UNIVERSITY OF SOUTHAMPTON

Coordination and Organometallic Chemistry of Stibine Ligands.

Michael David Brown

A Thesis submitted for the Degree of Doctor of Philosophy

Department of Chemistry

October 2006

UNIVERSITY OF SOUTHAMPTON

ABSTRACT

FACULTY OF ENGINEERING, SCIENCE AND MATHEMATICS

SCHOOL OF CHEMISTRY

Doctor of Philosophy

"COORDINATION AND ORGANOMETALLIC CHEMISTRY OF STIBINE LIGANDS."

by Michael David Brown

$\{CH_2(o\text{-}C_6H_4CH_2SbMe_2)\}_2$ (**VI**), has been prepared indirectly by coupling of the di-Grignard, $o\text{-}C_6H_4(CH_2MgCl)_2$ in concentrated thf solution followed by treatment with Me_2SbCl, and directly by treatment of the $\{CH_2(o\text{-}C_6H_4CH_2MgCl)\}_2$ with Me_2SbCl. **VI** has been characterised by ^1H and $^{13}C\{^1H\}$ NMR spectroscopy and high resolution EIMS. Oxidation of **VI** with Br_2 gives $\{CH_2(o\text{-}C_6H_4CH_2SbMe_2Br_2)\}_2$. **VI** shows a strong tendency to function as a *cis*-chelate in the complex $[PtMe_3I(\mathbf{VI})]$, forming an 11-membered ring and providing a stable Pt(IV) stibine complex, to Pt(II) in the complex $[PtCl_2(\mathbf{VI})]$ and to tungsten, in the complex $[W(CO)_4(\mathbf{VI})]$. This is also confirmed by single crystal X-ray structure determinations of each of these complexes.

The planar Pt(II) monomers $[PtMe_2(L\text{–}L)]$ and dimers $[(PtMe_2)_2(L'\text{-}L')_2]$ (L–L = $R_2Sb(CH_2)_3SbR_2$, $o\text{-}C_6H_4(CH_2SbMe_2)_2$; L'-L' = $R_2SbCH_2SbR_2$; R = Me or Ph) are obtained in good yield *via* reaction of $[PtMe_2(SMe_2)_2]$ with L–L or L'–L' in benzene. The Pt(IV) stibines, $[PtMe_3(L\text{–}L)I]$ (L–L = $R_2Sb(CH_2)_3SbR_2$, $o\text{-}C_6H_4(CH_2SbMe_2)_2$ or 2 × $SbPh_3$, $SbMePh_2$ or $SbMe_2Ph$) are obtained by treatment of $[PtMe_3I]$ with L–L in chloroform. The products have been characterised by ^1H, $^{13}C\{^1H\}$, ^{195}Pt NMR spectroscopy, electrospray mass spectrometry and analysis. Crystal structure determinations on 5 representative Pt(IV) complexes confirm the distorted octahedral environment at Pt. The C_1-distibines $R_2SbCH_2SbR_2$ afford the dinuclear species, $[(PtMe_3)_2(\mu\text{-}R_2SbCH_2SbR_2)(\mu\text{-}I)_2]$.

$[Rh(cod)(distibine)Cl]$, $[Rh(cod)(distibine)]BF_4$, $[Rh\{Ph_2Sb(CH_2)_3SbPh_2\}_2]BF_4$ and $[Rh(CO)(distibine)_2][Rh(CO)_2Cl_2]$ (distibine = $R_2Sb(CH_2)_3SbR_2$, and $o\text{-}C_6H_4(CH_2SbMe_2)$; R = Ph or Me) have been synthesized. The Ir(I) species $[Ir(cod)(distibine)]BF_4$ and $[Ir\{Ph_2Sb(CH_2)_3SbPh_2\}_2]BF_4$ have also been prepared. The complexes have been characterised by ^1H and $^{13}C\{^1H\}$ NMR and IR spectroscopy, electrospray mass spectrometry and microanalysis. The crystal structure of the anion exchanged $[Rh(CO)\{Ph_2Sb(CH_2)_3SbPh_2\}_2]PF_6\cdot 3/4CH_2Cl_2$ is also described.

$[CoX_2(o\text{-}C_6H_4(CH_2PPh_2)_2)]$ (X = Cl, Br or I), $[Rh(o\text{-}C_6H_4(CH_2PPh_2)_2)_2]^+$, $[M(cod)(o\text{-}C_6H_4(CH_2PPh_2)_2)]^+$ (M = Rh or Ir), $[NiX_2(o\text{-}C_6H_4(CH_2PPh_2)_2)]$ (X = Cl or Br), $[M'Cl_2(o\text{-}C_6H_4(CH_2PPh_2)_2)]$ (M' = Pd or Pt), $[Pd_2Cl_2(o\text{-}C_6H_4(CH_2PPh_2)_2)_2]^{2+}$, $[Pd(o\text{-}C_6H_4(CH_2PPh_2)_2)_2]^{2+}$, $[M''(o\text{-}C_6H_4(CH_2PPh_2)_2)_2]^+$ (M" = Cu, Ag or Au) and $[(AuCl)_2(o\text{-}C_6H_4(CH_2PPh_2)_2)]$ have been synthesised. Examples of Co(III), Ni(III) and Pt(IV) species are also reported. Where possible the products have been characterised by IR, UV-vis, NMR (^1H, ^{31}P, ^{63}Cu and ^{195}Pt as appropriate) spectroscopies, mass spectrometry and microanalysis. Crystal structures of six representative examples are also described.

The synthesis and characterisation of complexes of $R_2Sb(CH_2)_3SbR_2$ (R = Me or Ph) with a variety of metal carbonyls is described. These include *cis*-$[M(CO)_4\{R_2Sb(CH_2)_3SbR_2\}]$ (M = Cr, Mo or W), $[\{Fe(CO)_4\}_2\{\mu\text{-}R_2Sb(CH_2)_3SbR_2\}]$, $[\{Ni(CO)_3\}_2\{\mu\text{-}R_2Sb(CH_2)_3SbR_2\}]$, $[Co_2(CO)_6\{Ph_2Sb(CH_2)_3SbPh_2\}]$, $[Co_2(CO)_4\{Me_2Sb(CH_2)_3SbMe_2\}_3][Co(CO)_4]_2$ and $[Mn_2(CO)_8\{Ph_2Sb(CH_2)_3SbPh_2\}]$. The complexes have been characterised by analysis, mass spectrometry, IR and multinuclear NMR spectroscopy as appropriate.

Table of Contents

List of Figures

List of Tables

Acknowledgements

I would like to thank my supervisors Prof. Gill Reid and Prof. Bill Levason for all their help and advice throughout the course of my research degree, and the EPSRC for funding. I would also like to thank Dr. Mike Webster and Prof. Gill Reid for help with certain aspects of the *X*-ray crystallography, specifically the disorder models in some of the structures, and my advisor Dr. Andreas Danopoulos for his support over the three years.

Special thanks go to my colleagues in the research group, past and present, notably Charlie, Annie, Martin and Jo for continued encouragement. Additional thanks go to Jo Manning for preliminary work on the carbonyl stibine complexes, and Rebecca Watts for preliminary work on Pd and Pt complexes incorporating *o*-$C_6H_4(CH_2PPh_2)_2$. I would also like to thank the Mass Spectrometry, NMR Spectroscopy and *X*-ray crystallography departments for the use of instruments, and Prof. Gill Reid and Prof. Bill Levason for help with multinuclear NMR spectroscopy.

Finally I would like to thank my family and friends who I could not have done this without.

Abbreviations

Experimental Techniques

IR	Infra-red
ESMS	Electrospray Mass Spectrometry
EIMS	Electron Ionisation Mass Spectrometry
FAB	Fast Atom Bombardment
APCI	Atmospheric Pressure Chemical Ionisation
UV/vis	Ultra-violet/visible
NMR	Nuclear Magnetic Resonance

Solvents

EtOH	ethanol
MeCN	acetonitrile
thf	tetrahydrofuran
dmso	dimethylsulfoxide
d^6-dmso	deurerated dimethylsulfoxide
Et_2O	diethyl ether
^{n}BuOH	*n*-butanol
dmf	dimethylformamide

Ligands and Complexes

M	metal
L	ligand
L-L	bidentate ligand
X	halides (Cl, Br, I)
o-$C_6H_4(CH_2PPh_2)_2$	1,2-*bis*[diphenylphosphinomethyl]benzene
o-$C_6H_4(PPh_2)_2$	1,2-*bis*[diphenylphosphino]benzene
o-$C_6H_4(CH_2SbMe_2)_2$	1,2-*bis*[dimethylstibinomethyl]benzene
$Ph_2Sb(CH_2)_3SbPh_2$	1,3-*bis*(diphenylstibino)propane
$Me_2Sb(CH_2)_3SbMe_2$	1,3-*bis*(dimethylstibino)propane
$Ph_2SbCH_2SbPh_2$	1,1-*bis*(diphenylstibino)methane
$Me_2SbCH_2SbMe_2$	1,1-*bis*(dimethylstibino)methane
$Ph_2PCH_2PPh_2$	1,1-*bis*(diphenylphosphino)methane

$Ph_2P(CH_2)_2PPh_2$	1,2-*bis*(diphenylphosphino)ethane
$Ph_2P(CH_2)_3PPh_2$	1,3-*bis*(diphenylphosphino)propane
$Ph_2P(CH_2)_4PPh_2$	1,4-*bis*(diphenylphosphino)butane
cod	cyclooctadiene
coe	cyclooctene
tht	tetrahydrothiaphen

General

NBS	N-bromosuccinimide
Me	methyl (CH_3)
Et	ethyl (C_2H_5)
Ph	phenyl (C_6H_5)
R	alkyl or aryl group
I	nuclear spin
o-	*ortho* (1,2-)
m-	*meta* (1,3-)
p-	*para* (1,4-)
μ	bridging ligand
Å	Angström
δ	chemical shift
Hz	Hertz
m/z	mass to charge ratio
ν	vibrational frequency
cis	adjacent coordination
fac	facial coordination
mer	meridial coordination
trans	opposite coordination
ppm	parts per million
J	coupling constant
ε_{mol}	extinction coefficient
$w_{1/2}$	resonance width at half height
$\{^1H\}$	proton decoupled NMR spectroscopy
λ	Lamba (wavelength)
s	strong

(s)	singlet
m	medium
(m)	multiplet
(d)	doublet
(t)	triplet
w	weak
sh	shoulder
br	broad
vbr	very broad

Chapter 1

Introduction

1.1 Background

Phosphines and arsines have received much attention over the last hundred years. By varying the oxidation state of the metal and the substituent groups of the ligands, it was found that phosphines and arsines have an unprecedented coordination ability to hard and soft transition metal centres.[1] Initially phosphines were not investigated in as much depth as arsines, as many are more air sensitive, and there were no means of investigating these properties. Organoarsines generally had less complex preparations, and were easier to handle, making their coordination chemistry more desirable for the time.

In the 1960s however, intense studies on tertiary phosphines were developed, involving bonding organophosphines with hard and soft metal centres, to probe their coordination ability. This was made possible with advances in techniques, allowing research on more air sensitive compounds. Another desirable feature of phosphine chemistry is that there is an NMR spectroscopy probe involving the phosphorus-31 nucleus. Phosphorus-31 has a nuclear spin of ½, and therefore NMR spectroscopy can be used to probe the bonding characteristics of the phosphines and aid in the understanding of the particular systems.

Research on the organoantimony compounds (stibines), was very much neglected until the early part of the twentieth century, as it was widely believed that they were poor ligands, due to their weaker coordination, in particular, the weaker Sb–C bond, and the lack of commercially available examples. However a weaker donor ligand is not necessarily a poor ligand, as the compound can be tuned to different applications, depending on different bonding characteristics. The research into stibines was mainly confined to coordination to soft metals in low oxidation states, until post 1970, when more detailed research commenced on tertiary stibines.

Unfortunately, the only spin ½ nucleus in Group 15 is phosphorus-31. Arsenic, antimony and bismuth, the heavier elements in the group, have quadrupolar nuclei, which have low symmetry environments in ER_3 ligands (where E = As, Sb, Bi), and in NMR spectroscopy have no observable resonances due to the fast quadrupolar relaxation that occurs.

The work that is discussed in this Thesis describes the preparation and complexation of one tertiary diphosphine and a group of distibines to transition metals, and in particular draws interesting conclusions about the coordination ability of the wide angle, tertiary diphosphine, *o*-

$C_6H_4(CH_2PPh_2)_2$, the wide angle, tertiary distibine, *o*-$C_6H_4(CH_2SbMe_2)_2$ and the development of an unexpected novel distibine $\{CH_2(o\text{-}C_6H_4CH_2SbMe_2)\}_2$.

1.2 Electronic Characteristics

The areas of phosphine and stibine chemistry are of much interest to research chemists due to their unusual bonding characteristics. The trend in σ–donor power of the Group 15 tertiary ligands is shown below:

Fig 1.2.1: Trend of σ – donor power of Group 15 tertiary ligands.[1]

$$\mathbf{NR_3 > PR_3 > AsR_3 > SbR_3 >> BiR_3}$$

The trend above is due to the σ-donor orbitals becoming larger and more diffuse, as you descend Group 15. The concentration of electrons is therefore lower, which in turn causes a weakening of bonds. A similar trend is seen for the π-back bonding in PR_3, AsR_3, SbR_3 and BiR_3.[2,3]

Particular interest in phosphines and stibines is due to the ability to tune their bonding properties to accommodate specific transition metals, as a result of their σ-donor/π-acceptance properties. This can aid the understanding of why alkyl and aryl phosphines in particular can form stable complexes with many metals, in a wide range of oxidation states. Indeed, studies by Chatt [4] in 1951 and Orpen and Connelly[5] in 1985, have investigated the bonding characteristics of phosphines.

The Chatt model suggests that the lone pair on a PR_3 ligand (where R = alkyl or aryl group) is donated to the bonding metal, which forms the σ-bond. Chatt also suggested that in low metal oxidation states, there is π-back bonding, donating electrons into the empty phosphorus d-orbitals. Despite the relatively weak σ-bonding in certain transition metal – phosphine complexes, the M-P bond is strengthened by the π-back bonding component.

Fig 1.2.2: The Chatt model of PX_3 bonding to a metal centre.[4]

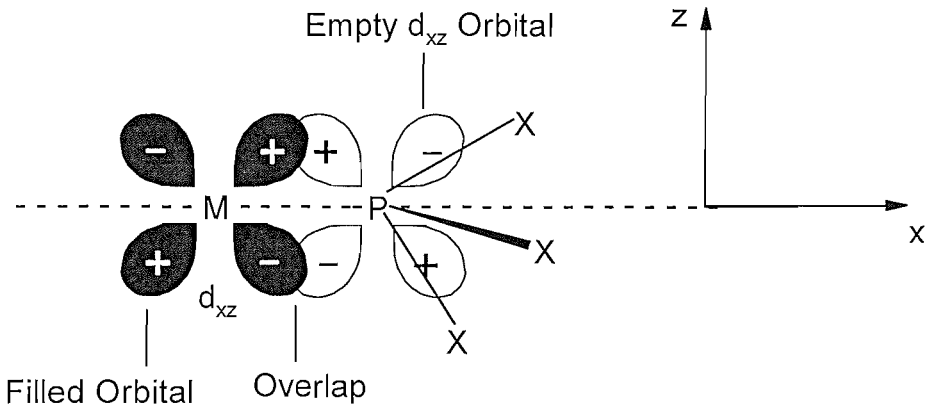

The Chatt model agrees with experimentally observed shortening and strengthening of the M-P bond, but later X-ray crystallographic data indicated there was also unexpected lengthening and weakening of the P-C bond. On the basis of this, Orpen and Connelly suggest that the π-back bonding component involves electrons being donated from the metal d orbitals to empty σ^* orbitals of the P-C bond.[5,6]

In conjunction with other studies,[7,8] Orpen and Connelly found that the LUMO of the PX_3 (X = H, CH_3, F) molecule has been shown to contain substantial P–X σ^* character in addition to some phosphorus 3d character. Figure 1.2.3 shows how the combination of phosphorus 3d and P–X σ^* orbitals of *e* symmetry leads to well hybridised π-acceptor orbitals.

Fig 1.2.3: Doubly degenerate PX_3 LUMO (C_{3v} local symmetry).[5,6]

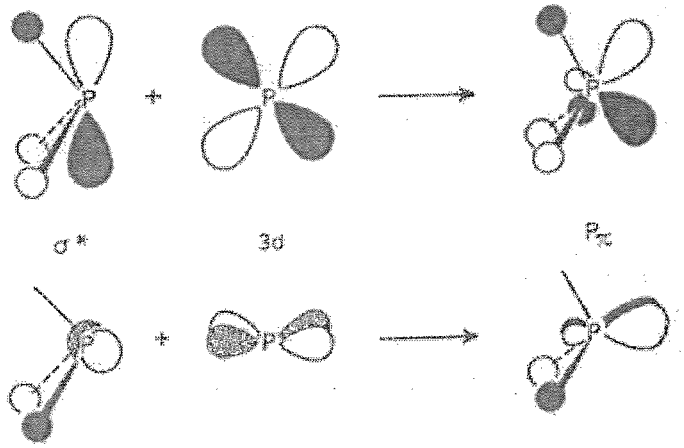

Orpen and Connelly predicted that in complexes where π-donation of electrons from the metal to the phosphorus is important there would be a weakening of the P–X bond. To test their hypothesis the results from crystallographic studies on pairs of transition metal phosphine and phosphite complexes related by electron transfer were examined. These were chosen as the M–P distances would not be affected by changes in ligands. Selected results of these studies can be seen in Table 1.3.1.

Table 1.3.1: Selected metal-phosphorus and phosphorus-substituent distances.[5]

Complex	Charge	Counter ion	M-P[a] (Å)	P-X[a] (Å)	Ref
$[Fe(CO)\{P(OMe)_3\}_2(\eta^4\text{-}C_4Ph_4)]$ (1)	0		2.146(1)	1.598(3)	5,6
	+1	BF_4	2.262(2)	1.579(6)	
$[\{Rh(CO)(PPh_3)\}_2(\eta^5\eta'^5\text{-fulvalene})]$ (2)	0		2.255(2)	1.844(5)	9
	+2	PF_6	2.322(4)	1.813(15)	
cis,trans-$[Ru(CO)_2(PPh_3)_2(o\text{-}O_2C_6Cl_4)]$ (3)	0		2.424(2)	1.829(5)	5,6
	+1	PF_6	2.429(2)	1.826(5)	
$[Co(PEt_3)_2(\eta\text{-}C_5H_5)]$ (4)	0		2.218(1)	1.846(3)	10
	+1	BF_4	2.230(1)	1.829(3)	
$[Fe(\eta^3\text{-}C_8H_{13})\{P(OMe)_3\}_3]$ (5)	0		2.138(1)	1.621(1)	11
	+1	BF_4	2.153(2)	1.600(2)	

a M-P and P-X distances are averaged over equivalent bonds, with the e.s.d.s in the least significant digit for *individual* bond lengths, as determined by least-squares.

Table 1.3.1 lists the M–P and P–X bond lengths for a selection of redox pairs, taken from the reported work of Orpen and Connelly.[5,6] The evidence (Electron Spin Resonance spectroscopy, Hückel calculations and structural analysis) indicates that the oxidations of **1, 2, 4** and **5** are largely metal based, with the HOMO of the neutral complex being of the 't_{2g}' type. For **3** the oxidation is largely ligand based. In each of the cases where the oxidation is known to be metal based, it can be seen that there was a marked increase in the M–P distance and a decrease in the P–X distance. The loss of electrons from the 't_{2g}' type orbitals leads to a direct loss of π-back-donation. Ligand based oxidation as in **3**, has very little effect on the M–P π-bonding and therefore on the M–P distances. The important conclusions that Orpen and Connelly made are that the changes in the M–P lengths are consistent with the M–P bonding in these complexes containing an important π-component. Metal–Ligand distances for purely σ-donors would be expected to decrease on metal-based oxidation owing to the contraction of the metal orbitals. Their conclusions are in accord

with work carried out by Aslanov *et al.*, who found variations in the M–P and M–Cl distances in high oxidation state *mer*-$[MCl_3(PR_3)_3]$ and *trans*-$[MCl_4(PR_3)_3]$ complexes (M = Re, Os, Ir).[12] Their study showed that the M(III)–P distances are shorter than M(IV)–P, and M(III)–Cl are longer than M(IV)–Cl. The second conclusion that Orpen and Connelly reported was that the decrease in P–X distance that accompanies the increase in the M–P distance were in accord with the predictions that the P–X σ^* orbitals participate in the M–P π-bonding.[5,6]

The heavier Group 15 elements in ligands of the type ER_3 (where E = As, Sb, Bi), are assumed to have similar bonding characteristics to phosphines. However, as you descend Group 15, there is a weaker σ–donation and weaker π – acceptance bonding characteristic. The weaker σ–donation can be explained by the fact that there is a larger separation between valence s- and p- orbitals as you go down the group. This is most obvious in the C–E–C angles along the series PPh_3 (103°), $AsPh_3$ (100°), $SbPh_3$ (96°), $BiPh_3$ (94°).[6] There is therefore more p-character in the E–C bond, and an increase of s-character in the lone pair of E. This leads to poor directional properties of the lone pair and more diffuse orbitals. The more diffuse the orbitals are, the weaker the bonds are, and so the ligating properties are diminished. The weaker π–acceptance can be attribruted to the reduced electronegativity of the acceptor atom, and the more diffuse orbitals. Orpen also carried out a detailed study of some 1860 examples of M–PPh_3 fragments, and found a correlation between the P–C distances and the C–P–C angles, but found that on coordination to a transition metal the geometry of the PPh_3 was little changed.[13]

Similar studies have been carried out to explore the effects of coordination of stibine ligands on the C–Sb–C angle.[14,15] Distibinomethane complexes which contain a $[M(\eta^1\text{-}Ph_2SbCH_2SbPh_2)]$ unit have been investigated, and the notable conclusion was that while the "free" $SbPh_2$ group was little changed from the uncoordinated stibine, the coordinated end of the ligand showed an increase in the C–Sb–C angle of $\leq 8°$.[14] This finding is explained by the greater p- character in the M–Sb bond and therefore less p- and more s- character in the Sb–C bonds. This increase in C–Sb–C angle has been seen in a more extensive study of complexes incorporating M – $SbPh_3$ units, where it was found that as the C–Sb–C angle increases the Sb–C bond shortens.[15] These findings are of great importance as they potentially conflict with the prediction that an increase in M–Sb π-bonding would lengthen the Sb–C bond. However, there are no known studies of the structures of redox pairs involving stibines in the literature.

Methods that are used to explore the electronic properties of Group 15 ligands are well known. For example Tolman has carried out extensive research on the electronic parameter, based on observations of the ν(CO) (a_1) stretching mode in $[Ni(CO)_3L]$ (L = tertiary phosphines) as mentioned in Chapter 6.[16] Research into the $\delta(^{13}C)$ NMR resonances of these complexes has also been carried out.[17] It has been shown experimentally (in Chapter 6 of this Thesis and in the literature)[18] that stibines and distibines place less electron density into the π^* (CO) orbitals than the phosphine analogues and exhibit the usual trends with differing R groups.

1.3 Steric Effects

The steric effects in complexes that involve phosphines, have been widely explained by Tolman's Cone angle model.[19] The volume of the cone, and hence the volume that the particular ligand occupies, is defined as enclosing all the van der waals radii of all the atoms in the ligand, over all rotational orientations starting from the M–P bond. Therefore, the angle of the cone depends on the size of the ligand that is coordinated to the metal centre, and it can be suggested that the larger the steric bulk of the ligand, the larger the size of the angle (θ). Indeed, the larger the value of θ the lower the coordination number that is favoured around the metal centre. Fig 1.3.1 shows the Tolman cone angle model.

Fig 1.3.1: Tolman's Cone Angle Model.[19]

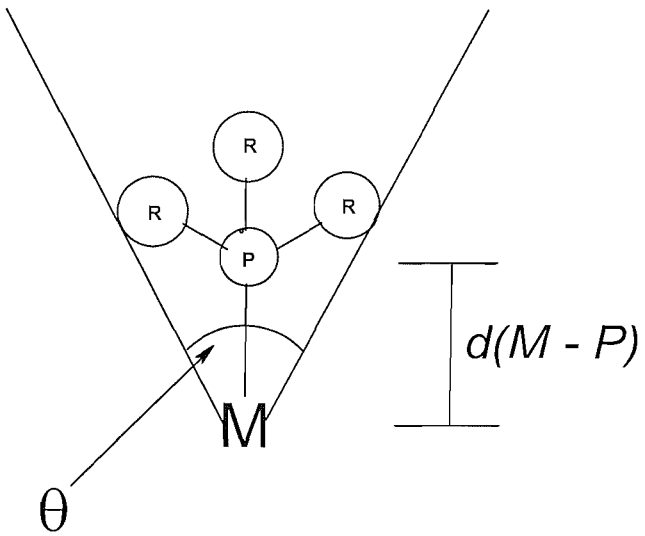

McAuliffe carried out a study on typical phosphine ligands and their cone angles when complexed to a rhodium metal centre. Selected findings from this can be seen in Table 1.3.2.

Table 1.3.2: Cone angles of common phosphine and stibine ligands.[20,21]

Ligand	Cone Angle / °	Ligand	Cone Angle / °
PMe_3	118	$SbMe_3$	119
PEt_3	132	$SbEt_3$	131
PMe_2Ph	122	Sb^nPr	121
PPh_3	145	$SbPh_3$	143
$P(o\text{-tolyl})_3$	194	$Sb(o\text{-tolyl})_3$	185
PH_3	87		
PH_2Ph	101		
$P(OMe)_3$	107		
$P(OPh)_3$	128		

It can be seen from Table 1.3.1 that the cone angle for $P(o\text{-tolyl})_3$ when incorporated in a transition metal complex, is 194° which suggests that a coordination number of two cannot be supported round the metal centre. However, as stated by Tolman himself, the model is a relative measure, as ligands are not uniformly cone shaped.[19] Ligands coordinate to metal centres, and intermesh due to cavities being present. Therefore bulky ligands can sometimes accommodate higher coordination numbers, even though it seems unlikely on the basis of cone angle. As long as the model is used as a model only, a relative understanding of whether a ligand is viable can be achieved. Another assumption of the Tolman model is that the distance of the M–P bond is 2.28 Å in phosphines, but of course slight variations of this length do occur depending on the complex involved, and the oxidation state of the metal. When applying this model to the other heavier elements in Group 15, for example stibines, it is vital to remember that d(M–P)<d(M–Sb), and that the C–Sb–C angle changes on coordination. Therefore, these two factors will have an effect on the cone angle and it is unclear that the "real cone angle" of a stibine is smaller, or even what value should be taken as a norm.

While steric effects seem to dominate bulky ligands and electronic effects seem to dominate small ligands, the debate as to how to separate electronic and steric effects and their significance

continues. There are observed differences noted in stibine complexes compared to their lighter analogues, four of which are:

1. Higher coordination numbers
2. Less dissociation in solution
3. More labile ligands
4. Different *cis-trans* isomer distributions.

Most of the above can be explained by electronic effects rather than sterics. For example, the fact that stibines place less electron density on the metal centre than phosphine or arsine analogues, results in reduced σ-donation and reduced π-acceptance. The differences seem to help explain the very different organometallic chemistry promoted by stibines.[22]

1.4 Synthesis of Primary and Secondary Phosphines

Primary phosphines

Primary phosphines can be synthesised relatively easily, but tend to be very volatile and toxic compounds. They have the general formula of PRH_2 (where R = alkyl or aryl) and can be used as synthons for poly-phosphines, but if the R group is small, for example a methyl group, the phosphines are pyrophoric, and difficult to handle.[23] Primary phosphines can also be prepared by reduction of RPX_2, $RP(S)X_2$ and $RP(O)X_2$ (X = Br, Cl, I) with $LiAlH_4$.[24,25] An example of this is $PhPH_2$ which can be prepared by the $LiAlH_4$ reduction of $PhPCl_2$[23] which can be seen in Fig. 1.4.1.

Fig 1.4.1: Preparation of primary phosphines.[23] (where R = aryl or alkyl group)

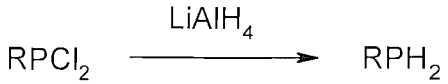

Secondary phosphines

Secondary phosphines generally have the formula PR_2H, and can be either prepared from primary phosphines above, or by treating a tertiary phosphine with lithium metal in thf to obtain the lithium salts *in situ*, then hydrolysing this to gain the product.[20,26] Secondary phosphines can also be

obtained by the hydrolysis of the corresponding phosphide or by alkylation and hydrolysis of MPRH.[20,26] The preparation of a secondary phosphine is shown in Fig 1.4.2.

Fig 1.4.2: Preparation of secondary phosphines.[20,26] (where R = aryl or alkyl group)

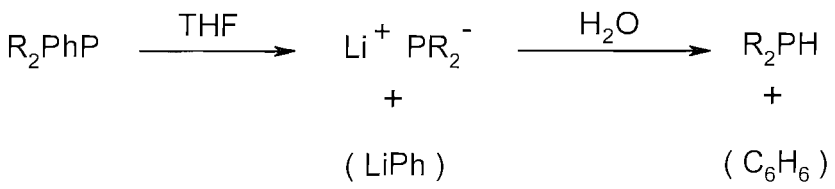

1.5 Tertiary phosphines

Tertiary phosphines can be easily prepared by reaction of PX_3, RPX_2, or R_2PX (X = Cl, Br, I) with a Grignard reagent or organolithium to yield PR'_3, RPR'_2 or R_2PR' respectively. Other methods for synthesising tertiary phosphines, involve reaction of alkali phosphides with alkyl halides. Mixed aryl and alkyl tertiary phosphines can be prepared by the reaction of Ph_2PCl or $PhPCl_2$ with an organolithium or Grignard reagent.[20,26]

1.6 Tertiary Stibines

The syntheses of antimony containing species are known, but the procedures are often lengthy and low yielding.[27] This is due to the weak Sb-C bond. Primary and secondary stibines are very unstable and therefore very difficult to handle. Organostibides are thermally unstable and therefore not attractive starting materials. Tertiary stibines SbR_3 are usually prepared by reaction of $SbCl_3$ and an appropriate Grignard reagent in Et_2O. Reaction of $SbCl_3$ and Ph_3Sb in a 2:1 or 1:2 ratio can yield $PhSbCl_2$ and Ph_2SbCl respectively as shown by Levason *et al.*[27-29] These can then be reacted with an organolithium or Grignard reagent to give mixed phenylalkylstibines. Other methods include the cleavage of a Sb-Ph bond in $SbPh_3$ in a sodium/liquid ammonia preparation to give a stibide, which can then be alkylated by reaction with an appropriate alkyl halide. However, once formed many tertiary stibines such as trialkylstibines (e.g. $SbMe_3$) are air sensitive oils, which make them very challenging to synthesise and handle.[27-29]

1.7 Diphosphines and Distibines

Diphosphines

Diphosphines are ligands with two phosphines incorporated, usually acting as bidentates. They can be prepared by reaction of phosphorus centres with dihalogenoalkanes. The reactions are carried out in an inert atmosphere and the products are achieved in high yield.[20]

Diphosphines of the form $Ph_2P(CH_2)_nPPh_2$ (n = 1-3) are prepared in high yield by reaction of $X(CH_2)_nX$ (X = Br, Cl) with $LiPPh_2$ in thf,[30] and diphosphines of the form $R_2P(CH_2)_2PR_2$ (R=Me, Et) can be prepared as highly air sensitive pyrophoric oils, by reacting $LiPR_2$ with an appropriate dihalogenoalkane.[23, 31] *cis*- and *trans*-1,2-bis(diphenylphosphino)ethylene ($Ph_2PCH=CHPh_2$) can be prepared by the reaction of *cis*- and *trans*-ClCH=CHCl with two equivalents of Ph_2PLi in thf.[32]

Diphosphines with a phenylene backbone, for example *o*-$C_6H_4(PPh_2)_2$ are more difficult to prepare. *p*-$C_6H_4(PPh_2)_2$ can be prepared in high yield by reaction of $LiPPh_2$ with either *p*-$C_6H_4Br_2$ or *p*-$C_6H_4ClSO_3Na$.[33,34] However *o*-$C_6H_4(PPh_2)_2$ can be prepared by reaction of $LiPPh_2$ and *o*-$C_6H_4F_2$ in thf.[35] This method can be seen in Fig 1.7.1 and is the preferred route. A more time consuming preparation is shown in Fig 1.7.2.[24]

Fig 1.7.1: Preferred synthetic route for *o*-$C_6H_4(PPh_2)_2$.[35]

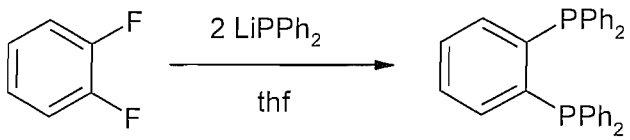

Fig 1.7.2: Alternative preparation of *o*-$C_6H_4(PPh_2)_2$.[24]

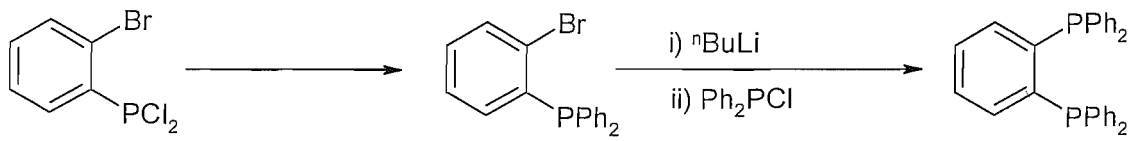

The methyl analogue o-$C_6H_4(PMe_2)_2$ can be prepared in low yield by the reaction of o-$C_6H_4X_2$ (X=Cl, Br) and $NaPMe_2$ in thf.[25] It can also be prepared by reduction of the corresponding phosphonate by $LiAlH_4$ to give the diphosphine o-$C_6H_4(PH_2)_2$ and then reacted with nBuLi and MeI to give the desired product.[36] This synthetic route can be seen in Fig 1.7.3. The coordination chemistry of diphosphines with rigid backbones is discussed in more detail in Chapter 5.

Fig 1.7.3: Preparation of o-$C_6H_4(PMe_2)_2$.[36]

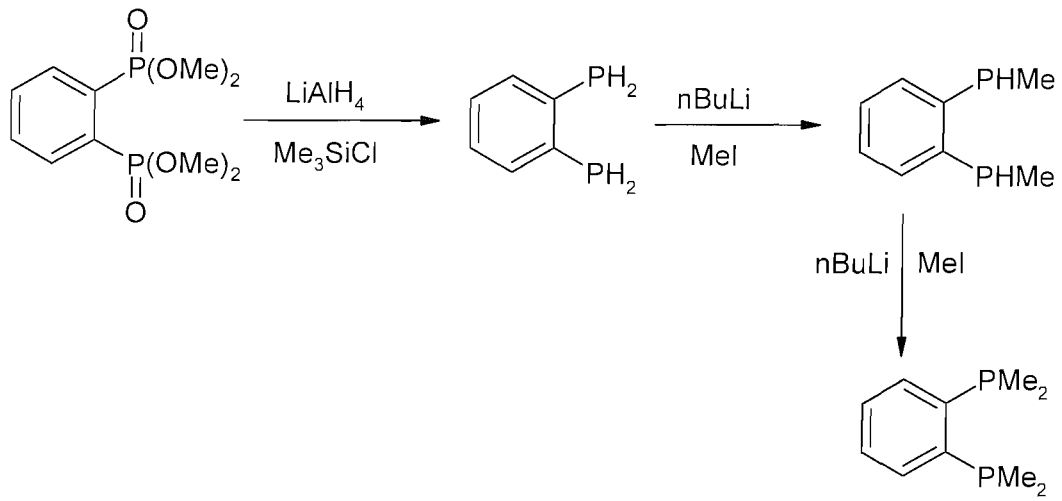

Distibines

Distibines are more challenging to synthesise and the yields are generally much lower due to the weak C-Sb bonds.[2] Nucleophiles such as alkyl-lithium or Grignard reagents can break existing Sb–C bonds as in Fig 1.7.8. Distibines of the form $R_2Sb(CH_2)_nSbR_2$ (n=1, 3 or 4) (R= Me, Ph) are readily made by the reaction of $NaSbR_2$ and a dihalogenoalkane in liquid ammonia.[37] $Ph_2Sb(CH_2)_3SbPh_2$ is an air stable white solid and is synthesised *via* a sodium/liquid ammonia route as shown in Fig 1.7.4.

Fig 1.7.4: Preparation of $Ph_2Sb(CH_2)_3SbPh_2$.[37]

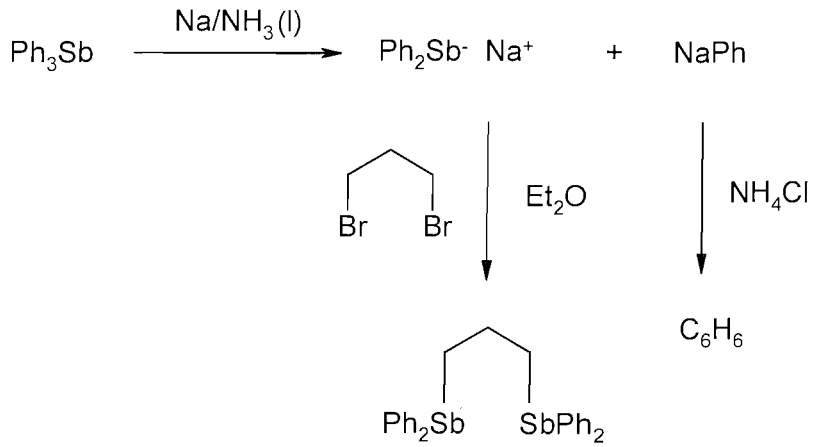

$Me_2Sb(CH_2)_3SbMe_2$ is an air sensitive oil and is prepared similarly as $Ph_2Sb(CH_2)_3SbPh_2$, however the air stable white solid, Me_3SbBr_2 is used as a starting material rather than $SbMe_3$ as the latter is very unstable and reactive. The synthesis of $Me_2Sb(CH_2)_3SbMe_2$ is shown in Fig. 1.7.5.

Fig 1.7.5: Preparation of $Me_2Sb(CH_2)_3SbMe_2$.[37]

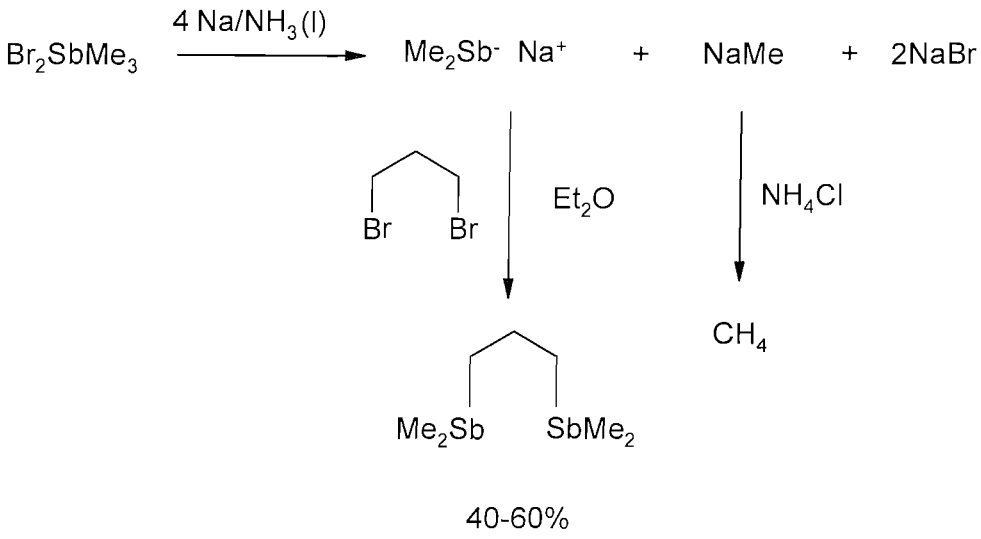

Fig 1.7.6: Preparation of $PhMeSb(CH_2)_3SbMePh$.[37]

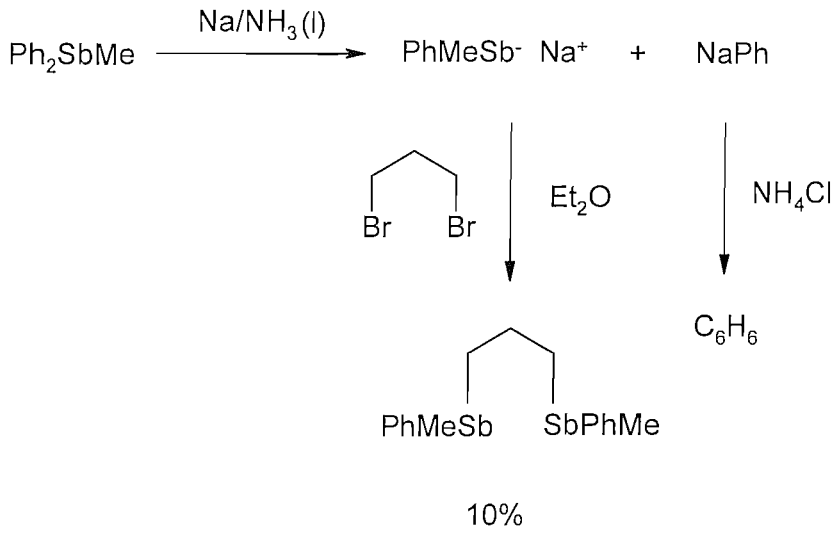

The synthesis of $PhMeSb(CH_2)_3SbPhMe$ as shown in Fig. 1.7.6, does not result in high yields due to the unreliable cleavage of Ph from Ph_2SbMe. The resultant air sensitive oil usually needs distilling to gain the pure product as the unreliable Ph cleavage results in unreacted starting material and decomposition products.[37] Attempts at the preparation of $R_2Sb(CH_2)_2SbR_2$ have been unsuccessful due to the elimination of ethane, and R_4Sb_2 is produced.[38] The synthesis of $R_2SbCH_2SbR_2$ (R = Me, Ph) is carried out in a similar manner to that of $R_2Sb(CH_2)_3SbR_2$ and can be seen in Fig 1.7.7a and Fig 1.7.7b.[37] Distibinoalkanes are soft moderate σ-donor ligands and in certain cases act as weak π-acceptors. They can promote higher coordination numbers which is due to their donor properties and small cone angles.

Fig 1.7.7a: Preparation of $R_2SbCH_2SbR_2$ (R = Ph).[37]

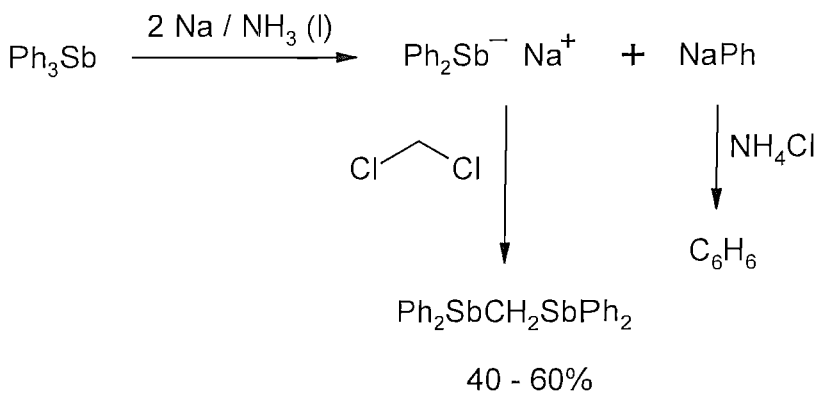

Fig 1.7.7b: Preparation of $R_2SbCH_2SbR_2$ (R = Me).[37]

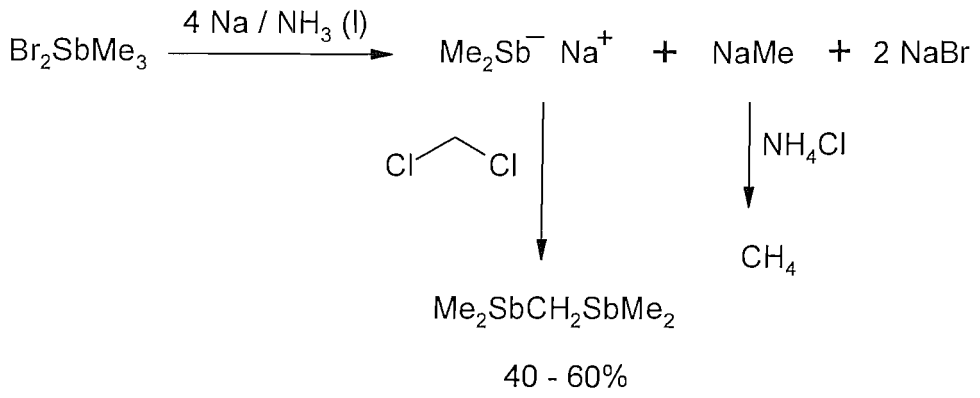

The ligands *o*-$C_6H_4(SbMe_2)_2$[25] and *o*-$C_6H_4(CH_2SbMe_2)_2$[18] have the strongest coordinating properties of the distibines.[2] Reaction of *o*-$C_6H_4Cl_2$ with $NaSbMe_2$ in liquid ammonia yields trace amounts of *o*-$C_6H_4(SbMe_2)_2$.[39] Attempts to prepare the phenyl analogue by this route have been unsuccessful, and yields of 5% and 9% have been obtained by using *o*-$C_6H_4Br_2$ and *o*-$C_6H_4I_2$ respectively.[40] Better yields have been obtained by a very lengthy preparation of *o*-$C_6H_4(SbMe_2)_2$. This route was developed by Levason *et al* and is shown in Fig 1.7.8.[25] The intermediate, $SbMe_3$ produced is hazardous, volatile and pyrophoric, but is reacted with either Br_2 or Cl_2 to afford an air stable white solid Me_3SbX_2, as used in the synthesis of $Me_2Sb(CH_2)_3SbMe_2$ in Fig 1.7.5. This is then, when required, decomposed to Me_2SbX by pyrolysis. The synthesis of *m*-$C_6H_4(SbMe_2)_2$[18] and *p*-$C_6H_4(SbMe_2)_2$[18] is shown in Fig 1.7.9 and the preparation of *o*-$C_6H_4(CH_2SbMe_2)_2$[18] can be seen in Fig 1.7.10. This ligand is discussed in more detail in Chapter 2, along with the synthesis of *p*-$C_6H_4(CH_2SbMe_2)_2$ and *m*-$C_6H_4(CH_2SbMe_2)_2$. The synthesis of *o*-$C_6H_4(SbPh_2)_2$[39] is shown in Fig 1.7.11.

Fig 1.7.8: The synthesis of *o*-$C_6H_4(SbMe_2)_2$.[25]

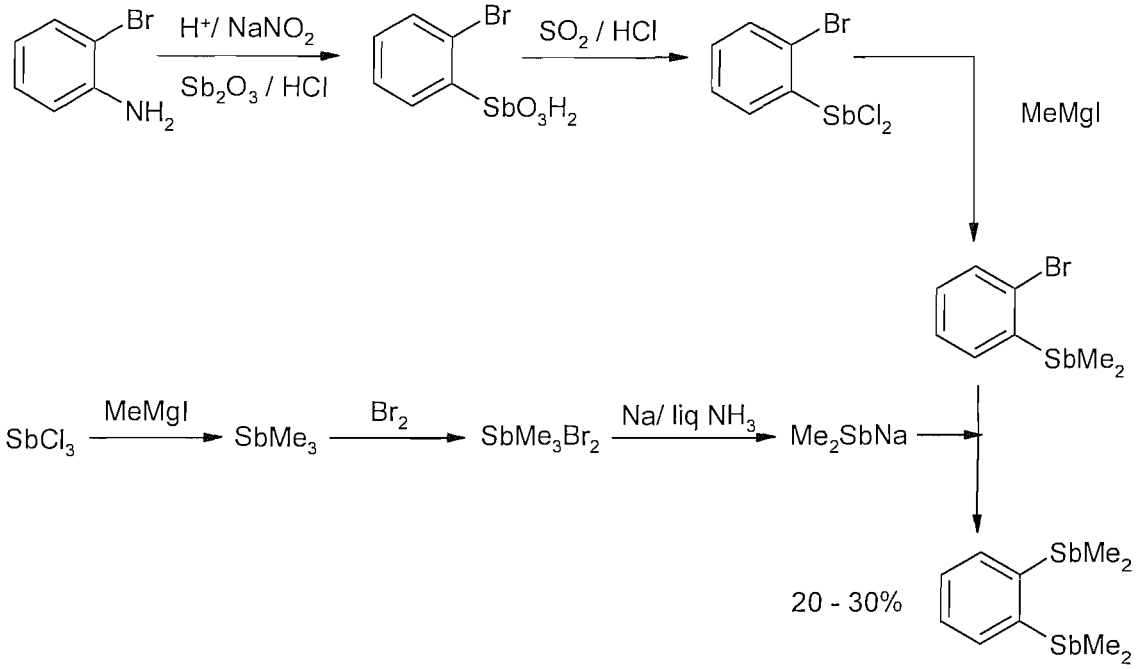

Fig 1.7.9: The preparation of *m*-$C_6H_4(SbMe_2)_2$ and *p*-$C_6H_4(SbMe_2)_2$.[18]

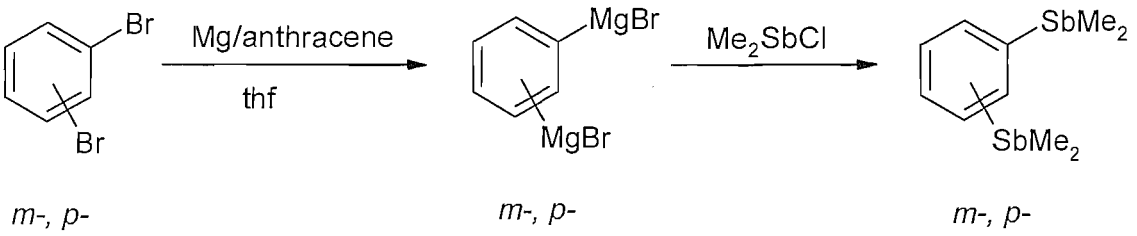

Fig 1.7.10: The synthesis of *o*-$C_6H_4(CH_2SbMe_2)_2$.[18]

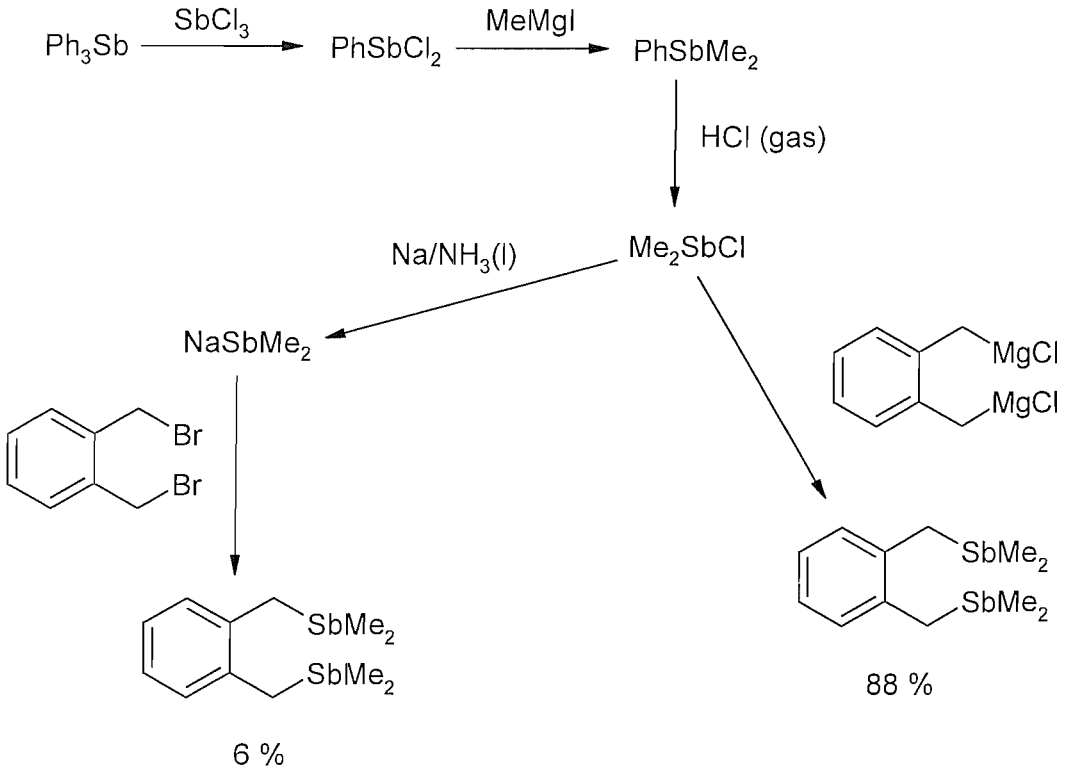

Fig 1.7.11: Preparation of *o*-$C_6H_4(CH_2SbPh_2)_2$.[39]

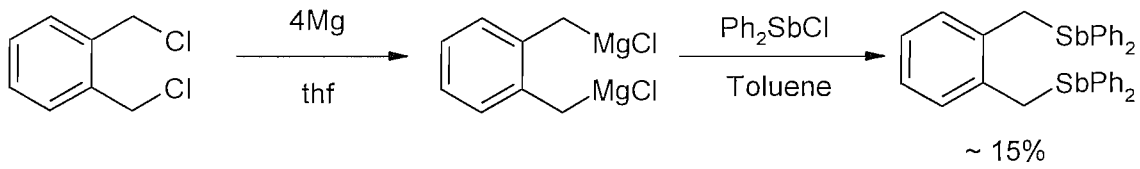

One tritertiary stibine $MeC(CH_2SbPh_2)_3$ has been prepared, by reaction of $MeC(CH_2Br)_3$ with $NaSbPh_2$ in liquid ammonia.[41] Interestingly the reaction of $NaSbPh_2$ and $MeC(CH_2Cl)_3$ afforded Sb_2Ph_4 as the only antimony containing species. It is hoped that by further research based on this Thesis new multidentate stibines can be synthesised in the future.

1.8 Chelate Effect

The term chelate effect, refers to the extra stability gained in a complex incorporating chelating ligands compared to a complex which involves analogous monodentate ligands.[31] Both enthalpic and entropic factors influence the stability of a complex. This is shown in the equations below:

$$\Delta G^{o} = \Delta H^{o} - T\Delta S^{o}$$

$$\Delta G^{o} = -RT\ln\beta$$

G = Gibbs free energy

H = enthalpy

S = entropy

T = Temperature

R = gas constant

β = formation/ stability constant

β increases as ΔG^{o} decreases. This can be achieved by either making ΔH^{o} more negative, or by making ΔS^{o} more positive.[31] Enthalpic differences arise from electrostatic interactions between the ligands in the system. The electrostatic repulsion between monodentate ligands increases as the ligands are brought together just before complexation. With chelating ligands, the electrostatic repulsion does not increase at complexation, as it is built into the ligand framework. The solvation of the chelating ligand is lower than that of monodentate analogues and therefore this does not influence the enthalpic differences as much.

Entropic differences between complexes involving monodentate and chelating ligands arise from the fact that there is a higher probability of the chelating ligand coordinating, as once one end of the ligand has bonded to the metal centre, the other is held in close proximity to the metal, and therefore there is a high probability of coordination. With long chain chelating ligands, however, the chelate effect is decreased due to the uncoordinated end of the ligand, not being in as close proximity to the metal centre.[42] In comparison to complexes with monodentate ligands, the binding of one ligand, has no influence on another ligand's coordination, so the probability of coordination is reduced.

1.9 Coordination Chemistry

In general ligands involving Group 15 elements, ER_3, (where E = P, As, Sb, and R = alkyl or aryl group), behave as monodentate ligands, complexing to one metal centre with one M–E bond. However, Werner and coworkers [22] have discovered some evidence for these ligands bridging between two metal centres, therefore creating two M–E bonds. This research is discussed in more detail in Chapter 4. Diphosphines, of the type $R_2P(CH_2)_nPR_2$ have been found to coordinate to metal centres as either bridging ligands or chelates, whereby both phosphorus centres bond to the same metal centre and form a chelate ring. The heavier elements of Group 15 also follow this trend, but due to the steric effects of larger heavier atoms, and the weaker E–C bond (E = AS, Sb, Bi) which has already been mentioned, there is more ring strain, so monodentate ligands have traditionally been preferred.

1.9.1 Advances in the coordination chemistry of distibines to transition metals

The coordination chemistry of ligands of the type $R_2SbYSbR_2$ (Y = CH_2, O, S) is interesting due to the short interdonor linkage and the large, weakly binding Sb atom. Chelation of these ligands when reacted with transition metals, is disfavoured due to the strained four-membered chelates that would be formed. Such ligands more commonly bond to transition metals as either monodentate ligands or bridging ligands. This result differs greatly to that of diphosphinomethanes where chelation is often found.[43]

Complexes that incorporate $R_2SbCH_2SbR_2$, (R = Ph, Me) with Group 6, Fe, Mn, Co and Ni carbonyls have been synthesised previously,[44] and these complexes are discussed in more detail in Chapter 6.

Complexes of the form $[M(CO)_5(\eta^1\text{-L})]$, $[(CO)_5M(\mu\text{-L})M(CO)_5]$, *cis*-$[(CO)_4M(\mu\text{-L})_2M(CO)_4]$ (where L = $Ph_2SbOSbPh_2$, $Ph_2SbSSbPh_2$, M = W, Mo, Cr)[45] have been prepared and fully characterised. Indeed $[Cr(CO)_5(\eta^1\text{-}Ph_2SbSSbPh_2)]$ and *cis*-$[(CO)_4Cr(\mu\text{-}Ph_2SbOSbPh_2)_2Cr(CO)_4]$ have also been characterised by single crystal X-ray diffraction. $Me_2SbOSbMe_2$, when reacted with 2 molar equivalents of *cis*-$[Cr(CO)_4$(norbornadiene)] gives *cis*-$[(CO)_4Cr(\mu\text{-}Me_2SbOSbMe_2)_2Cr(CO)_4]$, however, when the analogous reaction with $Me_2SbSSbMe_2$ is carried out two products were observed. The first was the expected *cis*-$[(CO)_4Cr(\mu\text{-}Me_2SbSSbMe_2)_2Cr(CO)_4]$ complex, whereas the second product was seen to be $[Cr(CO)_4\{MeSb(SSbMe_2)_2\}]$.[46] The latter complex contains a tristibine, $MeSb(SSbMe_2)_2$ which seems to have formed in a rearrangement that eliminates $SbMe_3$. The crystal structure of

$[Cr(CO)_4\{MeSb(SSbMe_2)_2\}]$ is shown in Fig 1.9.1. This result led to the detailed comparison of the carbonyl region of the IR spectra, which suggested that the $R_2SbCH_2SbR_2$ ligands are stronger σ-donors than $R_2SbYSbR_2$ (Y = O, S).[46]

Photolysis of $[(MeC_5H_4)Mn(CO)_3]$ in thf followed by addition of $R_2SbYSbR_2$ gave $[[(MeC_5H_4)Mn(CO)_2(\eta^1\text{-L})]$ and $[\{(MeC_5H_4)Mn(CO)_2\}_2(\mu\text{-L})]$ (Y = O, S; R = Ph, Me).[47]

Fig 1.9.1: Structure of $[Cr(CO)_4\{MeSb(SSbMe_2)_2\}]$ with numbering scheme adopted.[46]

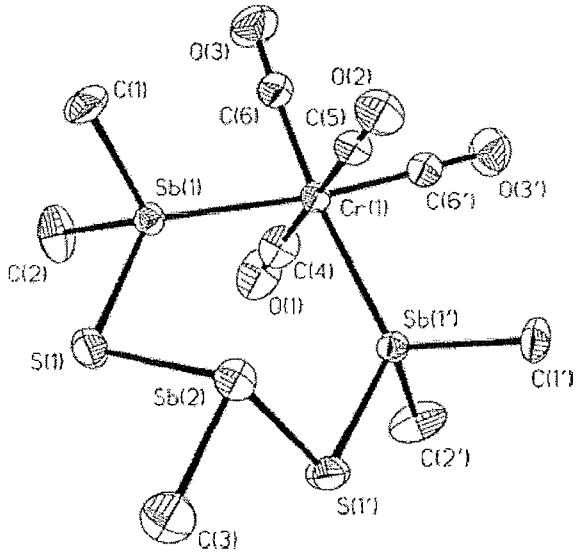

1.9.2 Ru and Os chemistry

The reaction of $Ph_2SbCH_2SbPh_2$ and $[Ru(dmf)_6][CF_3SO_3]_2$ and LiX (X = Cl, Br) in refluxing ethanol affords pink or brown solids which were found to be $[RuX_2(\eta^1\text{-}Ph_2SbCH_2SbPh_2)_4]$. The reaction of $[OsCl_2(dmso)_4]$ with the same ligand results in the formation of a yellow solid which was found to be $[OsCl_2(\eta^1\text{-}Ph_2SbCH_2SbPh_2)_4]$.[48] The complexes $[RuI_2(L)_3]$ and $[OsBr_2(L)_3]$ were prepared *via* similar reactions to that of above, however, as it can be seen, the stoichiometries are very different. Indeed the structure of $[RuI_2(L)_3]$ confirmed the first example of a chelating distibinomethane ligand,[28] and this can be seen in Fig 1.9.2.

As can be seen from Fig 1.9.2, two of the three ligands are bound to the Ru metal centre as monodentate ligands, and one is forming a strained 4-membered chelate ring with the Sb–C–Sb angle equal to 93.5°. This is in great contrast to the complexes incorporating η^1-ligands which

have Sb–C–Sb angles of about 118°. The Ru – Sb distance in $[RuI_2(L)_3]$ in the chelate ring is also longer than the Ru–Sb distance of the monodentate ligands. Both coordination modes are also present in the ^1H and $^{13}C\{^1H\}$ NMR spectra. It can be seen that the CH_2 resonances of the chelating ligand are shifted significantly to higher frequency than the η^1-$Ph_2SbCH_2SbPh_2$ ligands.[48]

Fig 1.9.2: Core geometry of $[RuI_2(Ph_2SbCH_2SbPh_2)_3]$, with phenyl groups and H atoms omitted for clarity.[48]

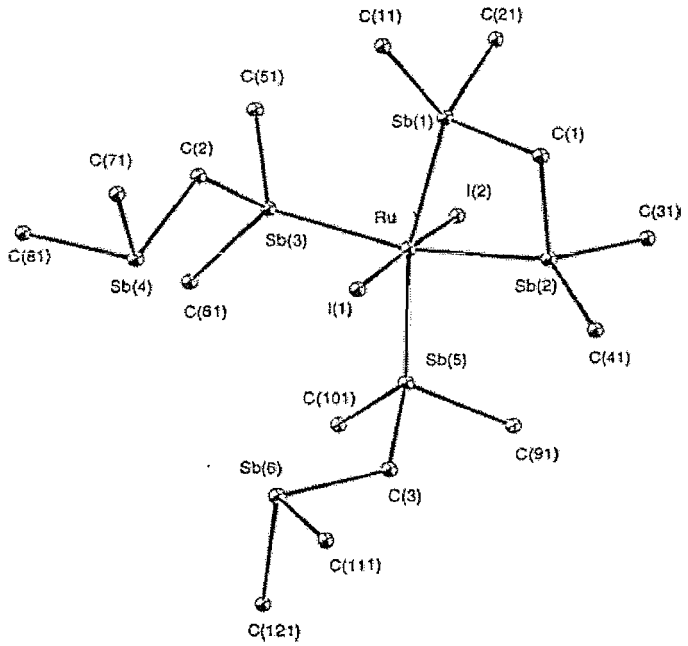

1.9.3 Pd and Pt Chemistry

Platinum(II) and palladium(II) halides form two different types of complexes with $Ph_2SbCH_2SbPh_2$, $[MX_2(L)_2]$ and $[M_2X_4(L)_2]$.[2] $[MX_2(L)_2]$ complexes are very unstable in solution, and decompose to $[M_2X_4(L)_2]$ and other species over time. However, multinuclear NMR spectroscopy was gained on freshly made samples, which showed a mixture of *cis*- and *trans*-isomers with η^1-$Ph_2SbCH_2SbPh_2$ for the platinum containing complexes and single isomers for the complexes that contained Pd.[48] An example of the instability of $[MX_2(L)_2]$ is $[PdCl_2(L)_2]$ which undergoes Sb–Ph cleavage in solution to form $[\{PdCl(\sigma\text{-}Ph)(L)\}_2]$ cleanly. It was found that the process was promoted by a photochemical reaction.[49] This particular decomposition process is minimal in the palladium(II) bromides and iodides, and does not occur with the platinum systems. Structures of dimers of the form $[M_2X_4(L)_2]$ show that the ligands are bridging the two metal

centres, and in the case of $[Pd_2I_4(L)_2]$ there is a *trans* geometry at each of the Pd centres. However, in the case of $[Pd_2Br_4(L)_2]$, $[Pt_2Br_4(L)_2]$ and $[Pt_2Cl_4(L)_2]$, one metal centre has *trans*-halides, whilst the other has *cis*-halides, and NMR spectroscopic studies suggest that these are the only major species in solution.[48] Fig 1.9.3 shows the structure of $[Pd_2Br_4(L)_2]$.

Fig 1.9.3: Structure of $[Pd_2Br_4(Ph_2SbCH_2SbPh_2)_2]$ with numbering scheme adopted, with phenyl rings and H atoms omitted for clarity.[48]

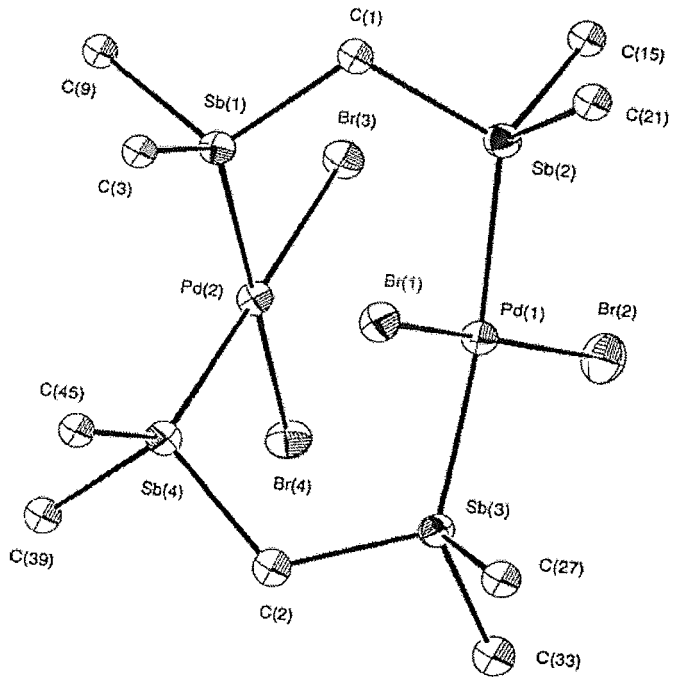

The reason for the geometries around the palladium(II) centres in $[Pd_2Br_4(L)_2]$ is unclear, indeed none of the many complexes incorporating $Ph_2PCH_2PPh_2$ [24] have shown this structure. The structural characterisation of $[Pt_2Cl_4(Ph_2AsCH_2AsPh_2)_2]$ recently, has shown the formation of the *trans-trans* isomer and the *cis-trans* isomer.[50]

Complexes of the form $[MCl_2(Me_2SbCH_2SbMe_2)]$ (M = Pt, Pd) were prepared, however due to insolubility in common solvents solution measurements were not obtained. FAB MS, however did show dimer ions present. The insolubility of these complexes is a property that is shared by the $Me_2PCH_2PMe_2$ and $Me_2AsCH_2AsMe_2$ analogues.[51] The organometallic chemistry of $R_2SbCH_2SbR_2$ (R = Me, Ph) with Pt(IV) is discussed in detail in Chapter 3.

1.9.4 Cu, Ag and Au chemistry

Complexes of the form $[M(R_2SbCH_2SbR_2)]Y$ (M = Cu(I), Ag(I), Au(I); R = Me, Ph; Y = BF_4, PF_6) have been formed, but are labile in solution. It is assumed that these species are ligand bridged oligomers in the solid state.[48] $[(AuCl)_2(Ph_2SbCH_2SbPh_2)]$ was prepared as a red-brown solid from [AuCl(tetrahydrothiophen)] and $Ph_2SbCH_2SbPh_2$.[51]

Details of the coordination chemistry of o-$C_6H_4(CH_2SbMe_2)_2$ with transition metal elements is discussed in Chapter 2 and the organometallic chemistry of Rh(I) and Ir(I) with $R_2SbCH_2SbR_2$ is discussed in detail in Chapter 4.

1.10 Characterisation Techniques

There are a wide range of analytical techniques available for the study of new ligands and their coordination chemistry, including ^1H, $^{13}C\{^1H\}$ and multinuclear NMR spectroscopy, IR and UV-Vis spectroscopy, mass spectrometry, single crystal X-ray diffraction and elemental analysis. Short accounts of some of these characterisation techniques are described in this section.

1.10.1 IR spectroscopy [52,53]

It is widely recognised that transition metal complexes involving M–X bonds (where X = halide) have stretching bands typically lying in the region 400 – 200 cm^{-1} in IR spectroscopy. Therefore in order to access the region, nujol mulls of complexes incorporating such metal halide bonds are made and supported on caesium iodide plates, which are transparent across the range 4000 – 180 cm^{-1} (as described in appendix 1). Transition metal complexes incorporating terminal M–CO bonds, commonly have stretching bands in the region 2200 – 1800 cm^{-1} in IR spectroscopy, and subsequently all such complexes in this Thesis were monitored by solution (CH_2Cl_2 where appropriate) IR spectroscopy to follow the formation of the complexes. Nujol mulls as described above were also carried out on the isolated solids. The group theory for both types of compounds is described in more depth in the relevant chapters. In order to predict the number of IR active bands expected for the complexes the reduction formula is applied to the reducible representation of symmetry operations within the molecules. The reduction formula can be seen in Fig 1.10.1.

Fig 1.10.1: Group theory reduction formula.

$$n_i = \frac{1}{h} \Sigma\, g_i\, \chi_I\, \chi_r$$

h = number of operations in the group

g_i = number of symmetry operations in the class

χ_I = character of irreducible representations

χ_r = character of reducible representations

1.10.2 Mass spectrometry[53]

The study of antimony containing species by mass spectrometry is aided by the two isotopes differing by 2 a.m.u., ^{121}Sb and ^{123}Sb with relative abundances of 57.3% and 42.7% respectively. These isotopes produce very characteristic isotope patterns in the mass spectra and therefore prove the number of antimony atoms present in the compounds. However, the relatively weak Sb–C bond can often result in significant fragmentation of the compounds. This fragmentation problem has been reduced by the introduction of methods such as positive ion electrospray, APCI and FAB. In this Thesis EI, ES^+, ES^- and APCI mass spectrometry have been used to characterise many of the complexes, and indeed ES^+ MS has been used extensively. Fig 1.10.2 shows the characteristic isotope patterns for antimony containing species.

Fig 1.10.2: Simulated isotope patterns for a) 1 Sb atom, b) 2 Sb atoms, c) 3 Sb atoms and d) 4 Sb atoms.

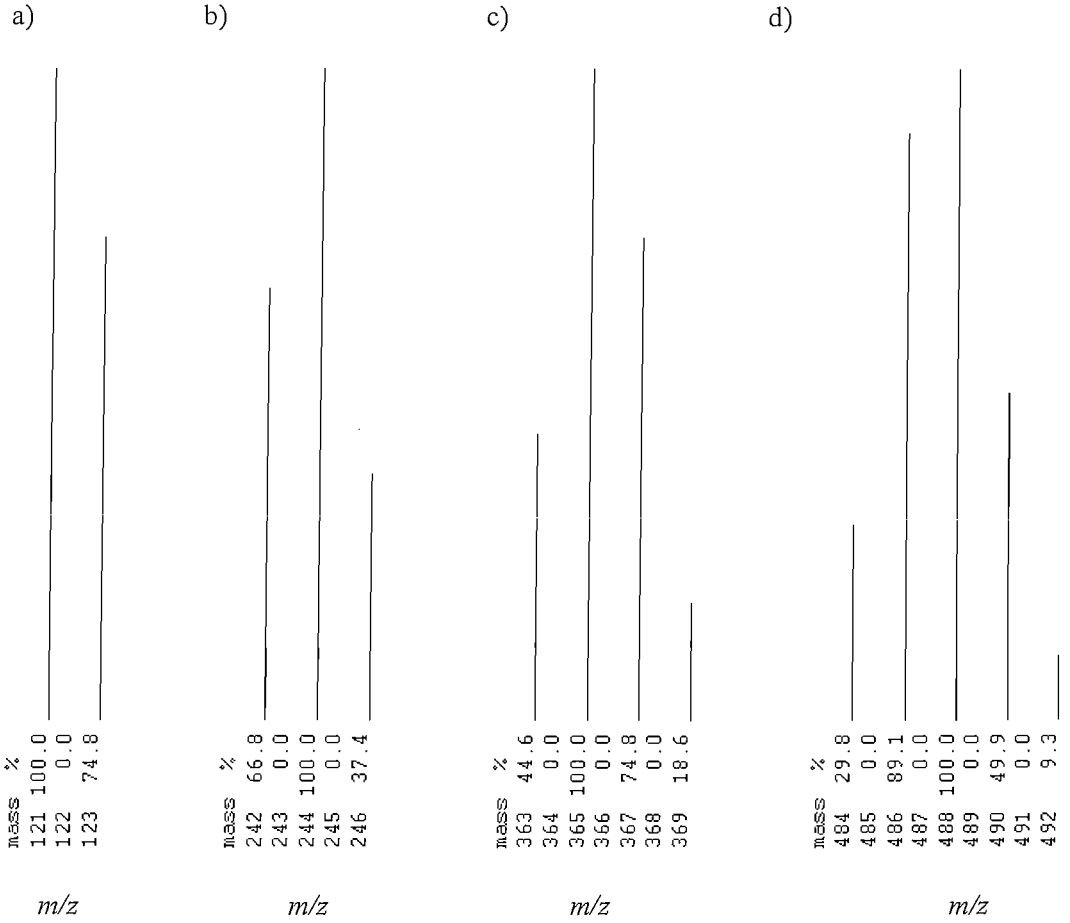

1.10.3 ^{195}Pt NMR spectroscopy

The only NMR active isotope of platinum is ^{195}Pt, with 33.8% abundance and I = ½. The receptivity with respect to ^{13}C is 19.9.[54] The widely used reference for ^{195}Pt NMR spectroscopy is aqueous 1 mol dm^{-3} $[PtCl_6]^{2-}$ in D_2O, with δ equal to zero. When undertaking a ^{195}Pt NMR spectroscopy experiment it is vital to make an educated assessment of where the resonance will occur as the chemical shift range is much larger than the spectroscopic window. Examples of the large chemical shift range can be seen from Pt(II)P_4 species that have δ(^{195}Pt) *ca.* -5500 ppm while other species such as $[PtF_6]^{2-}$ has a δ(^{195}Pt) *ca.* 12000 ppm.[22] The rapid relaxation rates for ^{195}Pt in fairly asymmetric environments allows for fast pulsing rates. This in turn enables fairly short acquisition times to be employed. The oxidation state and the donor set around the Pt centre can

change the chemical shift (δ) and coupling constant (*J*) significantly, along with the geometry around the ^{195}Pt centre.[54] For example the complexes *trans*-$[PtCl_2(PEt_3)_2]$[55] and *trans*-$[PtCl_4(PEt_3)_2]$[56] have platinum shifts of +595 Hz and +2925 Hz respectively. The ^{195}Pt chemical shift can also change by varying the substituent groups around the platinum centre. For example complexes of the type *trans*-$[PtCl_2(L)_2]$ have platinum shifts of +583 Hz (L = PMe_3), +753 Hz (L = $AsMe_3$) and -79 Hz (L = $SbMe_3$).[55]

1.10.4 $^{31}P\{^1H\}$ NMR spectroscopy [54]

^{31}P is 100% abundant and has spin I = ½ and a relative receptivity to ^{1}H of 6.6 x 10^{-2}. This enables the nucleus to be very useful, as studies of complexes incorporating M–P bonds, organophosphorus chemistry and reaction chemistry can be probed in great detail. In a ^{31}P NMR spectroscopy experiment, chemical shifts are referenced to an external 85% aqueous solution of H_3PO_4 set to zero. Chemical shifts of phosphines are very much dependent on the nature of the substituents around the P nucleus. For example, electron poor substituents result in a high frequency shift being observed, and in the case of electron rich substituents, the observed chemical shifts are to lower frequency. In metal complexes incorporating phosphines where a M–P bond is observed, the M–P σ bond involves the transfer of electron density from the phophine to the metal centre in most cases, which in turn causes the deshielding of the ^{31}P nucleus. This results in a shift to higher frequency of the uncoordinated phosphine. The size of this shift is found to be dependent on the metal centre involved and also the size of the chelate ring formed (when studying multidentate phosphines). Such studies have been carried out by Garrou, and some of the findings can be seen in Table 1.10.1.[57,58,59]

Table 1.10.4: The effect of chelate size on the $^{31}P\{^1H\}$ NMR chemical shift.[55]

Complex	$\delta(^{31}P\{^1H\})$ ppm	Chelate size	Ref
$[Me_2Pt(Ph_2PCH_2PPh_2)]$	-40.4	4	58
$[Me_2Pt(Ph_2P(CH_2)_2PPh_2)]$	+45.4	5	58
$[Me_2Pt(Ph_2P(CH_2)_3PPh_2)]$	+3.2	6	58
$[Me_2Pt(Ph_2P(CH_2)_4PPh_2)]$	+18.8	7	59
$[Me_2Pt(Ph_2PMe)_2]$	+6.4		55

1.11 Aims of the Research

This Thesis investigates the synthesis, coordination chemistry and organometallic chemistry of a novel distibine ligand, and other known distibine ligands to selected transition metal centres. The research aims to probe the coordination modes, spectroscopic properties and donor properties of the ligands, compared with related phosphines. The aims are summarised below:

- To develop novel distibine ligands in sufficiently high yields to carry out detailed studies of their coordination chemistry. Through the coordination of these novel distibines to transition metals, the aim of this work is to probe the coordinating ability of the ligand and gain a further understanding of the electronic properties of stibines.

- To investigate the coordination chemistry and organometallic chemistry of a range of distibine ligands, and the subsequent reaction chemistry of the complexes formed. In doing so, the coordination modes, spectroscopic properties and donor properties can be compared to other Group 15 ligands.

- The traditional view of stibine ligands, is that they support low to medium oxidation state transition metal centres. Therefore, we aim to explore the boundaries of this view, by synthesising a series of alkyl-Pt(IV) stibine complexes. In addition to this, an analogous series of alkyl-Pt(II) stibine complexes is also reported to give a comparison to the Pt(IV) species.

- Due to the elegant work by Werner and co-workers on bridging ER_3 (E = Sb, P, As) ligands[22] the organometallic chemistry of Rh(I) and Ir(I) stibine complexes is of great interest. This Thesis also aims to probe the ligating properties of the stibines when incorporated in Rh and Ir complexes involving cod and CO as co-ligands.

- Sterically demanding wide-angle diphosphine ligands have been of great interest, particularly when incorporated in transition metal complexes, as many exhibit remarkably high catalytic activities. This research aims to extend the work of Venanzi and co-workers[60,61,62] on the coordination chemistry of o-$C_6H_4(CH_2PPh_2)_2$ and push the boundaries of the chemistry in order to obtain a greater understanding of the coordination properties of the ligand.

1. 2 References

[1] C.A McAuliffe, in G. Wilkinson, J. A. McCleverty, R. D. Gillard (Eds.), Comprehensive Coordination Chemistry, 2, Pergamon Press, Oxford, 1987, 989.

[2] W. Levason, C. A. McAuliffe, *Coord. Chem. Rev.*, **19**, 1976, 173. G. Reid, W. Levason, *Coord. Chem. Rev.*, **250**, 2006, 2565.

[3] N. C. Norman, N. L. Pickett, *Coord. Chem. Rev.*, **145**, 1995, 27.

[4] J. Chatt, A. A. Williams, *J. Chem. Soc.*, 1951, 3061.

[5] A. G. Orpen, N. G. Connelly, *J. Chem. Soc. Chem. Commun.*, 1995, 1310.

[6] A. G. Orpen, N. G. Connelly, *Organometallics,* **9**, 1990, 1206.

[7] S-X. Xiao, W. C. Trogler, D. E. Ellis, Z. Berkovich-Yellin, *J. Am. Chem. Soc.,* 1983, **105,** 7033.

[8] D. S. Marynick, *J. Am. Chem. Soc.,* 1984, **106,** 4064.

[9] M. J. Freeman, A. G. Orpen, N. G. Connelly, I. Manners, S. J. Raven, *J. Chem. Soc., Dalton Trans.*, 1985, 2283.

[10] R. L. Harlow, R. J. McKinney, J. F. Whitney, *Organometallics,* 1983, **2**, 1839.

[11] R. L. Harlow, R. J. McKinney, S. D. Ittel, *J. Am. Chem. Soc.,* 1979, **101**, 7496; S. D. Ittel, R. L. Harlow, R. K. Brown, J. M. Williams, A. J. Schultz, G. D. Stucky, *ibid.,* 1980, **102**, 981.

[12] L. Aslanor, R. Mason, A. G. Wheeler, P. O. Whimp, *Chem. Commun.,* 1970, 30.

[13] B. J.Dunne, R. B. Morris, A. G. Orpen, *J. Chem. Soc., Dalton Trans.,* 1991, 653.

[14] A. M. Hill, N. J. Holmes, A. R. J. Genge, W. Levason, M. Webster, *J. Chem. Soc., Dalton Trans.*, 1998, 825.

[15] N. J. Holmes, W. Levason, M. Webster, *J. Chem. Soc., Dalton Trans.*, 1998, 3457.

[16] C. A. Tolman, *J. Am. Chem. Soc.,* 1970, **92**, 2953.

[17] G. M. Bodner, M. P. May, L. E. McKiney, *Inorg. Chem.,* 1980, **19**, 1951.

[18] W. Levason, M. L. Matthews, G. Reid, M. Webster, *Dalton Trans.*, 2004, 51.

[19] C. A. Tolman, *Chem. Rev.,* 1977, **77**, 313

[20] C. A. McAuliffe, "Phosphorus, Arsenic, Antimony and Bismuth Ligands", Chapter 14, Vol. 2, "Comprehensive Coordination Chemistry 1", G. Wilkinson, R. D. Gillard and J. A. McCleverty, Pergamon, (1987).

[21] H. Werner, P. Schwab, A. Heinemann, P. Steinert, *J. Organomet. Chem.,* 1995, **496**, 207.

[22] H. Werner, *Angew. Chem. Int. Ed.,* 2004, **43**, 938.

[23] K. Issleib, G. Doll, *Chem. Ber.,* 1963, **96**, 1544.

[24] L. Horner, P. Beck , V. G. Toscano, *Chem. Ber.,* 1961, **94**, 2122.

[25] W. Levason, K. G. Smith, C. A. McAuliffe, F. P. McCullough, R. D. Sedgwick, S. G. Murray, *J. Chem. Soc., Dalton. Trans.*, 1979, 1718.

[26] C. A. McAuliffe, W. Levason, "Studies in Inorganic Chemistry, Vol 1: Phosphine, Arsine and Stibine Complexes of the Transition Elements", Elsevier, Amsterdam, (1978).

[27] N. R. Champness, W. Levason, *Coord. Chem. Rev.*,1994, **133**, 115.

[28] M. Nunn, D. B. Sowerby, D. M. Wesolek, *J. Organomet. Chem.*, 1983, **251**, C45.

[29] S. P. Bone, D. B. Sowerby, *J. Chem. Soc., Dalton. Trans.*, 1979, 715.

[30] K. D. Crosbie, G. M. Sheldrick, *J. Inorg. Nucl. Chem.*, 1969, **31**, 3684.

[31] C. E. Wymore, J. C. Bailar, *J. Inorg. Nucl. Chem.*, 1960, **14**, 42.

[32] A. M. Aguiar, D. Daigle, *J. Am. Chem. Soc.*, 1964, **86**, 2299.

[33] H. Zorn, H. Schindlbauer, H. Hagen, *Monatsch.*, 1964, **95**, 422.

[34] H. Schindlbauer, *Monatsch.*, 1965, **96**, 2051.

[35] H. C. E. McFarlane, W. McFarlane, *Polyhedron*, 1983, **2**, 303.

[36] E. P. Kyba, S. T. Liu, R. L. Harris, *Organometallics*, 1983, **2**, 1877.

[37] K. Issleib, B. Hamann, *Z. Anorg. Allgem. Chem.*, 1966, **343**, 196.

[38] K. Issleib, B. Hamann, *Z. Anorg. Allgem. Chem.*, 1964, **332**, 179.

[39] W. Levason, C. A. McAuliffe, S. G. Murray, *J. Organomet. Chem.*, 1975, **88**, 171.

[40] E. Shewchuk, S. B. Wild, *J. Organomet. Chem.*, 1977, **128**, 115.

[41] J. Ellermann, A. Veit, *J. Organomet. Chem.*, 1985, **290**, 307.

[42] F. A. Cotton, G. Wilkinson, "Introduction to Ligands and Complexes", Chapter 2, "Advanced Inorganic Chemistry 5th Edition", Wiley Interscience, New York, (1987).

[43] G. K. Anderson, *Adv. Organomet. Chem.*, 1993, **35**, 1.

[44] A. M. Hill, W. Levason, M. Webster, I. Albers, *Organometallics*, 1997, **16**, 5641.

[45] M. Wieber, N. Graf, *Z. Anorg. Allgem. Chem.*,1993, **619**, 1991.

[46] H. J. Breunig, M. Jonsson, R. Rosler, E. Lork, *Z. Anorg. Allgem. Chem.*,1999, **625**, 2120.

[47] N. Graf, M. Wieber, *Z. Anorg. Allgem. Chem.*,1993, **619**, 2061.

[48] T. Even, A. R. J. Genge, A. M. Hill, N. J. Holmes, W. Levason, M.Webster, *J. Chem. Soc. Dalton Trans.*,2000, 655.

[49] A. F. Chiffey, J. Evans, W. Levason, M. Webster, *Organometallics*, 1995, **14**, 1522.

[50] A. Babai, G. B. Deacon, G. Meyer, *Z. Anorg. Allgem. Chem.*, 2004, **630**, 399.

[51] A. F. Chiffey, J. Evans, W. Levason, M. Webster, *Polyhedron*, 1996, **15**, 591.

[52] A. Vincent, "Molecular Symmetry and Group Theory", John Wiley& Sons, New York, 1977.

[53] D. H. Williams, I. Fleming, "Spectroscopic Methods in Organic Chemistry", 4th Edition, 1989, McGraw-Hill.

[54] R. J. Goodfellow, in *Multinuclear NMR*, J. Mason (ed.), Plenum, New York, 1987, Ch. 20.

[55] P. L. Goggin, R. J. Goodfellow, S. R. Haddock, B. F. Taylor, I. R. H. Marshall, *J. Chem. Soc., Dalton Trans.*, 1976, 459.

[56] D. W. W. Anderson, E. A. V. Ebsworth, D. W. H. Rankin, *J. Chem. Soc., Dalton Trans.*, 1973, 2370.

[57] P. E. Garrou, *Chem. Rev.*, 1981, 229.

[58] T. G. Appleton, M. A. Bennett, I. B. Tomkins, *J. Chem. Soc., Daton Trans.*, 1976, 439.

[59] S. Hietkamp, D. J. Stuffken, K. Vrieze, *J. Organomet.Chem.*, 1979, **169**, 107.

[60] F. Caruso, M. Camalli, H. Rimml, L. M. Venanzi, *Inorg. Chem.*, 1995, **34**, 673.

[61] H. Rimml, L. M. Venanzi, *Phosphorus Sulfur.*, 1987, **30**, 297.

[62] M. Camalli, F. Caruso, S. Chaloupka, E. M. Leber, H. Rimml, L. M. Venanzi, *Helv. Chim. Acta.*, 1990, **73**, 2263.

Chapter 2

Synthesis, Spectroscopic and Structural Properties of a Novel Distibine ligand and its coordination to selected transition metals

2.1 Introduction

In the last ten years there has been an increase in the research carried out into the applications of stibine ligands. Indeed work by Werner and co-workers has demonstrated that the donor properties of stibines are subtly different from that of their phosphine and arsine analogues in organometallics. By promoting different product distributions and by providing unprecedented examples of bridging SbR_3 ligands,[1,2] such as Sb^iPr_3 bridging two rhodium metal centres, Werner has proved that there is a wide area of antimony chemistry still to be probed. This research is discussed in more detail in Chapter 4.

Interest is further increased by the fact that stibine compounds have an increased tendency for higher coordination numbers and once complexed less tendency for M-SbR_3 dissociation.[3,4] Despite the above observations there are few examples of polystibines incorporating back-bones other than flexible polymethylene units. One of the reasons for this is the fragility of the C-Sb bond which can lead to decomposition of the compound during formation and on reaction of the organostibine with metal reagents.

However, recently work has been carried out to synthesise ligands such as *o*-$C_6H_4(CH_2SbMe_2)_2$[5,6] using electrophilic reactions of R_2SbCl (R = Me or Ph) with nucleophilic di-Grignard compounds. Fig 2.1.1 shows the synthesis of *o*-$C_6H_4(CH_2SbMe_2)_2$ *via* two routes. The contrast in yields using the two routes is striking. The route that reacts $NaSbMe_2$ with *o*-$C_6H_4(CH_2Br)_2$ in liquid ammonia has an extremely low yield which is in accord with reports that antimony nucleophiles have a tendency to break existing Sb–C bonds as well as C–X bonds.[3,4,7,8] The route using electrophilic reactions of R_2SbCl (R = Me or Ph) with nucleophilic di-Grignard compounds, seems to minimise C–Sb bond fission and gives much higher yields than using nucleophilic antimony reagents. Due to this optimised route, a new series of distibine ligands incorporating phenylene and xylylene linkages has been synthesised and their coordination to selected transition metal centres has been probed. Fig 2.1.2 shows reaction schemes of the synthesis of this series of distibine ligands.[5]

Fig 2.1.1: Synthesis of *o*-$C_6H_4(CH_2SbMe_2)_2$.[5]

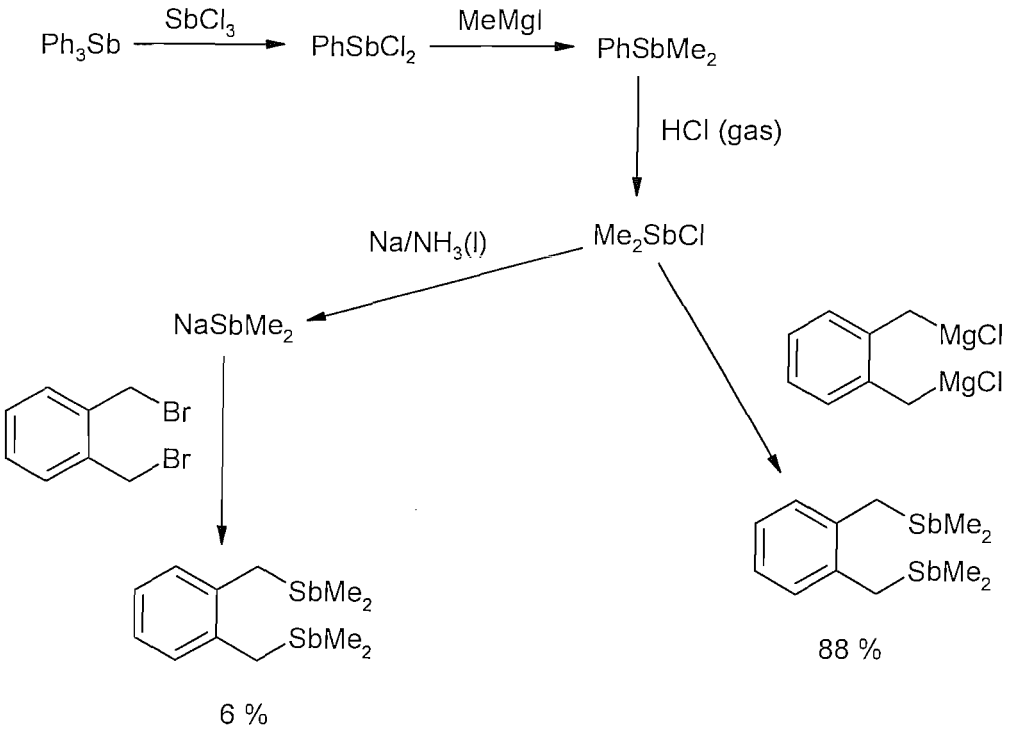

Fig 2.1.2: Scheme for the synthesis of *o*-, *m*- and *p*-$C_6H_4(CH_2SbMe_2)_2$, *o*-$C_6H_4(CH_2SbPh_2)_2$, *m*- and *p*-$C_6H_4(SbMe_2)_2$.[5]

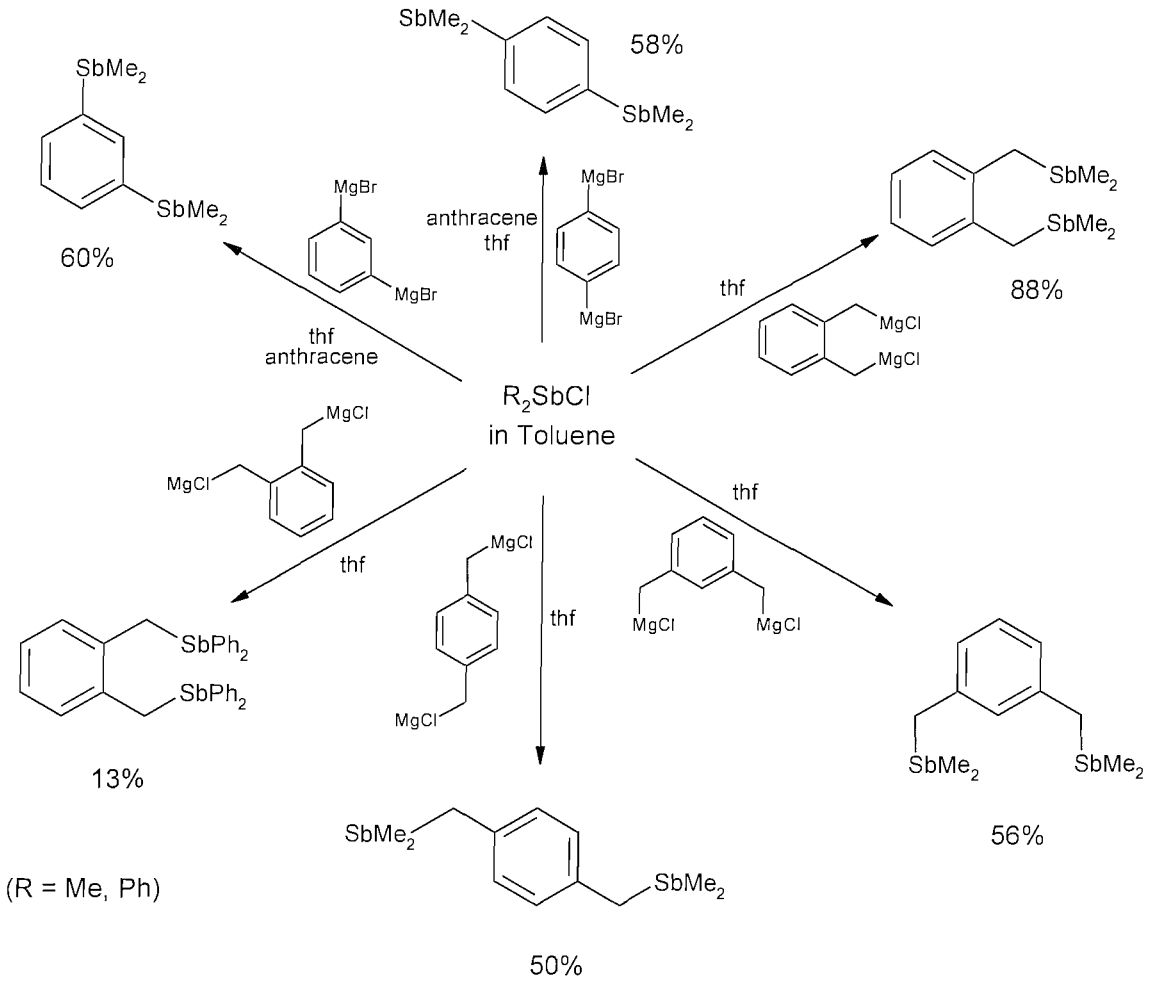

2.1.1 Recent Coordination chemistry of *o*-$C_6H_4(CH_2SbMe_2)_2$ and related ligands.

The versatile xylyl ligand, *o*-$C_6H_4(CH_2SbMe_2)_2$ can be reacted with one molar equivalent of $PdCl_2$ or $PtCl_2$ to produce complexes of the form $[MCl_2(o\text{-}C_6H_4(CH_2SbMe_2)_2)]$ (M = Pt, Pd) which exhibit a square planar geometry.[6] However, when MCl_2 is reacted with 2 molar equivalents of ligand in the presence of $TlPF_6$, complexes of the type $[M\{o\text{-}C_6H_4(CH_2SbMe_2)_2\}_2][PF_6]_2$ (M = Pt, Pd) can be formed. All these complexes have been fully characterised and in the case of $[M\{o\text{-}C_6H_4(CH_2SbMe_2)_2\}_2][PF_6]_2$, X-ray studies have been carried out. Fig 2.1.3 shows the crystal structure of $[Pt\{o\text{-}C_6H_4(CH_2SbMe_2)_2\}_2]^{+}$.[6]

Fig 2.1.3: Crystal structure of $[Pt\{o\text{-}C_6H_4(CH_2SbMe_2)_2\}_2]^+$.[6]

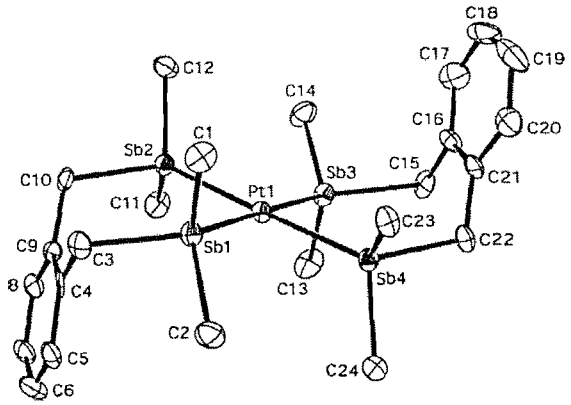

Platinum(IV) halide complexes of distibines have been described in the literature, but decompose very quickly in solution with halogenation of the stibine.[3] However, a series of alkyl-Pt(IV) distibine complexes are reported and discussed in detail in Chapter 3.

The reaction of $NiX_2.6H_2O$ and $Ni(ClO_4)_2.6H_2O$ (X = Br, I) with $o\text{-}C_6H_4(CH_2SbMe_2)_2$ in ^{n}BuOH resulted in the synthesis of a deep blue powder ($[NiBr\{o\text{-}C_6H_4(CH_2SbMe_2)_2\}_2]ClO_4$) and dark green powder ($[NiI\{o\text{-}C_6H_4(CH_2SbMe_2)_2\}_2]ClO_4$).[6] The UV-vis spectra showed that the complexes formed contained a low-spin trigonal pyramidal Ni(II) metal centre, and this was also confirmed by the X-ray structure of $[NiI\{o\text{-}C_6H_4(CH_2SbMe_2)_2\}_2]ClO_4$. Fig 2.1.4 shows the crystal structure of $([NiI\{o\text{-}C_6H_4(CH_2SbMe_2)_2\}_2]^+$.

Fig 2.1.4: Crystal structure of the cation $[NiI\{o\text{-}C_6H_4(CH_2SbMe_2)_2\}_2]^+$.[6]

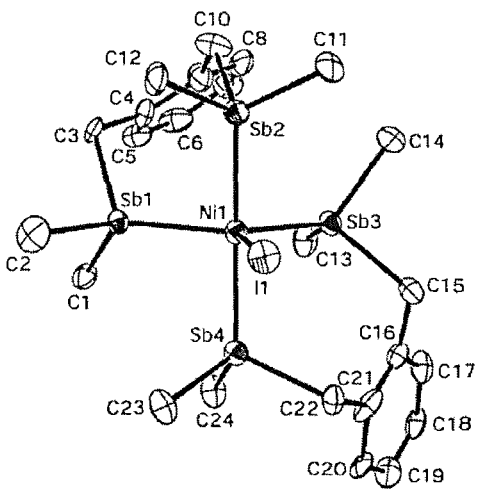

The reaction of $[Cu(MeCN)_4]BF_4$ and two equivalents of distibine in chlorocarbons, results in the formation of pseudo-tetrahedral copper(I) complexes of the form $[Cu(distibine)_2]BF_4$ (distibine = *o*-$C_6H_4(CH_2SbMe_2)_2$, *o*-$C_6H_4(SbMe_2)_2$ and $R_2Sb(CH_2)_3SbR_2$; R = Me, Ph).[6,9,10] The air stable colourless solids were analysed by ^{63}Cu NMR spectroscopy, and sharp peaks were seen in the spectra consistent with near cubic symmetry. This was further supported by the X-ray structure of $[Cu(o\text{-}C_6H_4(CH_2SbMe_2)_2)_2]BF_4$.[6] The synthetic route employed to form Ag(I) complexes incorporating distibine ligands can be seen in Fig 2.1.5. The colourless solids have been seen to exhibit varying degrees of light sensitivity.[6,10] The reaction of [AuCl(tht)] with 0.5 molar equivalents of *o*-$C_6H_4(CH_2SbMe_2)_2$ gives a yellow solid found to be $[(AuCl)_2\{o\text{-}C_6H_4(CH_2SbMe_2)_2\}]$. However, this is very unstable and decomposes even in the freezer over a couple of hours.[6]

Fig 2.1.5: Scheme showing the synthesis of $[Ag(distibine)_2]Y$ (distibine = *o*-$C_6H_4(CH_2SbMe_2)_2$, $R_2Sb(CH_2)_3SbR_2$; R = Me, Ph; Y = BF_4, CF_3SO_3).[6,10]

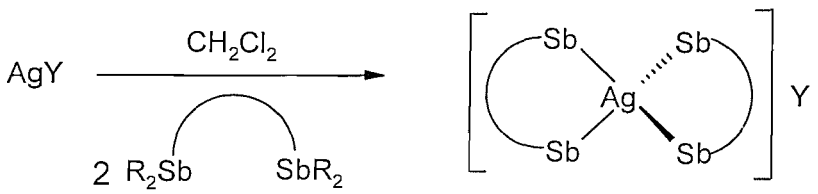

This Chapter concentrates on the in depth investigation into the synthesis of the above mentioned *o*-$C_6H_4(CH_2SbMe_2)_2$ ligand, the identity of a new coupled distibine, which has been identified as a by-product during the synthesis of *o*-$C_6H_4(CH_2SbMe_2)_2$ and it's direct synthesis. This Chapter also describes the attempted preparation of another novel distibine ligand, *o*-$C_6H_4(CH_2Sb^iPr_2)_2$, *via* a similar route to the synthesis of *o*-$C_6H_4(CH_2SbMe_2)_2$, incorporating ^{i}Pr substituents that are present in the bridging stibine complexes discovered by Werner.[1,2]

2.2 Results and Discussion

From research undertaken in the group previously on *o*-$C_6H_4(CH_2SbMe_2)_2$, it has been found that this compound may be obtained in very high yield (88%), without the need to distill. However, subsequent work undertaken as part of this Thesis has shown that sometimes the yield is much lower and its preparation is accompanied by formation of other Sb-containing compounds, including a substantial quantity of Me_4Sb_2, consistent with a deficit of *o*-$C_6H_4(CH_2MgCl)_2$. In an effort to probe the identity of the by-products further, we have investigated the less volatile species present after fractional distillation of *o*-$C_6H_4(CH_2SbMe_2)_2$ *in vacuo* from the reaction mixture. At high temperature (225°C, 0.5 mmHg), we obtained a colourless, viscous oil. The ^1H NMR spectrum of this shows singlets at 0.73 (Me), 2.88 ($SbCH_2$), 3.10 ($ArCH_2CH_2$) and a mulitplet at 7.0-7.6 (Ar-H) ppm. The notable difference to this fraction and the ^1H NMR spectrum of the desired ligand, is the presence of the singlet at 3.1 ppm that is assigned as an additional CH_2. The aromatic protons and SbMe protons integrated as 2:3 (rather than the 1:3 ratio expected for *o*-$C_6H_4(CH_2SbMe_2)_2$). The $^{13}C\{^1H\}$ NMR spectrum also showed similarities with the xylyl ligand with peaks at -2.3 SbMe, 20.9 $SbCH_2$ and peaks corresponding to *o*-C_6H_4. However, again the presence of a benzyl CH_2 at 35.0 ppm suggested a rearrangement of the ligand during the synthetic process. The EIMS of this fraction showed no evidence for *o*-$C_6H_4(CH_2SbMe_2)_2$ (which has been shown previously to appear as [P-Me], *m/z* = 393),[5] but rather the major fragment observed was centred at *m/z* = 497, consistent with loss of Me from the coupled compound $\{CH_2(o\text{-}C_6H_4CH_2SbMe_2)\}_2$, (**VI**). A minor mass peak at *m/z* = 512 was also evident and corresponded to $[\{CH_2(o\text{-}C_6H_4CH_2SbMe_2)\}_2]^+$ The simulated isotope patterns are fully consistent with these assignments and high resolution mass spectrometry confirms the formulation. Fig 2.2.1 shows the coupled compound (**VI**).

Fig 2.2.1: The coupled compound $\{CH_2(o\text{-}C_6H_4CH_2SbMe_2)\}_2$ (**VI**).

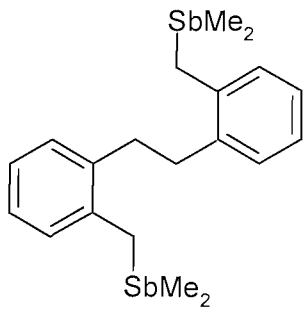

Noltes and co-workers have shown previously that the compounds $Me_2Sb(CH_2)_nSbMe_2$ (n = 3-6) undergo redistribution reactions at temperatures in excess of 200°C to eliminate Me_3Sb and give either polymeric species (n = 3, 6) or 1-methylstibacycloalkane (n = 4, 5).[11] However, no evidence of the formation of **VI** was observed when a sample of o-$C_6H_4(CH_2SbMe_2)_2$ was heated on the MS probe. Furthermore, no change was observed in the ^1H NMR spectrum of a pure sample of o-$C_6H_4(CH_2SbMe_2)_2$ after heating to 250°C for 1 h under static vacuum. These results suggest that **VI** does not form *via* thermolysis in the fractional distillation.

On this basis it is believed that the formation of **VI** occurs through partial coupling of the o-$C_6H_4(CH_2MgCl)_2$ di-Grignard in concentrated thf solution. The sensitivity of this di-Grignard to concentration has been noted by Lappert and co-workers, and the di-Grignard been shown to undergo C-C coupling above a critical concentration of 0.075 M, also producing bibenzyl species.[12,13]

Fig 2.2.2: Magnesium cylic system with xylyl backbone discovered by Lappert while investigating the coupling reactions of concentrated di-Grignards.

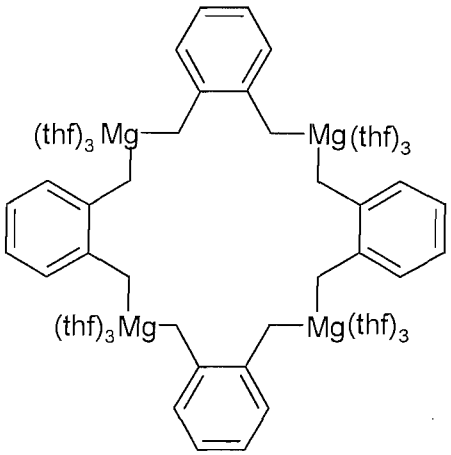

In order to prove that the coupling reaction occurred in the di-Grignard stage, $\{CH_2(o\text{-}C_6H_4CH_2D)\}_2$ was prepared.[12] o-$C_6H_4(CH_2Cl)_2$ was used as a starting material and the reaction was carried out with the critical concentration of 0.075 M of di-Grignard in mind. However, when o-C_6H_4-$(CH_2MgCl)_2$ was formed the volume of thf was reduced to ~15 cm^3 and the reaction was left to stir overnight. This was to see if the Grignard would couple when in a very high concentration. Indeed

after adding D_2O and an aqueous work-up, and isolation of the fawn oil, the ^1H NMR spectrum showed resonances for the bibenzyl CH_2CH_2 of the coupled ligand back-bone at 2.95 (s) [4H] and a broad singlet at 2.20 [4H] corresponding to CH_2D. As this experiment used o-$C_6H_4(CH_2Cl)_2$ as a starting material there was also evidence in the NMR spectrum of the CH_2D of o-$C_6H_4(CH_2D)_2$ at 2.1 ppm. This result proves beyond doubt that the coupling reaction took place in the Grignard stage of the synthesis.

Fig 2.2.3: Reaction scheme of the formation of the new coupled ligand (**VI**) as a by-product.

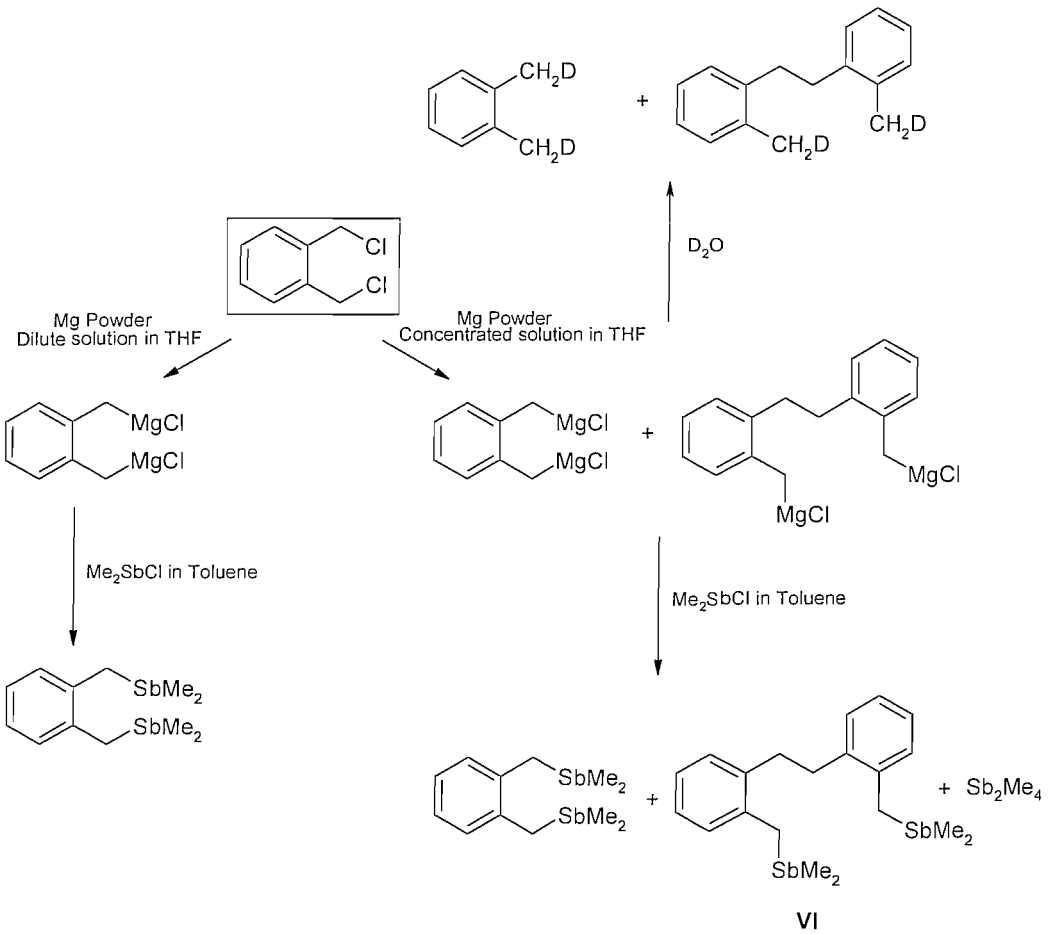

VI

2.2.1 Direct synthesis of VI

The new distibine **VI** was prepared directly from $\{CH_2(o\text{-}C_6H_4CH_2Cl)\}_2$ (Fig 2.2.4), itself obtained by slight modifications of the literature procedure.[14] Specifically, the conversion of the dialdehyde $\{CH_2(o\text{-}C_6H_4CHO)\}_2$ to the diol $\{CH_2(o\text{-}C_6H_4CH_2OH)\}_2$ was achieved in >90% yield using $LiAlH_4$

in Et_2O, and the conversion of $\{CH_2(o\text{-}C_6H_4CH_2OH)\}_2$ to $\{CH_2(o\text{-}C_6H_4CH_2Cl)\}_2$ using $SOCl_2$ required much longer (17 h) reflux to achieve complete conversion.

Fig 2.2.4: Synthesis of $\{CH_2(o\text{-}C_6H_4CH_2SbMe_2)\}_2$ **(VI)**

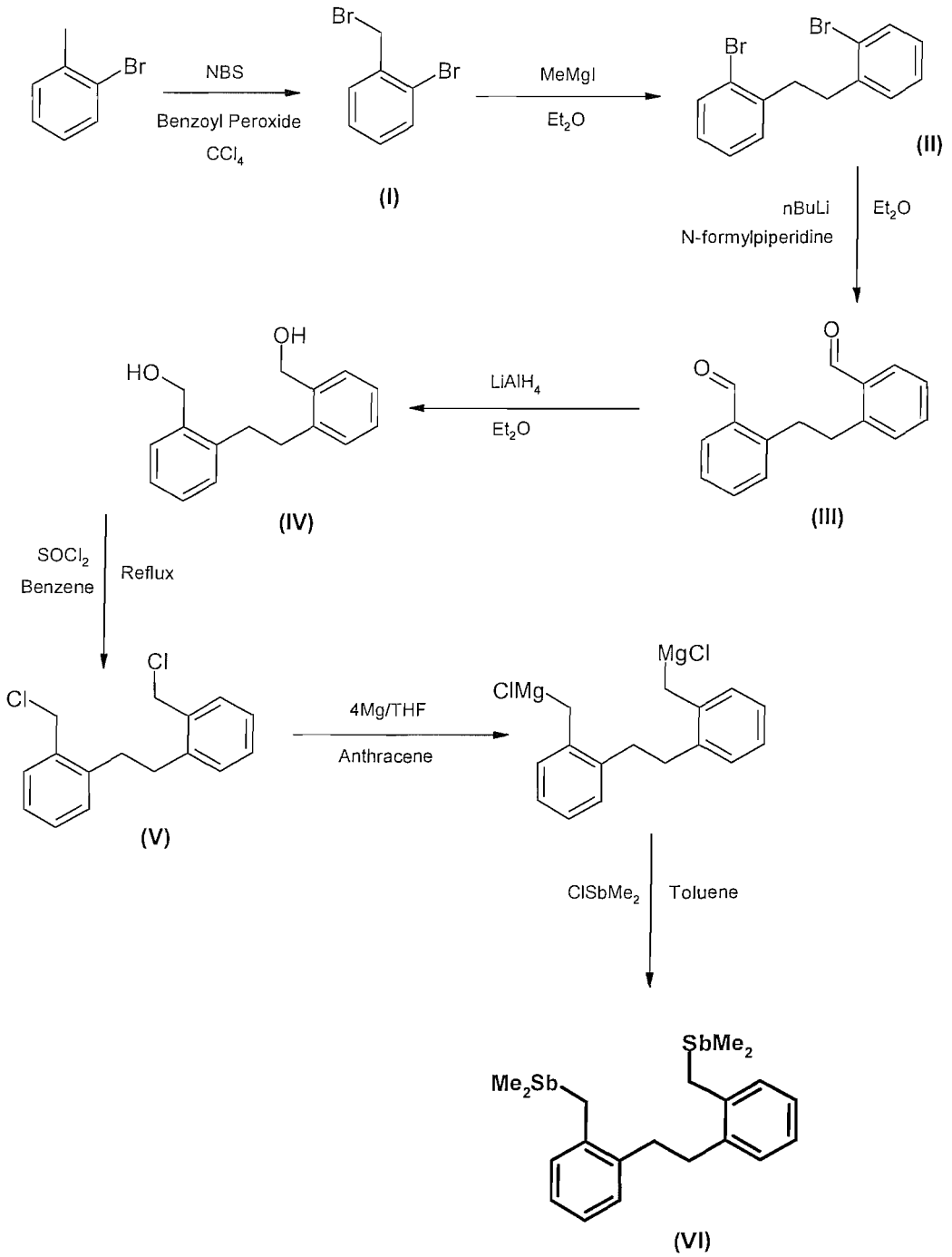

(I) was prepared from 2-bromotoluene and one equivalent of N-bromosuccinimide in CCl_4 in the presence of benzoyl peroxide. The resultant yellow oil was obtained in good yield and was found to be pure by ^1H and $^{13}C\{^1H\}$ NMR spectroscopy and EIMS. The ^1H NMR spectrum showed peaks at 7.65 – 7.10 (m) [4H] corresponding to the aromatic protons, and one singlet at 4.62 [2H] corresponding to the CH_2Br. The EIMS also confirmed that the oil was the desired compound with a peak at 250 corresponding to the parent ion.

(II) was prepared from a refluxing solution of MeMgI by slow addition of o-$C_6H_4(CH_2Br)(Br)$ in Et_2O. After an acid work-up the residues were recrystallised from CH_2Cl_2/MeOH. The resulting orange waxy solid was obtained in poor yield, due to excess of grignard being quenched at the work-up stage. This indicated that the coupling stage did not work properly. However the solid obtained was enough to carry on to the next stage, and was characterised by ^1H and $^{13}C\{^1H\}$ NMR spectroscopy and EIMS.

(III) was prepared from **(II)** and ^{n}BuLi in Et_2O at 0°C. N-formylpiperidine was then added to the lithium salt at 0 °C and the reaction was stirred at RT for 2 h. Following an aqueous work-up, drying over $MgSO_4$ then reducing to dryness, the residues were recrystallised from hexane. The white solid was obtained in moderate yield, and was characterised, by ^1H and $^{13}C\{^1H\}$ NMR spectroscopy and EIMS. Indeed the ^1H NMR spectrum showed an indicative singlet at 10.12 ppm corresponding to the proton of the aldehyde. The central CH_2CH_2 was shown as a singlet at 3.25 ppm. The $^{13}C\{^1H\}$ NMR spectrum also showed a peak indicative of the aldehyde at 191.60 ppm. The EIMS also proved the desired compound was formed by a mass peak at *m/z* 237 corresponding to $[\{CH_2(o\text{-}C_6H_4CHO)\}_2\text{-}H^+]^+$.

(IV) was prepared by reducing **(III)** with $LiAlH_4$ in Et_2O. After quenching with H_2O, dilute H_2SO_4 was added to precipitate a white solid, which was filtered off. The remaining Et_2O was also reduced to dryness and found to be the same as the filtered product and hence the products were combined. The white solid was obtained in good yield (91%). The ^1H NMR spectrum proved the desired product was formed with peaks at 7.3 – 7.0 (m) [8H] (Ar-H), 4.55 (s) [4H] (CH_2OH), 3.0 (s) [4H] (CH_2CH_2) ppm. The $^{13}C\{^1H\}$ NMR spectrum also corroborated this with peaks at 128.9, 128.1, 127.3, 125.5 (Ar-C), 62.5 (CH_2OH), 33.7 (CH_2CH_2) ppm. The absence of the aldehyde peaks in both NMR spectra also proved the reaction had worked. EIMS also showed the desired product was synthesised.

(V) was prepared by the reaction of **(IV)** with excess $SOCl_2$ in benzene with a few drops of pyridine. The reaction was refluxed for 17 h and following aqueous work-up an orange solid was obtained in good yield. Both ^1H and $^{13}C\{^1H\}$ NMR spectra suggested that the desired product was formed. The CH_2CH_2 resonances did not shift significantly from 3.0 ppm as seen in the ^1H NMR spectrum of **(IV)**, however the CH_2Cl resonance was found at 4.50 ppm, whereas the alcohol CH_2OH was at 4.55 ppm for **(IV)**. The $^{13}C\{^1H\}$ NMR CH_2Cl resonance was found at 43.2 ppm and the peak at 62.5 ppm corresponding to the CH_2OH had disappeared, which suggested that the alcohol had been converted to the chloride.

(VI) was prepared from $\{CH_2(o\text{-}C_6H_4CH_2MgCl)\}_2$, which was prepared from magnesium powder, anthracene and **(V)**, and $ClSbMe_2$ in thf and toluene, *via* the route described by Levason *et al.*[5] which was adapted from the di-Grignard preparation pioneered by Lappert and coworkers.[12,13] The waxy pale yellow solid was prepared in good yield, and was stored under an inert atmosphere and fully characterised by NMR spectroscopy and EIMS. The ^1H NMR spectrum agreed with the assignments that were made for the coupled ligand as the by-product, however the central CH_2CH_2 of the benzyl backbone and the CH_2Sb protons seem to be coincidental and appear as a singlet at 2.86 ppm. The $^{13}C\{^1H\}$ NMR spectrum also supports the conclusion that **(VI)** was successfully synthesised. Peaks at 33.29, 19.18 and -4.08 ppm correspond to CH_2CH_2, CH_2Sb and $SbMe_2$ respectively, which also prove that the assignment of the by-product fraction was also **(VI).** Furthermore, an EIMS was obtained from the waxy solid and fragments at *m/z* 497 and *m/z* 513 were observed which corresponded to $[P\text{-}Me]^+$ and $[P]^+$ respectively.

In order to fully characterise the ligand, the Sb(V) compound ($\{CH_2(o\text{-}C_6H_4CH_2SbBr_2Me_2)\}_2$) was prepared from **(VI)** and Br_2 in CH_2Cl_2. Hexane was used to precipitate a pale yellow solid in good yield. By ^1H and $^{13}C\{^1H\}$ NMR spectroscopy it can be seen that **(VII)** was the only product formed. The $SbCH_2$ (δ^1H: 4.24; $\delta^{13}C$: 46.33) and SbMe (δ^1H: 2.50; $\delta^{13}C$: 25.69) which are now bonded directly to the formally Sb(V) centres are significantly shifted to high frequency *cf* **VI.** Moreover the bibenzyl CH_2 groups are much less affected (δ^1H: 3.16; $\delta^{13}C$: 34.11).

Fig 2.2.5: ^{1}H NMR spectrum of **VII** ({CH_2(*o*-$C_6H_4CH_2SbBr_2Me_2$)}$_2$).

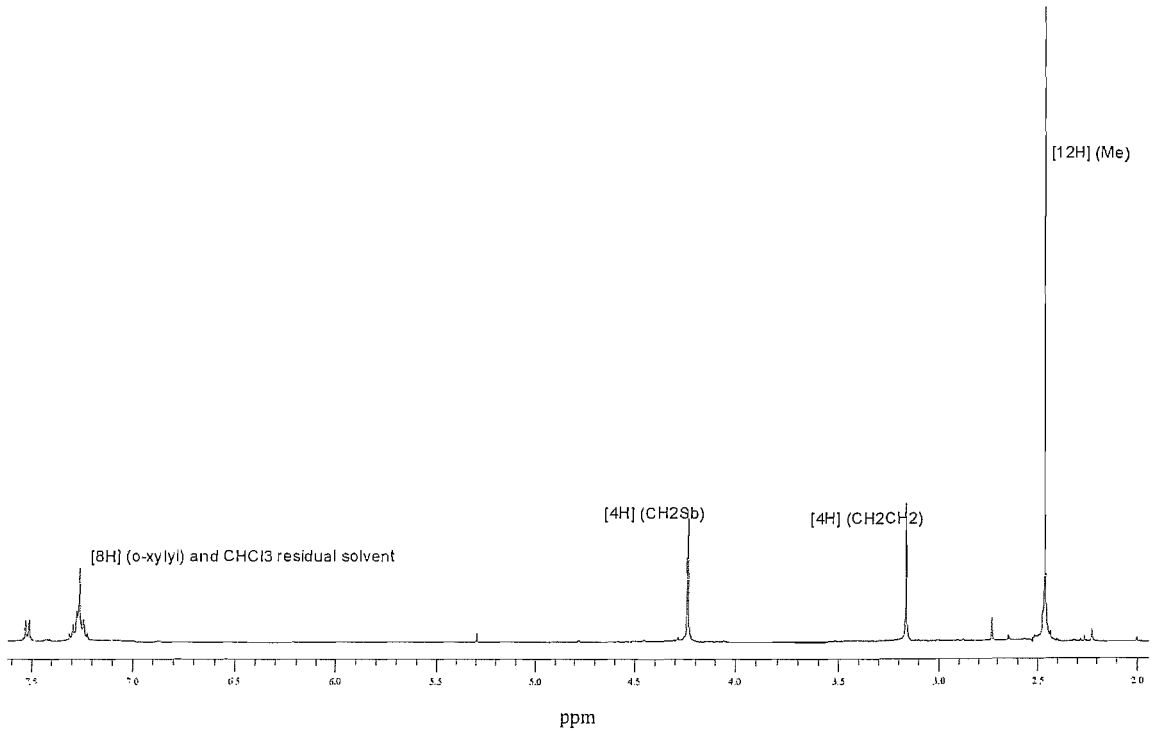

The synthesis of this novel distibine ligand is of interest in the field as the coordination of long chain diphosphine ligands of the form $R_2P(CH_2)_nPR_2$ (n = 6–16) to transition metals have been studied in detail and shown to give ligand bridged dimers, polymers and occasionally *trans* chelates. *Cis*-chelates are very rarely produced cleanly from such systems.[15] However, wide-angle *cis*-chelating phosphines are of considerable current interest owing to the very favourable catalytic properties displayed by their metal complexes, and this has led to major industrial usage.[16] The presence of the two *o*-xylyl substituted units in the backbone of the new distibine **VI** has led to speculation on whether **VI** has the potential to behave as a wide-angle chelate to metal centres.

2.2.2 Pt(II) and Pt(IV) complexes of VI

In order to explore the ligating properties of the novel ligand, the coordination chemistry of **VI** to selected transition metals was investigated. One mol. equiv. of [$PtMe_3I$] was reacted with **VI** in refluxing $CHCl_3$ solution under N_2. Following workup, the product [$PtMe_3I$(**VI**)] was isolated as a light yellow solid. Electrospray MS showed clusters of peaks with isotope patterns at *m/z* 706, 721 and 762 corresonding to [Pt(**VI**)]$^+$, [PtMe(**VI**)]$^+$ and [PtMe(**VI**)(MeCN)]$^+$ respectively. The ^{1}H and ^{13}C{^{1}H} NMR spectra also corroborated the formulation of [$PtMe_3I$(**VI**)] by the presence of three *fac*

Me ligands on Pt, one at very low frequency *trans* to I (δ^{13}C: -7.8) with a coupling constant of $^{1}J_{PtC}$ = 614 Hz and two *trans* to the Sb atoms shown by a peak at 6.2 ppm with a coupling constant of $^{1}J_{PtC}$ = 563 Hz. These data are in accord with other trimethyl-Pt(IV) stibine complexes.[14,17] Two singlet $^{13}C\{^{1}H\}$ resonances for the SbMe groups in the coordinated ligand **VI** were also evident, consistent with the absence of axial symmetry in the [$PtMe_3I$(**VI**)] complex. The ^{195}Pt NMR spectrum of the complex showed a single resonance at -4440 ppm, which is very similar to the platinum-195 NMR shifts for the Pt(IV) complexes reported in Chapter 3 of this Thesis.[17] These results suggest that **VI** behaves as a wide-angle *cis*-bidentate on Pt(IV), resulting in a very large 11-membered chelate ring. This complex along with the Pt(IV) complexes in Chapter 3 are the first reported examples of stable Pt(IV) stibine complexes. Literature examples of Pt(IV) stibine complexes are of the type [$PtCl_4$(distibine)], for example [$PtCl_4(Me_2Sb(CH_2)_3SbMe_2)$].[18] However, these complexes are extremely unstable and are formed *via* a chemical oxidation reaction, from the corresponding [$PtCl_2$(distibine)] with Cl_2.[18] In solution these complexes decompose instantaneously with chlorination of the stibine ligand.

A single crystal structure determination of [$PtMe_3I$(**VI**)] provided unambiguous confirmation of the identity of the coupled distibine compound. The structure (Fig. 2.2.6) shows **VI** occupying mutually *cis* coordination sites at a distorted octahedral Pt(IV) centre, with three facial Me ligands and the iodine completing the coordination environment. The Pt-Sb distances are 2.6279(4) and 2.6329(4) Å, substantially longer than in the Pt(II) distibines,[6] e.g. [$PtCl_2\{o\text{-}C_6H_4(CH_2SbMe_2)_2\}$] (2.4860(7), 2.4931(8) Å) and $[Pt\{o\text{-}C_6H_4(CH_2SbMe_2)_2\}_2]^{2+}$ (2.5690(8) – 2.5802(8) Å) – although of course the higher coordination number in the Pt(IV) species and the strong *trans* influence of the Me groups will both have a significant effect on d(Pt-Sb). We also note that the Sb2-Pt1-Sb1 angle in [$PtMe_3I$(**VI**)] is 95.957(12)°, whereas the corresponding Sb-Pt-Sb angle within the more common 6-membered chelate rings is < 90°.[17]

Fig 2.2.6: View of the structure of [$PtMe_3I$(**VI**)] with numbering scheme adopted. Note that there is disorder in the C21-Pt1-I1 region, the molecule shown is the major component. Ellipsoids are drawn at the 50% probability level and H atoms are omitted for clarity.

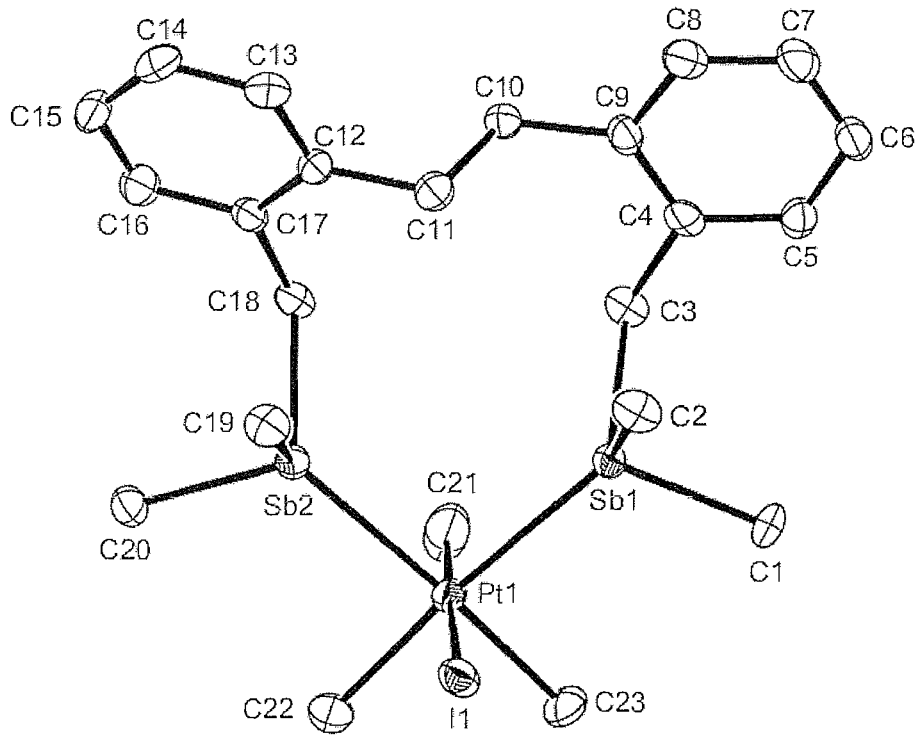

Table 2.2.1: Selected bond lengths (Å) and angles (°) from [$PtMe_3$(**VI**)I]

Pt1-Sb1	2.6329(4)	Sb1-Pt1-Sb2	95.957(12)
Pt1-C22	2.103(5)	Sb2-Pt1-C22	88.71(15)
Pt1-Sb2	2.6279(4)	Sb1-Pt1-C22	175.09(15)
Pt1-C23	2.108(5)	Sb2-Pt1-C23	174.63(15)
Pt1-I1	2.7573(5)[a]	Sb1-Pt1-C23	88.34(15)
Pt1-C21	2.377(3)[a]	Sb2-Pt1-I1	90.83(1)[a]
Sb1-C3	2.173(4)	Sb1-Pt1-I1	87.96(1)[a]
Sb2-C18	2.182(4)	C22-Pt1-C23	87.1(2)
Sb-C(Me)	2.122(5)-2.128(5)	Pt1-Sb1-C3	118.97(13)
Sb1···Sb2	3.908(1)	Pt1-Sb2-C18	116.53(13)
		Pt1-Sb-C(Me)	112.9(1)-121.6(1)

[a] The I1(C21A)–Pt1–C21(I1A) form a disordered group with chemically unreliable bond lengths (see text). The data given are for the major component.

It is believed that the *cis*-chelation observed for **VI** may be in part, due to the presence of the *o*-substituted aromatic units in the inter-donor linkage which are *cis*-directing, since long chain aliphatic linkages usually produce polymeric or occasionally *trans* chelating systems.

The reaction of $[PtCl_2(MeCN)_2]$ with **VI** in MeCN solution afforded a pale yellow solid in good yield, which was formulated as the Pt(II) complex $[PtCl_2(\mathbf{VI})]$. This was confirmed by IR spectroscopy, NMR spectroscopy, microanalysis and X-ray crystallography. The IR spectrum confirmed the presence of mutually *cis* Cl atoms with bands at 316 and 307 cm^{-1} corresponding to two Pt-Cl stretches. The platinum-195 NMR spectrum suggested that there was one platinum containing species present with a single resonance at -4960 ppm, which also indicates an Sb_2Cl_2 donor set at the Pt(II) metal centre.[19] A crystal structure of the product was obtained from slow evaporation from a solution of $[PtCl_2(\mathbf{VI})]$ in CH_2Cl_2 layered with Et_2O. Fig. 2.2.7 shows the crystal structure and Table 2.2.2 shows selected bond lengths and angles.

Fig 2.2.7: View of the structure of $[PtCl_2(\mathbf{VI})]$ with numbering scheme adopted. Note that only the major component of the disorder is shown (see Experimental). Ellipsoids are drawn at the 45% probability level and H atoms are omitted for clarity.

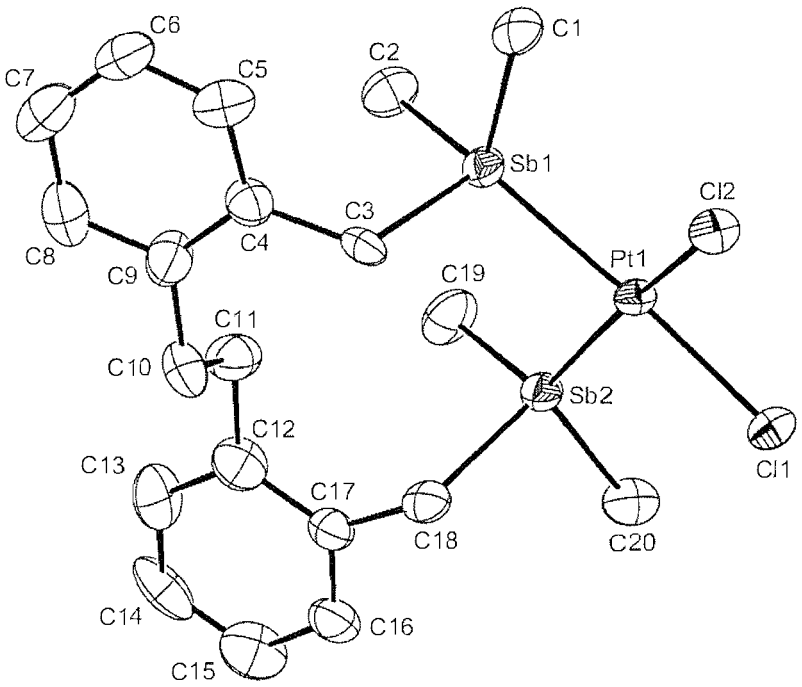

Table 2.2.2: Selected bond lengths (Å) and angles (°) from [$PtCl_2$(**VI**)]

Pt1-Cl1	2.338(2)	Cl1-Pt1-Cl2	90.48(9)
Pt1-Cl2	2.350(3)	Cl1-Pt1-Sb1	173.75(7)
Pt1-Sb1	2.4998(9)	Cl2-Pt1-Sb1	87.13(7)
Pt1-Sb2	2.5163(11)	Cl1-Pt1-Sb2	86.63(7)
Sb1-C1	2.095(10)	Cl2-Pt1-Sb2	171.45(7)
Sb1-C2	2.119(10)	Sb1-Pt1-Sb2	94.91(3)
Sb1-C3	2.162(10)		
Sb2-C20	2.104(10)		
Sb2-C19	2.138(10)		
Sb2-C18	2.169(11)		

In the structure in Fig 2.2.7, the distibine is coordinated to Pt(II) with two mutually *cis* Cl ligands completing the distorted square planar geometry, d(Pt-Sb) = 2.4998(9) and 2.5163 Å, d(Pt-Cl) = 2.338(2) and 2.350(3) Å. The chelate angle Sb1-Pt1-Sb2 = 94.91(3)°. There is some disorder at the Pt atom, and Fig 2.2.5 refers to the major (91%) component. These compare with d(Pt-Sb) = 2.4860(7) and 2.4931(8) Å, d(Pt-Cl) = 2.368(3), 2.376(3) Å and angle Sb-Pt-Sb = 97.58(2)° in the related species [$PtCl_2${*o*-$C_6H_4(CH_2SbMe_2)_2$}].[6] The [$PtCl_2$(**VI**)] molecules are distributed across a centre of symmetry such that the planes lie face to face, giving a weakly associated dimer with d(Pt1···Pt1a) = 3.176(1) Å. This is within the range observed for other weakly associated Pt(II) dimers and chains, for example [$PtCl_2(H_2NCH_2CH_2NH_2)$] d(Pt···Pt) = 3.381(3) Å.[20] Figure 2.2.8 shows the centre of symmetry and the weakly associated platinum dimer.

Fig 2.2.8: View of the weakly associated, centrosymmetric dimer formed by $[PtCl_2(\mathbf{VI})]$ (a: 1-x, -y, 2-z).

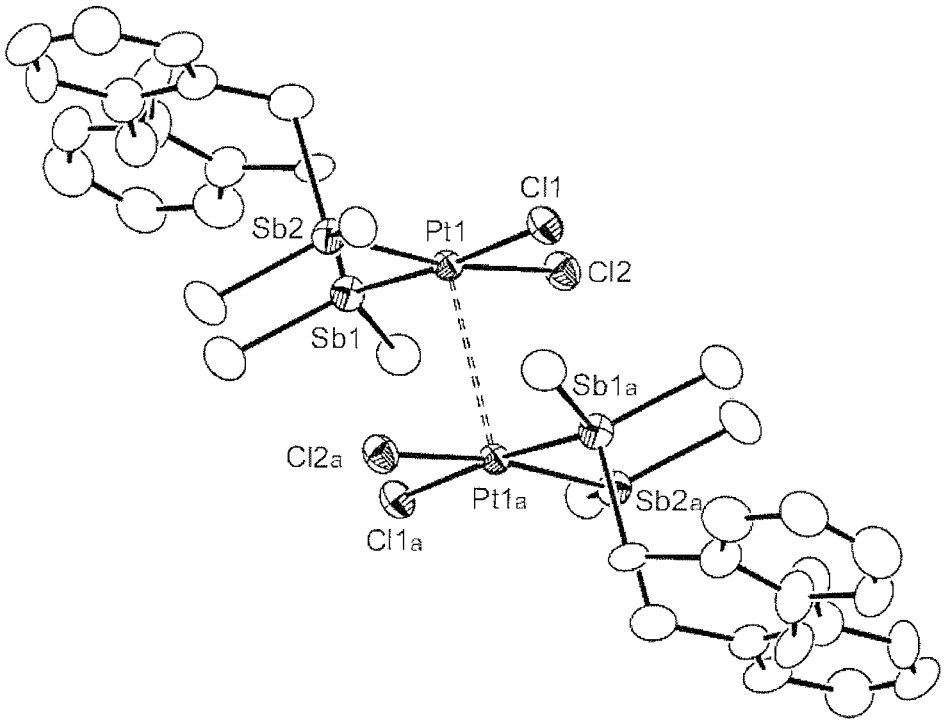

2.2.3 Synthesis of $[W(CO)_4(\mathbf{VI})]$

$[W(CO)_4(\mathbf{VI})]$ was prepared from $[W(CO)_4(piperidine)_2]$ and one molar equivalent of **VI** in refluxing EtOH. The light fawn powder was obtained in good yield, after work-up. The formulation of the complex was supported by the APCI mass spectrometry. The only significant cluster of mass peaks showing an isotope pattern consisent with the desired product was centred at *m/z* 809. This corresponded to $[W(CO)_4(\mathbf{VI}) + H]^+$ and microanalysis also confimed that the product was pure. The ^1H NMR spectrum showed the presence of coordinated ligand, and the nujol mull IR spectrum showed strong CO bands at 2011, 1898 and a shoulder at 1868 cm^{-1}. This is indicative of the formation of *cis*-$[W(CO)_4(\mathbf{VI})]$ and is similar to other complexes in the literature. For example *cis*-$[W(CO)_4\{o\text{-}C_6H_4(CH_2SbMe_2)_2\}]$[5] has CO bands at 2012, 1935, 1901 and 1863 cm^{-1} and *cis*-$[W(CO)_4\{Me_2Sb(CH_2)_3SbMe_2\}]$[21] has CO bands at 2011, 1896 and 1870 cm^{-1} in the IR spectrum. When $[W(CO)_4(piperdine)_2]$ and one molar equivalent of **VI** were refluxed in EtOH for a prolonged period of time (12 h) the only significant species was *cis*-$[W(CO)_4(\mathbf{VI})]$.

Fig 2.2.9: Positive ion electrospray mass spectrum (MeCN) of (a) $[W(CO)_4(\mathbf{VI}) + H]^+$ and (b) the relevant isotope simulation.

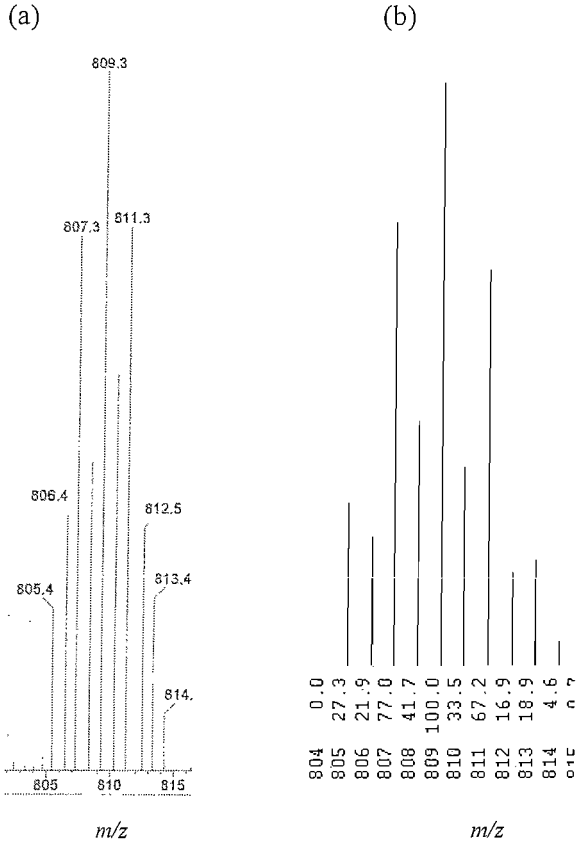

Crystals of two distinct polymorphs of this compound were obtained from slow evaporation from CH_2Cl_2/Et_2O solutions. The structures show that in each molecule the $W(CO)_4$ fragment is coordinated to two mutually *cis* Sb atoms of **VI** to give a *cis*-chelated distorted octahedral complex.

One of the polymorphs is shown in Figure 2.2.10a with selected bond lenghts and angles shown in Table 2.2.3a. There are molecules of $[W(CO)_4(\mathbf{VI})]$ in the asymmetric unit, one of which has the two aromatic rings of the ligand backbone in the same plane. The other molecule has some disorder in the distibine ligand backbone, suggesting that the ligand is very flexible and adopts two different conformations in the crystal lattice. The second polymorph is shown in Figure 2.2.10b and selected bond lengths and angles are shown in Table 2.2.3b. It is a very similar species to that shown in Figure 2.2.7a. The W-Sb bond lengths for both polymorphs are in the range of 2.7580(4) – 2.7736(4) Å, which are slightly longer than in other stibine complexes with tungsten carbonyl.[22] For example $[W(CO)_5\{Ph_2SbCH_2SbPh_2\}]$ has a W-Sb bond length of 2.743(1) Å and

[{$W(CO)_4(Me_2SbCH_2SbMe_2)$}$_2$] has W-Sb lengths of 2.752(1) – 2.7574(8) Å. This can be explained by the large 11-membered *cis*-chelate in the complex. The Sb–W–Sb chelate angles are in the range 90.34(1) to 93.26(1)°. The W-C distances are also sensitive to the *trans* ligand, being significantly longer for d(W-$C_{trans\ CO}$) *cf* d(W-$C_{trans\ Sb}$), reflecting the modest σ-donor/π-acceptor properties of the stibine compared to CO.

Fig 2.2.10a: View of the structure of one of the two crystallographically independent molecules of the first polymorph of [$W(CO)_4$(VI)] ($P2_1/n$) with numbering scheme adopted. Ellipsoids are drawn at the 50% probability level and H atoms are omitted for clarity. There is some disorder in the ligand backbone in the second molecule – see Experimental (section 2.3).

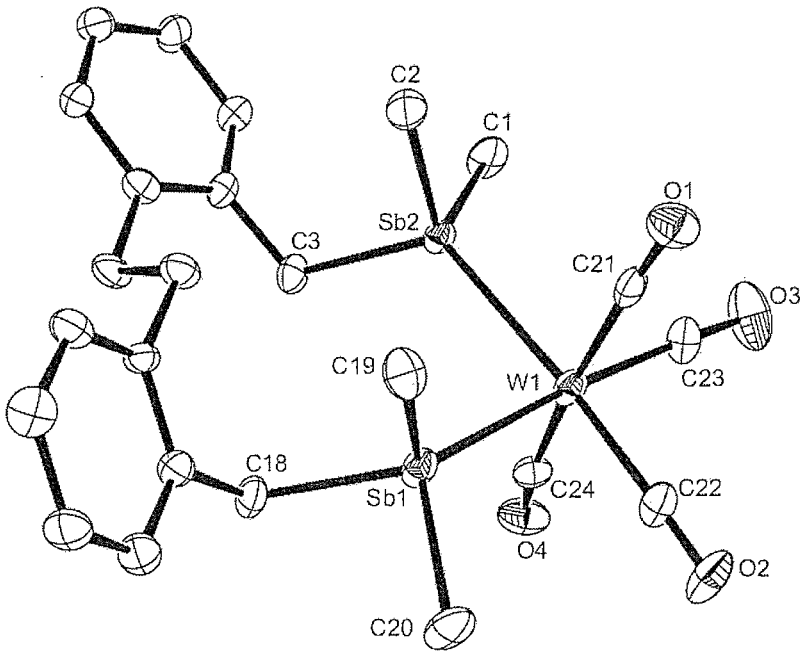

Table 2.2.3a: Selected bond lengths (Å) and angles (°) from $[W(CO)_4(\mathbf{VI})]$ ($P2_1/n$).

W1-Sb1	2.7736(4)	Sb1-W1-Sb2	91.947(12)
W1-Sb2	2.7590(4)	C21-W1-Sb1	88.46(11)
W1-C21	2.025(5)	C22-W1-Sb1	174.34(13)
W1-C22	1.968(5)	C23-W1-Sb1	94.31(14)
W1-C23	1.975(5)	C24-W1-Sb1	92.08(12)
W1-C24	2.019(5)	C-W1-C	85.2(2)-91.2(2)
Sb1-C3	2.188(4)	C24-W1-C21	171.45(18)
Sb2-C18	2.175(4)	W1-Sb1-C3	121.25(11)
Sb1···Sb2	3.978(1)	W1-Sb2-C18	127.20(11)
		Sb1-C3-C4	113.0(3)
		Sb2-C18-C17	110.3(3)

Fig 2.2.10b: View of the structure of one the second polymorph of $[W(CO)_4(\mathbf{VI})]$ (C*c*) with numbering scheme adopted. Ellipsoids are drawn at the 50% probability level and H atoms are omitted for clarity.

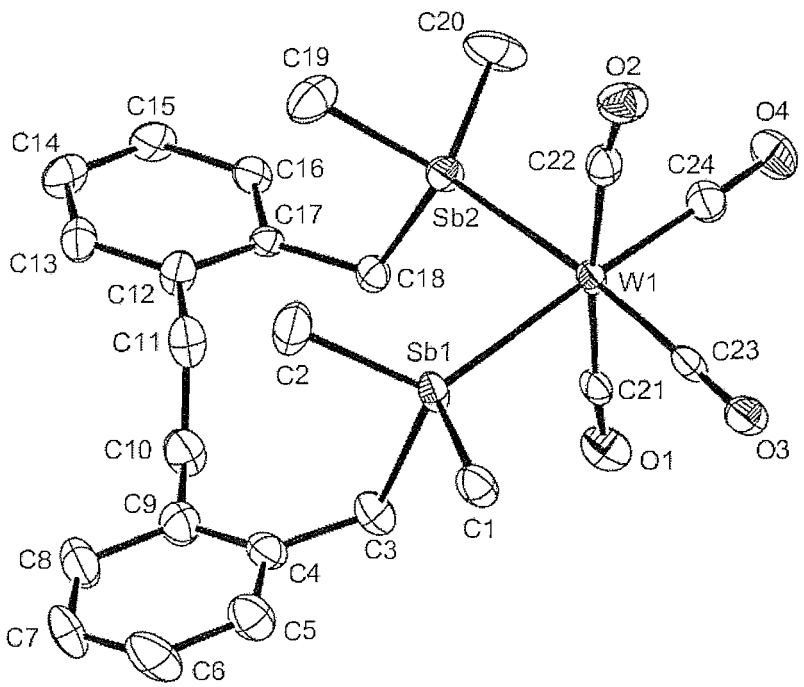

Table 2.2.3b: Selected bond lengths (Å) and angles (°) from [W(CO)$_4$(**VI**)] (C*c*).

W1-C23	1.966(5)	C23-W1-C24	94.8(2)
W1-C24	1.968(5)	C23-W1-C21	88.8(2)
W1-C21	2.021(5)	C24-W1-C21	88.4(2)
W1-C22	2.041(6)	C23-W1-C22	88.3(2)
W1-Sb1	2.7661(4)	C24-W1-C22	86.3(2)
W1-Sb2	2.7580(4)	C21-W1-C22	173.7(2)
		C23-W1-Sb1	85.04(14)
		C24-W1-Sb1	177.23(16)
		C21-W1-Sb1	88.80(13)
		C22-W1-Sb1	96.50(15)
		C23-W1-Sb2	174.31(13)
		C24-W1-Sb2	89.66(15)
		C21-W1-Sb2	87.78(14)
		C22-W1-Sb2	95.50(15)
		Sb2-W1-Sb1	90.339(14)

2.2.4 Attempted preparation of *o*-$C_6H_4(CH_2Sb^iPr_2)_2$

The preparation of *o*-$C_6H_4(CH_2Sb^iPr_2)_2$ was attempted in order to explore the ligating properties of bidentate distibine ligands that incorporate *iso*-propyl substituents as substituent groups coordinated to the antimony centres. This area of stibine chemistry is very interesting due to the work reported by Werner and co-workers involving bridging Sb^iPr_3 ligands in rhodium carbene complexes.[1] However, the study does not incorporate bidentate stibines of this type, indeed there are no examples of such ligands, and therefore it would be of interest to synthesise the above *o*-xylyl ligand.

Figure 2.2.11 shows the synthetic route that was employed in the attempted preparation of *o*-$C_6H_4(CH_2Sb^iPr_2)_2$, the analogous route to the synthesis of *o*-$C_6H_4(CH_2SbMe_2)_2$.[5]

In order to synthesise *o*-$C_6H_4(CH_2Sb^iPr_2)_2$, $PhSb^iPr_2$ was prepared from $PhSbCl_2$ and $BrMg^iPr_2$ in Et_2O. After aqueous work up, the desired product was distilled at 75°C / 0.2 mm Hg as a pale yellow oil in good yield. The ^{1}H NMR spectrum showed the presence of the ^{i}Pr groups bonded to the Sb centre with a septet at 1.98 (sept) [2H] (CH) and two doublets at 1.23 and 1.13 ppm (J = 7.2 Hz) which corresponded to the CH and CH_3 of the ^{i}Pr groups respectively. The reason for two ^{i}Pr

resonances is that in such situations the CH_3 groups in the different ^{i}Pr substituents are magnetically nonequivalent even if the energy barrier to rotation about the Sb – C bond is low. This effect is well documented and occurs for example, in PhP^iPr_2.[23] The $^{13}C\{^1H\}$ NMR spectrum also confirmed the desired product was formed by resonances at 22.5 (CH), 21.9 and 19.9 (CH_3) ppm.

Fig 2.2.11: Proposed synthetic route for the preparation of *o*-$C_6H_4(CH_2Sb^iPr_2)_2$.

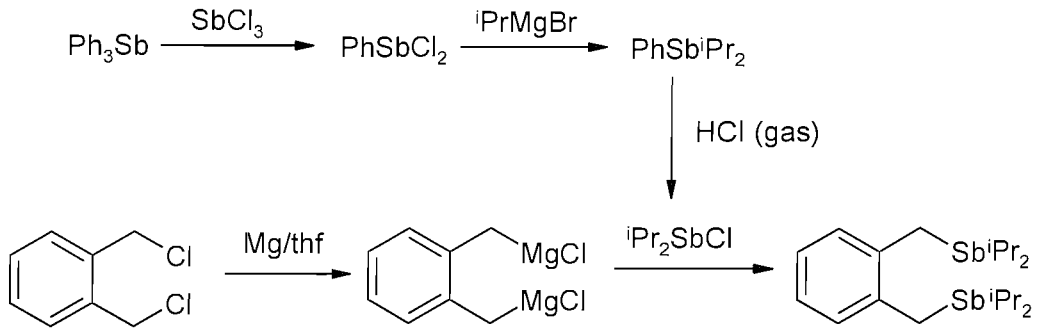

The use of HCl gas to cleave a Ph ring from $PhSbMe_2$ and replace it with a chloride is reported in the literature,[5] and has been used as routine in this Thesis. However, this procedure has not been carried out on ligands that contain R groups other than Me. It was therefore important to explore the reaction of HCl gas with PhSb^iPr_2 in toluene to see whether the cleavage of the Ph group and substitution with a Cl^- was as clean as with $PhSbMe_2$. Primary investigations suggested that the cleavage of the Ph group was not as easy as first predicted, as there was little change in the ^1H NMR spectrum. Indeed there was no evidence of Ph group resonances becoming diminished even with prolonged exposure to HCl gas. In addition to this it seemed that the presence of the HCl had caused other ^{i}Pr containing species to appear in the ^1H NMR spectrum. It was assumed that the reaction occurring at room temperature promoted rearrangements in the products and so the reaction was repeated at -40°C. HCl gas was bubbled through a solution of PhSb^iPr_2 in toluene at -40°C for 30 minutes. The reaction was then left for 1 h stirring still saturated with HCl, then the reaction was purged with N_2 to remove residual HCl. The ^1H NMR spectrum from this experiment indicated the resonances from the Ph groups had diminished in intensity, however the ^{i}Pr resonances were fairly complex and it was not clear what all the species were. There was however a septet at 1.85 ppm and a broad singlet at 1.22 ppm indicating the presence of $^iPr_2SbCl$. The literature data for $^iPr_2SbCl$ is in good accord with these findings.[24] There was also a small cluster of mass peaks centred at *m/z* 243 in the Electron Ionisation MS suggesting that

the desired compound was produced, however there was also evidence of other antimony containing species as well.

Due to the fact that $^{i}Pr_2SbCl$ was formed, even though it was clear that there was not complete substitution of the phenyl for a chloride, it was used in the reaction in Fig. 2.2.10 to form *o*-$C_6H_4(CH_2Sb^{i}Pr_2)_2$. By reacting *o*-$C_6H_4(CH_2MgCl)_2$ and a solution of $^{i}Pr_2SbCl$ in toluene, in thf, followed by aqueous work-up, a pale yellow oil was produced. After distilling at 140-145°C and 0.05 mm Hg a fawn air sensitive oil was obtained in low yield. Unfortunately even after distillation it was not clear by NMR spectroscopy whether the desired product was formed. There were indications in the ^{1}H NMR that the ligand was present, with indicative doublets for ^{i}Pr groups, however with the absence of a clearly defined CH_2 resonance and a complex aromatic region, it was not possible for positive assignment. The EIMS spectrum of the distilled product, did indicate that the desired product was formed. A cluster of peaks centred at *m/z* 477 corresponding to $[P-{}^{i}Pr]^{+}$ was seen. Due to this result an attempt to make a methiodide and a tetrabromide of the ligand was carried out. Unfortunately this failed, but the EIMS spectrum confirmed the presence of the ligand in the resultant oil. Fig 2.2.12 shows the EIMS spectrum of *o*-$C_6H_4(CH_2Sb^{i}Pr_2)_2$.

Fig 2.2.12: The EIMS spectrum of (a) $[o\text{-}C_6H_4(CH_2Sb^{i}Pr_2)_2 - {}^{i}Pr]^{+}$ and (b) the corresponding isotope simulation.

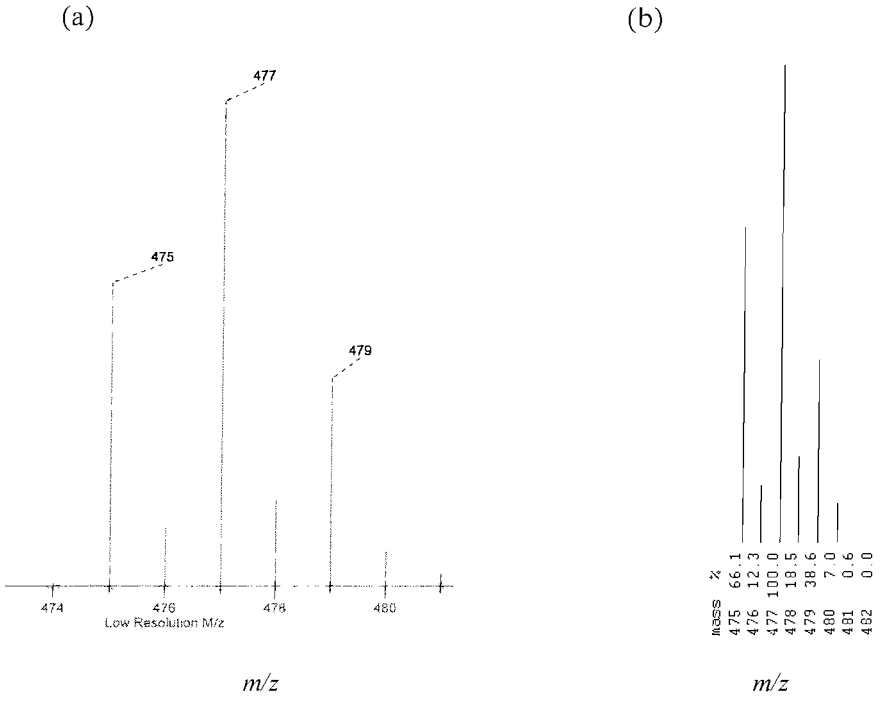

It is obvious that the unreliability of the reaction of $^{i}Pr_2SbPh$ with HCl gas to afford $^{i}Pr_2SbCl$ is one reason why the ligand was not prepared cleanly. It seems that the phenyl cleavage does not proceed cleanly with compounds of this nature, containing ^{i}Pr groups. Therefore another route needs to be devised to prepared the ligand. It could be suggested that this ligand could be synthesised from an Sb(V) precursor such as $^{i}Pr_3SbCl_2$ used in the preparation of ligands reported by Werner,[23] however this would need further investigation.

2.3 Conclusion

The work in this Chapter examined the preparation of *o*-$C_6H_4(CH_2SbMe_2)_2$ in more detail and found that there was significant dependence upon the concentration of the di-Grigard solution. As a result of this observation, the novel distibine {CH_2(*o*-$C_6H_4CH_2SbMe_2)_2$} (**VI**) was prepared *via* two methods. The first method was the indirect synthesis of **VI** by coupling of the di-Grignard *o*-$C_6H_4(CH_2MgCl)_2$ in concentrated thf solution followed by treatment with Me_2SbCl. The second method was the direct synthesis of **VI** by treatment of {CH_2(*o*-$C_6H_4CH_2MgCl)_2$} with Me_2SbCl. The latter method afforded the very oxygen sensitive distibine as a yellow oil in good yield. **VI** was fully characterised, and subsequent oxidation of the ligand with Br_2 gave the air stable tetrabromide {CH_2(*o*-$C_6H_4CH_2SbMe_2Br_2)_2$}. **VI** shows a surprising tendency for *cis*-chelation. The syntheses of [$PtMe_3I$(**VI**)], [$PtCl_2$(**VI**)] and [$W(CO)_4$(**VI**)] confirm the formation of an 11-membered chelate ring, and this was further supported by crystal structure determination of all three complexes.

The attempted preparation of the novel distibine *o*-$C_6H_4(CH_2Sb^iPr_2)_2$ was undertaken, from *o*-$C_6H_4(CH_2MgCl)_2$ and $^iPr_2SbCl$. However the cleavage of the phenyl group of $^iPr_2SbPh$ with HCl gas in toluene was not clean, and there was significant decomposition in the reaction. Therefore we were unable to isolate a pure sample even after distillation. The cleavage of the phenyl group from $PhSbMe_2$ with HCl is efficient and therefore $ClSbMe_2$ can be used to synthesise **VI** and other ligands such as *o*-$C_6H_4(CH_2SbMe_2)_2$.[5] However, it is clear that further research is needed in order to synthesise *o*-$C_6H_4(CH_2Sb^iPr_2)_2$. Possible precursors to this ligand could be using Sb(V) species such as $^iPr_3SbCl_2$, as used by Werner and co-workers for similar studies.[23] By reacting $^iPr_3SbCl_2$ with sodium in liquid ammonia, and subsequent reaction of the $NaSb^iPr_2$ produced with *o*-$C_6H_4(CH_2Br)_2$ the desired product may be synthesised.

2.4 Experimental

General experimental and instrumental techniques are described in the appendix. Solvents were dried prior to use and all preparations were undertaken using standard Schlenk techniques under a N_2 atmosphere. $[PtMe_3I]$[24] and $[W(CO)_4(pipieridine)_2]$[25] were obtained *via* literature methods.

o-$C_6H_4(CH_2Br)Br$ (I): 2-Bromotoluene (60 g, 0.35 mol), benzoyl peroxide (1.0 g, 0.004 mol) and CCl_4 (200 cm^3) were stirred to reflux under N_2. A suspension of N-bromosuccinimide (62.4 g, 0.35 mol) in CCl_4 (200 cm^3) was added dropwise and the reaction was heated at reflux until the reaction started. The reaction was then left to stir for a further 2 h. The insoluble succinimide was filtered off and the solution concentrated to afford a yellow oil. Yield (59.4 g, 68%). ^1H NMR ($CDCl_3$): δ 7.65 – 7.10 (m) [4H] (Ar-H), 4.62 (s) [2H] (CH_2) ppm. $^{13}C\{^1H\}$ NMR ($CDCl_3$): δ 133.38, 131.32, 130.15, 128.60 (Ar-C), 33.41 (CH_2) ppm. EIMS (CH_2Cl_2): *m/z* 250 [o-$C_6H_4(CH_2Br)Br]^+$. All spectroscopic data were in accord with the literature.[14]

{CH_2(o-C_6H_4Br)}$_2$ (II): MeMgI was prepared from MeI (75 g, 0.5 mol) and Mg turnings (12.5 g, 0.5 mol) in dry Et_2O (188 cm^3). A crystal of iodine was used to initiate the reaction. The mixture was stirred for 1 h to ensure complete reaction. The reaction was then warmed to reflux and o-$C_6H_4(CH_2Br)(Br)$ (41.4 g, 0.166 mol) in Et_2O (75 cm^3) was added dropwise over 1.5 h. After refluxing the mixture for a further 4 h, the reaction was cooled to RT and left to stir overnight. After refluxing the reaction for a further 4 h, it was cooled to RT and quenched with an aqueous 10% HCl solution and then H_2O (100 cm^3) was added. The organic layer was separated and the aqueous layer washed with Et_2O (2 x 100 cm^3). The combined organics were then dried over $MgSO_4$, filtered and reduced to dryness. The residues were then recrystallised from CH_2Cl_2 and MeOH to afford a waxy solid (9.5 g, 34 %) which was then dried *in vacuo*. ^1H NMR ($CDCl_3$): δ 7.55 – 6.90 (m) [8H] (Ar-H), 3.00 (s) [4H] (CH_2) ppm. $^{13}C\{^1H\}$ NMR ($CDCl_3$): δ 139.56, 131.75, 129.60, 126.79, 126.41, 123.46 (Ar-C), 35.41 (CH_2) ppm. EIMS (CH_2Cl_2): *m/z* 340 [{CH_2(o-C_6H_4Br)}$_2$]$^+$. All spectroscopic data were in accord with the literature.[14]

{CH_2(o-C_6H_4CHO)}$_2$ (III): {CH_2(o-C_6H_4Br)}$_2$ (1.5 g, 4.42 mmol) was dissolved in dry Et_2O (20 cm^3) and cooled to 0 °C with ice. *n*BuLi (7.6 cm^3, 19.0 mmol, 2.5 M in hexane) was added gradually and then the reaction was warmed to RT and stirred for 30 minutes. N-formylpiperidine (5 cm^3) was then added dropwise with ice cooling, and then the reaction was warmed to RT and stirred for 2 h. The mixture was quenched with 10 % HCl, and benzene (100 cm^3) was added. The organics were separated, washed with H_2O (50 cm^3), and then dried over $MgSO_4$. This was then filtered, and

reduced to dryness. The residues were recrystallised from hexane, filtered and the white solid (0.57 g, 54%) dried *in vacuo*. ^{1}H NMR ($CDCl_3$): δ 10.12 (s) [2H] (C<u>H</u>O), 7.80 – 7.10 (m) [8H] (Ar-<u>H</u>), 3.25 (s) [4H] (C<u>H</u>$_2$) ppm. ^{13}C{^{1}H} NMR ($CDCl_3$): δ 191.60 (<u>C</u>HO), 132.79, 131.78, 130.47, 125.86 (Ar-<u>C</u>), 33.76 (<u>C</u>H$_2$) ppm. EIMS (CH_2Cl_2): *m/z* 237 [{CH_2(o-C_6H_4CHO)}$_2$-H$^+$]$^+$. All spectroscopic data were in accord with the literature.[14]

{CH_2(o-$C_6H_4CH_2OH$)}$_2$ (IV): {CH_2(o-C_6H_4CHO)}$_2$ (0.88 g, 3.7 mmol) was added slowly to a solution of $LiAlH_4$ (0.28 g, 7.4 mmol) in dry Et_2O (100 cm^3). The mixture was refluxed for 3 hr, allowed to cool, and quenched with H_2O. Dilute H_2SO_4 (10 % in H_2O) was added until a white precipitate formed between the organic and aqueous layers. This was filtered and dried *in vacuo*. The organic layer was then dried over $MgSO_4$, filtered and reduced to dryness, to afford an off white solid. Both solids were found to be the alcohol product by NMR. (Yield 0.813 g, 91%). ^{1}H NMR ($CDCl_3$): δ 7.3 – 7.0 (m) [8H] (Ar-<u>H</u>), 4.55 (s) [4H] (C<u>H</u>$_2$OH), 3.0 (s) [4H] (C<u>H</u>$_2$CH$_2$) ppm. ^{13}C{^{1}H} NMR ($CDCl_3$): δ 128.9, 128.1, 127.3, 125.5 (Ar-<u>C</u>), 62.5 (<u>C</u>H$_2$OH), 33.7 (<u>C</u>H$_2$CH$_2$) ppm. EIMS (CH_2Cl_2): *m/z* 224 [$C_{16}H_{15}O$]$^+$. All spectroscopic data were in accord with the literature.[14]

{CH_2(o-$C_6H_4CH_2Cl$)}$_2$ (V): To a solution of {CH_2(o-$C_6H_4CH_2OH$)}$_2$ (0.685 g, 2.83 mmol) and a few drops of pyridine in benzene (60 cm^3), a solution of $SOCl_2$ (4 cm^3) in benzene (5 cm^3) was added dropwise over 10 minutes at RT. After refluxing the reaction for 17 h, it was allowed to cool to RT, was quenched with H_2O (30 cm^3), separated and dried over $MgSO_4$. The organics were then filtered and reduced to dryness. The light brown solid was then dried *in vacuo*. (Yield 95%). ^{1}H NMR ($CDCl_3$): δ 7.3 – 7.1 (m) [8H] (Ar-<u>H</u>), 4.5 (s) [4H] (C<u>H</u>$_2$Cl), 3.05 (s) [4H] (C<u>H</u>$_2$CH$_2$) ppm. ^{13}C{^{1}H} NMR ($CDCl_3$): δ 139.4, 134.3, 129.5, 128.9, 128.1, 125.8 (Ar-<u>C</u>), 43.2 (<u>C</u>H$_2$Cl), 32.9 (<u>C</u>H$_2$CH$_2$) ppm. All spectroscopic data were in accord with the literature.[14]

{CH_2(o-$C_6H_4CH_2SbMe_2$)}$_2$ (VI)

Method A: *o*-C_6H_4(CH_2MgCl)$_2$ was prepared from Mg powder (3.26 g, 134.3 mmol) in thf (150 cm^3) and *o*-C_6H_4(CH_2Cl)$_2$ (5.7 g, 32.75 mmol) in thf (50 cm^3) added dropwise over 1 h giving a 0.16 mol dm^{-3} solution. Me_2SbCl ($PhSbMe_2$ (15 g, 65.5 mmol) and HCl gas)[5] in toluene (50 cm^3) was added dropwise over 30 min., and the reaction was left to stir overnight. The mixture was then hydrolysed (100 cm^3 of 1 mol dm^{-3} aqueous NH_4Cl), the organics separated, the aqueous layer extracted with Et_2O (2 x 50 cm^3). After drying ($MgSO_4$), filtering and removing the solvent by distillation at atmospheric pressure, and fractionation of the *o*-C_6H_4(CH_2SbMe_2)$_2$ (200°C, 0.5 mmHg), **VI** was obtained as a clear oil by Kugelröhr distillation (225°C, 0.5 mmHg). (Yield 1.2 g,

14%). ^{1}H NMR ($CDCl_3$): δ 7.1–7.3 (m) [8H] (Ar-H), 2.96 (s) [8H] ($SbCH_2$, CH_2CH_2), 0.80 (s) [12H] ($SbCH_3$) ppm. $^{13}C\{^1H\}$ NMR ($CDCl_3$): δ 139.9, 138.8, 129.6, 128.5, 126.9, 125.5 (Ar-C), 34.9 (CH_2CH_2), 20.9 ($SbCH_2$), -2.3 ($SbCH_3$) ppm. EIMS: *m/z* 497 [parent – Me]$^+$, 513 [parent + H]$^+$. High resolution MS: calculated for [parent-Me] *m/z* = 497.00367; found: *m/z* = 496.9697.

Method B: $\{CH_2(o\text{-}C_6H_4CH_2MgCl)\}_2$ was prepared from magnesium powder (0.42 g, 17.3 mmol) and anthracene (0.31 g, 1.73 mmol), which was activated with 1,2-dibromoethane (0.1 cm^3) in thf (5 cm^3). After stirring for 5 min, thf (25 cm^3) was added, then $\{CH_2(o\text{-}C_6H_4CH_2Cl)\}_2$ (1.6 g, 5.73 mmol) in thf (170 cm^3) was added dropwise over 2 h. The mixture was stirred at RT overnight, then a solution of Me_2SbCl (prepared from $PhSbMe_2$ (2.62 g, 11.46 mmol) and HCl gas)[5] in toluene (50 cm^3) was added dropwise over 2 h, and the resulting mixture stirred at RT overnight. The reaction was hydrolysed with a solution of NH_4Cl (50 cm^3, 1 mol dm^{-3} in H_2O). The organics were separated and the aqueous layer washed with Et_2O (2 x 50 cm^3). The combined organics were then dried over $MgSO_4$, filtered and then reduced to dryness. The residues were dissolved in Et_2O (20 mL), the anthracene filtered off, and the pale yellow solution reduced to dryness *in vacuo*. Yellow oil. (Yield 2.0 g, 68%). ^{1}H NMR ($CDCl_3$): δ 7.2–7.0 (m) [8H] (Ar-H), 2.86 (s) [8H] (CH_2Sb, CH_2CH_2), 0.80 (s) [12H] ($SbCH_3$) ppm. $^{13}C\{^1H\}$ NMR ($CDCl_3$): δ 139.9, 138.7, 129.6, 128.8, 127.0, 125.5 (Ar-C), 34.9 (CH_2CH_2), 20.9 (CH_2Sb), -2.3 ($SbCH_3$) ppm. EIMS: *m/z* 497 [parent – Me]$^+$, 513 [parent + H]$^+$.

$\{CH_2(o\text{-}C_6H_4CH_2SbMe_2Br_2)\}_2$ (VII): **VI** (0.05 g, 0.098 mmol) was dissolved in dry CH_2Cl_2 (5 cm^3) and a solution of Br_2 (0.5 cm^3) in CH_2Cl_2 (10 cm^3) was added drop-wise until a yellow colour was observed. The reaction was then stirred for 2 h, reduced in volume to *ca.* 2 cm^3 and then hexane (5 cm^3) was added to precipitate a solid. The light yellow solid was isolated by filtration and dried *in vacuo*. (Yield 61%). Required for $C_{20}H_{28}Br_4Sb_2$: C, 28.9; H, 3.4. Found: C, 30.1; H, 3.4% (note that the NMR spectra of this compound and of **VI** itself show traces of anthracene from the original direct synthesis of **VI** which remain despite repeated washing, hence the poorer than normal fit for the analytical data). ^{1}H NMR ($CDCl_3$): δ 7.2–7.4 (m) [8H] (Ar-H), 4.24 (s) [4H] (CH_2Sb), 3.16 (s) [4H] (CH_2CH_2), 2.47 (s) [12H] (CH_3) ppm. $^{13}C\{^1H\}$ NMR ($CDCl_3$): δ 130.3, 129.5, 129.2, 127.9, 125.7 (Ar-C), 46.3 (CH_2Sb), 34.1 (CH_2CH_2), 25.7 (CH_3) ppm.

$PhSb^iPr_2$: ^{i}PrMgBr was prepared from ^{i}PrBr (44.28 g, 0.36 mol) and magnesium turnings (9.47 g, 0.39 mol) in dry Et_2O (750 cm^3) and then stirred for 45 minutes to ensure complete reaction. $PhSbCl_2$ (48.6 g, 0.18 mol) in dry Et_2O (200 cm^3) was added dropwise with stirring and the pale

yellow suspension was stirred at room temperature for 3 h. The reaction mixture was hydrolysed with a degassed solution of NH_4Cl (300 cm^3, 1 mol dm^{-3}), and the organic layer separated. The aqueous layer was washed with Et_2O (2 x 100 cm^3) and the combined organics dried over $MgSO_4$ overnight. The excess solvent was then removed by distillation at atmospheric pressure. The desired product was distilled as a pale yellow oil at 75 °C / 0.2 mm Hg. (Yield 28 g 54.7 %) ^1H NMR ($CDCl_3$): δ 7.41 (m), 7.19 (m) [5H] (Ar-H), 1.98 (sept) [2H] (CH), 1.23 (d, J = 7.2 Hz) [3H] (CH_3), 1.13 (d, J = 7.2 Hz) [3H] (CH_3) ppm. $^{13}C\{^1H\}$ NMR ($CDCl_3$): δ 136.8, 135.6, 127.6, 127.3 (Ar-C), 22.5 (CH), 21.9, 19.9 (CH_3) ppm. Due to the air sensitive nature of the ligand, microanalysis was not obtained.

Attempted preparation of o-$C_6H_4(CH_2Sb^iPr_2)_2$: o-$C_6H_4(CH_2MgCl)_2$ was prepared from magnesium powder (1.7 g, 70 mmol) activated with 1,2-dibromoethane (0.1 cm^3) in thf (5 cm^3). The reaction was stirred for 5 minutes, then thf (15 cm^3) was added followed by dropwise addition of o-$C_6H_4(CH_2Cl)_2$ (3.1.g, 17.7 mmol) in thf (220 cm^3) over 3 h. The reaction was then treated with a toluene (50 cm^3) solution of $ClSb^iPr_2$ (prepared as below † from $PhSb^iPr_2$ (14.24 g, 35 mmol) and HCl gas) added dropwise over 2 h. After stirring overnight the reaction mixture was hydrolysed with aqueous NH_4Cl (50 cm^3, 1 mol dm^{-3}), the organic layer separated, and the aqueous layer washed with Et_2O (2 x 50 mL). The combined organics were dried over $MgSO_4$ and the solvent removed *in vacuo*. The pale yellow residues were distilled *via* Kugelröhr distillation at 140-145 °C / 0.05 mm Hg as a fawn air sensitive oil (1.68 g, 18%). EIMS: *m/z* 477 [parent – $^iPr]^+$.

† $PhSb^iPr_2$ (14.24 g, 35 mmol) was dissolved in toluene (50 cm^3) and cooled to -40°C using an acetone/CO_2 slush. HCl gas was bubbled through the solution for 30 minutes. The solution was then stirred at -40 °C for 1 h, then purged with N_2 for 30 minutes to remove residual HCl.

[$PtMe_3I$(VI)]: Me_3PtI (0.075 g, 0.2 mmol) and **VI** (0.102 g, 0.2 mmol) were dissolved in dry $CHCl_3$ (20 cm^3) and refluxed under N_2 for 4 h. The light yellow solution was then pumped to dryness *in vacuo* to give a waxy solid which was triturated with hexane to produce a light yellow powder. (Yield: 60%). $C_{23}H_{37}IPtSb_2.CHCl_3$: C, 28.9; H, 3.8. Found: C, 28.2; H, 3.8%. ^1H NMR ($CDCl_3$): δ 0.65 (s) [6H] ($SbCH_3$), 0.89 (s) [3H] (Me *trans* I ($^2J_{PtH}$ = 71 Hz)), 1.16 (s) [6H] (SbMe), 1.52 (s) [6H] (Me *trans* Sb ($^2J_{PtH}$ = 66 Hz)), 3.10 (s) [4H] (CH_2CH_2), 3.28 (m) [4H] ($SbCH_2$), 7.00-7.28 (m) [4H] (Ar-H) ppm. $^{13}C\{^1H\}$ NMR ($CDCl_3$): δ -8.5 ($SbCH_3$), -7.8 (Me *trans* I ($^1J_{PtC}$ = 614 Hz)), -5.1 ($SbCH_3$), 6.2 (Me *trans* Sb ($^1J_{PtC}$ = 563 Hz)), 20.5 ($SbCH_2$), 34.9 (CH_2CH_2), 138.9-124.7 (Ar-C) ppm. ^{195}Pt NMR: -4440 ppm.

[$PtCl_2$(VI)]: $PtCl_2$ (51.95 mg, 0.195 mmol) was suspended in dry acetonitrile (20 cm^3) and refluxed for 1 h until all the solid was dissolved and a yellow solution was obtained. This was then cooled to room temperature, and **VI** (0.1 g, 0.195 mmol) in CH_2Cl_2 (5 cm^3) was added slowly. The reaction was stirred for 2 hr at room temperature, until an orange solution was obtained. The reaction mixture was then reduced to dryness. The residues were dissolved in minimum CH_2Cl_2 and hexane (10 cm^3) was added to precipitate a solid. The orange solid was isolated and dried *in vacuo* to afford an orange powder. The orange solid was isolated and dried *in vacuo*. (Yield 55 %). Required for $C_{20}H_{28}Cl_2PtSb_2.CH_2Cl_2$: C, 29.2; H, 3.5. Found: C, 29.0; H, 3.9%. ^{1}H NMR ($CDCl_3$): δ 7.0–7.3 (m) [8H] (Ar-H), 5.30 (s) (CH_2Cl_2), 3.36 (s) [4H] (CH_2Sb), 2.93 (s) [4H] (CH_2CH_2), 1.25 (s) [12H] (CH_3) ppm. ^{195}Pt{^{1}H} NMR (CH_2Cl_2/$CDCl_3$): δ -4960 ppm. IR (Nujol mull): ν 316 w, 307 w (ν(Pt-Cl)) cm^{-1}.

[$W(CO)_4$(VI)]: [$W(CO)_4$(piperidine)$_2$] (0.18 g, 0.39 mmol) and **VI** (0.20 g, 0.39 mmol) were refluxed in EtOH (20 cm^3) for 2 h, cooled to room temperature and the reaction mixture was filtered. The EtOH was removed *in vacuo* and the residues were dissolved in minimum CH_2Cl_2. Hexane (10 cm^3) was added to precipitate a solid, and the light brown powder was isolated and dried *in vacuo*. (Yield 40%). Required for $C_{24}H_{28}O_4Sb_2W$: C, 35.7; H, 3.5. Found: C, 35.7; H, 3.5%. ^{1}H NMR ($CDCl_3$): δ 7.1–7.4 (m) [8H] (Ar-H), 3.25 (s) [4H] (CH_2Sb), 2.74 (s) [4H] (CH_2CH_2), 1.08 (s) [12H] (CH_3) ppm. IR (Nujol mull): ν 2011 s, 1898 vs, 1868 sh (CO) cm^{-1}. APCI MS (MeCN): *m/z* = 809; calculated for [$W(CO)_4$(**VI** + H)]$^+$.

2.4.1 Crystallography

Details of the crystallographic data collection and refinement parameters are given in Table 2.3.1. Yellow single crystals of [$PtMe_3I$(**VI**)], [$PtCl_2$(**VI**)] and two polymorphs of [$W(CO)_4$(**VI**)] were obtained by diffusion of hexane into a CH_2Cl_2 solution, by diffusion of Et_2O into a solution of the complex in CH_2Cl_2 or by slow evaporation from a solution of the complex in CH_2Cl_2/Et_2O respectively. Data collection used a Nonius Kappa CCD diffractometer (T = 120 K) and with graphite-monochromated Mo-Kα X-radiation (λ = 0.71073 Å). Structure solution and refinement were routine,[26-28] except for some disorder between the I and C atoms within the *trans*-I–Pt–Me unit in [$PtMe_3I$(**VI**)]. This was modelled using partial atom positions, with the sum of the occupancies of the two I and two C components each being one. Distinct partial C atom and partial I atoms could not be identified, hence these units were refined with identical atomic coordinates and atom displacement parameters. Consequently the Pt–I and Pt–C distances in the *trans*-I–Pt–C unit are weighted averages, and should not be used in comparative studies. The H atoms associated

with the disordered Me groups were not included in the final structure factor calculation. The structure of [$PtCl_2$(**VI**)] shows some disorder in the position of the $PtCl_2$ fragment. This was evident from a residual unassigned peak in the difference map which based upon the thermal ellipsoids, coordination environment, the distances and angles relative to the Sb_2PtCl_2 plane could not be assigned to a light atom. The disorder model presented gave a very satisfactory refinement for two alternative positions for the Pt atom with relative occupancies of 91% and 9%. This leads to two Sb_2PtCl_2 planes with different orientations, and examination of the centrosymmetric dimer shows that the Cl atoms associated with the minor Pt component and those on the symmetry related Pt1a are common. The discussion and the geometric parameters in Table 2.2.2 refer to the major component.

Some disorder was also found in the backbone of one of the two crystallographically independent [$W(CO)_4$(**VI**)] molecules in the asymmetric unit of the first polymorph ($P2_1/n$; (a)). This was modelled very satisfactorily using split C atom occupancies in the disordered region, revealing two slightly different ligand conformations. Selected bond lengths and angles for these species are presented in Tables 2.2.1, 2.2.2, 2.2.3a and 2.2.3b.

Table 2.4.1: Crystallographic data collection and refinement parameters.[a]

Complex	**[$Me_3Pt(VI)$]**	**[$PtCl_2(VI)$]**	**[$W(CO)_4(VI)$] (a)**	**[$W(CO)_4(VI)$] (b)**
Formula	$C_{23}H_{37}IPtSb_2$	$C_{20}H_{28}Cl_2PtSb_2$	$C_{24}H_{28}O_4Sb_2W$	$C_{24}H_{28}O_4Sb_2W$
M	879.02	777.91	807.81	807.81
Crystal system	Monoclinic	Monoclinic	Monoclinic	Monoclinic
Space Group	$P2_1/n$ (no.14)	$P2_1/c$ (no.14)	$P2_1/n$ (no.14)	Cc (no. 9)
a/ Å	12.2870(15)	14.243(5)	12.9641(15)	17.705(3)
b/ Å	12.7061(10)	13.068(3)	23.323(3)	11.6869(15)
c/ Å	16.623(2)	12.380(4)	17.0599(15)	12.4991(10)
β/°	91.307(6)	90.302(12)	96.210(5)	94.506(10)
U/ $Å^3$	2594.5(5)	2304.1(12)	5128.0(9)	2758.2(5)
Z	4	4	4	4
μ(Mo-Kα)/mm^{-1}	8.64	8.62	6.59	6.56
R_{int}	0.034	0.148	0.048	0.0251
Total no. of obsns.	29152	25377	58518	17199
Unique obsns.	5928	5290	11741	5633
No. of parameters	245	240	605	281
R1 [$I_o > 2\sigma(I_o)$]	0.029	0.057	0.028	0.024
R1 [all data]	0.036	0.147	0.046	0.0254
wR_2 [$I_o > 2\sigma(I_o)$]	0.062	0.090	0.054	0.0489
wR_2 [all data]	0.064	0.109	0.059	0.0495

[a] Common items: temperature = 120 K; wavelength (Mo-Kα) = 0.71073 Å; θ(max) = 27.5°.
$R1 = \Sigma\big|\,|F_o| - |F_c|\,\big|_i / \Sigma|F_o|$; $wR_2 = [\Sigma w(F_o^2 - F_c^2)^2 / \Sigma\, wF_{oi}^4]^{1/2}$

2.5 References

[1] H. Werner, *Angew. Chem. Int. Ed.*, 2004, **43**, 938.

[2] H. Werner, D. A. Ortmann, O. Gevert, *Chem. Ber.*, 1996, **129**, 411.

[3] N. R. Champness, W. Levason, *Coord. Chem. Rev.*, 1994, **133**, 115; W. Levason and G. Reid, *Coord. Chem. Rev.*, 2006, **250**, 2565.

[4] W. Levason, G. Reid in *Comprehensive Coordination Chemistry II*, Eds. J. A. McCleverty and T. J. Meyer, Volume 1, Elsevier, Amsterdam, 2004.

[5] W. Levason, M. L. Matthews, G. Reid, M. Webster, *Dalton Trans.*, 2004, 51.

[6] W. Levason, M. L. Matthews, G. Reid, M. Webster, *Dalton Trans.*, 2004, 554.

[7] C. A. McAuliffe, *"Phosphine, Arsine and Stibine Complexes of the Transition Metal Elements"* Elsevier, New York, 1979.

[8] W. Levason, K. G. Smith, C.A. McAuliffe, F. P. McCullough, R. D. Sedgewick, S. G. Murray, *J. Chem. Soc., Dalton Trans.*, 1979, 1718.

[9] J. R. Black, W. Levason, M. D. Spicer, M. Webster, *J. Chem. Soc., Dalton Trans.*, 1993, 3129.

[10] A. M. Hill, W. Levason, M. Webster, *Inorg. Chem.*, 1996, **35**, 3428.

[11] H. A. Meinema, H. F. Martens, J. G. Noltes, *J. Organomet. Chem.*, 1976, **110**, 183.

[12] M. F. Lappert, T. R. Martin, C. L. Raston, *Inorg. Synth.*, 1989, **26**, 144.

[13] M. F. Lappert, T. R. Martin, C. L. Raston, B. W. Skelton, A. H. White, *J. Chem. Soc., Dalton Trans.*, 1982, 1959.

[14] T. Yamato, N. Sakaue, M. Komine, Y. Nagano, *J. Chem. Res. (S)*, 1997, 246; *J. Chem. Res. (M)*, 1997, 1708.

[15] F. L. March, R. Mason, K. M. Thomas, B. L. Shaw, *J. Chem. Soc., Chem. Commun.*, 1975, 584; A. J. Pryde, B. L. Shaw, B. Weeks, *J. Chem. Soc., Chem. Commun.*, 1973, 947; *J. Chem. Soc., Dalton Trans.*, 1976, 322; W. E. Hill, D. M. A. Minehan, J. C. Taylor, C. A. McAuliffe, *J. Am. Chem. Soc.*, 1982, **104**, 6001; B. L. Shaw, *J. Organomet. Chem.*, 1980, **200**, 307.

[16] P. W. N. M. van Leeuwen, P. C. J. Kamer, J. N. H. Reek, P. Dierkes, *Chem. Rev.*, 2000, **100**, 2741 and references therein.

[17] M. D. Brown, W. Levason, G. Reid, M. Webster, *Dalton Trans.*, 2006, 1667.

[18] D. J. Gulliver, W. Levason, K. G. Smith, *J. Chem. Soc., Dalton Trans.*, 1981, 2153.

[19] E. G. Hope, W. Levason, N. A. Powell, *Inorg. Chim. Acta*, 1986, **115**, 187.

[20] J. Iball, M. MacDougall, S. Scrimgeour, *Acta Crystallogr., Sect. B*, 1975, **31**, 1672.

[21] M. D. Brown, W. Levason, J. M. Manning, G. Reid, *J. Organomet. Chem.*, 2005, **690**, 1540.

[22] A. M. Hill, N. J. Holmes, A. R. J. Genge, W. Levason, M. Webster, S. Rutschow, *J. Chem. Soc., Dalton Trans.*, 1998, 825.

[23] M. Manger, J. Wolf, M. Laubender, M. Teichert, D. Stalke, H. Werner, *Chem. Eur. J.*, 1997, **3**(9) 1442.

[24] J. C. Baldwin, W. C. Kaska, *Inorg. Chem.*, 1975, **14**, 2020.

[25] D. J. Darensbourg, R. L. Kump, *Inorg. Chem.*, 1978, **17**, 2680.

[26] G. M. Sheldrick, SHELXS-97, program for crystal structure solution, University of Göttingen, Germany, 1997.

[27] G. M. Sheldrick, SHELXL-97, program for crystal structure refinement, University of Göttingen, Germany, 1997.

[28] H. D. Flack, *Acta Crystallogr., Sect. A,* 1983, **39**, 876.

Chapter 3

Preparation, properties and structures of the first series of organometallic Pt(II) and Pt(IV) complexes with stibine co-ligands

3.1. Introduction

Many transition metal based homogeneous catalysts incorporate phosphines as co-ligands. The chemistry of these complexes has been investigated in great detail, due to the potential of these compounds being well documented. Therefore a great deal is known of the reaction chemistry of the complexes and indeed the electronic and steric influences of the ligands on the metal ion fragments.

In contrast to phosphines, little of the analogous organometallic chemistry incorporating stibine ligands has been investigated, with the exception of selected metal carbonyl species.[1,2] There are however, exceptions to this statement, such as the very elegant work carried out by Werner and co-workers, which has been described in chapter 2 of this Thesis.[3-6] Werner's work demonstrates that these stibine species promote different product distributions and therefore result in very interesting reaction chemistry. These findings show that stibine ligands have subtly distinct electronic properties and are therefore important to explore in greater detail. Other advances in the area prove that stibines as ligands are particularly valuable in industry. One such example is the efficient nickel catalysed styrene polymerisation using $[Ni(CH_2C(Me)CH_2)(SbPh_3)_3]^+$.[7] Employing this catalyst the reaction reached a 2000 min^{-1} turnover. Further studies revealed that by replacing the $SbPh_3$ co-ligand with $AsPh_3$ a similar turnover and catalytic activity was achieved. Moreover, a trend is observed in the degree of oligomerization of styrene as a function of the co-ligand used: passing from PPh_3 to $SbPh_3$ through $AsPh_3$ causes an increase in the amount of dimer and a reduction in the amount of higher oligomers. $[Ni(CH_2C(Me)CH_2)(SbPh_3)_3]^+$ and $[Ni(CH_2C(Me)CH_2)(AsPh_3)_3]^+$ have also been found to be active towards the oligomerization of dienes and other olefins. From this study it becomes clear that stibine ligands may play an important role in the future development of highly active nickel catalysts for olefin oligomerization.[7] Figure 3.1.1 shows the reaction of styrene to produce polystyrene and Figure 3.1.2 shows the nickel cation used as the catalyst.

Fig 3.1.1: Reaction scheme of the polymerisation of styrene.[7]

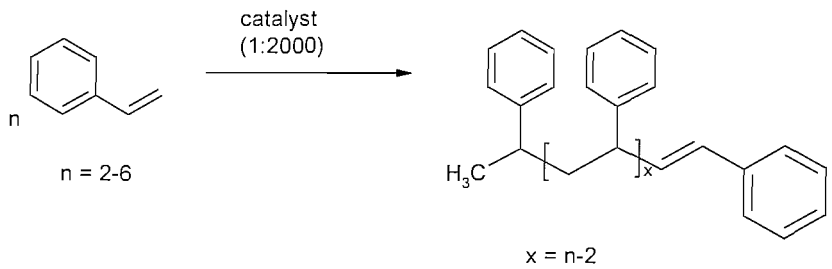

Fig 3.1.2: Crystal structure of $[Ni(CH_2C(Me)CH_2)(SbPh_3)_3]^+$ used in the polymerisation of styrene.[7]

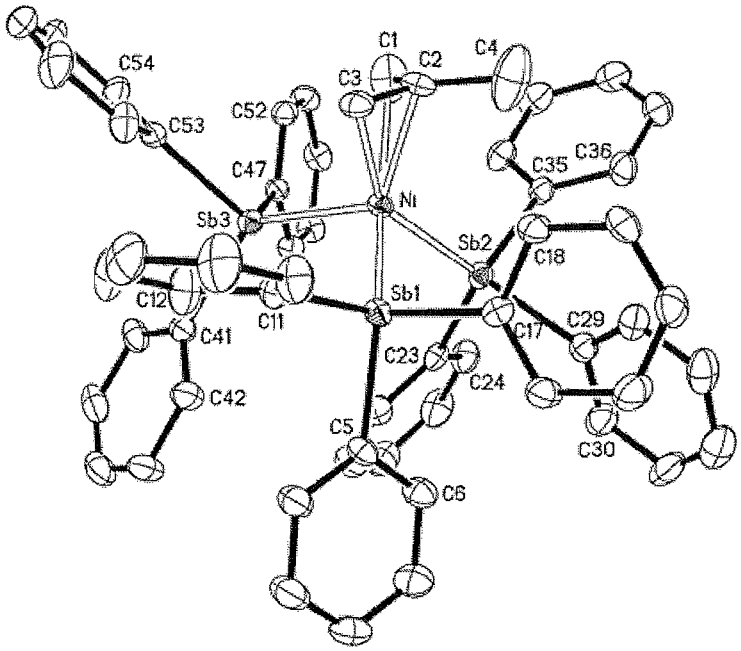

Selected bond lengths (Å) and angles (°): Ni–C(2) 2.013(5), Ni–C(3) 2.076(5), Ni–C(1) 2.228(9), Ni–Sb(1) 2.5175(7), Ni–Sb(2) 2.5222(7), Ni–Sb(3) 2.5650(7), C(1)–C(2) 1.355(9), C(2)–C(3) 1.403(7), C(2)–C(4) 1.466(10), Sb(1)–Ni–Sb(2) 100.35(3), Sb(1)–Ni–Sb(3) 110.24(2), Sb(2)–Ni–Sb(3) 99.76(2), C(1)–C(2)–C(3) 116.1(6).[7]

The literature data on transition metal complexes that incorporate stibines suggest that they prefer low or medium oxidation states. However this could be misleading as not much research has been carried out on higher oxidation state transition metal complexes involving stibines. There are however a small number of Pt(IV) stibines of the form *cis*-$[PtCl_4(distibine)]$ that have been obtained. These complexes tend to decompose very rapidly in solution, in particular *via* chlorination of the stibine ligand and corresponding reduction of the Pt(IV) centre.[8] Table 3.1.1 summarises a selection of the *cis*-$[PtCl_4(distibine)]$ already known in the literature.

Table 3.1.1: Selected Pt(IV) halide complexes.[8]

Compound	ν(Pt-X) /cm^{-1}	10^{-3} E_{max} /cm^{-1}
$[Pt(Me_2Sb(CH_2)_3SbMe_2)Cl_4]$	326s, 300s, 278s	21.30sh, 26.50
$[Pt(o\text{-}C_6H_4(SbPh_2)_2)Cl_4]$	347m, 325s, 295s	25.80br
$[Pt(Me_2Sb(CH_2)_3SbMe_2)Br_4]$	240m	19.30w, 23.60sh, 26.50
$[Pt(Ph_2Sb(CH_2)_3SbPh_2)Br_4]$	245m	24.60br
$[Pt(o\text{-}C_6H_4(SbPh_2)_2)Cl_4]$	246m	19.60sh, 26.70br
$[Pt(SbMe_3)_2Cl_4]$	349m, 327s, 310s, 283s	18.80sh, 25.70
$[Pt(SbMe_3)_2Br_4]$	242m	19.60sh, 26.70

There are no reported Pt(IV) stibine complexes in the literature which incorporate alkyl co-ligands, with the exception of $[PtMe_3\{CH_2(o\text{-}C_6H_4CH_2SbMe_2)\}_2I]$ described in Chapter 2 of this thesis.[9] There is however, some early work on some platinum(II) dialkyl complexes that employ $SbPh_3$ as co-ligands. These complexes are of the form *cis*-$[PtR_2(SbPh_3)_2]$ (R = Me, Ph, o/m/p-C_6H_4Me) and are formed by reaction of $[PtR_2(C_8H_8)]$ with two molar equivalents of $SbPh_3$ in refluxing benzene. However, there have been no spectroscopic or structural data included in the report.[10] Other compounds of the form $[PtR'_2(Ph_2SbCH_2SbPh_2)]$ (R' = various substituted phenyl ligands) have also been reported and their photochemical activity explored, but again these compounds were not characterised spectroscopically or structurally.[11]

The coordination of distibine ligands of the form $R_2Sb(CH_2)_3SbR_2$, $R_2SbCH_2SbR_2$ R = Me or Ph) and o-$C_6H_4(CH_2SbMe_2)_2$ with $[Me_3PtI]$ and $[Me_2Pt(SMe_2)_2]$ starting materials is reported in this Chapter. Together with the synthesis of these complexes, their spectroscopic and structural properties are also described. Selected examples with monostibines are also prepared for comparative purposes. Crystal structures of five representative examples involving Pt(IV) are described which provide the basis for comparisons of the Pt-Sb bonding in these species.

This work also provides a useful comparison with the synthesis and reaction chemistry of a wide range of Pt(II)-dimethyl and Pt(IV)-trimethyl complexes that incorporate phosphine and arsine ligands, that have been studied previously.[12]

3.2. Results and Discussion

3.2.1. Pt(II) Complexes

$[PtMe_2\{Ph_2Sb(CH_2)_3SbPh_2\}]$ was obtained as a light yellow solid in good yield through the reaction of $[PtMe_2(cod)]$ and one molar equivalent of $Ph_2Sb(CH_2)_3SbPh_2$ stirred for 12 h in toluene. The microanalysis results support the formulation of the desired product and indeed, the ^1H NMR spectrum showed the coordination of the ligand to the Me_2Pt fragment showing a single Pt-Me resonance at 1.05 ppm ($^2J_{Pt\text{-}H}$ 85 Hz). There were also peaks at 2.40-2.15 (m) and 7.10-7.60 (m) corresponding to methylene and phenyl protons respectively, proving the coordination of the ligand. The $^{13}C\{^1H\}$ NMR spectrum showed a singlet at -3.63 ppm ($^1J_{PtC}$ = 716 Hz) corresponding to the methyl groups directly coordinated to the platinum metal centre, along with resonances corresponding to the coordinated, bidentate, stibine ligand. There was no evidence of residual cod in either NMR spectra, which shows clean substitution had taken place. It is interesting to note that the $^1J_{PtC}$ coupling constant is significantly larger than the analogous phosphine complex, $[PtMe_2\{Ph_2P(CH_2)_3PPh_2\}]$ ($^1J_{PtC}$ = 595 Hz),[13] which can be explained by the fact that the stibine is lower in the *trans* influence series than the phosphine ligand. The ^{195}Pt NMR spectrum showed one resonance at -4804 ppm, indicating that the isolated yellow solid contained only one platinum containing species.

Attempts to make the corresponding $[PtMe_2(L\text{-}L)]$ (L-L = $Me_2Sb(CH_2)_3SbMe_2$ or o-$C_6H_4(CH_2SbMe_2)_2$) by a similar route to above were not successful, as there was evidence in the NMR spectra that there had been only partial substitution of the cod. Even with prolonged reaction times (>24 h) and heating of the reaction mixture the substitution did not go to completion and often led to decompostion, which was indicated by the solution turning brown/black. The alternative starting material, $[PtMe_2(SMe_2)_2]$, was therefore employed due to the more labile SMe_2 ligand. Reaction of $[PtMe_2(SMe_2)_2]$ and one molar equivalent of $Ph_2Sb(CH_2)_3SbPh_2$ in CH_2Cl_2 produced $[PtMe_2\{Ph_2Sb(CH_2)_3SbPh_2\}]$ very cleanly in high yield, and all the data agreed with that discussed above for the complex. $Me_2Sb(CH_2)_3SbMe_2$ and *o*-$C_6H_4(CH_2SbMe_2)_2$, however, did not react cleanly in CH_2Cl_2 with $[PtMe_2(SMe_2)_2]$, but gentle warming a solution of the appropriate ligand and one molar equivalent of the platinum starting material in benzene, generated the mononuclear $[PtMe_2(L\text{-}L)]$ (L-L = $Me_2Sb(CH_2)_3SbMe_2$, *o*-$C_6H_4(CH_2SbMe_2)_2$) in good yield as a pale yellow oil and a light yellow solid respectively. With C_1 linked distibine ligands, complexes of the form $[(PtMe_2)_2(L'\text{-}L')_2]$ (L'-L' = $Me_2SbCH_2SbMe_2$ or $Ph_2SbCH_2SbPh_2$) were obtained. The reaction scheme for these reactions is show in Figure 3.2.1.

Fig 3.2.1: Reaction scheme for $[PtMe_2(L\text{-}L)]$ and $[(PtMe_2)_2(L'\text{-}L')_2]$ where L-L = $R_2Sb(CH_2)_3SbR_2$ or *o*-$C_6H_4(CH_2SbMe_2)_2$ and L'-L' = $R_2SbCH_2SbR_2$ (R = Me, Ph).

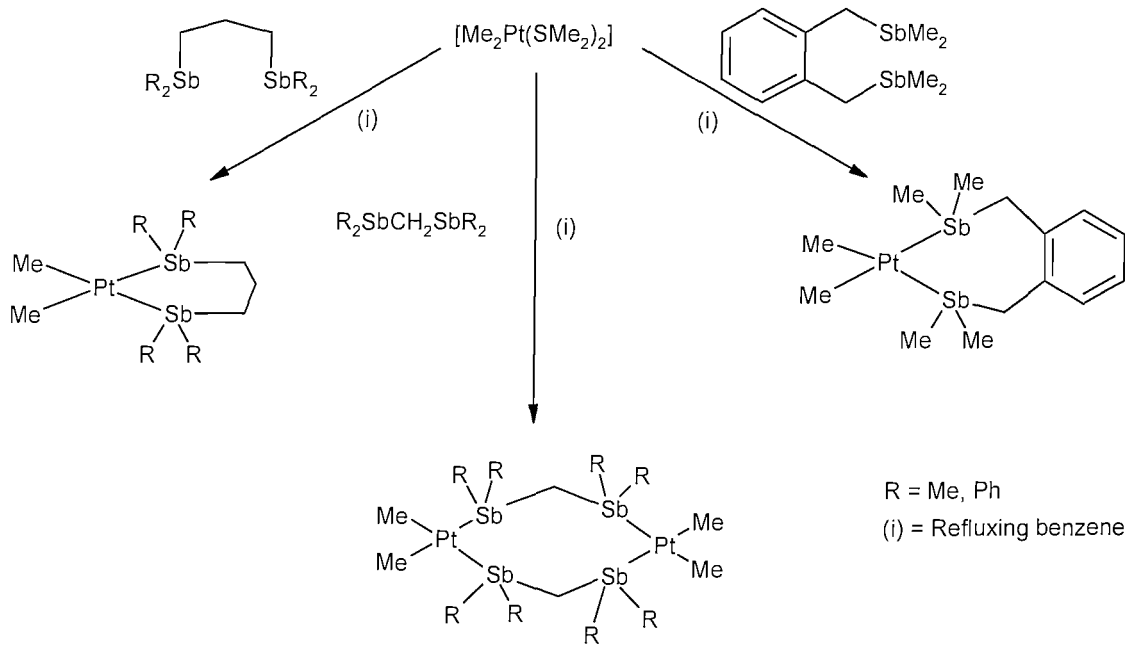

The electrospray mass spectrometry (MeCN) of all the Pt(II) complexes described above showed the major species resulting from loss of Me from the parent compound, $[Parent\text{-}Me]^+$. This strongly supports the formulations of the structures made above for both the monomeric and dimeric species. Surprisingly, decomposition in chlorinated solvents and benzene was observed in all cases apart from $[PtMe_2\{Ph_2Sb(CH_2)_3SbPh_2\}]$. The most extensive decomposition was seen for $[(PtMe_2)_2(Ph_2SbCH_2SbPh_2)_2]$ where we were unable to obtain a resonance in the ^{195}Pt NMR spectrum. Selected NMR spectroscopic data for the platinum(II) complexes are presented in Table 3.2.1 showing that they are similar to $[PtMe_2\{Ph_2Sb(CH_2)_3SbPh_2\}]$. As expected they have similar Pt-C and Pt-H couplings within the dialkyl-Pt unit. The ^{195}Pt NMR shifts are all *ca.* -4800 ppm, significantly shifted to low frequency of the Pt(IV) complexes reported below, and the ^{195}Pt NMR spectrum of $[PtMe_2\{o\text{-}C_6H_4(CH_2SbMe_2)_2\}]$ is shown in Figure 3.2.2. Little platinum-195 NMR data on stibine complexes is available, however $\delta(^{195}Pt)$ for $[PtCl_2\{Ph_2Sb(CH_2)_3SbPh_2\}]$ and $[PtCl_2\{Me_2Sb(CH_2)_3SbMe_2\}]$ are -4556 and -4553 respectively, some 250 ppm to high frequency of the Pt(II) methyl analogues in this work.[14]

Table 3.2.1: Selected NMR spectroscopy data for the platinum(II) complexes.

Complex	$\delta(^{13}C\{^1H\})$ (ppm)	$^1J_{PtC}$ / Hz	$\delta(^{195}Pt)$ (ppm)
$[PtMe_2\{Ph_2Sb(CH_2)_3SbPh_2\}]$	-3.63 PtMe	716	-4804
$[PtMe_2\{Me_2Sb(CH_2)_3SbMe_2\}]^a$	-4.98 PtMe	[b]	-4722
$[PtMe_2\{o\text{-}C_6H_4(CH_2SbMe_2)_2\}]^a$	-3.85 PtMe	726	-4687
$[(PtMe_2)_2(Me_2SbCH_2SbMe_2)_2]^a$	-3.96 PtMe	711	-4802

[a] Spectra recorded in d^6-benzene; others in $CDCl_3$. [b] Pt-C coupling unclear.

Fig 3.2.2: ^{195}Pt NMR Spectrum for $[Me_2Pt\{o\text{-}C_6H_4(CH_2SbMe_2)_2\}]$ in d^6-benzene.

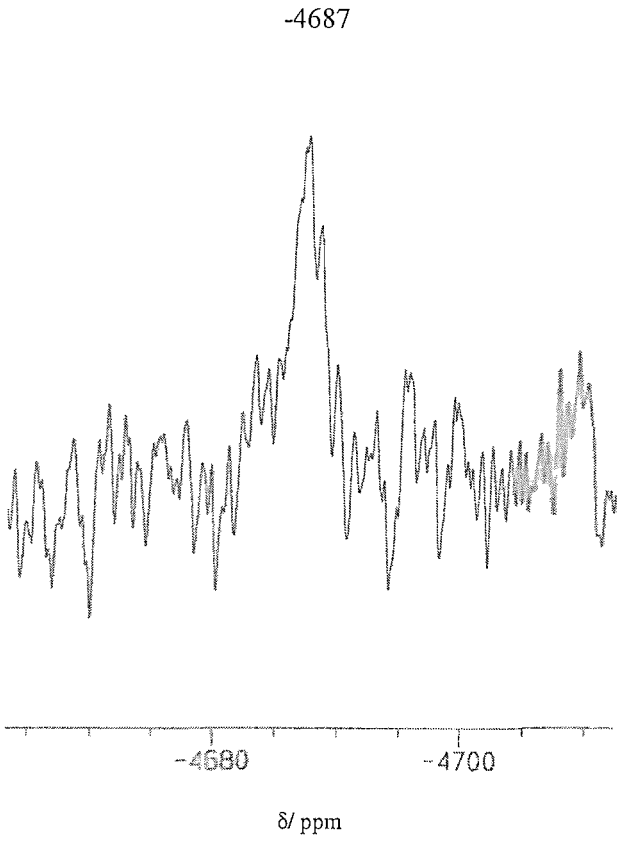

3.2.2 Pt(IV) Complexes

Complexes of the form $[PtMe_3(L\text{-}L)I]$ (L-L = $R_2Sb(CH_2)_3SbR_2$; R = Me or Ph; *o*-$C_6H_4(CH_2SbMe_2)_2$ or L-L = 2 x $SbPh_3$, $SbPh_2Me$ or $SbPhMe_2$) were prepared by reaction of $[PtMe_3I]$ with one molar equivalent of the appropriate bidentate ligands and two equivalents of the monodentate ligands in refluxing $CHCl_3$. The complexes were obtained in high yield, as air stable yellow solids, with the exception of $[PtMe_3(SbPhMe_2)_2I]$ which was obtained as a pale yellow oil. Complexes of the form $[\{PtMe_3I\}_2(\mu\text{-}R_2SbCH_2SbR_2)]$ were prepared by similar reaction, even when a 1:1 Pt:distibine ratio was used. It can be suggested that this was due to the short methylene linkage in the ligand, between the two Sb centres, which is not preorganised for chelation. Research by Puddephatt and co-workers supports this argument as they reported the formation of $[(PtMe_3)_2(\mu\text{-}Ph_2PCH_2PPh_2)_2(\mu\text{-}I)_2]$.[15] The reaction schemes for the first series of stable formally Pt(IV) distibine complexes are shown in Fig. 3.2.3.

Fig 3.2.3: Reaction scheme of $[PtMe_3(L\text{-}L)I]$ and $[(PtMe_3)_2(\mu\text{-}R_2SbCH_2SbR_2)(\mu\text{-}I)_2]$ where L-L = $R_2Sb(CH_2)_3SbR_2$, o-$C_6H_4(CH_2SbMe_2)_2$ or 2 x $SbPh_3$, $SbPh_2Me$ or $SbPhMe_2$ (R = Me, Ph).

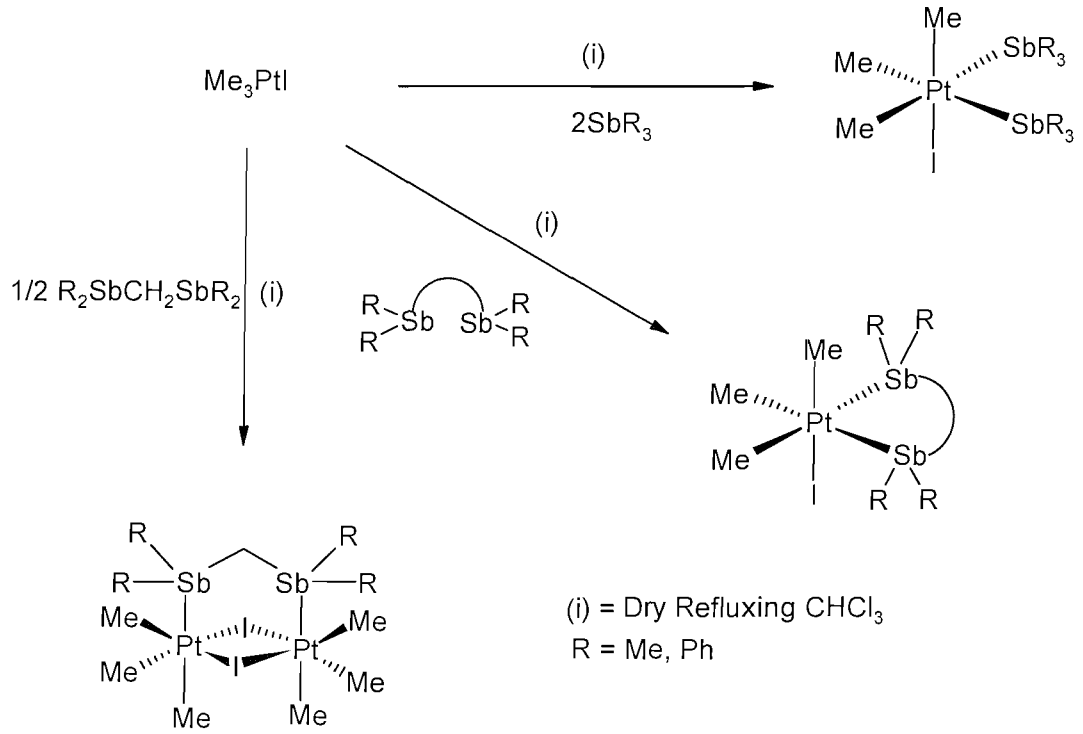

The NMR spectroscopic data for the above compounds show that the desired complexes have been formed. For example, the ^{1}H NMR data for [$Me_3Pt(Ph_2Sb(CH_2)_3SbPh_2)I$] showed peaks at 1.20 (s), ($^2J_{PtH}$ = 72 Hz), Me *trans* I, 1.70 (s) ($^2J_{PtH}$ = 65 Hz), Me *trans* Sb, and 2.10-2.80 (m) CH_2, 7.20-7.75 (m) Ph, with corresponding platinum satellites and coupling constants. The other complexes in the family show similar resonances. The ^{13}C {^{1}H} NMR spectrum also supports the ^{1}H NMR data, with peaks at -3.17 ($^1J_{PtC}$ = 616 Hz) Me *trans* I, 5.31 ($^1J_{PtC}$ = 575) Me *trans* Sb, 18.30 $SbCH_2$, 24.12 $CH_2CH_2CH_2$ and 127.23-136.90 Ph. A summary of the ^{195}Pt {^{1}H} NMR spectroscopy and ^{13}C {^{1}H} NMR spectroscopy data of all the Pt(IV) complexes is shown in Table 3.2.2. All the platinum shifts for the Pt(IV) complexes are around -4400 ppm, indicating that the geometries and platinum environments are similar.

Table 3.2.2: Selected NMR spectroscopic data for the Pt(IV) complexes.

Complex	$\delta(^{13}C\{^1H\})$ (ppm)	$^1J_{PtC}$ / Hz	$\delta(^{195}Pt)$ (ppm)
[$Me_3Pt\{Ph_2Sb(CH_2)_3SbPh_2\}I$]	-3.17 (1C) PtMe *trans* I	616	-4381
	5.31 (2C) PtMe *trans* Sb	575	
[$Me_3Pt\{Me_2Sb(CH_2)_3SbMe_2\}I$]	-6.20 (1C) PtMe *trans* I	628	-4491
	1.85 (2C) PtMe *trans* Sb	553	
[$Me_3Pt\{o\text{-}C_6H_4(CH_2SbMe_2)_2\}I$]	-6.20 (1C) PtMe *trans* I	611	-4384
	3.82 (2C) PtMe *trans* Sb	562	
[$(PtMe_3)(\mu\text{-}Ph_2SbCH_2SbPh_2)(\mu\text{-}I)_2$]	5.53 (2C) PtMe *trans* I	655	-4360
	8.27 (1C) PtMe *trans* Sb	684	
[$(PtMe_3)(\mu\text{-}Me_2SbCH_2SbMe_2)(\mu\text{-}I)_2$]	4.17 (2C) PtMe *trans* I	692	-4509
	12.78 (1C) PtMe *trans* Sb	571	
[$Me_3Pt(SbPh_3)_2I$]	-3.72 (1C) PtMe *trans* I	606	-4380
	10.43 (2C) PtMe *trans* Sb	542	
[$Me_3Pt(SbMePh_2)I$]	-5.04 (1C) PtMe *trans* I	611	-4419
	7.59 (2C) PtMe *trans* Sb	566	
$Me_3Pt(SbMe_2Ph)I$]	-5.87 (1C) PtMe *trans* I	643	-4471
	5.16 (2C) PtMe *trans* Sb	564	

Electrospray mass spectrometry (MeCN) supported the NMR spectroscopic data for the Pt(IV) complexes incorporating chelating distibine ligands, by showing the major peaks as corresponding to $[PtMe(L\text{-}L)]^+$ and $[PtMe(L\text{-}L)(MeCN)]^+$. In the case of the complexes incorporating

monodentate stibines or the bridging ligands, the only significant peaks were that of $[PtMe_3(MeCN)_n]^+$ (n = 1, 2 and 3). This suggests that under the mass spectrometry conditions the Pt-Sb bond is cleaved easily.

From Table 3.2.2 it can be seen that the general trends in the chemical shifts for these novel Pt(IV) complexes are similar to those observed for phosphine and arsine derivatives.[16] For example the ^1H NMR spectra for all the complexes show two Pt-Me resonances, one for the Me ligand *trans* to Sb and the other, with larger coupling constant (see Table 3.2.2), for the Me ligand *trans* to iodine. The ^1H and $^{13}C\{^1H\}$ NMR spectra showed two SbMe resonances for the Me-substituted distibine ligands, and in some cases there was clear evidence of ^{195}Pt coupling through the quadrupolar antimony centres. For example in the case of $[(PtMe_3)_2(\mu\text{-}Me_2SbCH_2SbMe_2)(\mu\text{-}I)_2]$ the resonances that correspond to protons of SbMe and $SbCH_2$ showed Pt-H couplings of 3-4 Hz in the ^1H NMR spectrum. Fig 3.2.4 shows the ^1H NMR spectrum of $[(PtMe_3)_2(\mu\text{-}Me_2SbCH_2SbMe_2)(\mu\text{-}I)_2]$.

Fig 3.2.4: ^1H NMR spectrum of $[(PtMe_3)_2(\mu\text{-}Me_2SbCH_2SbMe_2)(\mu\text{-}I)_2]$ ($CDCl_3$).

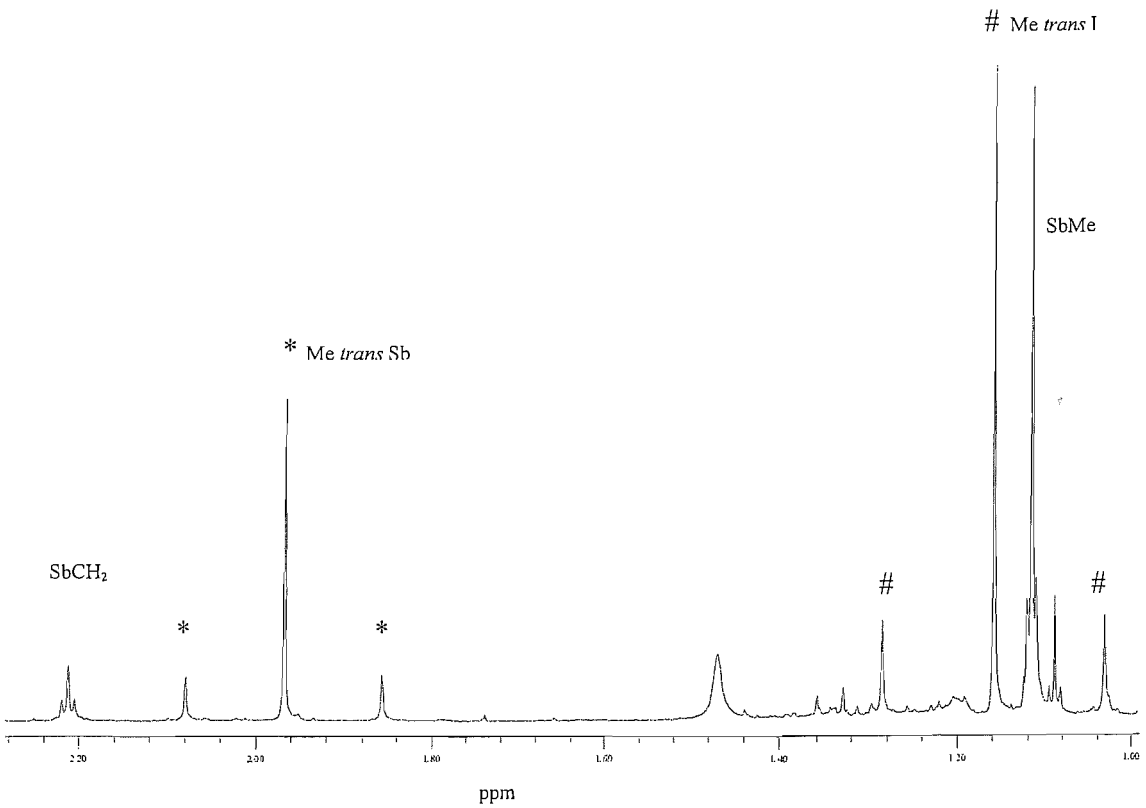

From Table 3.2.2, it is evident that all the Pt(IV) complexes have one platinum containing species in the bulk. This is shown by one single resonance in the ^{195}Pt NMR spectrum at *ca.* -4400 ppm. This is of significance as these resonances are some 400 ppm to higher frequency than the corresponding dimethyl-Pt(II) species reported earlier in this chapter (Table 3.2.1), indicating the different electronic environment around the platinum centre. Literature examples of related methyl Pt(II) and Pt(IV) phosphines and arsines show very similar trends with oxidation state in ^{195}Pt NMR shifts, but it must also be noted that the nature of the Group 15 donor atom of the ligand does have a significant effect. For example in the case of $[PtMe_3I(PMe_2Ph)_2]$ and $[PtMe_3I(SbMe_2Ph)_2]$ the $\delta(^{195}Pt)$ values are –4277 ppm and –4471 ppm respectively, in addition $[PtMe_3I(PMePh_2)_2]$ and $[PtMe_3I(SbMePh_2)_2]$ have $\delta(^{195}Pt)$ values of –4227 and –4582 ppm respectively.[16] This can be explained by the incorporation of the heavier antimony atom in the ligand rather than phosphorus. It is also interesting to note that the dinuclear species $[(PtMe_3)_2(\mu\text{-}R_2SbCH_2SbR_2)(\mu\text{-}I)_2]$, has $\delta(^{195}Pt)$ values of -4360 ppm (R = Ph) and -4509 ppm (R = Me). These values are not significantly shifted from the mononuclear $[PtMe_3I(L\text{-}L)]$ complexes despite having two bridging iodo ligands. This suggests that changing a heavy I ligand for another heavy atom such as Sb does not have a significant effect electronically. Indeed Goodfellow and co-workers have seen this 'heavy atom effect' in their studies of platinum-195 chemical shifts.[17] For example with a I_3Sb donor set in $[PtI_3(SbMe_3)]^-$ the $\delta(^{195}Pt)$ value is -5642 ppm, whereas with a I_2Sb_2 donor set in $[PtI_2(SbMe_3)_2]$ the $\delta(^{195}Pt)$ value is -5815 ppm. The coupling constants ($^1J_{Pt\text{-}C}$) for the Pt(IV) complexes reported by Goodfellow are also consistent with the work reported here, *ca.* 550-650 Hz, with the larger couplings occurring for Me *trans* I.

The synthesis of this novel series of stable Pt(IV) distibines is interesting as it extends the boundaries of the chemistry and the ligating properties of the ligands, however the reaction chemistry of the complexes is also important as it gives indications as to possible application for the future. There have been detailed studies by Puddephatt and co-workers on the reaction chemistry of analogous alkyl-Pt complexes with phosphine ligands. They have shown that reaction of the dimethyl-Pt(II) complexes with MeI leads to the oxidative addition of the MeI and yields the expected Pt(IV) complex of the form $[PtMe_3I(diphosphine)]$. Moreover these trimethyl-Pt(IV) species can then be thermolysed and readily undergo reductive elimination of ethane.[18] Similarly to these studies we have shown that treating $[PtMe_2\{Me_2Sb(CH_2)_3SbMe_2\}]$ in d^6-benzene with MeI gives a quantitative conversion (by ^{1}H NMR spectroscopy) of the dimethyl-Pt(II) complex to $[PtMe_3I\{Me_2Sb(CH_2)_3SbMe_2\}]$. Furthermore, thermogravimetric analysis of $[PtMe_3I(SbPh_3)_2]$ shows a mass loss at 170°C indicative of reductive elimination of ethane. These

results are significant, as they prove that despite the fragility of the Sb-C bonds the stibine ligands are tightly enough bound to support both Pt(II) and Pt(IV) centres and indeed *via* simple reactions can undergo oxidative addition or reductive elimination reaction chemistry to convert between the two oxidation states. The stability of these complexes can be attributed to the strong ligand field effects in the Pt-methyl complexes in contrast to other Pt(IV) tetrachloro distibine complexes of the form [$PtCl_4$(distibine)], which are extremely unstable.[8]

3.2.3 Structural Studies

In order to provide unambiguous assignment of the Pt(IV) stibine complexes geometries, five crystal structures of representative examples of these complexes have been obtained. The structures also allow comparisons with similar complexes in the literature, in particular complexes incorporating Pt(II) centres.

The structure of [$PtMe_3\{Ph_2Sb(CH_2)_3SbPh_2\}I$] is shown in Figure 3.2.5 and selected bond lengths and angles are shown in Table 3.2.3. The structure is a distorted octahedral Pt(IV) centre coordinated to three fac Me groups, one I ligand and two Sb atoms from a chelating distibine. [$PtMe_3\{Me_2Sb(CH_2)_3SbMe_2\}I$] adopts a very similar arrangement and is shown in Figure 3.2.6 and selected bond lengths and angles are shown in Table 3.2.4. However, in the structure of [$PtMe_3\{Me_2Sb(CH_2)_3SbMe_2\}I$] the platinum centre, C6, and I1 occupy a mirror plane, which cuts the distibine ligand in two. Similar geometries are seen in the crystal structures of [$PtMe_3\{o\text{-}C_6H_4(CH_2SbMe_2)_2\}I$] (Fig. 3.2.7, Table 3.2.5) and [$PtMe_3(SbPh_3)_2I$] (Fig. 3.2.8, Table 3.2.6).

Fig 3.2.5: View of the structure $[Me_3Pt\{Ph_2Sb(CH_2)_3SbPh_2\}I]$ with numbering scheme adopted. H atoms have been omitted for clarity and ellipsoids are shown at 50 % probability level.

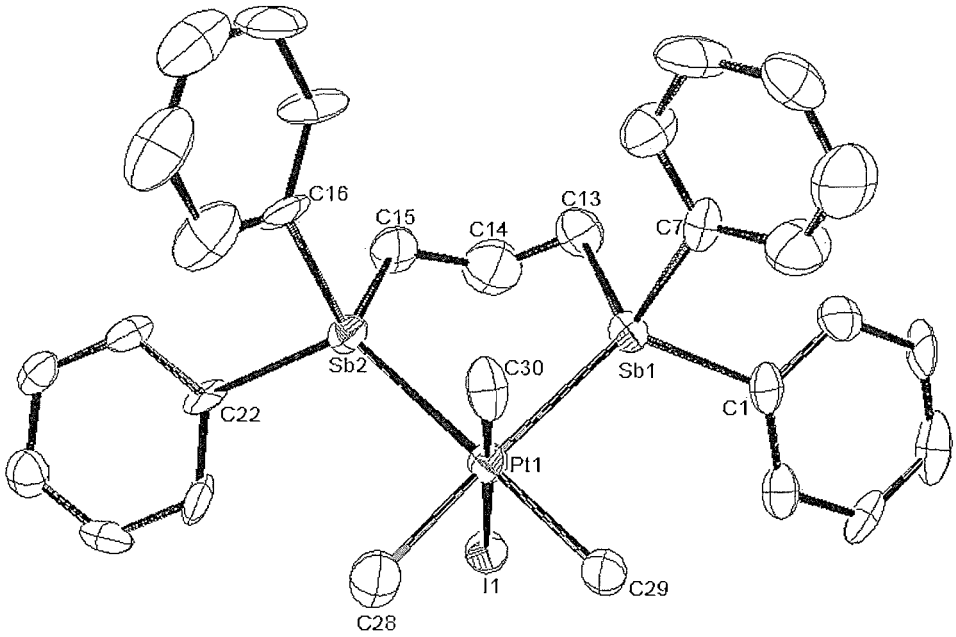

Table 3.2.3: Selected bond lengths (Å) and angles (°) for $[Me_3Pt\{Ph_2Sb(CH_2)_3SbPh_2\}I]$.

Pt1-C30	2.066(13)	C30-Pt1-C28	88.0(5)
Pt1-C29	2.098(12)	C29-Pt1-Sb1	92.7(3)
Pt1-C28	2.107(12)	C28-Pt1-Sb1	177.2(4)
Pt1-Sb1	2.6026(11)	C30-Pt1-Sb2	92.2(4)
Pt1-Sb2	2.6344(11)	C29-Pt1-Sb2	179.6(3)
Pt1-I1	2.7829(11)	Sb1-Pt1-Sb2	87.68(3)
		C30-Pt1-I1	179.2(3)
		C29-Pt1-I1	92.8(4)

Fig 3.2.6: View of the structure $[Me_3Pt\{Me_2Sb(CH_2)_3SbMe_2\}I]$ with numbering scheme adopted. H atoms have been omitted for clarity and ellipsoids are shown at 50 % probability level. There is a mirror plane passing through Pt1, I1, C4 and C5, with symmetry operation: a = x, ½ - y, z.

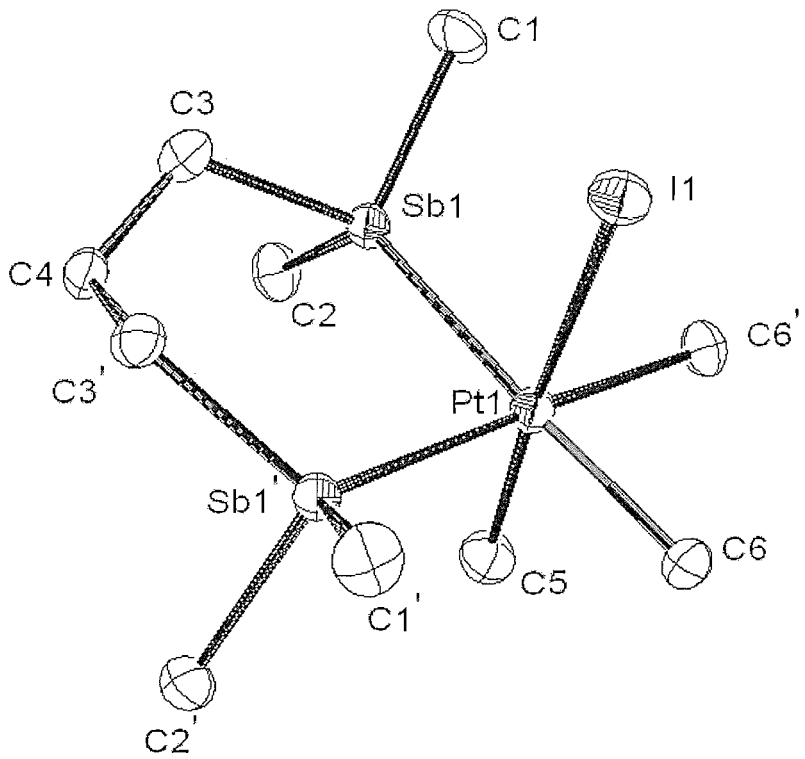

Table 3.2.4: Selected bond lengths (Å) and angles (°) for $[Me_3Pt\{Me_2Sb(CH_2)_3SbMe_2\}I]$.

Pt1-C5	2.076(9)	C5-Pt1-C6	86.9(3)
Pt1-C6	2.141(6)	C5-Pt1-Sb1	93.9(2)
Pt1-Sb1	2.6169(6)	C6-Pt1-Sb1	177.09(19)
Pt-I1	2.7777(9)	Sb1-Pt1-Sb1	89.63(2)
Sb1-C1	2.113(7)	C5-Pt1-I1	176.5(3)
Sb1-C2	2.125(6)	C6-Pt1-I1	90.52(18)
Sb1-C3	2.129(6)	Sb1-Pt1-I1	88.532(16)

Fig 3.2.7: View of the structure $[Me_3Pt\{o\text{-}C_6H_4(CH_2SbMe_2)_2\}I]$ with numbering scheme adopted. H atoms have been omitted for clarity and ellipsoids are shown at 50 % probability level.

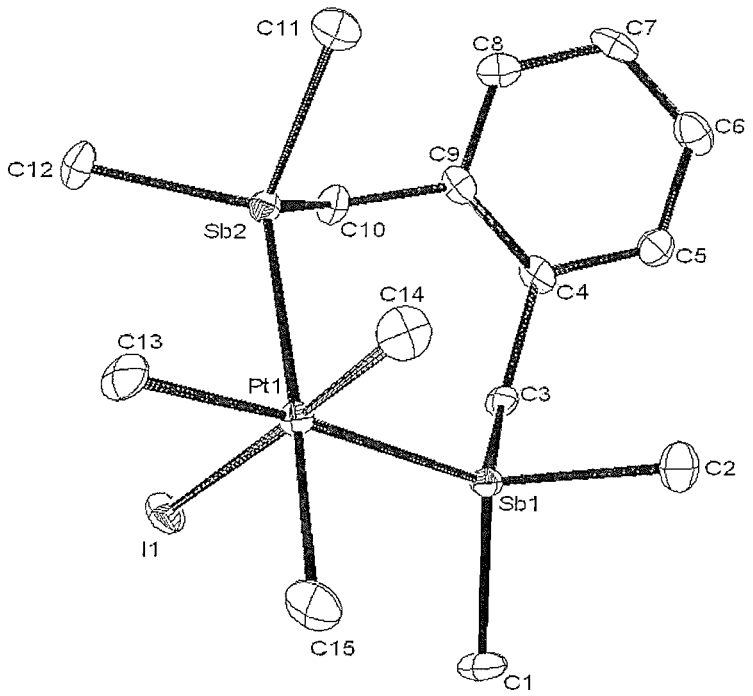

Table 3.2.5: Selected bond lengths (Å) and angles (°) for $[Me_3Pt\{o\text{-}C_6H_4(CH_2SbMe_2)_2\}I]$.

Pt1 C14	2.070(6)	C14 Pt1 C15	86.8(3)
Pt1 C15	2.108(7)	C14 Pt1 Sb2	94.6(2)
Pt1 C13	2.109(6)	C15 Pt1 Sb2	177.0(2)
Pt1 Sb2	2.6054(7)	C14 Pt1 Sb1	96.4(2)
Pt1 Sb1	2.6204(15)	C15 Pt1 Sb1	87.25(19)
Pt1 I1	2.7811(10)	C13 Pt1 Sb1	175.93(18)
		Sb2 Pt1 Sb1	95.245(15)
		C14 Pt1 I1	178.3(2)
		C15 Pt1 I1	94.7(2)
		Sb2 Pt1 I1	83.90(3)
		Sb1 Pt1 I1	84.569(I5)

Fig 3.2.8: View of the structure of one of the crystallographically independent molecules of $[PtMe_2(SbPh_3)_2I]$ with numbering scheme adopted (the other molecule in the assymetric unit is essentially indistinquishable). H atoms are omitted for clarity, and ellipsoids are shown at 50 % probability level. There is diorder in the I2-Pt2-C77 unit (see text).

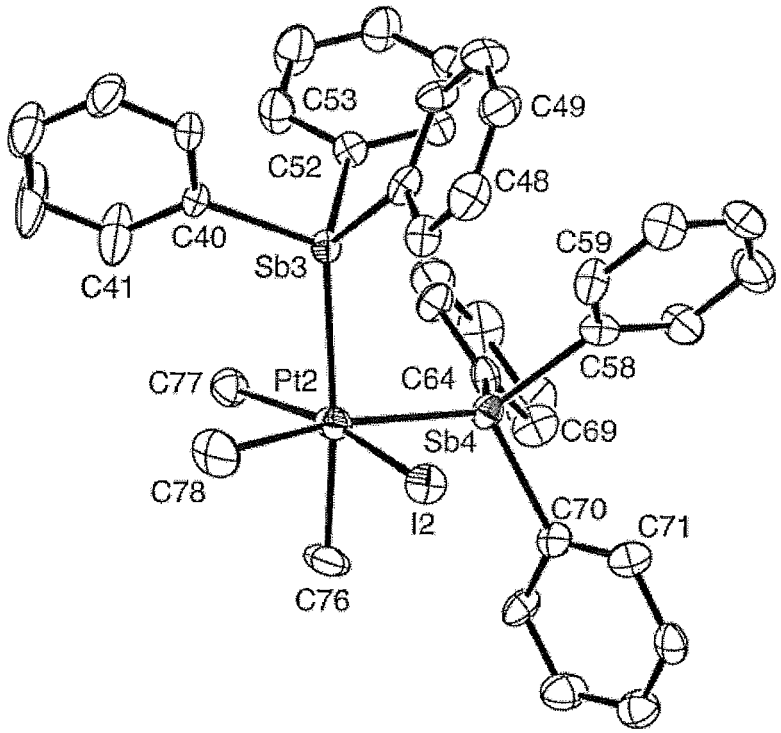

Table 3.2.6: Selected bond lengths (Å) and angles (°) for $[Me_3Pt\{SbPh_3)_2\}I]$.[a]

Pt2-C78	2.098(9)	C78-Pt2-C76	85.3(4)
Pt2-C77	2.5679(14)[b]	C76-Pt2-C77	87.0(4)[b]
Pt2-Sb4	2.6551(7)	C76-Pt2-I2	85.5(4)[b]
Pt2-C76	2.102(9)	C78-Pt2-Sb4	171.4(3)
Pt2-I2	2.6302(12)[b]	C77-Pt2-Sb4	95.31(3)[b]
Pt2-Sb3	2.6651(7)	C78-Pt2-Sb3	91.7(3)
		Sb4-Pt2-Sb3	96.48(2)
		C77-Pt2-I2	170.81(4)[b]
		I2-Pt2-Sb4	89.46(3)[b]

[a] Bond lengths and angles for the second molecule invloving Pt1, I1, Sb1, Sb2 and C1-C39 are similar and also have disorder in the *trans* I1-Pt1-C fragment. [b] Disordered group I2/C77A-Pt2-C77/I2A with chemically unreliable bond lengths and angles. This is most marked in the Pt2-C77 bond length when comparing with other Pt-C distances.

The Sb-Pt(IV) bond distances in all of the chelated distibine complexes lie in the range 2.6025(11) –2.6342(11) Å, significantly longer than in Pt(II) distibines,[19] for example $[PtCl_2\{o\text{-}C_6H_4(CH_2SbMe_2)_2\}]$ has Pt-Sb bonds of 2.4860(7) and 2.4931(8) Å and $[Pt\{o\text{-}C_6H_4(CH_2SbMe_2)_2\}_2]^{2+}$ has Pt-Sb bonds of length 2.5690(8)–2.5802(8) Å. This lengthening of the Pt-Sb bond could be attributed to the higher coordination number of the Pt(IV) distibine complexes and the strong *trans* influence of the methyl groups around the platinum centre.

The Sb-Pt-Sb angles in the Pt(IV) stibine complexes reflect the different chelate ring sizes, with the $o\text{-}C_6H_4(CH_2SbMe_2)_2$ ligand, which forms a 7-membered ring chelate, giving a wide bite angle of 95.246(11)°. With the ligands that form 6-membered chelates ($R_2Sb(CH_2)_3SbR_2$) the Sb-Pt-Sb angles are less than 90°. The same trend is seen in the non-bonded Sb···Sb distances within the chelates. Therefore the Sb···Sb distance is *ca.* 0.17 Å greater for the $o\text{-}C_6H_4(CH_2SbMe_2)_2$ complex than the $R_2Sb(CH_2)_3SbR_2$ complexes. These comparisions can be seen in Table 3.2.7. Moreover, the Pt-Sb distances (2.6457(7)–2.6656(7) Å), and Sb-Pt-Sb angles (96.48(2), 96.74(2)°) in $[PtMe_3I(SbPh_3)_2]$ are similar the bond lengths and angles found in $[PtMe_3I\{o\text{-}C_6H_4(CH_2SbMe_2)_2\}_2]$ which can be attributed to the substantial steric bulk of the $SbPh_3$ ligand in $[PtMe_3I(SbPh_3)_2]$.

Table 3.2.7: Comparison of the non-bonded Sb···Sb distances within the distibine chelates rings of the Pt(IV) complexes.

Complex	Non-bonded Sb···Sb distance / Å
$[Me_3Pt(Ph_2Sb(CH_2)_3SbPh_2)I]$	3.627
$[Me_3Pt(Me_2Sb(CH_2)_3SbMe_2)I]$	3.689
$[Me_3Pt(o\text{-}C_6H_4(CH_2SbMe_2)_2)I]$	3.860
$[Me_3Pt(\{CH_2(o\text{-}C_6H_4CH_2SbMe_2\}_2)I]$ (Chapter 2)	3.902

Another trend in the crystal structures is that the $Pt\text{-}C_{trans\ Sb}$ distances are all *ca.* 2.1 Å, which is longer than the $Pt\text{-}C_{trans\ I}$ distances. It can be suggested that this is due to the stibine exerting a stronger *trans* influence than the iodide ligand. It has been observed that structures that incorporate $SbPh_3$ and $Ph_2SbCH_2SbPh_2$ as ligands have an increase in C-Sb-C bond angle of about 8 degrees when complexed to a medium oxidation state transition metal due to the rehybridisation which takes place at antimony upon coordination to a metal centre.[20] It is also important to note

that when comparing the data reported here with known Pt(II) stibines it can be seen that the Sb-Pt-Sb angles are essentially unaffected by changes in oxidation state.

Figure 3.2.9 and Table 3.2.8 shows the structure, selected bond lengths and angles of $[(PtMe_3I)_2\{Ph_2SbCH_2SbPh_2\}]$. It confirms that the short C_1-linked distibine ligands bridge two $PtMe_3$ fragments. Completing the distorted octahedral geometry around the platinum metal centres are two bridging iodo ligands, giving an edge shared bioctahedral structure. The NMR spectroscopic studies on the above compound and that of $[(PtMe_3I)_2\{Me_2SbCH_2SbMe_2\}]$ are consistent with the crystal structure. The Pt-Sb bond distances of 2.6530(5) and 2.6793(5) Å are longer (by *ca.* 0.05 Å) than those in the mononuclear species above. This may be a consequence of the short C_1-linked distibine ligand having difficulty in spanning the two Pt centres. The rather open Sb1-C16-Sb2 angle (116.2(2)°) is also consistent with this. Puddephatt and co-workers synthesised $[(PtMe_3)_2(\mu\text{-}I)\{\mu\text{-}R_2PCH_2PR_2\}_2]I$ (R = Et, Me), and these complexes were fully characterised.[18] A crystal structure of $[(PtMe_3)_2(\mu\text{-}I)\{\mu\text{-}Me_2PCH_2PMe_2\}_2]I$ was also obtained, and it is interesting to note that the $Me_2PCH_2PMe_2$ ligand is more strained spanning the two platinum centres, due to the shorter P–C distances of 1.835(10) and 1.823(10) Å than the Sb–C distances in $[(PtMe_3I)_2\{Ph_2SbCH_2SbPh_2\}]$ of 2.136(5) and 2.318(6) Å. It is also of interest to note that the C–P–C angle of the two ligands spanning the two platinum centres is 125.8(5)° some 10° larger than in the stibine complex above.

Fig 3.2.9: View of the structure $[(PtMe_3I)_2\{Ph_2SbCH_2SbPh_2\}]$ with numbering scheme adopted. H atoms have been omitted for clarity and ellipsoids are shown at 50 % probability level.

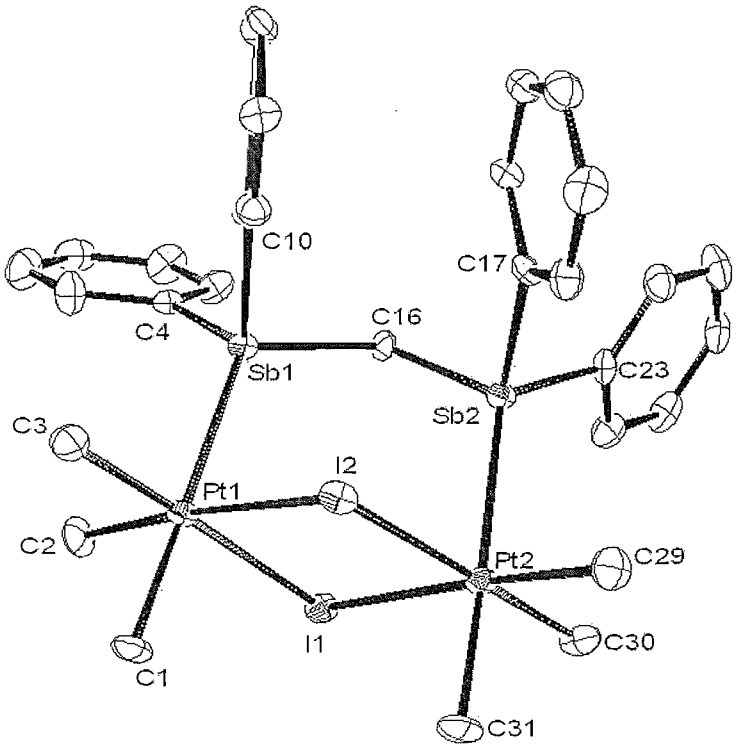

Table 3.2.8: Selected bond lengths (Å) and angles (°) for $[(PtMe_3I)_2\{Ph_2SbCH_2SbPh_2\}]$.

Pt1-C1	2.064(6)	C2-Pt1-C1	87.8(3)
Pt1-C2	2.054(6)	C2-Pt1-Sb1	93.18(19)
Pt1-C3	2.064(6)	C1-Pt1-Sb1	178.36(19)
Pt1-Sb1	2.6491(4)	C2-Pt1-I2	174.9(2)
Pt1-I1	2.7946(5)	C1-Pt1-I2	88.51(19)
Pt1-I2	2.7897(4)	Sb1-Pt1-I2	90.594(13)
		Sb1-Pt1-I1	88.361(15)
		I2-Pt1-I1	85.712(14)

3.3 Conclusions

A novel series of stable formally Pt(IV) stibine complexes have been prepared in high yield and are of the form $[Me_3Pt(L\text{-}L)I]$ and $[(PtMe_3)(\mu\text{-}R_2SbCH_2SbR_2)(\mu\text{-}I)_2]$ (L-L = $R_2Sb(CH_2)_3SbR_2$, *o*-$C_6H_4(CH_2SbMe_2)_2$, 2 x $SbPh_3$, $PhMe_2Sb$ or Ph_2MeSb, R = Ph, Me). Also a series of alkyl-Pt(II) stibine complexes of the form $[Me_2Pt(L\text{-}L)]$ and $[\{PtMe_2\}_2(R_2SbCH_2SbR_2)_2]$ (L-L = $R_2Sb(CH_2)_3SbR_2$, *o*-$C_6H_4(CH_2SbMe_2)_2$, R = Me, Ph) have been prepared in good yield. From these results it can be seen that stibine ligands can bond effectively to organometallic fragments in both medium and high oxidation states. The dialkyl-Pt(II) stibine species readily undergo oxidative addition of MeI to form the trialkyl-Pt(IV) species, which in turn can undergo reductive elimination of ethane to form complexes incorporating a MePtI fragment. This reaction chemistry suggests that the systems are very versatile. It is also interesting to note that these novel, trimethyl-Pt(IV) stibine complexes contrast greatly with the very unstable tetrachloro Pt(IV) species $[PtCl_4(distibine)]$, and it is likely that the methyls around the platinum centre help to stabilise the complexes.

3.4 Experimental

Solvents were dried prior to use and all preparations were undertaken using standard Schlenk techniques under a N_2 atmosphere. The $[PtMe_3I]_4$,[21] $[PtMe_2(cod)]$,[22] $[PtMe_2(SMe_2)_2]$[23] and the stibine ligands were prepared as described previously.[24-26]

3.4.1. Platinum(II) compounds:

$[PtMe_2\{Ph_2Sb(CH_2)_3SbPh_2\}]$:

Method A: $[Me_2Pt(cod)]$ (0.042 g, 0.125 mmol) and $Ph_2Sb(CH_2)_3SbPh_2$ (0.075 g, 0.125 mmol) were dissolved in toluene (15 cm^3) and stirred under N_2 for 12 hrs. The resulting yellow solution was filtered, reduced in volume to ~ 1 cm^3 and hexane (10 cm^3) was added to precipitate a solid. The solution was decanted off and the yellow solid dried *in vacuo*. (Yield: 70%). Required for $[C_{29}H_{32}PtSb_2]$: C, 42.5; H, 3.9. Found: C 42.6; H, 3.8%. ^1H NMR: δ 1.05 (s) [6H], (Pt-C$\underline{H}_3$) ($^2J_{PtH}$ = 85 Hz), 2.40-2.15 (m) [6H] (C$\underline{H}_2$), 7.1-7.6 (m) [20H] (Ph). $^{13}C\{^1H\}$ NMR: δ -3.63 (Pt-$\underline{C}H_3$) ($^1J_{PtC}$ = 716 Hz), 18.57 ($\underline{C}H_2Sb$), 23.99 ($CH_2\underline{C}H_2CH_2$), 129.21, 130.04, 131.41, 135.91 (Ph).

Method B: $[Me_2Pt(SMe_2)_2]$ (0.060 g, 0.17 mmol) and $Ph_2Sb(CH_2)_3SbPh_2$ (0.1 g, 0.17 mmol) were dissolved in dry $CHCl_3$ (15 cm^3) and stirred at RT for 1 hr. The excess solvent was removed under reduced pressure, and the residues were triturated with hexane to afford a pale yellow solid. This was then dried *in vacuo*. ^1H and $^{13}C\{^1H\}$ NMR spectroscopy as for Method A.

$[PtMe_2\{Me_2Sb(CH_2)_3SbMe_2\}]$: $[Me_2Pt(SMe_2)_2]$ (0.060 g, 0.17 mmol) and $Me_2Sb(CH_2)_3SbMe_2$ (0.058 g, 0.17 mmol) were dissolved in dry C_6H_6 (5 cm^3) and stirred at RT for 15 minutes. The excess solvent was removed under reduced pressure, and the residues were triturated with hexane to afford a pale yellow oil which was dried *in vacuo*. (Yield: 65%). ES^+ MS (MeCN): 555 ($[^{195}PtMe\{Me_2{}^{121}Sb(CH_2)_3{}^{123}SbMe_2\}]^+$ 556). ^1H NMR (C_6D_6): δ 0.70 (s) [12H] (SbC$\underline{H}_3$) ($^3J_{PtH}$ = 7 Hz), 1.14 (m) [6H] (C$\underline{H}_2$), 1.48 (s) [6H] (Pt-C$\underline{H}_3$) ($^2J_{PtH}$ = 83 Hz). $^{13}C\{^1H\}$ NMR (C_6D_6): δ -6.1 (Sb$\underline{C}H_3$), -4.98 (Pt-$\underline{C}H_3$), 15.26 ($\underline{C}H_2Sb$), 24.47 ($CH_2\underline{C}H_2CH_2$). Due to decomposition of the complex in air over time, microanalytical data were not obtained.

$[PtMe_2\{o\text{-}C_6H_4(CH_2SbMe_2)_2\}]$: Method as for $[PtMe_2\{Me_2Sb(CH_2)_3SbMe_2\}]$. (Yield: 63%). Required for $[C_{14}H_{26}PtSb_2].0.5C_6H_{14}$: C, 30.2; H, 4.9. Found: C, 30.3; H, 4.1 % ES^+ MS (MeCN): 658 ($[^{195}Pt\{o\text{-}C_6H_4(CH_2{}^{121/123}SbMe_2)_2\}(MeCN)]^+$ 659), 617 ($[^{195}PtMe\{o$-

$C_6H_4(CH_2{}^{121/123}SbMe_2)_2\}]^+$ 618). ^1H NMR (C_6D_6): δ 0.73 (s) [12H] (SbC$\underline{H}_3$) ($^3J_{PtH}$ = 9 Hz), 1.26 (s) [6H] (Pt-C$\underline{H}_3$) ($^2J_{PtH}$ = 82 Hz), 2.88 (br s) [4H] (C$\underline{H}_2$), 6.6-6.9 (m) [4H] (Ar-$\underline{H}$). $^{13}C\{^1H\}$ NMR (C_6D_6): δ -5.55 (Sb$\underline{C}H_3$), -3.85 (Pt-$\underline{C}H_3$) ($^1J_{PtC}$ = 726 Hz), 23.15 ($\underline{C}H_2$). Due to decomposition of the complex in air over time, microanalytical data were not obtained.

$[(PtMe_2)_2(Ph_2SbCH_2SbPh_2)_2]$: Method as for $[PtMe_2\{Me_2Sb(CH_2)_3SbMe_2\}]$. (Yield = 70%). Required for $[C_{54}H_{56}Pt_2Sb_4].0.5C_6H_6$: C, 42.2; H, 3.7. Found: C, 42.4; H, 3.6 %. ES^+ MS (MeCN): 1569 ($[^{195}Pt_2Me_3(Ph_2{}^{121}SbCH_2{}^{123}SbPh_2)_2]^+$ 1567), 1341 ($[^{195}PtMe(Ph_2{}^{121}SbCH_2{}^{123}SbPh_2)_2]^+$ 1342). ^1H NMR (C_6D_6): δ 1.43 (s) [6H] (Pt-C$\underline{H}_3$) ($^2J_{PtH}$ = 82 Hz), 2.20 (br s) [2H] (C$\underline{H}_2$), 6.9-7.4 (m) [20H] (Ph).

$[(PtMe_2)_2(Me_2SbCH_2SbMe_2)_2]$: Method as for $[PtMe_2\{Me_2Sb(CH_2)_3SbMe_2\}]$. ES^+ MS (MeCN): 1071 ($[^{195}Pt_2Me_3(Me_2{}^{121}SbCH_2{}^{123}SbMe_2)_2]^+$ 1071), 845 ($[^{195}PtMe(Me_2{}^{121}SbCH_2{}^{123}SbMe_2)_2]$+ 846). ^1H NMR (C_6D_6): δ 0.95 (s) [12H] (SbC$\underline{H}_3$) ($^3J_{PtH}$ = 6 Hz), 1.17 (s) [6H] (Pt-C$\underline{H}_3$) ($^2J_{PtH}$ = 80 Hz), 1.27 (s) [2H] (C$\underline{H}_2$). $^{13}C\{^1H\}$ NMR (C_6D_6): δ -5.89 (Sb$\underline{C}H_3$), -3.96 (Pt-$\underline{C}H_3$) ($^1J_{PtC}$ = 711 Hz), -3.46 ($\underline{C}H_2$). Due to decomposition of the complex in air over time, microanalytical data were not obtained.

3.4.2. Platinum(IV) compounds:

$[PtMe_3\{Ph_2Sb(CH_2)_3SbPh_2\}I]$: Me_3PtI (0.065 g, 0.177 mmol) and $Ph_2Sb(CH_2)_3SbPh_2$ (0.105 g, 0.177 mmol) were dissolved in dry $CHCl_3$ (20 cm^3) under argon and refluxed for 4 hr. The light yellow solution was then pumped to dryness *in vacuo* to give a light yellow waxy solid which was triturated with hexane to produce a light yellow powder. (Yield: 80 mg, 50%). Required for $[C_{30}H_{35}IPtSb_2].0.5CHCl_3$: C, 35.9; H, 3.5%. Found: C, 36.4; H, 4.0%. ^1H NMR: δ 1.20 (s) [3H] (Me *trans* I) ($^2J_{PtH}$ = 72 Hz), 1.70 (s) [6H] (Me *trans* Sb) ($^2J_{PtH}$ = 65 Hz), 2.10-2.80 (m) [6H] (C$\underline{H}_2$), 7.20-7.75 (m) [20H] (Ph). $^{13}C\{^1H\}$ NMR: δ -3.17 (Me *trans* I) ($^1J_{PtC}$ = 616 Hz), 5.31 (Me *trans* Sb) ($^1J_{PtC}$ = 575), 18.30 (Sb$\underline{C}H_2$), 24.12 ($CH_2\underline{C}H_2CH_2$), 127.23-136.90 (Ph).

$[PtMe_3\{Me_2Sb(CH_2)_3SbMe_2\}I]$: Method as above. (Yield: 45%). Required for $[C_{10}H_{27}IPtSb_2]$: C, 16.8; H, 3.8%. Found: C, 16.3; H, 3.9%. ES^+ MS (MeCN): 596 ($[^{195}PtMe\{Me_2{}^{121}Sb(CH_2)_3{}^{123}SbMe_2\}(MeCN)]^+$ 597), 555 ($[^{195}PtMe\{Me_2{}^{121}Sb(CH_2)_3{}^{123}SbMe_2\}]^+$ 556). ^1H NMR: δ 0.97 (s) [6H] (SbC$\underline{H}_3$), 1.07 (s) [3H] (Me *trans* I) ($^2J_{PtH}$ = 78 Hz), 1.27 (s) [6H]

(SbC$\underline{H}_3$), 1.45 (s) [6H] (Me *trans* Sb) ($^2J_{PtH}$ = 65 Hz), 2.0 (m) [6H] (CH_2). $^{13}C\{^1H\}$ NMR: δ -11.22 (SbC$\underline{H}_3$), -7.58 (Sb$\underline{C}H_3$), -6.20 (Me *trans* I) ($^1J_{PtC}$ = 628 Hz), 1.85 (Me *trans* Sb) ($^1J_{PtC}$ = 553 Hz), 14.31(Sb$\underline{C}H_2$), 24.30 ($CH_2\underline{C}H_2CH_2$).

[PtMe$_3${*o*-C$_6$H$_4$(CH$_2$SbMe$_2$)$_2$}I]: Method as above. (Yield: 60%). Required for [$C_{15}H_{29}IPtSb_2$].¼C_6H_8: C, 24.9; H, 4.1. Found: C, 24.7; H, 3.7%. ^1H NMR: δ 0.78 (s) [6H] (SbC$\underline{H}_3$), 0.82 (s) [3H] (Me *trans* I) ($^2J_{PtH}$ = 76 Hz), 1.20 (s) [6H] (Me *trans* Sb) ($^2J_{PtH}$ = 65 Hz), 1.31 (s) [6H] (SbC$\underline{H}_3$), 3.12 (m) [2H] ($C\underline{H}_2$), 4.08 (d) [2H] ($C\underline{H}_2$), 6.88-7.05 (m) [4H] (Ar-$\underline{H}$). $^{13}C\{^1H\}$ NMR: δ -11.57 (SbC$\underline{H}_3$), -6.20 (Me *trans* I) ($^1J_{PtC}$ = 611 Hz), -6.05 (Sb$\underline{C}H_3$), 3.82 (Me *trans* Sb) ($^1J_{PtC}$ = 562 Hz), 21.37 (Sb$\underline{C}H_2$), 126.16, 130.53, 136.45 (Ar-$\underline{C}$).

[(PtMe$_3$I)$_2$(Ph$_2$SbCH$_2$SbPh$_2$)]: Method as above, but using a Pt : $Ph_2SbCH_2SbPh_2$ ratio of 2 : 1. (Yield: 50%). Required for [$C_{31}H_{40}I_2Pt_2Sb_2$]: C, 28.6; H, 3.1%. Found: C, 29.4; H, 3.1%. ^1H NMR: δ 1.36 (s) [12H] (Me *trans* I) ($^2J_{PtH}$ = 76 Hz), 2.25 (s) [6H] (Me *trans* Sb) ($^2J_{PtH}$ = 69 Hz), 2.92 (s) [2H] ($C\underline{H}_2$), 7.10-7.40 (m) [20H] (Ph). $^{13}C\{^1H\}$ NMR: δ 5.53 (Me *trans* I) ($^1J_{PtC}$ = 655 Hz), 8.27 (Me *trans* Sb) ($^1J_{PtC}$ = 694 Hz), 14.70 (Sb$\underline{C}H_2$), 138.8-128.8 (Ph).

[(PtMe$_3$I)$_2$(Me$_2$SbCH$_2$SbMe$_2$)]: Method as above, but using a Pt : $Me_2SbCH_2SbMe_2$ ratio of 2 : 1. (Yield: 55%). Required for [$C_{11}H_{32}I_2Pt_2Sb_2$].1/3 hexane: C, 14.4; H, 3.4. Found: C, 14.6; H, 3.6%. ^1H NMR: δ 1.18 (s) [12H] (SbC$\underline{H}_3$) ($^3J_{PtH}$ = 3 Hz), 1.23 (s) [12H] (Me *trans* I) ($^2J_{PtH}$ = 76 Hz), 2.04 (s) [6H] (Me *trans* Sb) ($^2J_{PtH}$ = 67 Hz), 2.28 (s) [2H] ($C\underline{H}_2$) ($^3J_{PtH}$ = 4.5 Hz). $^{13}C\{^1H\}$ NMR: δ -6.91 (SbC$\underline{H}_3$), -0.05 (Sb$\underline{C}H_2$), 4.17 (Me *trans* I) ($^1J_{PtC}$ = 629 Hz), 12.78 (Me *trans* Sb) ($^1J_{PtC}$ = 571 Hz).

[PtMe$_3$(SbMe$_2$Ph)$_2$I]: Method as above giving a light yellow oil. (Yield 70%). ^1H NMR: δ 0.93 (s) [3H] (Me *trans* I) ($^2J_{PtH}$ = 71 Hz), 1.21 (s) [6H] (SbC$\underline{H}_3$), 1.43 (s) [6H] (Me *trans* Sb) ($^2J_{PtH}$ = 66 Hz), 7.30-7.40 (m) [10H] (Ph). $^{13}C\{^1H\}$ NMR: δ -5.87 (Me *trans* I) ($^1J_{PtC}$ = 643 Hz), -2.98 (Sb$\underline{C}H_3$), 5.16 (Me *trans* Sb) ($^1J_{PtC}$ = 564 Hz), 129.23, 129.92, 134.73 (Ph). Due to the complex being an oil, microanalysis was not obtained.

[PtMe$_3$(SbMePh$_2$)$_2$I]: Method as above. (Yield 55%). Required for [$C_{29}H_{35}IPtSb_2$]: C, 36.7; H, 3.7. Found: C, 36.2; H, 3.7%. ^1H NMR: δ 1.08 (s) [3H] (Me *trans* I) ($^2J_{PtH}$ = 71 Hz), 1.38 (s) [3H] (SbC$\underline{H}_3$), 1.55 (s) [6H] (Me *trans* Sb) ($^2J_{PtH}$ = 67 Hz), 7.10-7.40 (m) [20H] (Ph). $^{13}C\{^1H\}$ NMR: δ -5.05 (Me *trans* I) ($^1J_{PtC}$ = 611 Hz), -1.73 (Sb$\underline{C}H_3$), 7.60 (Me *trans* Sb) ($^1J_{PtC}$ = 566 Hz), 129.0 – 136.9 (Ph).

[$PtMe_3(SbPh_3)_2I$]: Method as above. (Yield 70%). Required for [$C_{39}H_{39}IPtSb_2$]: C, 43.6; H, 3.7. Found: C, 43.4; H, 3.4%. ^1H NMR: δ 1.27 (s) [3H] (Me *trans* I) ($^2J_{PtH}$ = 70 Hz), 1.83 (s) [6H] (Me *trans* Sb) ($^2J_{PtH}$ = 68 Hz), 7.05-7.50 (m) [30H] (Ph). $^{13}C\{^1H\}$ NMR: δ -3.72 (Me *trans* I) ($^1J_{PtC}$ = 606 Hz), 10.43 (Me *trans* Sb) ($^1J_{PtC}$ = 542 Hz), 129.3 – 136.9 (Ph).

3.4.3. X-ray crystallography

Details of the crystallographic data collection and refinement parameters are given in Table 3.4.1. Pale yellow crystals of [$PtMe_3\{Ph_2Sb(CH_2)_3SbPh_2\}I$], [$PtMe_3\{Me_2Sb(CH_2)_3SbMe_2\}I$], [$PtMe_3\{o\text{-}C_6H_4(CH_2SbMe_2)_2\}I$], [$PtMe_3(SbPh_3)_2I$] and [$(PtMe_3I)_2(Ph_2SbCH_2SbPh_2\}$] were obtained by liquid diffusion of hexane into a CH_2Cl_2 solution of the compound. Data collection used a Nonius Kappa CCD diffractometer (T = 120 K) and with graphite-monochromated Mo-K_α X-radiation (λ = 0.71073 Å). Structure solution and refinement were largely routine,[27,28] except for [$PtMe_3(SbPh_3)_2I$] which revealed some disorder of the *trans*-I-Pt-Me unit. This was modelled using partial atom positions, with the sum of the occupancies of the two I and two C components each being one. Distinct partial C atom and partial I atoms could not be identified, hence these units were refined with identical atomic coordinates and atom displacement parameters. Consequently the Pt-I and Pt-C distances in the *trans* I-Pt-C units are weighted averages, and should not be used in comparative studies. The H atoms associated with the disordered Me groups were not included in the final structure factor calculation.

Table 3.4.1: Crystallographic Parameters

Complex	**[$PtMe_3\{Ph_2Sb(CH_2)_3SbPh_2\}I$]**	**[$PtMe_3\{Me_2Sb(CH_2)_3SbMe_2\}I$]**	**[$PtMe_3\{o\text{-}C_6H_4(CH_2SbMe_2)_2\}I$]**	**[$PtMe_3\{SbPh_3\}_2I$]**	**[$(PtMe_3I)_2\{Ph_2SbCH_2SbPh_2\}$]**
Formula	$C_{30}H_{35}IPtSb_2$	$C_{10}H_{27}IPtSb_2$	$C_{15}H_{29}IPtSb_2$	$C_{39}H_{39}IPtSb_2$	$C_{31}H_{40}I_2Pt_2Sb_2$
M	961.07	712.81	774.87	1073.19	1300.11
Crystal System	Monoclinic	Orthorhombic	Monoclinic	Triclinic	Triclinic
Space Group	$P2_1/c$ (no. 14)	*Pnma* (no. 62)	$P2_1/c$ (no. 14)	P-*1* (no. 2)	P-*1* (no. 2)
a/Å	12.611(3)	14.035(4)	11.7559(16)	9.6674(10)	9.7960(10)
b/Å	12.557(5)	10.851(3)	9.2374(12)	18.681(3)	11.7470(10)
c/Å	19.535(5)	11.349(2)	19.124(2)	19.993(3)	15.3850(10)
α/°	90	90	90	81.604(7)	103.790(6)
β/°	105.48(2)	90	102.258(6)	89.966(8)	93.514(5)
γ/°	90	90	90	83.681(8)	90.628(4)
U/Å^3	2981.4(16)	1728.4(8)	2029.4(5)	3549.7(7)	1715(3)
Z	4	4	4	4	2
μ(Mo-Kα)/cm^{-1}	7.532	12.937	11.030	6.338	11.504
R_{int}	0.1915	0.0611	0.0336	0.0943	0.0299
Total Reflections	41792	10988	18921	75972	33362
Unique Reflns	6924	2081	4624	16313	7793
No. of params.	307	74	172	777	334
$R1$ [$I_o > 2\sigma(I_o)$]	0.0600	0.0346	0.0252	0.0572	0.0284
$R1$ [all data]	0.1687	0.0558	0.0314	0.1066	0.0320
wR_2 [$I_o > 2\sigma(I_o)$]	0.0968	0.0644	0.0573	0.0906	0.0851

3.5 References

[1] W. Levason and N. R. Champness, *Coord. Chem. Rev.*, 1994, **133**, 115; W. Levason, G. Reid, *Coord. Chem. Rev.*, 2006, **250**, 2565.

[2] W. Levason, G. Reid in *Comprehensive Coordination Chemistry II*, Eds. J. A. McCleverty and T. J. Meyer, Volume 1, Elsevier, Amsterdam, 2004, p377.

[3] H. Werner, *Angew. Chem. Int. Ed.*, 2004, **43**, 938.

[4] H. Werner, D. A. Ortmann, O. Gevert, *Chem. Ber.*, 1996, **129**, 411.

[5] H. Werner, C. Grunwald, P. Steinert, O. Gevert, J. Wolf, *J. Organomet. Chem.*, 1998, **565**, 231.

[6] M. Mattias, J. Wolf, M. Laubender, M. Teichert, D. Stalke, H. Werner, *Chem. Eur. J.*, 1997, **3**, 1442.

[7] M. Jiminez-Tenorio, M. C. Puerta, I. Salcedo, P. Valerga, S. L. Costa, P. T. Gomes, K. Mereiter, *Chem. Commun.*, 2003, 1168.

[8] D. J. Gulliver, W. Levason, K. G. Smith, *J. Chem. Soc., Dalton Trans.*, 1981, 2153.

[9] M. D. Brown, W. Levason, G. Reid, M. Webster, *Dalton Trans.*, 2006, DOI: 10.1039/b611544f.

[10] C. R. Kistner, J. D. Blackman, W. C. Harris, *Inorg. Chem.*, 1969, **8**, 2165.

[11] H.-A. Brune, R. Klotzbucher, G. Schmidtberg, *J. Organomet. Chem.*, 1989, **371**, 113.

[12] For examples see: F. R. Hartley, in *Comprehensive Organometallic Chemistry I*, Eds. G. Wilkinson, F. G. A. Stone, E. W. Abel, Pergamon, Oxford, 1982, Vol. 6, ch 39, p.421; G. K. Anderson, in *Comprehensive Organometallic Chemistry II*, Eds. G. Wilkinson, F. G. A.. Stone, E. W. Abel, Pergamon, Oxford, 1995, Vol. 9, ch 7, p. 391.

[13] S. Hietkamp, D. J. Stufkens, K. Vrieze, *J. Organomet. Chem.*, 1979, **169**, 107.

[14] E. G. Hope, W. Levason, T. Kemmitt, *Inorg. Chim. Acta*, 1986, **115**, 187.

[15] M. Rashidi, Z. Fakhroeian, R. J. Puddephatt, *J. Organomet. Chem.*, 1990, **406**, 261.

[16] J. D. Kennedy, W. McFarlane, R. J. Puddephatt, P. J. Thompson, *J. Chem. Soc., Dalton Trans.*, 1976, 874.

[17] P. L. Goggin, R. J. Goodfellow, S. R. Haddock, B. F. Taylor, I. R. H. Marshall, *J. Chem. Soc., Dalton Trans.*, 1976, 459.

[18] For examples see M. P. Brown, R. J. Puddephatt, C. E. E. Upton, *J. Chem. Soc., Dalton Trans.*, 1974, 2457; M. Crespo, R. J. Puddephatt, *Organometallics*, 1987, **6**, 2548; S. S. M. Ling, I. R. Jobe, L. Manojlovic-Muir, K. W. Muir, R. J. Puddephatt, *Organometallics*, 1985, **4**, 1198; T. G Appleton, H. C. Clark, L. E. Manzer, *J. Organomet. Chem.*, 1974, **65**, 275; B. L. Shaw, J. D. Vessey, *J. Chem. Soc., Dalton Trans.*, 1992, 1929.

[19] W. Levason, M. L. Matthews, G. Reid, M. Webster, *Dalton Trans.*, 2004, 554.

[20] N. J. Holmes, W. Levason, M. Webster, *J. Chem. Soc., Dalton Trans.*, 1998, 3457.

[21] J. C. Baldwin, W. C. Kaska, *Inorg. Chem.*, 1975, **14**, 2020.

[22] R. Bassan, K. H. Bryars, L. Judd, A. W. G. Platt, P. G. Pringle, *Inorg. Chim. Acta*, 1986, **121**, L41.

[23] G. S. Hill, M. J. Irwin, C. J. Levy, L. M. Rendina, R. J. Puddephatt, *Inorg. Synth.*, 1998, **32**, 149.

[24] W. Levason, M. L. Matthews, G. Reid, M. Webster, *Dalton Trans.*, 2004, 51.

[25] S. Sato, Y. Matsumura, R. Okawara, *J. Organomet. Chem.*, 1972, **43**, 333.

[26] H. A. Meinema, H. F. Martens, J. G. Noltes, *J. Organomet. Chem.*, 1976, **110**, 183.

[27] SHELXS-97, program for crystal structure solution, G. M. Sheldrick, University of Göttingen, Germany 1997.

[28] SHELXL-97, program for crystal structure refinement, G. M. Sheldrick, University of Göttingen, Germany 1997.

Chapter 4

Synthesis and properties of Rh(I) and Ir(I) distibine complexes with organometallic co-ligands.

4.1 Introduction

The organometallic chemistry of organoantimony ligands has been studied very little, with the exception of $SbPh_3$ as it is commercially available. In comparison to lighter Group 15 analogues such as phosphines,[1,2] this area of chemistry is very much in its infancy.

As mentioned in earlier Chapters stibines are traditionally seen as weaker/poorer ligands compared to phosphines and arsines, due to the weaker C-Sb bond. As antimony is a larger element with more diffuse orbitals, C-Sb bond fission is easier, resulting in the chemistry being more challenging. Indeed even though the C-Sb bond is weaker, compounds containing such groups could promote very different reaction chemistry, and may therefore have useful applications where phosphines and arsines are not suitable. The different electronic properties of stibines compared to phosphines and arsines has already been seen to promote different product distributions in work pioneered by Werner *et al* which led to the discovery of bridging ER_3 (E = P, Sb, As) ligands.[3] Moreover, it was found that in order to achieve the phosphine or arsine bridged complexes, it was necessary to start with complexes incorporating the bridging stibine, Sb^iPr_3. It is therefore suggested that due to the larger antimony centre, the stibine ligand can easily bridge between the rhodium centres.[3]

Fig 4.1.1: The first example of bridging stibines.[3]

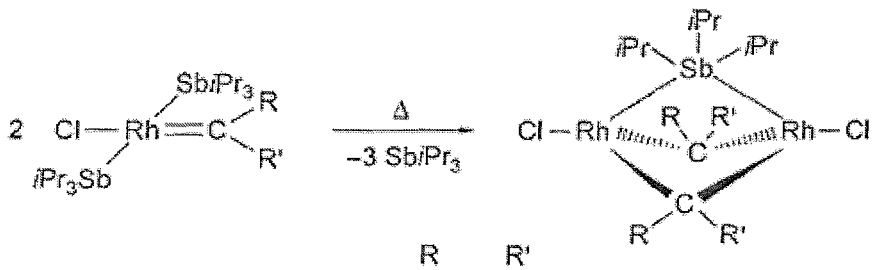

R	R'
Ph	Ph
p-Tol	*p*-Tol
Ph	*p*-Tol

Werner and co-workers have also explored the organometallic Rh, Ir and Ru chemistry in great depth, and have shown that complexes incorporating Sb^iPr_3 as ligands exhibit different reactivity to complexes incorporating the analogous phosphine or arsine.[4]

4.1.1 Rh, Ir, Ru and Os Chemistry

In the last ten years there have been significant advances in the understanding of stibine chemistry. Werner and co-workers have carried out a large proportion of this work.[4] Just over a decade ago, the synthesis of a series of monomeric rhodium(I) complexes of the form *trans*-[RhCl(L)(E^iPR_3)$_2$] (L = isocyanides; CNR, α, β-unsaturated carbonyl compounds; CH_2=CHC(=O)R, alkynes, and diynes, E = As, Sb) was achieved. Full characterisation of these compounds and the *X*-ray crystal structure of *trans*-[RhCl(CNMe)(Sb^iPr_3)$_2$] (Fig.4.1.2) were also obtained.[4] The unexpected reaction chemistry of *trans*-[RhCl(C_2H_4)(Sb^iPr_3)$_2$] was also reported. Instead of reacting with RCCR (R = Ph, CO_2Me, ^{t}Bu) to form *trans*-[RhCl(=C=CHR)(Sb^iPr_3)$_2$] like the analogous arsine complex, the complex catalysed the formation of the corresponding E-enynes, RCHCHCCR.[5]

Fig 4.1.2: View of the crystal structure of *trans*-[RhCl(CNMe)(Sb^iPr_3)$_2$].[5]

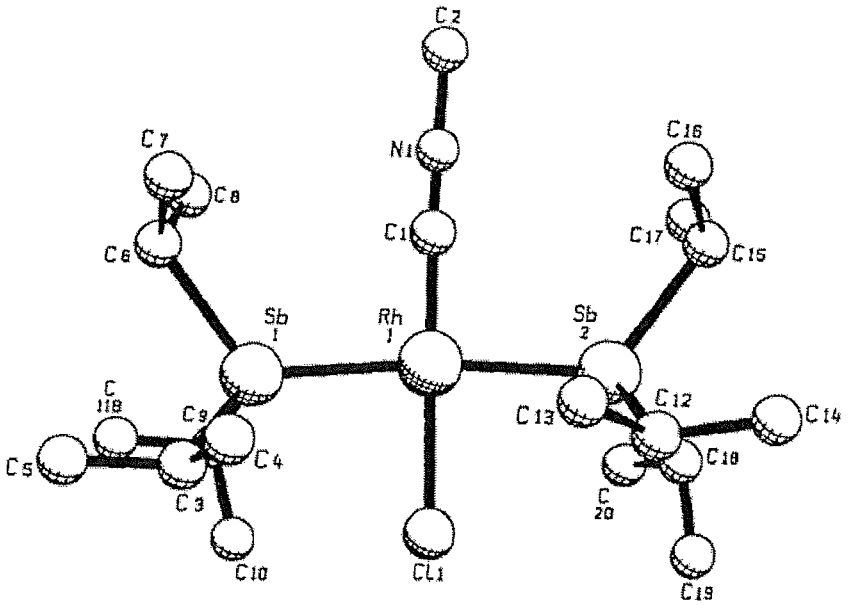

Werner and co-workers also developed a series of (η^5-Indenyl)rhodium(I) complexes of the general form [(η^5-C_9H_7)Rh(=CPh_2)(L)] (L = Sb^iPr_3, P^iPr_3, PPh_3, P^iPrPh_2 and P^iPr_2Ph) which were prepared from the square planar precursors *trans*-[RhCl(=CPh_2)(L)] and C_9H_7K in thf.[6] The reaction scheme for these reactions is shown in Fig. 4.1.3. Again, after exploring some of the reaction chemistry of these (η^5-Indenyl)rhodium(I) complexes, Werner and colleagues found some interesting results. In

particular when treating $[(\eta^5\text{-}C_9H_7)Rh(=CPh_2)(L)]$ with CO gas, there was an unusual migratory insertion of the carbene ligand into one of the five membered rings of the indenyl unit. The resulting complexes were of the general formulation $[\{\eta^5\text{-}C_9H_6(CHPh_2)\}Rh(CO)(L)]$ and were obtained in very high yields. The reaction scheme for these reactions is also shown in Fig. 4.1.3.[6]

Fig 4.1.3: Reaction schemes to form $[(\eta^5\text{-}C_9H_7)Rh(=CPh_2)(L)]$ and $[\{\eta^5\text{-}C_9H_6(CHPh_2)\}Rh(CO)(L)]$.[6]

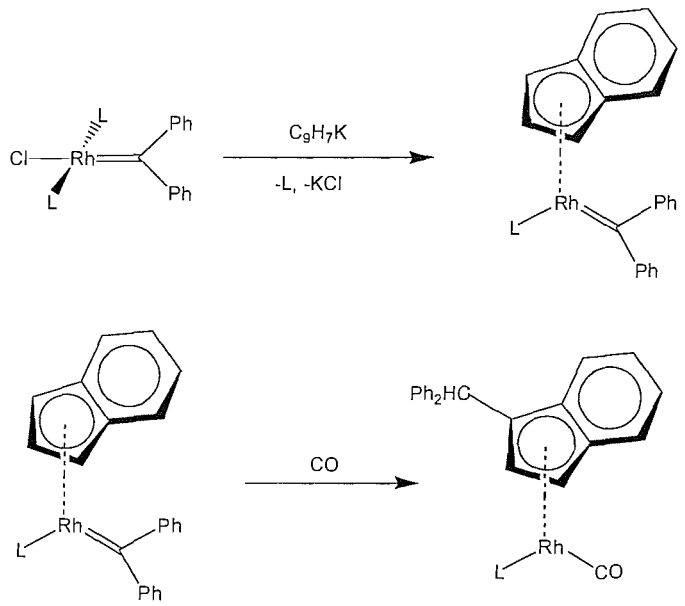

As well as advances in rhodium stibine chemistry Werner and co-workers have prepared ruthenium and osmium carbonyl complexes incorporating Sb^iPr_3 as a co-ligand.[7] Treating $RuCl_3.H_2O$ in ethanol with Sb^iPr_3 affords the monocarbonyl $[RuCl_2(CO)(Sb^iPr_3)_3]$ species. Subsequent exposure to CO also affords the dicarbonyl species $[RuCl_2(CO)_2(Sb^iPr_3)_2]$. In the presence of Na_2CO_3, $RuCl_3.H_2O$ in ethanol resulted in a chloro(hydrido) species being formed of the form $[RuHCl(CO)(Sb^iPr_3)_3]$. The analogous osmium complex was also prepared, *via* an analogous route. Subsequent reactions of $[OsHCl(CO)(Sb^iPr_3)_3]$ with C_2H_4, $NaBF_4$ and $C_2(CO_2Me)_2$ can be seen in Figure 4.1.4.[7]

Fig 4.1.4: Reaction scheme of the reaction chemistry of $[OsHCl(CO)(Sb^iPr_3)_3]$.[7]

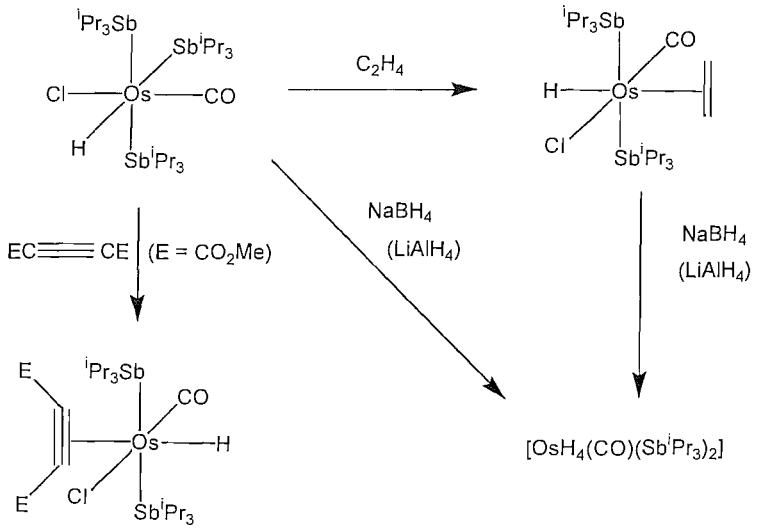

Reaction of $[RuHCl(CO)(Sb^iPr_3)_3]$ with $C_2(CO_2Me)_2$, HCCPh and $HCCCPh_2OH$ afforded $[RuHCl(CO)(C_2(CO_2Me)_2)Sb^iPr_3)_2]$, the alkynyl ruthenium(II) complex $[RuCl(CCPh)(CO)(Sb^iPr_3)_3]$, and the allenylidene ruthenium(II) complex $[RuCl_2(=C=C=CPh_2)(CO)(Sb^iPr_3)_2]$ respectively. These results suggested that Ru and Os complexes incorporating monodentate stibines are very versatile and support some very interesting reaction chemistry.[7]

As well as rhodium and ruthenium chemistry, Werner *et al.* have recently investigated some iridium stibine chemistry.[8] In particular the coordination and reaction chemistry of Sb^iPr_3 has been explored. For example, the mixed phosphine-stibine compound $[IrCl(C_2H_4)(P^iPr_3)(Sb^iPr_3)]$ can be synthesised from $[Ir_2(C_2H_4)_2(P^iPr_3)_2Cl_2]$ and two equivalents of Sb^iPr_3 as a bright orange solid in nearly quantitative yield.[8] $[IrCl(C_2H_4)(P^iPr_3)(Sb^iPr_3)]$ can be stored under argon, but is very labile in solution and decomposes in chlorinated solvents. However, by reacting it with N_2CR_2 (R = Ph, p-Tol) in benzene, carbene complexes of the form $[IrCl(=CR_2)(P^iPr_3)(Sb^iPr_3)]$ can be formed. $[IrCl(C_2H_4)(P^iPr_3)(Sb^iPr_3)]$ can also react with CO, diphenylacetylene and H_2 by ligand substitution or oxidative addition. In contrast to these findings however, treatment of $[IrCl(C_8H_{14})(P^iPr_3)(Sb^iPr_3)]$ or *trans*-$[IrCl(C_8H_{14})(Sb^iPr_3)_2]$ with $C_5Cl_4N_2$ affords the diazoalkane complexes *trans*-$[IrCl(N_2C_5Cl_4)(P^iPr_3)(Sb^iPr_3)]$ and *trans*-$[IrCl(N_2C_5Cl_4)(Sb^iPr_3)_2]$ without elimination of N_2.[8] The cyclooctene iridium(I) complex *trans*-$[IrCl(C_8H_{14})(Sb^iPr_3)_2]$, mentioned above, can be prepared from $[IrCl(C_8H_{14})_2]_2$ and 4 equivalents of Sb^iPr_3 in excellent yield, but interestingly it rearranges in hexane

at room temperature to form *anti.exo*-[IrHCl(η^3-C_8H_{13})(Sb^iPr_3)$_2$] which when dissolved in benzene is in equilibrium with the *anti.endo*- isomer. The reaction to prepare [IrHCl(η^3-C_8H_{13})(Sb^iPr_3)$_2$] even occurs in the solid state. Similar reactions can be achieved with 1-hexene and propene. Other reaction chemistry of *trans*-[IrCl(C_8H_{14})(Sb^iPr_3)$_2$] can be seen in Fig 4.1.5.[8]

Fig 4.1.5: Reaction chemistry of *trans*-[IrCl(C_8H_{14})(L)$_2$] (L = Sb^iPr_3) with CO or H_2.[8]

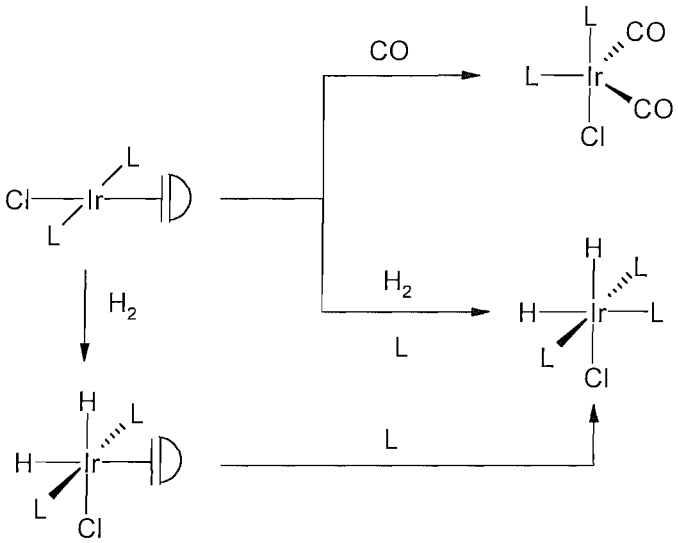

4.1.2 Rh(I)-cod-stibine and Rh(I)-carbonyl stibine complexes

A number of Rh(I) complexes involving the $SbPh_3$ have been described previously. [1] Specific examples include the interaction of $SbPh_3$ with [$Rh_2Cl_2(CO)_4$][9-12] and it has been shown that the yellow, planar, four coordinate species *trans*-[Rh(CO)($SbPh_3$)$_2$Cl] can be synthesised as well as the red, trigonal bipyramidal, five-coordinate [Rh(CO)($SbPh_3$)$_3$Cl]. These species have been structurally characterised,[11] along with the planar [Rh(CO)($SbPh_3$)$_2$I].[11] It has also been seen that [Rh(CO)($SbPh_3$)$_3$Cl] oxidatively adds various substrates. For example the reaction of [Rh(CO)($SbPh_3$)$_3$Cl] and MeI results in the formation of [Rh(CO)($SbPh_3$)$_2$$I_2$(Me)], whose structure shows *trans* stibines and *cis* iodines.[10,12-14]

Other studies have established that the reaction of $SbPh_3$ and [$Rh_2Cl_2(cod)_2$] gives [Rh($SbPh_3$)$_2$(cod)Cl] as an orange solid on the basis of spectroscopic and analytical data.[15] It has also been seen that reacting C_1-linked distibine ligands of the form $R_2SbCH_2SbR_2$ (R = Me or Ph) with [$Rh_2Cl_2(CO)_4$] gives ligand bridged dimers of the form *trans*-[{Rh(CO)Cl}$_2$(μ-

$R_2SbCH_2SbR_2)_2]$.[16,17]

4.1.2 Applications of complexes incorporating stibines

Applications for complexes incorporating stibines as ligands, have already been discovered, with the use of nickel-$SbPh_3$ complexes [Ni(2-methylallyl)$(SbPh_3)_3$][BARF] (BARF = [B{C_6H_3-3,5-$(CF_3)_2$}$_4$]$^-$ and *trans*-[Ni$(C_6Cl_2F_3)_2(SbPh_3)_2$] in the catalysis of styrene polymerization and norbornene insertion polymerisation respectively.[18,19]

4.1.3 Distibines

As there is a limited amount of commercially available stibines and also very few distibine ligands known in comparison with phosphines, development of novel synthetic procedures for making such ligands is vital. Indeed recent research incorporating the reaction of R_2SbCl and di-Grignard reagents has led to the synthsis of *m*- and *p*-phenylene and *o*-, *m*- and *p*-xylylene distibines in remarkably high yields.[20] Also advances that are reported in this Thesis include the synthesis of the unprecedented wide angle distibine {CH_2(*o*-$C_6H_4CH_2SbMe_2$)}$_2$ as seen in Chapter 2.

Previous studies involving the versatile *o*-$C_6H_4(CH_2SbMe_2)_2$ ligand have included exploring the ligating properties of the ligand with a large range of transition metal carbonyls and transition metal halides.[21] The *o*-$C_6H_4(CH_2SbMe_2)_2$ ligand has been seen to adjust the size of the chelate bite angle changing the Sb···Sb by as much as 0.5 Å depending on the metal ion that it is coordinated to. Indeed, the work in Chapter 3 further supports the evidence that distibine ligands can promote some very interesting reaction chemistry. The synthesis of the first stable fully characterised examples of Pt(IV) stibine complexes ([$PtMe_3I$(distibine)] and [$(PtMe_3)(\mu$-$I)_2(\mu$-$R_2SbCH_2SbR_2)$] (R = Me or Ph)) is very interesting in the field, and the fact that they can undergo reductive elimination of ethane upon thermolysis[22] shows that these systems are versatile and could in the future have applications in catalysis.

In this Chapter the coordination and organometallic chemistry of Rh(I) and Ir(I) complexes incorporating distibine ligands is discussed, with the majority of the work focusing on the $Ph_2Sb(CH_2)_3SbPh_2$, $Me_2Sb(CH_2)_3SbMe_2$ and *o*-$C_6H_4(CH_2SbMe_2)_2$ ligands. The synthesis and spectroscopic properties and the crystal structure of [Rh(CO){$Ph_2Sb(CH_2)_2SbPh_2$}$_2$]PF_6 is also reported. Moreover some very interesting reaction chemistry involving the Rh(I) and Ir(I) complexes incorporating $Ph_2Sb(CH_2)_3SbPh_2$ is also reported.

4.2 Results and Discussion

4.2.1 Rhodium(I) –cod–stibine systems

$[Rh(SbPh_3)_2(cod)Cl]$[15] was prepared previously, but for the purposes of this work, it was necessary to synthesise it, to gain an understanding of the chemistry that could then be used to obtain other such complexes. The addition of $[Rh_2Cl_2(cod)_2]$ to a refluxing solution of excess $SbPh_3$ in EtOH under argon, was followed by the filtration of the red precipitate formed. The high yield of red solid was found to be the 1:2 Rh:$SbPh_3$ species with the analytical data in agreement with that in the literature.[15] In addition to the previously reported data, the integration of the resonances in the ^1H NMR spectrum, and electrospray mass spectrometry that showed a cluster of peaks at *ca. m/z* 917 corresponding to $[Rh(cod)(SbPh_3)_2]^+$ confirmed the formulation of the product. Attempts were made to grow crystals of $[Rh(SbPh_3)_2(cod)Cl]$ from $EtOH/Et_2O$, to compare the unit cell with the literature structure, however the crystals that were grown were found to be *mer*-$[RhCl_2(SbPh_3)_3(Ph)]$ which has already been reported in the literature.[23]

Fig 4.2.1: Crystal structure of $[RhCl_2(SbPh_3)_3(Ph)]$ with selected atoms labeled. H atoms are omitted for clarity and ellipsoids are shown at the 50 % probability level.

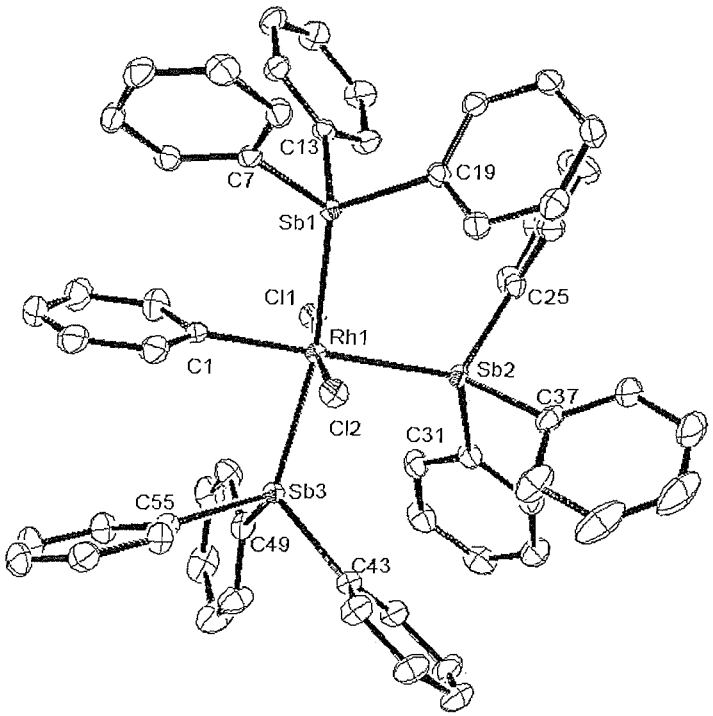

Table 4.2.1: Selected bond lengths and angles from the crystal structure of $[RhCl_2(SbPh_3)_3(Ph)]$.

Rh1 – Sb1	2.5803(4)	Cl1 – Rh1 – Cl2	173.65(3)
Rh1 – Sb2	2.6770(4)	C1 – Rh1 – Sb1	84.48(8)
Rh1 – Sb3	2.5975(5)	C1 – Rh1 – Sb2	171.88(9)
Rh1 – Cl1	2.3547(9)	C1 – Rh1 – Sb3	84.42(8)
Rh1 – Cl2	2.3649(8)	Sb1 – Rh1 – Sb2	97.141(15)
Rh1 – C1	2.1260(3)	Sb1 – Rh1 – Sb3	166.874(12)
		Sb2 – Rh1 – Sb3	94.828(15)

As the analytical data proves the isolated product was that of $[Rh(SbPh_3)_2(cod)Cl]$, it can be postulated that a re-arrangement occurred during crystallisation, along with cleavage of phenyl groups from a molecule of $SbPh_3$.

A simple modification of the procedure above, was used to synthesise $[Rh(cod)\{Ph_2Sb(CH_2)_3SbPh_2\}Cl]$ and $[Rh(cod)\{Me_2Sb(CH_2)_3SbMe_2\}Cl]$, by reacting 2 molar equivalents of the appropriate ligand with $[Rh_2Cl_2(cod)_2]$ in dry EtOH at room temperature under argon. Following concentration to dryness of the orange solutions, the residues were triturated in hexane to afford orange solids in good yields. The microanalytical data for both compounds suggests the desired products were formed and indeed the ^1H NMR spectroscopic data also supported this, with the presence of both cod and the distibine. However, the 18 electron, 5 coordinate complexes seem to be fluxional at room temperature, but after cooling to 223 K the ^1H NMR spectrum showed separate broad peaks for the different cod proton environments. For example the $[Rh(cod)\{Ph_2Sb(CH_2)_3SbPh_2\}Cl]$ ^1H NMR spectrum showed broad peaks at 4.20 (cod CH), 2.43 (cod CH_2) and 1.78 (cod CH_2). In the case of $[Rh(cod)\{Me_2Sb(CH_2)_3SbMe_2\}Cl]$ there was also a multiplet corresponding to the SbMe groups at 1.35–1.20 ppm. The electrospray mass spectrometry also supported the formulation of the complexes with mass peaks at *m/z* 805 and *m/z* 557 corresponding to the ions $[Rh(cod)\{Ph_2Sb(CH_2)_3SbPh_2\}]^+$ and $[Rh(cod)\{Me_2Sb(CH_2)_3SbMe_2\}]^+$ respectively. The possibility that these complexes were four coordinate 16 electron cationic species, $[Rh(cod)\{R_2Sb(CH_2)_3SbR_2\}]Cl$, was reduced significantly by conductivity measurements in CH_2Cl_2 which suggested that the complexes were 18 electron neutral species.

Rh(cod){*o*-$C_6H_4(CH_2SbMe_2)_2$}Cl] was prepared similarly as an orange solid, and indeed the electrospray mass spectrometry showed mass peaks at *m/z ca.* 619 corresponding to [Rh(cod){*o*-$C_6H_4(CH_2SbMe_2)_2$}]$^+$. Unfortunately, even after recrystallisation, the complex was not isolated as an analytically pure sample. Moreover the ^{1}H NMR spectrum was seen to be more complicated than first thought and so this complex was not pursued. No crystals were obtained of either of the complexes of the form [Rh(cod)(distibine)Cl], and therefore the structure of the complexes were not proved beyond doubt. However we expect the five-coordinate Rh(I) distibine complexes to adopt a similar geometry to [Ir$(C_2H_4)_2$(Sb^{i}Pr$_3$)$_2$Cl].[4] The distorted trigonal bipyramid of [Ir$(C_2H_4)_2$(Sb^{i}Pr$_3$)$_2$Cl] shows equatorial olefins and one axial and one equatorial stibine, and the crystal structure is shown in Figure 4 2.2 below.

Fig 4.2.2: Crystal structure of [Ir$(C_2H_4)_2$(Sb^{i}Pr$_3$)$_2$Cl].[4]

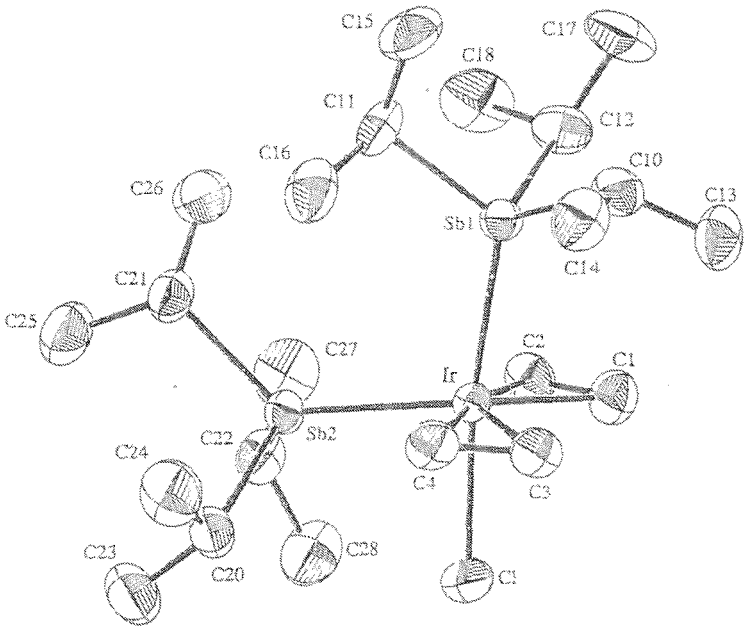

Planar, 16 electron Rh(I) complexes of the form [Rh(cod)(L–L)]BF_4 (L–L = $Ph_2Sb(CH_2)_3SbPh_2$, $Me_2Sb(CH_2)_3SbMe_2$, *o*-$C_6H_4(CH_2SbMe_2)_2$) were obtained in good yield, from reaction of [$Rh_2Cl_2(cod)_2$] with two molar equivalents of $AgBF_4$, in acetone, removal of the AgCl *via* filtration, and then treatment of the resultant yellow solution with a toluene solution of two molar equivalents of the appropriate ligand. The products were obtained as yellow/orange solids in good yield. The microanalytical data confirmed the formulations of the 16 electron rhodium(I) species, and the

positive ion electrospray showed the Rh(I) cations to be present and were indistinguishable from those of the neutral Rh(I) species [Rh(cod)(L–L)Cl] reported above with clusters of mass peaks at *m/z ca.* 805, 557 and 619 for $[Rh(cod)(Ph_2Sb(CH_2)_3SbPh_2)]BF_4$, $[Rh(cod)(Me_2Sb(CH_2)_3SbMe_2)]BF_4$ and $[Rh(cod)(o\text{-}C_6H_4(CH_2SbMe_2)_2)]BF_4$ respectively. Figure 4.2.3 shows the positive ion electrospray for $[Rh(cod)(Ph_2Sb(CH_2)_3SbPh_2)]BF_4$.

Fig 4.2.3: Positive ion electrospray (MeCN), and isotope simulation, for $[Rh(cod)(Ph_2Sb(CH_2)_3SbPh_2)]BF_4$ showing $[Rh(cod)(Ph_2Sb(CH_2)_3SbPh_2)]^+$.

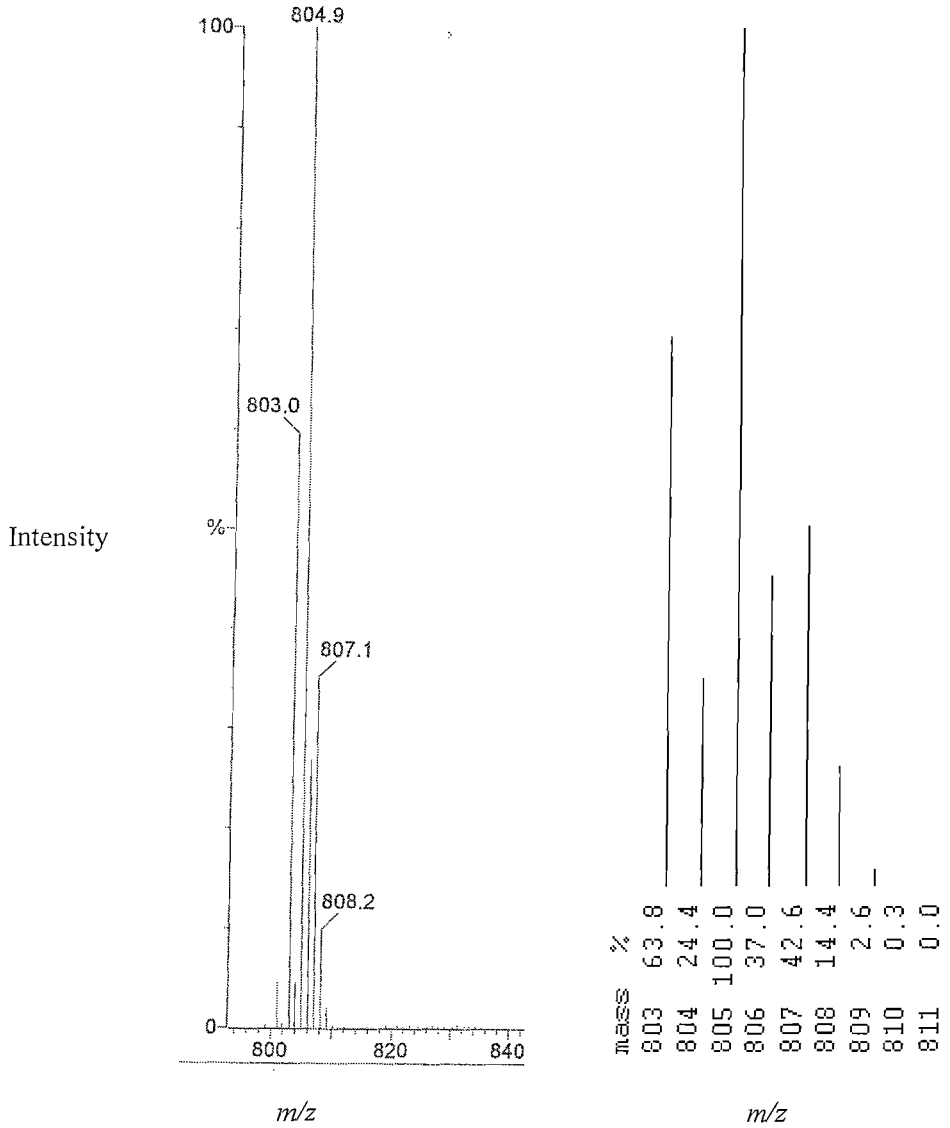

The IR spectra showed the presence of the ionic BF_4^- anion at 1054 cm^{-1}, which also supported the

formulation of the products. The ^{1}H and $^{13}C\{^{1}H\}$ NMR spectra were simpler than that of the five coordinate Rh(I) neutral species above but were consistent with the formulation of static planar cationic species. For example the ^{1}H NMR spectrum for $[Rh(cod)(Me_2Sb(CH_2)_3SbMe_2)]BF_4$ showed peaks at 4.0, 2.4, 2.1–2.4 (br) and 1.7 (br) ppm corresponding to cod CH, cod CH_2, methylene groups of the ligand and SbMe groups respectively. The $^{13}C\{^{1}H\}$ NMR spectrum for this complex showed peaks at 79.31 (cod CH), 31.45 (cod CH_2), 23.94 ($CH_2\underline{C}H_2CH_2$), 18.75 ($SbCH_2$) and -6.00 (SbMe) corroborating the determination of the product. Figure 4.2.4 shows a summary of the reaction schemes for the rhodium(I) –cod–stibine systems.

Fig 4.2.4: Reaction scheme of rhodium(I) –cod–stibine systems (R = Me, Ph).

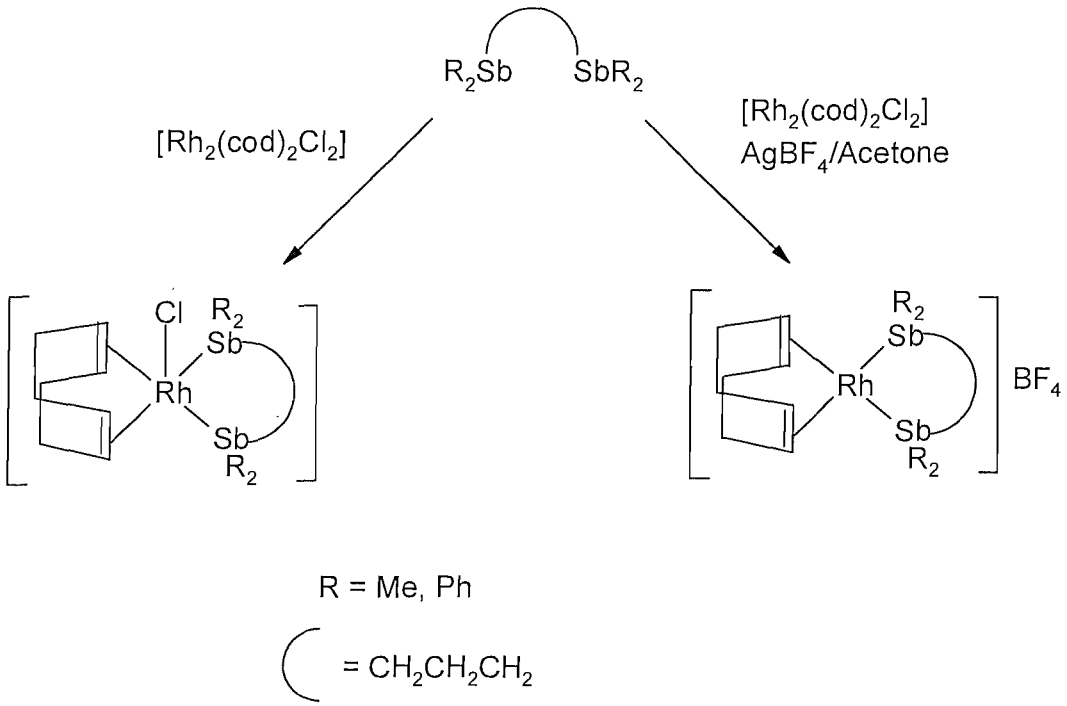

4.2.2 Rhodium(I)-*bis*(distibine) systems

Attempts to obtain $[Rh(L\text{-}L)_2]BF_4$ (L-L = $Ph_2Sb(CH_2)_3SbPh_2$, $Me_2Sb(CH_2)_3SbMe_2$ or *o*-$C_6H_4(CH_2SbMe_2)_2\}_2$) using $[Rh_2Cl_2(cod)_2]$ and two molar equivalents of $AgBF_4$, removal of the AgCl *via* filtration, and then addition of 4.1 equivalents of L-L in toluene were unsuccessful. Even when the reaction mixture was heated to temperatures up to 90 °C for 1h the spectroscopic data suggested that the resulting orange solid was a mixture of $[Rh(cod)(L\text{-}L)]BF_4$ and $[Rh(L\text{-}L)_2]BF_4$

with the major product being the former. This result indicates the incomplete substitution of the cod by the distibine, indicating that the distibine is not basic enough to force the substitution. This directly contrasts the work carried out by Pignolet and co-workers, who have carried out similar reactions with diphosphines obtaining $[Rh(diphosphine)_2]BF_4$ in good yield even at room temperature.[24,25] For example $[Rh(Ph_2PCH_2PPh_2)_2]BF_4$ and $[Rh(Ph_2P(CH_2)_4PPh_2)_2]BF_4$ were prepared very easily via a similar route to that above. These results serve to emphasise the different basicities of distibines *vs* diphosphines.

$[Rh\{Ph_2Sb(CH_2)_3SbPh_2\}_2]BF_4$ was successfully prepared by employing a slight modification to that of the preparation of $[Rh(cod)(L\text{-}L)]BF_4$. The red solid was obtained in good yield from substitution of the more labile coe ligand in $[Rh_2(coe)_4Cl_2]$ and two equivalents of $AgBF_4$ in acetone, removal of the AgCl *via* filtration, followed by addition of the resulting yellow solution to a toluene solution of 2 molar equivalents of $Ph_2Sb(CH_2)_3SbPh_2$ at room temperature. Microanalysis agreed with the formulation of the product, and IR spectroscopy showed the presence of the ionic BF_4^- anion with a peak at 1064 cm^{-1}. The positive ion electrospray of the product suggested the presence of the rhodium(I) cation with clusters of peaks at *m/z ca.* 1291 and 1013 which correspond to $[Rh\{Ph_2Sb(CH_2)_3SbPh_2\}_2]^+$ and $[Rh\{Ph_2Sb(CH_2)_3SbPh_2\}_2 - SbPh_2]^+$ respectively. The ^1H NMR spectrum showed coordinated ligand with resonances at 6.8–7.5 (m) and 2.3–2.7 (br) ppm corresponding to phenyl and methylene groups respectively. Evidence of the coordinated ligand was also seen in the $^{13}C\{^1H\}$ NMR spectrum with strong resonances for the methylene groups of the ligand at 24.71 ($CH_2\underline{C}H_2CH_2$) and 21.62 ($SbCH_2$). Some of the reaction chemistry of this complex is described later in the Chapter.

Fig 4.2.5: Reaction scheme for the preparation of $[Rh\{Ph_2Sb(CH_2)_3SbPh_2\}_2]BF_4$.

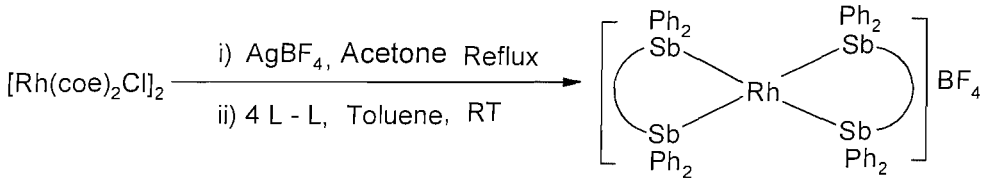

$[Rh\{Me_2Sb(CH_2)_3SbMe_2\}_2]BF_4$ was not attempted due to significant decomposition being observed

in the formation of $[Rh(cod)\{Me_2Sb(CH_2)_3SbMe_2\}]BF_4$. However attempts to obtain $[Rh\{o\text{-}C_6H_4(CH_2SbMe_2)_2\}_2]BF_4$ were carried out. Using the reaction conditions for the formation of $[Rh\{Ph_2Sb(CH_2)_3SbPh_2\}_2]BF_4$ the orange solid was obtained in good yield. However when analysed by positive ion electrospray, the major cluster of mass peaks was observed at *m/z* 924, some 5 mass units higher than expected. This corresponded to $[Ag\{o\text{-}C_6H_4(CH_2SbMe_2)_2\}_2]^+$ formed by reaction of the slight excess (0.2 equivalents) of $AgBF_4$ used in the reaction. A smaller cluster of mass peaks was observed at *m/z ca.* 919, which suggested that the desired product $[Rh\{o\text{-}C_6H_4(CH_2SbMe_2)_2\}_2]^+$ was also present. The ^1H and $^{13}C\{^1H\}$ NMR spectra indicated that the ligand was coordinated to the metal centre, however due to the mixture of products, microanalysis was not obtained. When $TlPF_6$ was used instead of $AgBF_4$ the spectroscopic data were inconclusive, and therefore not pursued.

4.2.3 Rhodium(I)–carbonyl–stibine systems

$[Rh(CO)(SbPh_3)_2Cl]$ which has been prepared previously in the literature [10] was obtained by reaction of $[Rh_2Cl_2(CO)_4]$ and two molar equivalents of $SbPh_3$ in the dry CH_2Cl_2. After monitoring the reaction by solution IR spectroscopy, the solvent was removed *in vacuo* and the residues were triturated with hexane to give the red product. The microanalytical data was consistent with the formulation proposed and indeed the IR and ^1H NMR spectroscopic data confirmed this and were in line with the literature.[10] In addition, the $^{13}C\{^1H\}$ NMR spectroscopic data showed the presence of the carbonyl group in the complex, with a doublet at 184.3 ($J_{Rh\text{-}C}$ = 57 Hz), and positive ion electrospray MS showed the major mass peak at 837 which corresponded to $[Rh(CO)(SbPh_3)_2]^+$.

$[Rh(CO)(SbPh_2Me)_2Cl]$ was synthesized using the above method, however attempts to synthesise $[Rh(CO)(SbPhMe_2)_2Cl]$ in a pure form were not as successful. $[Rh(CO)(SbPh_2Me)_2Cl]$ was prepared in good yield, and the ^1H NMR spectrum suggested that the desired product was formed, with resonances at 7.80–7.30 (m) and 1.35 (s) ppm corresponding to aromatic protons and methyl protons, respectively. The $^{13}C\{^1H\}$ NMR spectrum did confirm the coordination of the ligand to the rhodium(I) metal centre, however there was no evidence of a CO resonance which could be due to the CO being fluxional. It could also be due to the complex being fairly unstable, as microanalysis could not be obtained due to decomposition. The positive ion electrospray MS showed a cluster of mass peaks at *ca.* 1003 and 713 with the correct isotopic distribution, corresponding to $[Rh(CO)(SbPh_2Me)_3]^+$ and $[Rh(CO)(SbPh_2Me)_2]^+$ respectively, suggesting that

there may be two species present in the product, however both solution and solid IR spectroscopy suggest that the desired species was formed with bands at 1956 cm^{-1} and 1962 cm^{-1}, for solution and solid respectively. It is clear that this system is more complex than first thought, with the $^{13}C\{^1H\}$ NMR spectrum suggesting there is no carbonyl in the product, whereas the mass spectrum suggests there is CO in the product, but there is a mixture of di- and tri- substituted rhodium complexes. Unfortunately we were unable to separate these two products due to the instability of the system.

The attempted preparation of $[Rh(CO)(SbPhMe_2)_2Cl]$ resulted in a red/brown oil being obtained in moderate yield. The ^1H NMR spectrum confirmed the coordination of $SbPhMe_2$ to the rhodium(I) centre, but the complex did not seem to fly by positive ion electrospray and the IR spectrum was complex with three bands at 2019 w, 1998 w, 1969 w in the solution IR spectrum and two at 2012 m 1964 w in the solid IR spectrum, all corresponding to CO stretches. As the product was an oil, microanalytical data could not be obtained and the $^{13}C\{^1H\}$ NMR was inconclusive. Therefore the attempted preparation of $[Rh(CO)(SbPh_2Me)_2Cl]$ and $[Rh(CO)(SbPhMe_2)_2Cl]$ did not produce clean products and were not pursued.

$[Rh(CO)\{Ph_2Sb(CH_2)_3SbPh_2\}_2][Rh(CO)_2Cl_2]$ was prepared from $[Rh_2Cl_2(CO)_4]$ and two equivalents of $Ph_2Sb(CH_2)_3SbPh_2$ in dry, degassed CH_2Cl_2, as an orange solid in good yield. The reaction was monitored by solution IR spectroscopy until no change occurred, and bands at 2068 s and 1989 m cm^{-1} corresponded to the $Rh(CO)_2Cl_2]^-$ anion,[26] and the band at 1968 (m) cm^{-1} corresponded to $[Rh(CO)\{Ph_2Sb(CH_2)_3SbPh_2\}_2]^+$. Similar rhodium(I) phosphine complexes, for example $[Rh(CO)(Ph_2P(CH_2)_3PPh_2)_2]^+$ (ν(CO) = 1930 cm^{-1}) have ν(CO) bands to low frequency of these distibine analogues, which is consistent with the phosphine complexes having a more electron rich rhodium centre.[27] Other spectroscopic data on the complex suggested that formulation was correct, with the ^1H NMR spectrum showing peaks at 7.60–7.40 (m), 2.85 (bs) and 2.05 (s) corresponding to aromatic protons, CH_2Sb and CH_2 respectively. The $^{13}C\{^1H\}$ NMR spectrum showed a doublet at 182.3 ($^1J_{RhC}$ = 71 Hz) corresponding to the $[Rh(CO)_2Cl_2]^-$ anion, but there was no doublet for the $[Rh(CO)\{Ph_2Sb(CH_2)_3SbPh_2\}_2]^+$ cation, suggesting that the carbonyl in the cation is fluxional. Studies of the complex using electrospray MS revealed that the desired product was evident. For example in the positive ion electrospray MS there were clusters of peaks at *ca.* 1289 (100%) and 1317 (5%) corresponding to $[Rh\{Ph_2Sb(CH_2)_3SbPh_2\}_2]^+$ and $[Rh(CO)\{Ph_2Sb(CH_2)_3SbPh_2\}_2]^+$ and in the negative ion electrospray MS there was only one

peak at *ca.* 229 corresponding to the $[Rh(CO)_2Cl_2]^-$ anion. A conductivity experiment also confirmed the ionic nature of the species, and microanalysis suggested the purity of the sample.

In order to probe the boundaries of the chemistry in more detail $[Rh(CO)\{Ph_2Sb(CH_2)_3SbPh_2\}_2][Rh(CO)_2Cl_2]$ was subsequently treated with 2 molar equivalents of $Ph_2Sb(CH_2)_3SbPh_2$ in dry CH_2Cl_2 to form $[Rh(CO)\{Ph_2Sb(CH_2)_3SbPh_2\}_2]Cl$. In situ monitoring by IR spectroscopy saw the loss of the bands at 2068 (s) and 1989 (m) corresponded to the $Rh(CO)_2Cl_2]^-$ anion, leaving the ν(CO) at 1966 cm^{-1} which corresponded to the $[Rh(CO)\{Ph_2Sb(CH_2)_3SbPh_2\}_2]^+$ cation. This was confirmed by the electrospray MS, in particular the absence of the mass peak at 229 ($[Rh(CO)_2Cl_2]^-$ anion) in the negative ion electrospray MS.

Further studies on this system involved reacting $[Rh(CO)\{Ph_2Sb(CH_2)_3SbPh_2\}_2][Rh(CO)_2Cl_2]$ with 2 molar equivalents of ligand and two molar equivalents of NH_4PF_6 in CH_2Cl_2 at room temperature. This reaction was almost instantaneous, and the NH_4Cl was filtered off. The resulting orange solution was then reduced in volume and Et_2O was added to precipitate a solid. The orange solid was obtained in good yield, and the ^1H NMR spectrum was similar to that of $[Rh(CO)\{Ph_2Sb(CH_2)_3SbPh_2\}_2][Rh(CO)_2Cl_2]$. Indeed the positive ion electrospray showed the same mass peaks at *ca.* 1291 and 1317 as in the cases of $[Rh(CO)\{Ph_2Sb(CH_2)_3SbPh_2\}_2][Rh(CO)_2Cl_2]$ and $[Rh(CO)\{Ph_2Sb(CH_2)_3SbPh_2\}_2]Cl$, but the nujol mull IR spectrum, in addition to seeing the band at 1952 cm^{-1} corresponding to the $[Rh(CO)\{Ph_2Sb(CH_2)_3SbPh_2\}_2]^+$, showed bands at 837 and 557 cm^{-1} confirming the presence of ionic PF_6^-. Literature examples of rhodium(I) carbonyl complexes incorporating phosphines have been reported, although these have been synthesised by bubbling CO through solutions of the planar 16 electron $[Rh(diphosphine)_2]^+$ cations.[24,25] For example $[Rh(CO)\{Ph_2P(CH_2)_3PPh_2\}_2]BF_4$ and $[Rh(CO)\{Ph_2PCH_2PPh_2\}_2]BF_4$ have been synthesised by Pignolet and co-workers and have been found to have CO stretches of 1929 and 1945 cm^{-1} in the IR spectra.[20] Figure 4.2.6 shows the solution IR spectra (CO region) of $[Rh(CO)\{Ph_2Sb(CH_2)_3SbPh_2\}_2][Rh(CO)_2Cl_2]$, $[Rh(CO)\{Ph_2Sb(CH_2)_3SbPh_2\}_2]Cl$ and $[Rh(CO)\{Ph_2Sb(CH_2)_3SbPh_2\}_2]PF_6$ and Figure 4.2.7 shows the reaction scheme for the reactions involving $[Rh_2Cl_2(CO)_4]$ and $Ph_2Sb(CH_2)_3SbPh_2$.

Fig 4.2.6: Solution (CH_2Cl_2) IR spectra of (a) $[Rh(CO)\{Ph_2Sb(CH_2)_3SbPh_2\}_2][Rh(CO)_2Cl_2]$, (b) $[Rh(CO)\{Ph_2Sb(CH_2)_3SbPh_2\}_2]Cl$ and (c) $[Rh(CO)\{Ph_2Sb(CH_2)_3SbPh_2\}_2]PF_6$ showing the CO stretching region.

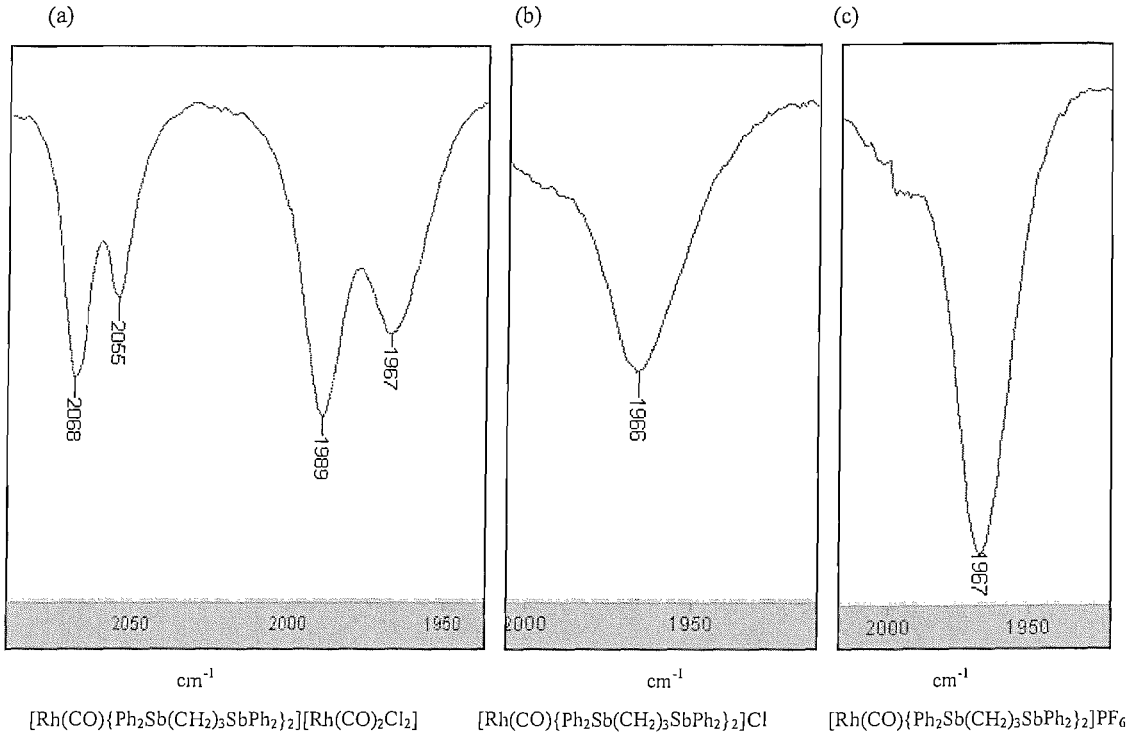

$[Rh(CO)\{Ph_2Sb(CH_2)_3SbPh_2\}_2]^+$ cation: ν = 1966/1967 cm^{-1}.$[Rh(CO)_2Cl_2]^-$ anion: ν = 2068, 1989 cm^{-1}.

CH_2Cl_2 solvent overtone: 2055 cm^{-1}.

Fig 4.2.7: Reaction scheme summarising reaction of $[Rh(CO)_2Cl]_2$ and $Ph_2Sb(CH_2)_3SbPh_2$.

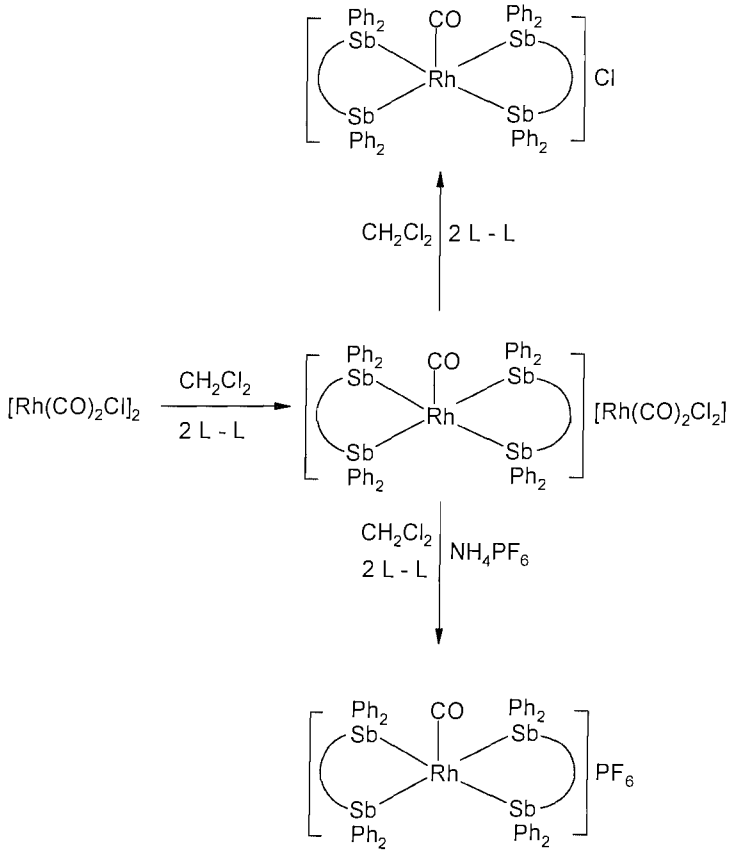

In order to investigate the structural properties of the above complexes, crystals of $[Rh(CO)\{Ph_2Sb(CH_2)_3SbPh_2\}_2]PF_6.¾CH_2Cl_2$ were obtained by layering a solution of the complex in CH_2Cl_2 with hexane. The crystal structure shows two independent cations and anions in the asymmetric unit. There are also two partially occupied sites containing CH_2Cl_2 molecules. Both of the rhodium(I) cations are indistinguishable. Figure 4.2.8 shows one of the $[Rh(CO)\{Ph_2Sb(CH_2)_3SbPh_2\}_2]^+$ cations in a distorted trigonal bipyramidal coordination environment with two chelating $Ph_2Sb(CH_2)_3SbPh_2$ ligands and one CO in the equatorial position. Comparing the Rh-Sb distances and Rh-CO distances of this crystal structure with literature examples such as $[RhCl_2\{Ph_2Sb(CH_2)_3SbPh_2\}_2]^+$,[28] $[Rh(CO)(Ph_2PCH_2PPh_2)_2]^+$ [20] and $[Rh_2(CO)_4\{Ph_2P(CH_2)_4PPh_2\}_3]^{2+}$[25] suggests that they are similar. For example the Rh–Sb distances in this Rh(I) species are 2.5404(6) – 2.6062(7) Å and in $[RhCl_2\{Ph_2Sb(CH_2)_3SbPh_2\}_2]^+$ they are 2.594(2) and 2.611(2) Å. The Rh-CO distances are also comparable with this species having distances in the range of 1.875(7)-1.856(7) Å compared to

$[Rh_2(CO)_4\{Ph_2P(CH_2)_4PPh_2\}_3]^{2+}$ (d(Rh–CO) = 1.886(4) and 1.922(5) Å) while $[Rh(CO)(Ph_2PCH_2PPh_2)_2]^+$ has d(Rh–CO) = 1.894(6) Å. Table 4.2.2 shows selected bond lengths and angles from the crystal structure of the cation of $[Rh(CO)\{Ph_2Sb(CH_2)_3SbPh_2\}_2]PF_6.¾CH_2Cl_2$.

Fig 4.2.8: Crystal structure of the cation of $[Rh(CO)\{Ph_2Sb(CH_2)_3SbPh_2\}_2]PF_6.¾CH_2Cl_2$ with numbering scheme adopted. The second cation in the structure is very similar. Ellipsoids are shown at the 50 % probability level and H atoms are omitted for clarity.

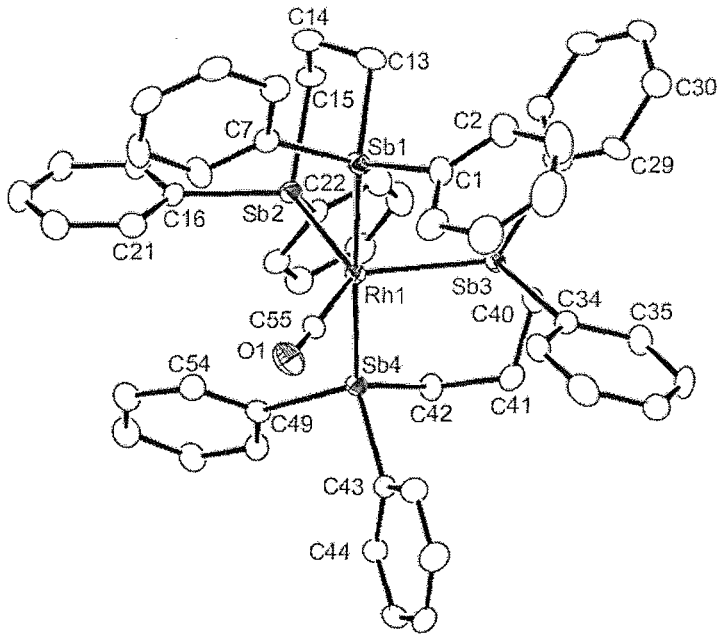

Table 4.2.2: Selected bond lengths (Å) and angles (°) of $[Rh(CO)\{Ph_2Sb(CH_2)_3SbPh_2\}_2]^+$

Rh1–Sb1	2.5404(6)	C55–Rh1–Sb1	88.67(19)
Rh1–Sb2	2.5967(7)	C55–Rh1–Sb2	128.5(2)
Rh1–Sb3	2.6062(7)	C55–Rh1–Sb3	125.2(2)
Rh1–Sb4	2.5579(6)	C55–Rh1–Sb4	91.36(19)
Rh1–C55	1.875(7)	Sb1–Rh1–Sb2	87.70(2)
Sb–C	2.119(7) – 2.152(6)	Sb1–Rh1–Sb3	91.26(2)
C55–O1	1.141(8)	Sb1–Rh1–Sb4	177.99(2)
		Sb2–Rh1–Sb3	106.16(2)
		Sb2–Rh1–Sb4	93.85(2)
		Sb3–Rh1–Sb4	87.08(2)

The reaction of $[Rh_2Cl_2(CO)_4]$ with four molar equivalents of either $Me_2Sb(CH_2)_3SbMe_2$ or *o*-$C_6H_4(CH_2SbMe_2)_2$ in dry CH_2Cl_2 led to the formation of dark brown solids over a period of about 2 minutes. Substantial decomposition was also observed in these reactions, and resulting analytical data of the brown solids revealed no well-defined products. Similar reactions of Rh(I) complexes involving distibinomethanes have been reported in the literature, where decomposition readily occurs, even in the solid state.[17] However when the reaction was repeated with $[Rh_2Cl_2(CO)_4]$ and 2 molar equivalents of $Me_2Sb(CH_2)_3SbMe_2$, in CH_2Cl_2 at -15 °C for 30 minutes, an orange/brown solid was obtained. By electrospray MS this compound was seen to contain the $[Rh(CO)\{Me_2Sb(CH_2)_3SbMe_2\}_2]^+$ cation. Indeed the positive ion electrospray MS showed a cluster of mass peaks at *m/z ca.* 865, 795 and 641 corresponding to $[Rh(CO)\{Me_2Sb(CH_2)_3SbMe_2\}_2.MeCN]^+$, $[Rh\{Me_2Sb(CH_2)_3SbMe_2\}_2]^+$, and $[Rh\{Me_2Sb(CH_2)_3SbMe_2\}_2 - SbMe_2]^+$ respectively. IR spectroscopy also confirmed the Rh(I) cation being present. For example the solution IR spectrum showed a carbonyl band at 1966 cm^{-1}. There were however two more CO bands at 2069 and 1988 cm^{-1} corresponding to the $[Rh(CO)_2Cl_2]^-$ anion. This was further supported in the $^{13}C\{^1H\}$ NMR spectrum with doublets at 193.0 ($^1J_{RhC}$ = 65 Hz) and 181.7 ($^1J_{RhC}$ = 79 Hz) ppm corresponding to $[Rh(CO)\{Me_2Sb(CH_2)_3SbMe_2\}_2]^+$ and $[Rh(CO)_2Cl_2]^-$ respectively. The ^1H NMR spectrum also showed coordinated ligand, and the microanalysis supported the formulation of $[Rh(CO)\{Me_2Sb(CH_2)_3SbMe_2\}_2][Rh(CO)_2Cl_2]$. The compound decomposed significantly in solution at room temperature over a period of minutes and even in the solid state there was significant decomposition over a few days, which suggests that the complex is very reactive and unstable. Treatment of the complex with excess $Me_2Sb(CH_2)_3SbMe_2$ or addition of NH_4PF_6 did not result in the replacement of the $[Rh(CO)_2Cl_2]^-$ anion, but resulted in decomposition of the complex. It can therefore be postulated that the bulky $[Rh(CO)_2Cl_2]^-$ anion stablises the Rh(I) cation species.

The corresponding $[Rh(CO)\{o\text{-}C_6H_4(CH_2SbMe_2)_2\}_2][Rh(CO)_2Cl_2]$ was obtained as a brown solid in moderate yield. Positive ion electrospray MS confirmed the presence of the rhodium(I) cation with mass peaks at *ca.* 947, and the negative ion electrospray MS showed a mass peak at *ca.* 229 corresponding to the $[Rh(CO)_2Cl_2]^-$ anion. ^1H NMR spectroscopy also confirmed the formulation of the complex with resonances corresponding to coordinated ligand. Unfortunately the complex decomposed readily in solution, and it was not possible to obtain a clear $^{13}C\ \{^1H\}$ NMR spectrum or a solution IR spectrum. The Nujol mull IR spectrum did however show further evidence for the

formulation of $[Rh(CO)\{o\text{-}C_6H_4(CH_2SbMe_2)_2\}_2][Rh(CO)_2Cl_2]$ with bands at 2075, 2007 v br ($[Rh(CO)_2Cl_2]^-$), and a shoulder at 1974 ($[Rh(CO)\{o\text{-}C_6H_4(CH_2SbMe_2)_2\}_2]^+$) (CO) cm^{-1}.

A further reaction of interest is the reaction of $[Rh_2Cl_2(CO)_4]$ and 4 molar equivalents of $Ph_2SbCH_2SbPh_2$ in CH_2Cl_2. Initially the reaction pathway forms the known Rh(I) dimer $[Rh_2(CO)_2Cl_2\{Ph_2SbCH_2SbPh_2\}_2]$,[17] with an IR band at 2000 cm^{-1}, but if the reaction is left to proceed further, another CO containing species is produced. This is evident with the appearance of another CO band at 1970 cm^{-1}, which may be the Rh(I) cationic species $[Rh(CO)\{Ph_2SbCH_2SbPh_2\}_2]^+$. However, even with further stirring or the addition of NH_4PF_6, to drive the reaction forward, there is not complete conversion of the dimer species to the Rh(I) cationic species, and a substantial amount of the dimer species remains. The positive ion electrospray MS supports this with mass peaks at *ca.* 1429 and *ca.* 1263 corresponding to $[Rh_2(CO)_2Cl\{Ph_2SbCH_2SbPh_2\}_2]^+$ and $[Rh(CO)\{Ph_2SbCH_2SbPh_2\}_2]^+$ respectively. Unfortunately, due to the incomplete conversion of the dimer to the cationic species it was impossible to obtain an analytically pure sample. This reaction however does suggest that distibinomethane ligands can chelate, albeit with a much lower tendency than analogous diphosphinomethanes.

4.2.4 Rhodium(I) reaction chemistry

The reaction chemistry of Rh(I) complexes incorporating $Ph_2Sb(CH_2)_3SbPh_2$ will be focused on in this study, due to these complexes being more stable than complexes that incorporate the methyl-substituted distibine ligands, in the solid state and in solution.

An alternative route to form the $[Rh(CO)\{Ph_2Sb(CH_2)_3SbPh_2\}_2]^+$ cation was by bubbling CO through a solution of $[Rh\{Ph_2Sb(CH_2)_3SbPh_2\}_2]BF_4$ in acetone. This was confirmed by the appearance of a single CO band at 1966 cm^{-1}, being present in the solution IR spectrum. However when the monocarbonyl species is exposed to an atmosphere of CO for a long period of time (in excess of 1 h) the single CO band is replaced by two CO bands at 2020 and 1993 cm^{-1}. It is thought that this shows the formation of a *cis*-dicarbonyl Rh(I) complex. Moreover in the absence of a CO atmosphere, the dicarbonyl species readily reverts quantitatively back to the monocarbonyl species. It can be suggested that the conversion of the monocarbonyl $[Rh(CO)\{Ph_2Sb(CH_2)_3SbPh_2\}_2]^+$ cation to the dicarbonyl complex, could occur *via* one of two routes, the first of which being dissociation of one distibine ligand to give $[Rh(CO)_2\{Ph_2Sb(CH_2)_3SbPh_2\}]^+$ and free ligand. The second route is *via* chelate ring opening,

which would form a 16 electron 5 coordinate Rh(I) $[Rh(CO)_2\{Ph_2Sb(CH_2)_3SbPh_2\}\{\kappa^1\text{-}Ph_2Sb(CH_2)_3SbPh_2\}]^+$ species. This route may be more appropriate as it would be easily reversible. Comparison of similar complexes in the literature is shown in Table 4.2.3.

Table 4.2.3: IR Spectroscopy data of selected literature Rh(I) carbonyl complexes compared with this study.

Complex	IR ν(CO) cm^{-1}	Ref
$[Rh(CO)\{Ph_2Sb(CH_2)_3SbPh_2\}_2]^+$ + excess CO	2020, 1993	*a*
cis-$[Rh(CO)_2\{Ph_2P(CH_2)_2Ph_2\}]^+$	2100, 2055	29
$[\{(CO)_2\{Ph_2P(CH_2)_4PPh_2\}Rh\}_2\{\mu\text{-}Ph_2P(CH_2)_4PPh_2\}]$	2020, 1965	25
$[Rh(CO)_2(SbPh_3)_3][AlCl_4]$	2009	30

[a] This study

From the comparison of the literature data in Table 4.2.2, and that it is observed that the dicarbonyl species converts reversibly back to $[Rh(CO)\{Ph_2Sb(CH_2)_3SbPh_2\}_2]^+$ it can be postulated that the most likely product is the five coordinate $[Rh(CO)_2\{Ph_2Sb(CH_2)_3SbPh_2\}\{\kappa^1\text{-}Ph_2Sb(CH_2)_3SbPh_2\}]^+$ species. Unfortunately structural identification of the dicarbonyl species could not be obtained.

It has also been observed that $[Rh(CO)\{Ph_2Sb(CH_2)_3SbPh_2\}_2]PF_6$ undergoes oxidative addition of bromine in CH_2Cl_2. The resultant complex of the reaction is the known cationic species *trans*-$[RhBr_2\{Ph_2Sb(CH_2)_3SbPh_2\}_2]^+$, which has been synthesised previously.[28] From IR and NMR spectroscopy and by mass spectrometry it was seen that the conversion was quantitative. However when $[Rh(CO)\{Ph_2Sb(CH_2)_3SbPh_2\}_2]PF_6$ or $[Rh\{Ph_2Sb(CH_2)_3SbPh_2\}_2]BF_4$ was reacted with MeI in CH_2Cl_2 no reaction was observed, even when the reaction was heated.

$[Rh(CO)\{Ph_2Sb(CH_2)_3SbPh_2\}_2]PF_6$ was dissolved in CH_2Cl_2 and the solution was saturated with excess HCl gas. The solution rapidly changed from deep red to pale yellow, and following *in situ* solution IR spectroscopy studies, it was observed that the CO stretching vibration disappeared. After removing the solvent, the yellow powder was dried *in vacuo* and spectroscopic studies suggested that there was a mixture of products. ^1H NMR spectroscopy was used to identify one of

the rhodium containing species. A doublet at -18.95 ppm with $^{1}J_{RhH}$ = 7.2 Hz was observed which suggests the presence of a rhodium-hydride, and indeed a tentative formulation of this complex is a rhodium(III) hydride, $[RhHCl_2\{Ph_2Sb(CH_2)_3SbPh_2\}]$. Comparison of literature data on $[RhHCl_2(SbPh_3)_2]$, reported by Wilkinson *et al* which has a hydride resonance at -18.3 ppm and $^{1}J_{RhH}$ = 7 Hz seems to support the formulation. [31]

A second rhodium containing species was discovered when crystals were grown from a solution of the products in $CHCl_3$. The crystal structure is that of a very unexpected Rh(III) complex of formula $[RhCl_2\{Ph_2Sb(CH_2)_3SbPh_2\}\{PhClSb(CH_2)_3SbClPh\}]Cl.CHCl_3$. A view of the crystal structure can be seen in Figure 4.2.9, and shows one rhodium metal atom surrounded by two *trans* chloride ligands, and four antimony centres. Two of these are incorporated in a chelating $Ph_2Sb(CH_2)_3SbPh_2$ and the other two antimony centres are from a *bis*(phenylchlorostibino)propane ligand. There is also a Cl^- anion which forms a long range secondary interaction between the Sb atoms of the *bis*(phenylchlorostibino)propane ligand, and is also present to provide a charge balance. Selected bond lengths and angles can be seen in Table 4.2.4.

Fig 4.2.9: Crystal structure of $[RhCl_2\{Ph_2Sb(CH_2)_3SbPh_2\}\{PhClSb(CH_2)_3SbClPh\}]Cl.CHCl_3$ with atom numbering scheme. Ellipsoids are drawn at the 50% probability level and H atoms are omitted for clarity.

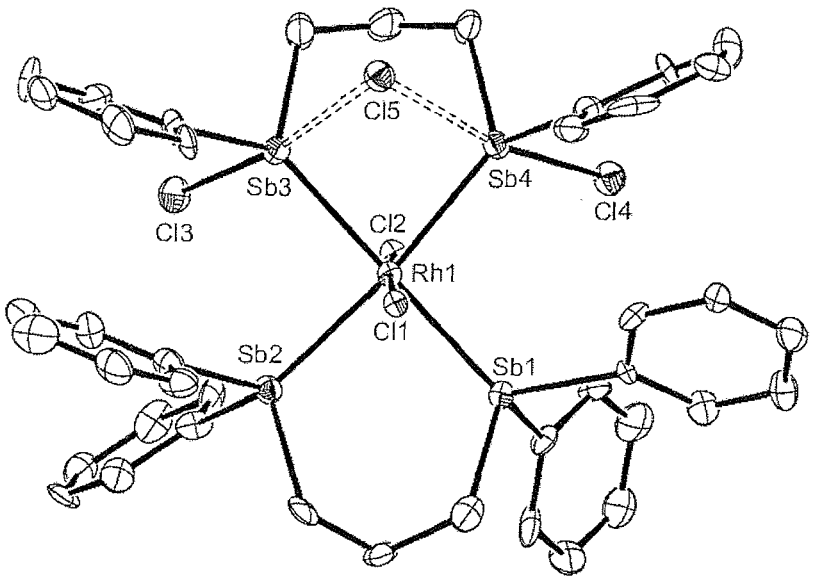

Table 4.2.4: Selected bond lengths (Å) and angles (°) for $[RhCl_2\{Ph_2Sb(CH_2)_3SbPh_2\}\{PhClSb(CH_2)_3SbClPh\}]Cl$.

Rh1–Cl2	2.371(3)	Cl2–Rh1–Cl	1174.86(11)
Rh1–Cl1	2.410(3)	Sb1–Rh1–Sb2	89.56(4)
Rh1–Sb1	2.5896(13)	Sb1–Rh1–Sb4	97.75(5)
Rh1–Sb2	2.5920(14)	Sb2–Rh1–Sb4	170.86(5)
Rh1–Sb4	2.6045(14)	Sb1–Rh1–Sb3	176.92(5)
Rh1–Sb3	2.6261(13)	Sb2–Rh1–Sb3	91.09(4)
Sb3–Cl3	2.440(3)	Sb4–Rh1–Sb3	81.90(4)
Sb3···Cl5	2.736(3)	Sb3···Cl5···Sb4	76.13(8)
Sb4–Cl4	2.435(4)		
Sb4···Cl5	2.823(3)		

Detailed comparisons of the crystallographic parameters for this crystal structure with other structures is not reliable due to the data being weak, and the final residuals being rather high, but it is clear that one phenyl group on both antimony of one of the ligands has been cleaved. The crystal structure in Figure 4.2.9 is very interesting and important in the exploration of stibine chemistry, as structural examples involving R_2SbCl units are rare, while secondary Sb···Cl interactions are well known, in compounds such as antimony chloride anions. As can be seen from Table 4.2.4, the Sb···Cl distances are 2.736(3) Å and 2.823(3) Å, relatively short in comparison to secondary interactions in chloro-antimony anions (2.9-3.2 Å). For example in the complex $[Sb_2Cl_6\{o\text{-}C_6H_4(AsMe_2)_2\}]$ the Sb···Cl distances are 3.020(3), 3.171(2) and 3.267(3) Å.[32] It can be suggested that this unusually short interaction could be due to either the C_3-unit of the ligand back-bone, the geometric constraints of the Sb coordinated to the Rh centre, or the less electron rich Sb centre as a result of the rhodium coordination, which in turn would lead to stronger Sb···Cl interactions.

Due to the harsh reaction conditions involved in this system, ie. HCl gas saturated solution, it can be suggested that the phenyl rings could have been cleaved by the excess HCl. In an attempt to probe this a dilute solution of HCl in CH_2Cl_2 was added to $[Rh(CO)\{Ph_2Sb(CH_2)_3SbPh_2\}_2]PF_6$ and the reaction analysed by ^1H NMR spectroscopy and IR spectroscopy. The same hydride species was observed in the ^1H NMR spectrum and the absence of the CO stretching frequency in the IR spectrum was also observed. Unfortunately we were unable to obtain single crystals to prove the

reproducibility of the second product. Moreover the planar 16 electron $[Rh\{Ph_2Sb(CH_2)_3SbPh_2\}_2]BF_4$ was also treated with an HCl saturated acetone solution and the Rh-hydride product ($\delta^1H = -18.95$, $^1J_{RhH} = 7.2$ Hz) was identified from *in situ* ^1H NMR studies. In the IR spectrum there was also a weak band at 1998 cm^{-1} which may be tentatively assigned as the Rh-H stretch.

It has been seen that organostibines incorporating phenyl groups can undergo phenyl cleavage and Sb-Cl bond formation readily when exposed to a saturated HCl solution. Indeed in preparing the *o*-$C_6H_4(CH_2SbMe_2)_2$ this technique is used to convert $PhSbMe_2$ to $ClSbMe_2$. However it is generally accepted that chlorostibines are not considered as good ligands for metal centres. Moreover the Rh(III) complex reported here is the first structurally characterised example of a metal coordinated to a chlorostibine. Unfortunately, not much is known about the reaction mechanism in the cleavage reaction. It is unclear whether the cleavage of the Ph groups occurs while the ligand is coordinated to the metal centre, or whether dissociation of the ligand occurs, followed by cleavage of the Ph group along with substitution for the Cl^-, and then association of the new chlorostibine. This exciting discovery is of great interest in the field however, as it may pave the way forward for template syntheses of new polydentate and macrocylic stibines. Figure 4.2.10 summarises the reaction chemistry of $[Rh\{Ph_2Sb(CH_2)_3SbPh_2\}_2]BF_4$.

Fig 4.2.10: Summary of the reaction chemistry of $Rh\{Ph_2Sb(CH_2)_3SbPh_2\}_2]BF_4$.

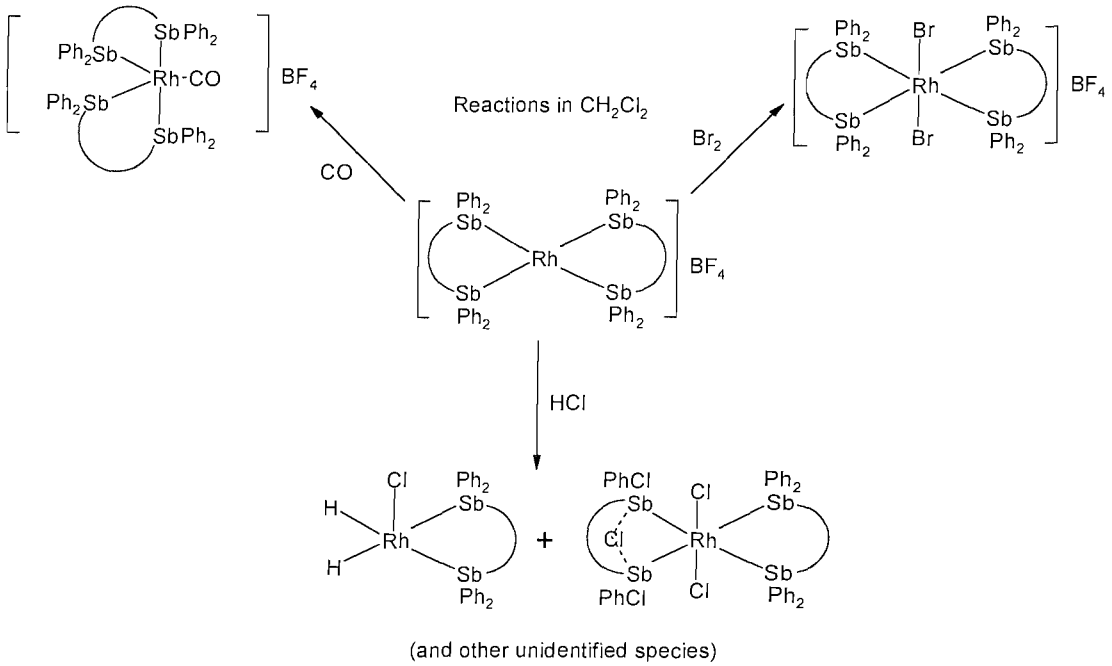

4.2.5 Iridium(I)-stibine complexes

There are very few examples of Ir(I) complexes incorporating stibine ligands,[1] one of which is shown in Figure 4.2.2. None of these known complexes involve distibine ligands however and therefore were interested to probe the chemistry of Ir(I) species with distibines.

Complexes of the form $[Ir(cod)\{L\text{-}L\}]BF_4$ (where L-L = $Ph_2Sb(CH_2)_3SbPh_2$ and *o*-$C_6H_4(CH_2SbMe_2)_2$) were prepared by the reaction of $[Ir_2Cl_2(cod)_2]$ and two molar equivalents of $AgBF_4$, filtration of the AgCl produced, followed by the addition of a toluene solution of the appropriate distibine ligand. $[Ir(cod)\{Ph_2Sb(CH_2)_3SbPh_2\}]BF_4$ and $[Ir(cod)\{o\text{-}C_6H_4(CH_2SbMe_2)_2\}]BF_4$ were obtained as pink and orange solids respectively, in good yield. Microanalysis suggested that the above formulations were correct, along with the IR spectroscopy and mass spectrometry data. For example the positive ion electrospray mass spectra for $[Ir(cod)\{Ph_2Sb(CH_2)_3SbPh_2\}]BF_4$ showed mass peaks centred at *m/z* 895 ($[Ir(cod)\{Ph_2Sb(CH_2)_3SbPh_2\}]^+$) and for $[Ir(cod)\{o\text{-}C_6H_4(CH_2SbMe_2)_2\}]BF_4$ showed mass peaks centred at *m/z* 707. For both complexes the nujol mull IR spectrum showed a band at 1064 cm^{-1}, corresponding to the BF_4^- anion. NMR spectroscopic studies of the complexes also supported the formulations with the resonances indicating the presence of coordinated distibine ligand and cod. Unfortunately single crystals of these complexes were not obtained, but the spectroscopic data provides strong evidence that the compounds were formed. Attempts to synthesise $[Ir(cod)\{Me_2Sb(CH_2)_3SbMe_2\}]BF_4$ were not as successful due to significant decomposition occurring as a black precipitate. This is probably due to the very reactive nature of the C_3-linked methyl substituted distibine ligand and was also seen when synthesising $[Rh(cod)\{Me_2Sb(CH_2)_3SbMe_2\}]BF_4$. Positive ion electrospray MS was obtained which showed mass peaks centred at *m/z* 647 corresponding to $[Ir(cod)\{Me_2Sb(CH_2)_3SbMe_2\}]^+$. A nujol mull IR spectrum was also obtained which showed a strong band at 1054 cm^{-1} corresponding to the BF_4^- anion. This evidence supports the formulation above, and proves that the complex was formed, however solution NMR spectroscopic studies were not obtained due to substantial decomposition when the complex is in solution. Therefore, we are not able to suggest that the reaction was clean. Due to the sensitive nature of the complex, microanalytical data were not obtained.

Another iridium(I) complex that has been obtained in this study is the planar 16-electron species, $[Ir\{Ph_2Sb(CH_2)_3SbPh_2\}_2]BF_4$. In an analogous reaction to that of the preparation of $[Rh\{Ph_2Sb(CH_2)_3SbPh_2\}_2]BF_4$, $[Ir_2(coe)_4Cl_2]$ in acetone, and two equivalents of $AgBF_4$, were

stirred at room temperature. The resulting yellow solution was filtered to remove AgCl, and a toluene solution of the ligand was added. Following work up, the solid was isolated and dried *in vacuo* to produce a pale yellow solid in good yield. Microanalysis supported the formulation of the complex, along with ^{1}H and $^{13}C\{^{1}H\}$ NMR spectroscopy. For example it was shown that the complex incorporated coordinated ligand in the ^{1}H NMR spectrum with resonances at 7.0–7.4 (m), 2.8 (br) and 2.3 (br) corresponding to aromatic protons, $C\underline{H}_2CH_2$ and CH_2Sb respectively. IR spectroscopy also showed the presence of the BF_4^- anion.The complexes above are of great importance in the exploration of distibine ligands and their coordination chemistry with iridium(I) metal centres, and it is vital that the reaction chemistry of these complexes is also investigated to help the understanding of the area. In due course the results of such studies could be used to develop applications for these compounds. In an attempt to study some reaction chemistry $[Ir\{Ph_2Sb(CH_2)_3SbPh_2\}_2]BF_4$ was dissolved in dry acetone, and the solution was saturated with CO gas. *In situ* IR spectroscopy and positive ion electrospray MS studies were undertaken, and CO stretches at 2020 and 1991 cm^{-1} were observed in the IR spectrum, and mass peaks at 1407 and 1435 corresponding to $[Ir(CO)\{Ph_2Sb(CH_2)_3SbPh_2\}_2]^+$, and $[Ir(CO)_2\{Ph_2Sb(CH_2)_3SbPh_2\}_2]^+$ were seen in the mass spectrometry spectrum. This suggested that a dicarbonyl and a monocarbonyl species were present. However, when the yellow solid was isolated, (the CO atmosphere was not present) the nujol mull IR spectrum showed only one CO stretching band at 2002 cm^{-1}, suggesting that the monocarbonyl was the only major product isolated. The ^{1}H NMR spectrum was similar to that of $[Ir(CO)\{Ph_2Sb(CH_2)_3SbPh_2\}_2]BF_4$ showing coordinated ligand, however we were unable to obtain a clean $^{13}C\ \{^{1}H\}$ NMR spectrum. From these data it is evident that the monocarbonyl iridium(I) complex was formed *in situ* along with a dicarbonyl species. However after work up the major species was seen to be that of $[Ir(CO)\{Ph_2Sb(CH_2)_3SbPh_2\}_2]BF_4$. Fig 4.2.11 shows a summary of the Ir(I) chemistry in this Chapter.

Fig 4.2.11: Coordination chemistry of $R_2Sb(CH_2)_3SbR_2$ and o-$C_6H_4(CH_2SbMe_2)_2$ (R = Me, Ph) with Ir(I).

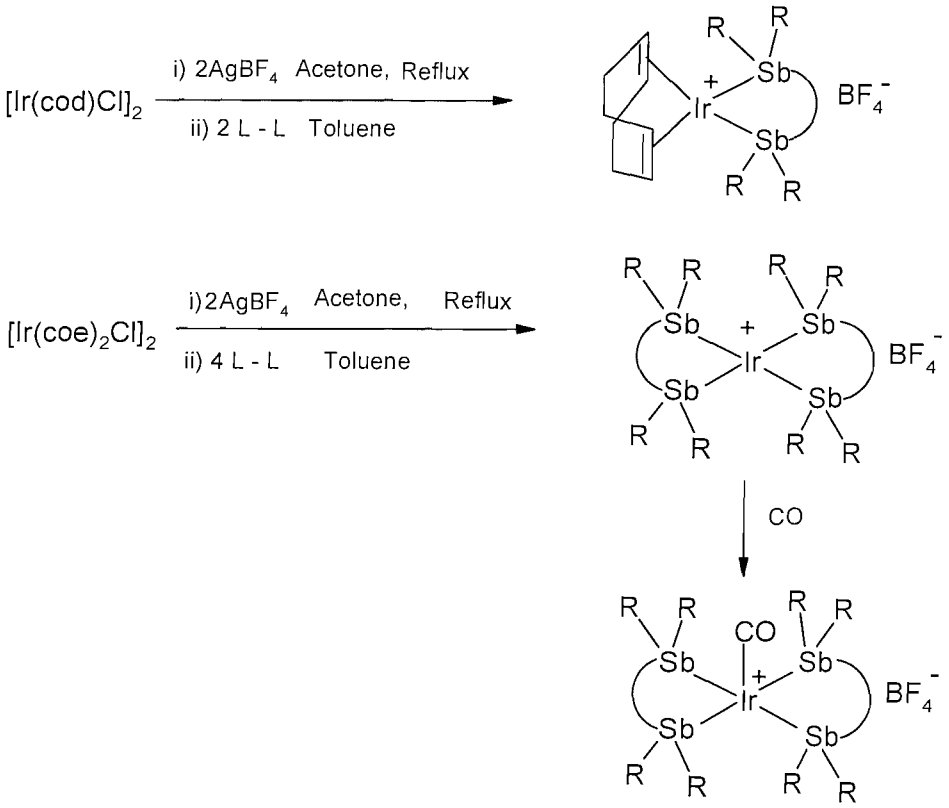

Attempts were made to synthesise a selection of iridium(I) carbonyl species directly, using dimethylformamide decarbonylation.[33] Serp and co-workers used dmf as a source of CO in the coordination chemistry of rhodium, ruthenium, iridium and platinum.[33] This method was employed in the attempted preparation of $[Ir(CO)(SbPh_3)_2Cl]$ and $[Ir(CO)\{Ph_2Sb(CH_2)_3SbPh_2\}_2]Cl$. Vaska's compound $[Ir(CO)(PPh_3)_2Cl]$ [34] was also prepared to explore the synthetic procedure. $IrCl_3.6H_2O$ and dilute HCl were refluxed in dmf, and after cooling, two molar equivalents of PPh_3 were added and stirred at room temperature. Upon aqueous work-up the yellow solid was isolated in good yield. By $^{31}P\{^1H\}$ NMR spectroscopy the product was seen to be pure, with one single resonance at 24.8 ppm. Solution IR spectroscopy also confirmed the desired product with one CO band at 1964 cm^{-1}. These data are in good accord with the literature data.[33] The attempted preparation of $[Ir(CO)(Ph_2Sb(CH_2)_3SbPh_2)_2]Cl$ was carried out using an analogous method to that of the preparation of $[Ir(CO)(PPh_3)_2Cl]$. Two molar equivalents of $Ph_2Sb(CH_2)_3SbPh_2$ and $[Ir(CO)_2Cl_2]^-$ (made *in situ* from the above route) were reacted together in dmf. There was an immediate colour change from orange to yellow and after stirring, the dmf was removed under reduced pressure, and the residues

recrystallised from CH_2Cl_2/hexane. The yellow solid was obtained in good yield. The ^1H NMR spectrum showed coordinated ligand, and the $^{13}C\{^1H\}$ NMR spectrum showed one CO resonance at 187.4 ppm. The positive ion electrospray showed clusters of mass peaks centred at *ca. m/z* 1380 and 1408, corresponding to $[Ir(Ph_2Sb(CH_2)_3SbPh_2)_2]^+$ and $[Ir(CO)(Ph_2Sb(CH_2)_3SbPh_2)_2]^+$ respectively. However the negative ion electrospray showed a cluster of mass peaks centred at *m/z* 405 corresponding to $([Ir(CO)Cl_4(dmf)]\text{-}CO)^-$. This suggests that some of the $[Ir(CO)Cl_4(dmf)]^-$ formed in the reaction of $IrCl_3.6H_2O$ with dilute HCl did not convert fully to $[Ir(CO)_2Cl_2]^-$ on heating, and therefore did not react with the ligand. This mixture of products was also confirmed in the IR spectra. In the solution IR spectrum, two carbonyl bands were seen at 2068 and 1946 cm^{-1} corresponding to $[Ir(CO)Cl_4(dmf)]^-$ and $[Ir(CO)(Ph_2Sb(CH_2)_3SbPh_2)_2]^+$ respectively. Similar findings were observed in the nujol mull IR spectrum with bands at 2054 and 1930 cm^{-1}. Further attempts to produce $[Ir(CO)(Ph_2Sb(CH_2)_3SbPh_2)_2]Cl$ cleanly, by refluxing the $IrCl_3.6H_2O$ and dilute HCl for longer periods of time, were unsuccessful and hence this method was not pursued.

Due to the problems of purifying $[Ir(CO)\{Ph_2Sb(CH_2)_3SbPh_2\}_2]Cl$ a modified method to the one above was employed in an attempt to synthesise $[Ir(CO)(SbPh_3)Cl]$. $[Ir(CO)_2Cl_2][AsPh_4]$ was prepared *via* the literature route above.[33] This complex was then reacted with 2 molar equivalents of $SbPh_3$ in CH_2Cl_2 and stirred under nitrogen. After reducing the volume to *ca.* 2 cm^3, hexane was added to precipitate a solid. The yellow solid was isolated in good yield. The IR spectroscopic data for the product showed three CO bands at 2055 and 1994 ($[Ir(CO)_2Cl_2]^-$) and 1968 cm^{-1} ($[Ir(CO)(SbPh_3)_2Cl]$. The positive ion electrospray showed the only major cationic species to be $[AsPh_4]$ with a cluster of mass peaks at *m/z* 383. These data suggest that the desired product was not synthesised cleanly, and further attempts to push the reaction to completion *via* heating were unsuccessful.

The "facile" route to carbonylhalogenometal complexes by dmf decarbonylation developed by Serp *et al.* does not seem to work for these systems, due to problems associated with purification. It is clear that the desired complexes form, however the employment of dmf and the conversion of $[IrCl_4(CO)(dmf)]^-$ to $[Ir(CO)_2Cl_2]^-$ *in situ* seemed unpredictable, and the stibine ligands do not seem to substitute cleanly. Due to these observations the reactions were not pursued further.

4.3 Conclusions

Neutral Rh(I) distibine complexes of the form [M(cod){L-L}Cl], along with cationic species of the form $[M(cod)\{L\text{-}L\}]^+$, $[M\{L\text{-}L\}_2]^+$ and $[M(CO)\{L\text{-}L\}_2]^+$ (where L-L = $Ph_2Sb(CH_2)_3SbPh_2$ and M = Rh, Ir) have been prepared in good yield. In addition $[Rh(cod)\{L'\text{-}L'\}]BF_4$, $[Rh(CO)\{L'\text{-}L'\}_2][Rh(CO)_2Cl_2]$ and $[Rh(CO)(L)_2Cl]$, (where L'-L' = $Me_2Sb(CH_2)_3SbMe_2$ and *o*-$C_6H_4(CH_2SbMe_2)_2$, and L = $SbPh_3$, Ph_2SbMe) have been isolated and characterised. The structural determination of $[Rh(CO)\{Ph_2Sb(CH_2)_3SbPh_2\}_2]PF_6$ has also been achieved *via* single crystal *X*-ray diffraction.

The results prove that a variety of four- and five-coordinate Rh(I) and Ir(I) distibine complexes involving cod or CO as co-ligands can be synthesised using selected metal precursors, and subtle variations in reaction conditions. It can be seen that complexes incorporating $Ph_2Sb(CH_2)_3SbPh_2$ are more stable, and this is probably due to the phenyl substituents on the distibine ligands. This therefore leads to less electron rich and less reactive complexes compared to the complexes with the more electron rich $-SbMe_2$ units on the ligands. These complexes seem to undergo Sb-C fission more readily resulting in decomposition in some of the reaction reported.

$[Rh(CO)\{Ph_2Sb(CH_2)_3SbPh_2\}_2]PF_6$ and $[Rh\{Ph_2Sb(CH_2)_3SbPh_2\}_2]BF_4$ undergo oxidative addition with Br_2 to form the known Rh(III) cationic species, *trans*-$[RhBr_2\{Ph_2Sb(CH_2)_3SbPh_2\}_2]^+$.[24] Oxidative addition of HCl to $[Rh(CO)\{Ph_2Sb(CH_2)_3SbPh_2\}_2]PF_6$ or $[Rh\{Ph_2Sb(CH_2)_3SbPh_2\}_2]BF_4$ results in the same two major rhodium containing species being formed. The first product is tentatively assigned as $[RhHCl_2\{Ph_2Sb(CH_2)_3SbPh_2\}]$ due to comparisons with literature data on $[RhHCl_2\{SbPh_3\}_2]$[27] and the second unexpected product is shown to be $[RhCl_2\{Ph_2Sb(CH_2)_3SbPh_2\}\{PhClSb(CH_2)_3SbClPh\}]Cl$ by single crystal *X*-ray diffraction. This represents the first structurally characterised example of a coordinated chlorostibine, and this work in the future could lead to other reactions of mixed organoantimony chlorides with transition metals and the reaction chemistry thereof, possibly including the template syntheses of macrocyclic stibines.

4.4 Experimental

General experimental techniques and instrumentation can be found in the appendix. Percentage yields are based upon the metal. The Rh(I) and Ir(I) precursors $[Rh_2Cl_2(CO)_4]$,[35] $[M_2Cl_2(cod)_2]$,[36,37] $[M_2Cl_2(coe)_4]$ [38] (M = Rh or Ir) and the ligands were prepared as described previously.[20,39,40]

4.4.1 Rhodium(I) and Ir(I) compounds

[Rh(cod)($SbPh_3$)$_2$Cl]: $[Rh_2Cl_2(cod)_2]$ (0.049 g, 0.10 mmol) was added to a refluxing solution of $SbPh_3$ (1.0 g, 2.9 mmol) in dry EtOH (10 cm^3) under argon. An orange precipitate formed immediately, was filtered off, washed with CH_2Cl_2/hexane and dried *in vacuo*. (Yield 0.2 g, 100%). Required for $[C_{44}H_{42}ClRhSb_2].½CH_2Cl_2$: C, 53.7; H, 4.4%. Found: C, 53.7; H, 3.8%. ^{1}H NMR ($(CD_3)_2CO$, 300 K): δ 7.50–7.30 (m) [30H] (Ph), 4.25 (br) [4H] (cod C<u>H</u>), 2.45 (m) [4H] (cod C<u>H$_2$</u>), 1.85 (br) [4H] (cod C<u>H$_2$</u>) ppm. $^{13}C\{^1H\}$ NMR ($(CD_3)_2CO$, 225 K): δ 136.3 (s), 135.7 (s), 134.8 (s), 129.1 (s), 128.8 (s) (Ph), 78.0 (d) (^1J = 15 Hz) (cod <u>C</u>H) (cod <u>C</u>H$_2$ resonances obscured by solvent) ppm. ES^+ MS (MeCN): *m/z* 563 $[Rh(cod)(SbPh_3)]^+$, 841 $[Rh(SbPh_3)_2Cl_2]^+$, 917 $[Rh(cod)(SbPh_3)_2]^+$. Conductivity Λ_M/Ω^{-1} cm^2 mol^{-1} (10^{-3} mol dm^{-3} in CH_2Cl_2): 1.39.

[Rh(cod){$Ph_2Sb(CH_2)_3SbPh_2$}Cl]: Reaction as above using $[Rh_2Cl_2(cod)_2]$ (0.062 g, 0.126 mmol) and $Ph_2Sb(CH_2)_3SbPh_2$ (0.15 g, 0.25 mmol). The deep orange solution was reduced to dryness and stirred in dry hexane (20 cm^3) until a precipitate formed. The orange solid was filtered off and dried *in vacuo*. (Yield 0.093 g, 44%). Required for $[C_{35}H_{38}ClRhSb_2].CH_2Cl_2$: C, 46.7; H, 4.4%. Found: C, 47.4; H, 4.1%. ^{1}H NMR ($(CD_3)_2CO$, 300 K): δ 7.60–7.20 (m) [20H] (Ph), 4.20 (br) [4H] (cod C<u>H</u>), 2.43 (br) [4H] (cod C<u>H$_2$</u>), 2.33 (br) [6H] (C<u>H$_2$</u>), 1.78 (br) [4H] (cod C<u>H$_2$</u>) ppm. ES^+ MS (MeCN): *m/z* 805 $[Rh(cod)\{Ph_2Sb(CH_2)_3SbPh_2\}]^+$. Conductivity Λ_M/Ω^{-1} cm^2 mol^{-1} (10^{-3} mol dm^{-3} in CH_2Cl_2): 4.68.

[Rh(cod){$Me_2Sb(CH_2)_3SbMe_2$}Cl]: Reaction as above, except at room temperature using $[Rh_2Cl_2(cod)_2]$ and $Me_2Sb(CH_2)_3SbMe_2$. The orange precipitate was dried *in vacuo*. (Yield 46%). Required for $[C_{15}H_{30}ClRhSb_2].2CH_2Cl_2$: C, 26.8; H, 4.5%. Found: C, 27.2; H, 5.0%. ^{1}H NMR ($(CD_3)_2CO$): δ 4.18 (br) [4H] (cod C<u>H</u>), 2.43 (br) [4H] (cod C<u>H$_2$</u>), 1.76 (br) [6H] (C<u>H$_2$</u>), 1.76 (br) [4H] (cod C<u>H$_2$</u>), 1.35–1.20 (m) [12H] (SbC<u>H$_3$</u>) ppm. ES^+ MS (MeCN): *m/z* 557 $[Rh(cod)\{Me_2Sb(CH_2)_3SbMe_2\}]^+$. Conductivity Λ_M/Ω^{-1} cm^2 mol^{-1} (10^{-3} mol dm^{-3} in CH_2Cl_2): 2.25.

[Rh(cod){*o*-$C_6H_4(CH_2SbMe_2)_2$}Cl]: Prepared at room temperature as above using $[Rh_2Cl_2(cod)_2]$ and *o*-$C_6H_4(CH_2SbMe_2)_2$. Orange solid. (Yield 40%). ES^+ MS (MeCN): *m/z* 619 [Rh(cod){*o*-$C_6H_4(CH_2SbMe_2)_2$}]$^+$. ^1H NMR ($(CD_3)_2CO$): δ 7.0–7.4 (m) [4H] (*o*-$C_6\underline{H}_4$), 4.18 (br) [4H] (cod C$\underline{H}$), 2.40 (br) [4H] (cod C$\underline{H}_2$), 2.32 (br) [6H] (C$\underline{H}_2$), 1.75 (br) [4H] (cod C$\underline{H}_2$), 1.30 1.40 (m) [12H] (SbC$\underline{H}_3$) ppm. Microanalysis was not obtained due to decomposition.

[Rh(cod){$Ph_2Sb(CH_2)_3SbPh_2$}]BF_4: $[Rh_2Cl_2(cod)_2]$ (0.047 g, 0.095 mmol) and $AgBF_4$ (0.043 g, 0.22 mmol) were dissolved in degassed acetone (20 cm^3) and heated to reflux for 30 minutes, where upon a white precipitate was formed. The yellow solution was filtered and added dropwise to a solution of $Ph_2Sb(CH_2)_3SbPh_2$ (0.225 g, 0.38 mmol) in degassed toluene (15 cm^3). The resulting orange solution was stirred at room temperature for *ca.* 1 h. and then reduced to dryness *in vacuo*. The residues were recrystallised in CH_2Cl_2/Et_2O to give a yellow/orange solid, which was filtered off and dried *in vacuo*. (Yield 0.12 g, 74%). Required for $[C_{35}H_{38}BF_4RhSb_2]$: C, 47.1; H, 4.3%. Found: C, 47.0; H, 4.1%. ^1H NMR ($CDCl_3$): δ 6.9–7.6 (m) [20H] (Ph), 4.2 (br) [4H] (cod C$\underline{H}$), 2.3–2.5 (br) [14H] (C$\underline{H}_2$) ppm. $^{13}C\{^1H\}$ NMR ($CDCl_3$): δ 128.22–133.40 (Ph), 80.98 (cod $\underline{C}$H), 31.48 (cod $\underline{C}H_2$), 17.36, 17.15 ($\underline{C}H_2$) ppm. ES^+ MS (MeCN): *m/z* 805 [Rh(cod){$Ph_2Sb(CH_2)_3SbPh_2$}]$^+$. IR (Nujol mull):ν 1054 s (BF_4^-) cm^{-1}.

[Rh(cod){$Me_2Sb(CH_2)_3SbMe_2$}]BF_4: Method as above using $[Rh_2Cl_2(cod)_2]$, $AgBF_4$ and $Me_2Sb(CH_2)_3SbMe_2$. The product was recrystallised from Me_2CO and Et_2O. (Yield 56%). Required for $[C_{15}H_{30}BF_4RhSb_2]$.¼toluene: C, 30.2; H, 4.8. Found: C, 30.1; H, 4.5%. ^1H NMR ($(CD_3)_2CO$): δ 4.0 (s) [4H] (cod C$\underline{H}$), 2.4 (s) [8H] (cod C$\underline{H}_2$), 2.1–2.4 (br) [6H] (C$\underline{H}_2$), 1.7 (br) (12H) (SbC$\underline{H}_3$) ppm (signals due to associated toluene solvent are also evident). $^{13}C\{^1H\}$ NMR ($(CD_3)_2CO$): δ 79.31 (d) (^1J = 15 Hz) (cod $\underline{C}$H), 31.45 (cod $\underline{C}H_2$), 23.94 ($CH_2\underline{C}H_2CH_2$), 18.75 (Sb$\underline{C}H_2$), -6.00 (Sb$\underline{C}H_3$) ppm. ES^+ MS (MeCN): *m/z* 557 [Rh(cod){$Me_2Sb(CH_2)_3SbMe_2$}]$^+$. IR (Nujol Mull): ν 1054 s (BF_4^-) cm^{-1}.

[Rh(cod){*o*-$C_6H_4(CH_2SbMe_2)_2$}]BF_4: Method as above using $[Rh_2Cl_2(cod)_2]$, $AgBF_4$ and *o*-$C_6H_4(CH_2SbMe_2)_2$. (Yield 60%). Required for $[C_{20}H_{32}BF_4RhSb_2]$: C, 34.0; H, 4.6. Found: C, 33.4; H, 4.5%. ^1H NMR ($(CD_3)_2CO$): δ 7.0–7.7 (m) [4H] (o-$C_6\underline{H}_4$), 4.3 (br) [4H] (Sb$C\underline{H}_2$), 4.1 (s) [4H] (cod C$\underline{H}$), 2.4 (s) [8H] (cod C$\underline{H}_2$), 1.7 (d) [12H] ($SbMe_2$) ppm. $^{13}C\{^1H\}$ NMR ($(CD_3)_2CO$): δ 124.74–130.70 (*o*-$\underline{C}_6H_4$), 78.34 (d) (^1J = 15 Hz) (cod $\underline{C}$H), 30.57 (Sb$\underline{C}H_2$), 29.80 (cod $\underline{C}H_2$), 0.89 (Sb$\underline{C}H_3$) ppm. IR (Nujol mull): ν 1054 s (BF_4^-) cm^{-1}.

[Ir(cod){$Ph_2Sb(CH_2)_3SbPh_2$}]BF_4: $[Ir_2Cl_2(cod)_2]$ (0.0806 g, 0.12 mmol) and $AgBF_4$ (0.0493 g, 0.253 mmol) were dissolved in degassed acetone (10 cm^3) and heated gently for 30 min., whereupon a white precipitate was formed. After filtering, the yellow solution was added drop-wise to a solution of $Ph_2Sb(CH_2)_3SbPh_2$ (0.15 g, 0.253 mmol) in degassed toluene (15 cm^3). The resulting pink solution was stirred for 30 min. at room temperature and reduced in volume to *ca.* 2 cm^3 whereupon a pink/orange solid formed. This was then filtered off and dried *in vacuo*. (Yield 0.18 g, 76%). Required for $[C_{35}H_{38}BF_4IrSb_2]$: C, 42.8; H, 3.9. Found: C, 43.6; H, 4.1%. ^1H NMR ($CDCl_3$): δ 7.0–7.6 (m) [20H] (Ph), 3.76 (s) [4H] (cod C<u>H</u>), 2.59 (br) [8H] (cod C<u>H</u>$_2$), 2.00–2.15 (m) [6H] (C<u>H</u>$_2$) ppm. $^{13}C\{^1H\}$ NMR ($CDCl_3$): δ 128.22–133.40 (Ph), 63.77 (cod <u>C</u>H), 36.53 (cod <u>C</u>H$_2$), 23.37 (CH$_2$<u>C</u>H$_2$CH$_2$), 19.59 (Sb<u>C</u>H$_2$) ppm. ES^+ MS (MeCN): *m/z* 895 $[Ir(cod)\{Ph_2Sb(CH_2)_3SbPh_2\}]^+$. IR (Nujol mull): ν 1064 s (BF_4^-) cm^{-1}.

Attempted preparation of [Ir(cod){$Me_2Sb(CH_2)_3SbMe_2$}]BF_4: Method as above using $[Ir_2Cl_2(cod)_2]$, $AgBF_4$ and $Me_2Sb(CH_2)_3SbMe_2$. (Yield: 35%). ES^+ MS (MeCN): *m/z* 647 $[Ir(cod)\{Me_2Sb(CH_2)_3SbMe_2\}]^+$. IR (Nujol mull): ν 1054 s (BF_4^-) cm^{-1}. Due to decomposition of the complex in air over time, microanalytical data were not obtained.

[Ir(cod){*o*-$C_6H_4(CH_2SbMe_2)_2$}]BF_4: Method as above using $[Ir_2Cl_2(cod)_2]$, $AgBF_4$ and *o*-$C_6H_4(CH_2SbMe_2)_2$. (Yield 65%). Required for $[C_{20}H_{32}BF_4IrSb_2]$: 30.2; H, 4.1. Found: C, 30.2; H, 4.1%. ^1H NMR ($(CD_3)_2CO$): δ 7.2–7.7 (m) [4H] (*o*-C$_6$<u>H</u>$_4$), 3.8 (br) [8H] (cod C<u>H</u>, SbC<u>H</u>$_2$), 2.5 (br) [8H] (cod C<u>H</u>$_2$), 1.4 (s) [12H] (SbC<u>H</u>$_3$) ppm. $^{13}C\{^1H\}$ NMR ($(CD_3)_2CO$): δ 126.4–136.7 (*o*-<u>C</u>$_6$H$_4$), 59.16 (cod <u>C</u>H), 33.60 (cod <u>C</u>H$_2$), 24.73 (Sb<u>C</u>H$_2$), -4.87 (Sb<u>C</u>H$_3$) ppm. ES^+ MS (MeCN): *m/z* 707 $[Ir(cod)\{o\text{-}C_6H_4(CH_2SbMe_2)_2\}]^+$. IR (Nujol mull): ν 1064 s (BF_4^-) cm^{-1}.

[Rh{$Ph_2Sb(CH_2)_3SbPh_2$}$_2$]BF_4: $[Rh_2Cl_2(coe)_4]$ (0.064 g, 0.09 mmol) and $AgBF_4$ (0.043 g, 0.22 mmol) were dissolved in degassed acetone (10 cm^3) and stirred for 45 min. at room temperature, where upon a white precipitate formed. After filtering, the orange solution was added drop-wise to a solution of $Ph_2Sb(CH_2)_3SbPh_2$ (0.225 g, 0.38 mmol) in degassed toluene (15 cm^3). The deep red solution was left to stir for 30 minutes, and reduced to dryness. The residues were dissolved in minimum acetone, and Et_2O (10 cm^3) was added to precipitate a solid. The red solid was filtered off and dried *in vacuo*. (Yield 0.2 g, 81%). Required for $[C_{54}H_{52}BF_4RhSb_4].CH_2Cl_2$: C, 45.2; H, 3.7. Found: C, 45.4; H, 3.9%. ^1H NMR ($(CD_3)_2CO$): δ 6.8–7.5 (m) [40H] (Ph), 2.3–2.7 (br) [12H] (C<u>H</u>$_2$) ppm (CH_2Cl_2 solvent is also evident). $^{13}C\{^1H\}$ NMR ($(CD_3)_2CO$): δ 129.42–137.07 (Ph),

24.71 ($CH_2\underline{C}H_2CH_2$), 21.62 ($Sb\underline{C}H_2$) ppm. ES^+ MS (MeCN): *m/z* 1291 $[Rh\{Ph_2Sb(CH_2)_3SbPh_2\}_2]^+$, 1013 $[Rh\{Ph_2Sb(CH_2)_3SbPh_2\}_2 - SbPh_2]^+$. IR (Nujol mull): ν 1064 s (BF_4^-) cm^{-1}.

$[Ir\{Ph_2Sb(CH_2)_3SbPh_2\}_2]BF_4$: $[Ir_2(coe)_4Cl_2]$ (0.08 g, 0.09 mmol) and $AgBF_4$ (0.043 g, 0.22 mmol) were dissolved in degassed acetone (10 cm^3) and stirred at room temperature for 1 h. The white precipitate was filtered off and the orange solution was added dropwise to a solution of $Ph_2Sb(CH_2)_3SbPh_2$ (0.225 g, 0.38 mmol) in degassed toluene (10 cm^3). The reaction was stirred for 30 minutes and then the reaction was pumped to dryness. The yellow residues were dissolved in minimum acetone, and Et_2O (10 cm^3) was added to precipitate a solid. The yellow solid was isolated by filtration and dried *in vacuo*. (Yield 0.19 g, 72%). Required for $[C_{54}H_{52}BF_4IrSb_4].CH_2Cl_2$: C, 42.5; H, 3.5. Found: C, 41.9; H, 3.7%. ^1H NMR ($(CD_3)_2CO$): δ 7.0–7.4 (m) [40H] (Ph), 2.8 (br) [4H] ($C\underline{H}_2$), 2.3 (br) [8H] ($C\underline{H}_2$). $^{13}C\{^1H\}$ NMR ($(CD_3)_2CO$): δ 130.0–136.6 (Ph), 25.0 ($CH_2\underline{C}H_2CH_2$), 23.1 ($Sb\underline{C}H_2$). IR (Nujol mull): ν 1067 s (BF_4^-) cm^{-1}.

$[Rh(CO)(SbPh_3)_2Cl]$: $[Rh_2Cl_2(CO)_4]$ (0.082 g, 0.21 mmol) and $SbPh_3$ (0.30 g, 0.92 mmol) were dissolved in dry CH_2Cl_2 (10 cm^3) and stirred for 2 h. The reaction was monitored by solution IR spectroscopy, and the reaction mixture was reduced to dryness and the residues were stirred in dry hexane (30 cm^3) until a dark red precipitate was formed. This was filtered and the red solid was dried *in vacuo*. (Yield 0.2 g, 100%). Required for $[C_{37}H_{30}ClORhSb_2]$: C, 50.9; H, 3.5. Found: C, 50.6; H, 3.1%. ^1H NMR ($CDCl_3$): δ 7.90–7.30 (m) [30H] (Ph) ppm. $^{13}C\{^1H\}$ NMR ($CDCl_3$): δ 184.3 (d) (^1J = 57 Hz) ($\underline{C}O$), 134.9, 130.7, 128.9, 127.9 (Ph) ppm. ES^+ MS (MeCN): *m/z* 837 $[Rh(CO)(SbPh_3)_2]^+$. IR (CH_2Cl_2): ν 1967 s (CO) cm^{-1}. IR (Nujol mull): ν 1952 s (CO) cm^{-1}. Conductivity Λ_M/Ω^{-1} cm^2 mol^{-1} (10^{-3} mol dm^{-3} in CH_2Cl_2): 0.

$[Rh(CO)(SbPh_2Me)_2Cl]$: Method as above using $[Rh_2Cl_2(CO)_4]$ and $SbPh_2Me$. The red/brown solid was dried *in vacuo*. (Yield 55%). ^1H NMR ($CDCl_3$): δ 7.80–7.30 (m) [20H] (Ph), 1.35 [6H] ($C\underline{H}_3$) ppm. $^{13}C\{^1H\}$ NMR ($CDCl_3$): δ 136.4, 135.5, 130.1, 129.3 (Ph), -1.23 ($\underline{C}H_3$) ppm. ES^+ MS (MeCN): *m/z* 1003 $[Rh(CO)(SbPh_2Me)_3]^+$, 713 $[Rh(CO)(SbPh_2Me)_2]^+$. IR (CH_2Cl_2): ν 1956 s (CO) cm^{-1}. IR (Nujol mull): ν 1962 s (CO) cm^{-1}. Due to decomposition of the complex in air over time, microanalytical data were not obtained.

Attempted preparation of [Rh(CO)(SbPhMe$_2$)$_2$Cl]: Method as above using [$Rh_2Cl_2(CO)_4$] and $SbPhMe_2$. The red/brown oil was dried *in vacuo*. (Yield 45%). ^{1}H NMR ($CDCl_3$): δ 7.50–7.30 (m) [20H] (Ph), 1.20 [6H] ($C\underline{H}_3$) ppm. IR (CH_2Cl_2): ν 2019 w, 1998 w, 1969 w (CO) cm^{-1}. IR (Nujol mull): ν 2012 m 1964 w (CO) cm^{-1}. Due to decomposition of the complex in air over time, microanalytical data were not obtained.

[Rh(CO){Ph$_2$Sb(CH$_2$)$_3$SbPh$_2$}$_2$][Rh(CO)$_2$Cl$_2$]: Reaction as above with [$Rh_2Cl_2(CO)_4$] (0.049 g, 0.126 mmol) and $Ph_2Sb(CH_2)_3SbPh_2$ (0.15 g, 0.25 mmol). The orange precipitate was dried *in vacuo*. (Yield 0.13 g, 68%). Required for [$C_{57}H_{52}Cl_2O_3Rh_2Sb_4$]: C, 44.2; H, 3.3. Found: C, 43.4; H, 3.0%. ^{1}H NMR ($(CD_3)_2CO$): δ 7.60–7.40 (m) [20H] (Ph), 2.85 (bs) [4H] ($C\underline{H}_2Sb$), 2.05 (s) [2H] ($C\underline{H}_2$) ppm. $^{13}C\{^1H\}$ NMR ($CDCl_3$): δ 182.3 (d) (^1J = 71 Hz) ([$Rh(CO)_2Cl_2$]$^-$), 136.1, 134.7, 131.2, 129.9 (Ph), 23.7 ($\underline{C}H_2$), 18.9 ($\underline{C}H_2Sb$) ppm. ES$^+$ MS (MeCN): *m/z* 1289 [Rh{$Ph_2Sb(CH_2)_3SbPh_2$}$_2$]$^+$, 1317 [Rh(CO){$Ph_2Sb(CH_2)_3SbPh_2$}$_2$]$^+$. ES$^-$ MS (MeCN): *m/z* 229 [$Rh(CO)_2Cl_2$]$^-$. IR (CH_2Cl_2): ν 2068 s, 1989 m, 1968 m (CO) cm^{-1}. IR (Nujol mull): ν 2058 s, 1977 s, 1953 bs (CO) cm^{-1}.

[Rh(CO){Ph$_2$Sb(CH$_2$)$_3$SbPh$_2$}$_2$]Cl: A further two mol. equivalents of $Ph_2Sb(CH_2)_3SbPh_2$ were added to the [Rh(CO){$Ph_2Sb(CH_2)_3SbPh_2$}$_2$][$Rh(CO)_2Cl_2$] prepared above, in dry CH_2Cl_2 (10 cm^3), and the reaction was stirred under an argon atmosphere for 12 h. The progress of the reaction was monitored by solution IR spectroscopy. An orange solid was isolated. IR (CH_2Cl_2): ν 1966 s (CO) cm^{-1}. ES$^+$ MS (MeCN): *m/z* 1289 [Rh{$Ph_2Sb(CH_2)_3SbPh_2$}$_2$]$^+$, 1317 [Rh(CO){$Ph_2Sb(CH_2)_3SbPh_2$}$_2$]$^+$. †

[Rh(CO){Ph$_2$Sb(CH$_2$)$_3$SbPh$_2$}$_2$]PF$_6$: [Rh(CO){$Ph_2Sb(CH_2)_3SbPh_2$}$_2$][$Rh(CO)_2Cl_2$] (0.067 g, 0.043 mmol) and $Ph_2Sb(CH_2)_3SbPh_2$ (0.051 g, 0.0865 mmol) and NH_4PF_6 (0.016 g, 0.0865 mmol) were dissolved in dry CH_2Cl_2 (20 cm^3). Solution IR spectroscopy indicated that the reaction was complete after 5 min. The fine white precipitate (NH_4Cl) was removed by filtration and the resultant orange solution was concentrated to *ca.* 1 cm^3. Et_2O (10 cm^3) was added to precipitate an orange solid, which was isolated by filtration and dried *in vacuo*. (Yield 60%). ^{1}H NMR ($CDCl_3$): δ 7.40–7.05 (m) [20H] (Ph), 1.90 (bs) [2H] ($C\underline{H}_2CH_2$), 1.80 (bs) [4H] ($C\underline{H}_2Sb$) ppm. ES$^+$ MS (MeCN): *m/z* 1291 [Rh{$Ph_2Sb(CH_2)_3SbPh_2$}$_2$]$^+$, 1317 [Rh(CO){$Ph_2Sb(CH_2)_3SbPh_2$}$_2$]$^+$. IR (CH_2Cl_2): ν 1967 s (CO) cm^{-1}. IR (Nujol mull): ν 1952 s (CO), 837 s ν(PF_6^-), 557 s δ(PF_6^-) cm^{-1}. †

[Rh(CO){$Me_2Sb(CH_2)_3SbMe_2$}$_2$][$Rh(CO)_2Cl_2$]: Method as for [Rh(CO){$Ph_2Sb(CH_2)_3SbPh_2$}$_2$][$Rh(CO)_2Cl_2$] above, except the solutions were maintained at ~-15 °C with an ice-salt bath. Orange/brown solid. (Yield 50%). Required for [$C_{17}H_{36}Cl_2O_3Rh_2Sb_4$]: C, 19.4; H, 3.5; found: C, 20.2; H, 3.6%. ^{1}H NMR ($CDCl_3$): δ 1.8 – 1.3 (br) [6H] ($C\underline{H}_2$), 1.22 (s) [12H] ($SbC\underline{H}_3$). $^{13}C\{^1H\}$ NMR ($CDCl_3$, 250 K): δ 193.0 (d) (^1J = 65 Hz) [Rh($\underline{C}O$){$Me_2Sb(CH_2)_3SbMe_2$}$_2$]$^+$, 181.7 (d) (^1J = 79 Hz) ([Rh($\underline{C}O)_2Cl_2$]$^-$), 23.04 ($\underline{C}H_2$), 16.89 ($\underline{C}H_2$), -0.16 ($Sb\underline{C}H_3$). ES$^+$ MS (MeCN): *m/z* 865 [Rh(CO){$Me_2Sb(CH_2)_3SbMe_2$}$_2$.MeCN]$^+$, 795 [Rh{$Me_2Sb(CH_2)_3SbMe_2$}$_2$]$^+$, 641 [Rh{$Me_2Sb(CH_2)_3SbMe_2$}$_2$ – $SbMe_2$]$^+$. IR (CH_2Cl_2): ν 2069, 1988, 1966 (CO) cm^{-1}. IR (Nujol mull): ν 2047 sh, 1953 ν br (CO) cm^{-1}.

[Rh(CO){*o*-$C_6H_4(CH_2SbMe_2)_2$}$_2$][$Rh(CO)_2Cl_2$]: Method as above using [$Rh_2Cl_2(CO)_4$] and *o*-$C_6H_4(CH_2SbMe_2)_2$. Orange/brown solid. (Yield 55%). ^{1}H NMR ($CDCl_3$, 210 K): δ 7.0–7.5 (m) [8H] (*o*-$C_6\underline{H}_4$), 3.3–3.5 (m) [8H] ($C\underline{H}_2$), 1.15–1.22 (m) [24H] ($SbC\underline{H}_3$). ES$^+$ MS (MeCN): found *m/z* = 947 [Rh(CO){*o*-$C_6H_4(CH_2SbMe_2)_2$}$_2$]$^+$. ES$^-$ MS (MeCN): found *m/z* = 229 [$Rh(CO)_2Cl_2$]$^-$. IR (Nujol mull): ν 2075, 2007 ν br, 1974 sh (CO) cm^{-1}. Due to decomposition of the complex in air over time, microanalytical data were not obtained.

[Ir(CO)(PPh_3)$_2$Cl]: $IrCl_3.6H_2O$ (0.1 g, 0.28 mmol) and HCl (0.05 cm^3, 37% in H_2O) in dmf (10 cm^3), were heated to reflux for 50 minutes. In this time the reaction mixture turned from deep red to orange. A further portion of HCl (0.03 cm^3, 37% in H_2O) was added and the mixture refluxed for a further 10 minutes. The reaction was then allowed to cool and two molar equivalents of PPh_3 (0.15 g, 0.57 mmol) were added. The reaction was then stirred for 1 h. at room temperature, and monitored by solution IR spectroscopy. Once the reaction had gone to completion, degassed H_2O (15 cm^3) was added to precipitate a solid. This was filtered and dried *in vacuo* to afford a yellow powder (Yield: 0.17 g, 77%). IR (CH_2Cl_2): ν 1964 s cm^{-1}. $^{31}P\{^1H\}$ NMR (CH_2Cl_2/$CDCl_3$): δ 24.8 ppm. Spectroscopic data were in accord with the literature data.[34]

Attempted preparation of [Ir(CO)($SbPh_3$)$_2$Cl]: [$Ir(CO)_2Cl_2$][$AsPh_4$] (0.07 g, 0.099 mol) and 2 molar equivalents of $SbPh_3$ (0.07 g, 0.199 mmol) were dissolved in dry CH_2Cl_2 (5 cm^3) and stirred under N_2. The reaction was monitored by solution IR spectroscopy. The reaction was reduced in volume to *ca.* 2 cm^3 and hexane (5 cm^3) was added to precipitate a solid. This was filtered and dried *in vacuo*. Yellow solid (Yield: 0.048 g, 56%). IR (CH_2Cl_2): ν 2055 s, 1994 w, 1968 w cm^{-1}. ES$^+$ MS (MeCN): found *m/z* 383 [$AsPh_4$]$^+$. ‡

Attempted preparation of $[Ir(CO)(Ph_2Sb(CH_2)_3SbPh_2)_2]Cl$: $IrCl_3.6H_2O$ (0.1 g, 0.28 mmol) and HCl (0.05 cm^3, 37% in H_2O) in dmf, were heated to reflux for 50 minutes. In this time the reaction mixture turned from deep red to orange. A further portion of HCl (0.03 cm^3, 37% in H_20) was added and the mixture refluxed for a further 10 minutes. The reaction was then allowed to cool and 2 molar equivalents of $Ph_2Sb(CH_2)_3SbPh_2$ (0.33 g, 0.56 mmol) were added in dmf (7.5 cm^3). There was an immediate colour change from orange to yellow, and the reaction was monitored by solution IR spectroscopy. After stirring overnight there was no change observed. The reaction was heated to reflux for 2 h. then allowed to cool and stirred for 72 h. The dmf was then removed under reduced pressure, and the residues were dissolved in minimum CH_2Cl_2 and hexane was added to precipitate a solid. The yellow solid was filtered and dried *in vacuo*. Yellow solid (Yield: 0.19 g, 49%). ^1H NMR ($CDCl_3$): δ 7.45 – 7.15 (m) [40H] (Ph), 2.60 [12H] ($C\underline{H}_2$) ppm. $^{13}C\{^1H\}$ NMR: δ 187.4 ($\underline{C}O$), 136.0 – 129.6 (Ph), 23.6 ($\underline{C}H_2CH_2$), 17.1 ($\underline{C}H_2Sb$) ppm. ES^+ MS (MeCN): found *m/z* 1380 $[Ir(Ph_2Sb(CH_2)_3SbPh_2)_2]^+$, 1408 $[Ir(CO)(Ph_2Sb(CH_2)_3SbPh_2)_2]^+$. ES^- MS (MeCN): found *m/z* 405 $([Ir(CO)Cl_4(dmf)]-CO)^-$IR (CH_2Cl): ν 2068 s, 1946 s cm^{-1}. IR (Nujol mull): ν 2054 m, 1930 m cm^{-1}. ‡

Attempted preparation of $[Ir(CO)\{Ph_2Sb(CH_2)_3SbPh_2\}_2]BF_4$: $[Ir\{Ph_2Sb(CH_2)_3SbPh_2\}_2]BF_4$ (0.050 g, 0.034 mmol) was dissolved in dry acetone (10 cm^3) and purged with CO gas for 30 minutes. The reaction mixture was reduced to ca. 2 cm^3, Et_2O (10 cm^3) was added to precipitate a solid, and the yellow solid filtered and dried *in vacuo*. Yield 0.035 g, 68%. ^1H NMR ($(CD_3)_2CO$): δ 6.9–7.5 (m) [20H] (Ph), 2.60 (s) [4H] ($C\underline{H}_2CH_2$), 2.20 (br s) [2H] ($SbC\underline{H}_2$). ES^+ MS (MeCN): found *m/z* 1407 $[Ir(CO)\{Ph_2Sb(CH_2)_3SbPh_2\}_2]^+$, 1435 $[Ir(CO)_2\{Ph_2Sb(CH_2)_3SbPh_2\}_2]^+$. IR ($CH_2Cl_2$): ν 2020, 1991 (CO) cm^{-1}. IR (Nujol mull): ν 2002 w (CO), 1061 (BF_4^-) cm^{-1}. ‡

† Microanalysis was not obtained due to the cationic species in the complex, having identical spectroscopic data to the cationic species in $[Rh(CO)\{Ph_2Sb(CH_2)_3SbPh_2\}_2][Rh(CO)_2Cl_2]$.

‡ Microanalysis was not obtained due to a mixture of starting material and products being formed.

4.4.2 X-Ray Crystallography

Details of the crystallographic data collection and refinement parameters are given in Table 4.4.1. Crystals of $[Rh(CO)\{Ph_2Sb(CH_2)_3SbPh_2\}_2]PF_6.¾CH_2Cl_2$ were obtained by diffusion of hexane

into a CH_2Cl_2 solution of the compound. Data collection used a Nonius Kappa CCD diffractometer (T = 120 K) and with graphite-monochromated Mo-Kα X-radiation (λ = 0.71073 Å). Structure solution and refinement were routine.[41,42]

Table 4.4.1: Crystallographic parameters for $[Rh(CO)\{L\text{-}L\}_2]PF_6.¾CH_2Cl_2$ and $[RhCl_2\{L\text{-}L\}\{PhClSb(CH_2)_3SbClPh\}]Cl.CHCl_3$ (where L-L = $Ph_2Sb(CH_2)_3SbPh_2$).

Complex	**$[Rh(CO)\{L\text{-}L\}_2]PF_6.¾CH_2Cl_2$**	**$[RhCl_2\{L\text{-}L\}\{PhClSb(CH_2)_3SbClPh\}]Cl.CHCl_3$**
Formula	$C_{55.75}H_{53.5}Cl_{1.5}F_6OPRhSb_4$	$C_{43}H_{43}Cl_8RhSb_4$
Mwt	1527.54	1433.28
Crystal System	Triclinic	Monoclinic
Space Group	P-*1* (no. 2)	$P2_1/c$
a/Å	13.5141(10)	28.147(6)
b/Å	20.129(3)	0.9609(16)
c/Å	21.133(3)	15.724(3)
α/°	74.016(5)	90
β/°	80.152(7)	104.095(8)
γ/°	82.929(7)	90
U/Å^3	5427.5(10)	4705.2(15)
Z	4	4
μ(Mo-Kα)/mm^{-1}	2.426	3.096
R_{int}	0.065	0.089
Total no. reflns.	94727	31249
Unique reflections	24949	9970
No. of parameters	1265	505
$R1$ [$I_o > 2\sigma(I_o)$]	0.0509	0.1057
$R1$ [all data]	0.0824	0.1508
wR_2 [$I_o > 2\sigma(I_o)$]	0.0996	0.1492
wR_2 [all data]	0.1109	0.1730

$R1 = \Sigma \| |F_o| - |F_c| \| / \Sigma |F_o|$; $wR_2 = [\Sigma w(F_o^2 - F_c^2)^2 / \Sigma wF_{oi}^4]^{1/2}$; T = 120 K; λ(Mo-K_α) = 0.71073 Å

4.4 References

[1] W. Levason and N. R. Champness, *Coord. Chem. Rev.*, 1994, **133**, 115; W. Levason and G. Reid, *Coord. Chem. Rev.*, 2006, **250**, 2565.

[2] W. Levason and G. Reid in *Comprehensive Coordination Chemistry II*, Eds. J. A. McCleverty and T. J. Meyer, Volume 1, Elsevier, Amsterdam, 2004, p. 377.

[3] H. Werner, *Angew. Chem. Int. Ed.*, 2004, **43**, 938.

[4] H. Werner, D. A. Ortmann and O. Gevert, *Chem. Ber.*, 1996, **129**, 411; M. Mattias, J. Wolf, M. Laubender, M. Teichert, D. Stalke and H. Werner, *Chem. Eur. J.*, 1997, **3**, 1442; D. A. Ortmann, B. Weberndörfer, K. Ilg, M. Laubender and H. Werner, *Organometallics*, 2002, **21**, 2369; D. A. Ortmann, O. Gevert, M. Laubender and H. Werner, *Organometallics*, 2001, **20**, 1776.

[5] H. Werner, P Schwab, A. Heinemann and P. Steinert, *J. Organomet. Chem.*, 1995, **496**, 207.

[6] E. Bleuel, O. Gevert, M. Laubender and H. Werner, *Organometallics*, 2000, **19**, 3109.

[7] H. Werner, C. Grunwald, P. Steinert, O. Gevert and J. Wolf, *J. Organomet. Chem.*, 1998, **565**, 231.

[8] D. A. Ortmann, B. Weberndörfer, J. Schöneboom and H. Werner, *Organometallics*, 1999, **18**, 952.

[9] L. M. Vallarino, *J. Chem. Soc.*, 1957, 2287.

[10] S. Otto and A. Roodt, *Inorg. Chim. Acta*, 2002, **331**, 199.

[11] S. Otto and A. Roodt, *Acta Crystallogr. Sect. C*, 2002, **58**, m565.

[12] A. Kayan, J.C. Gallucci and A. Wojcicki, *Inorg. Chem. Commun.*, 1998, **1**, 446.

[13] A. Kayan, J.C. Gallucci and A. Wojcicki *J. Organomet. Chem.*, 2001, **630**, 44.

[14] A. Kayan and A. Wojcicki, *Inorg. Chim. Acta*, 2001, **319**, 187.

[15] K. Vrieze, H. C. Volgar and A. P. Praat, *J. Organomet. Chem.*, 1968, **14**, 185.

[16] P. E. Garrou and G. E. Hartwell, *J. Organomet. Chem.*, 1974, **69**, 445.

[17] T. Even, A. R. J. Genge, A. M. Hill, N. J. Holmes, W. Levason and M. Webster, *J. Chem. Soc., Dalton Trans.*, 2000, 655.

[18] M. Jiminez-Tenorio, M. C. Puerta, I. Salcedo, P. Valerga, S. L. Costa, P. T. Gomes and K. Mereiter, *Chem. Commun.*, 2003, 1168.

[19] J. A. Casares, P. Espinet, J. M. Martin-Alverez, J. M. Martinez-Ilarduya and G. Salas, *Eur. J. Inorg. Chem.*, 2005, 3825.

[20] W. Levason, M. L. Matthews, G. Reid and M. Webster, *Dalton Trans.*, 2004, 51.

[21] W. Levason, M. L. Matthews, G. Reid and M. Webster, *Dalton Trans.*, 2004, 554.

[22] M. D. Brown, W. Levason, G. Reid and M. Webster, *Dalton Trans.*, 2006, 1667.

[23] A. Haynes, B. E. Mann, G. E. Morris, P. M. Maitlis, *J. Am. Chem. Soc.*, 1993, **115**, 4093.

[24] L. H. Pignolet, D. H. Doughty, S. C. Nowicki and A. L. Casalnuovo, *Inorg. Chem.*, 1980, **19**, 2172.

[25] L. H. Pignolet, D. H. Doughty, S. C. Nowicki, M. P. Anderson and A. L. Casalnuovo, *J. Organomet. Chem.*, 1980, **202**, 211.

[26] L. M. Vallarino, *Inorg. Chem.*, 1965, **4**, 161.

[27] B. R. James and D. Mahajan, *Can. J. Chem.*, 1980, **58**, 996.

[28] A. M. Hill, W. Levason and M. Webster, *Inorg. Chim. Acta*, 1998, **271**, 203.

[29] P. Albano and M. Aresta, *J. Organomet. Chem.*, 1980, **190**, 243.

[30] W. Hieber and V. Frey, *Chem. Ber.*, 1966, **99**, 2614.

[31] J. T. Mague and G. Wilkinson, *J. Chem. Soc. (A)*, 1966, 1736.

[32] A. R. J. Genge, N. J. Hill, W. Levason and G. Reid, *J. Chem. Soc., Dalton Trans.*, 2001, 1007.

[33] P. Serpe, M. Hernandez, B. Richards, P. Kalck, *Eur. J. Inorg. Chem.*, 2001, 2327.

[34] L. Vaska, *J. Am. Chem. Soc.*, 1961, **83**, 2784.

[35] J. A. McCleverty and G. Wilkinson, *Inorg. Synth.*, 1966, **8**, 211.

[36] G. Giordano and R. H. Crabtree, *Inorg. Synth.*, 1979, **19**, 218.

[37] J. L. Herde, J. C. Lambert and C. V. Senoff, *Inorg. Synth.*, 1974, **15**, 18.

[38] A. Van der Ent and A. L. Onderdelinden, *Inorg. Synth.*, 1990, **28**, 90.

[39] S. Sato, Y. Matsumura and R. Okawara, *J. Organomet. Chem.*, 1972, **43**, 333.

[40] H. A. Meinema, H. F. Martens and J. G. Noltes, *J. Organomet. Chem.*, 1976, **110**, 183.

[41] SHELXS-97, program for crystal structure solution, G. M. Sheldrick, University of Göttingen, Germany 1997.

[42] SHELXL-97, program for crystal structure refinement, G. M. Sheldrick, University of Göttingen, Germany 1997.

Chapter 5

Synthesis, Spectroscopic and Structural Properties of Transition Metal Complexes of the *o*-Xylyl Diphosphine *o*-$C_6H_4(CH_2PPh_2)_2$

5.1 Introduction

Sterically demanding wide-angle diphosphine ligands have been of great interest, particularly when incorporated in transition metal complexes, as many exhibit remarkably high catalytic activity. For example there is great interest in the rhodium-catalysed hydroformylation of alkenes,[1] and the mechanism for this reaction was first proposed by Heck and Breslow, and is shown in Fig.5.1.1.

Fig 5.1.1: The rhodium-catalysed hydroformylation of alkenes.[2,3]

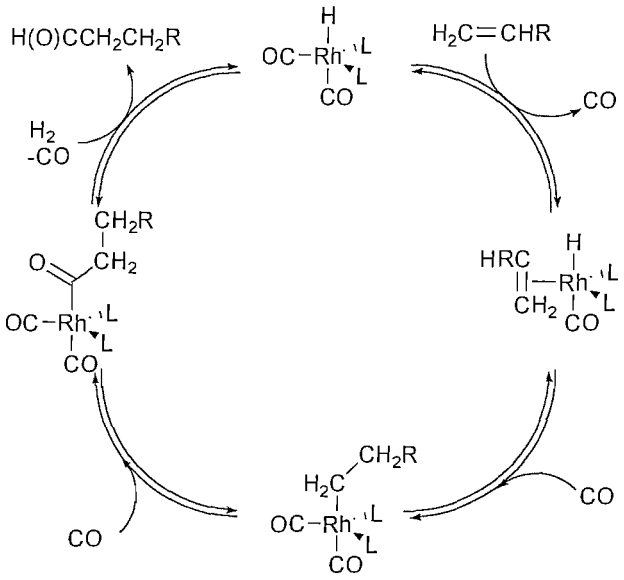

Hydroformylation of alkenes is one of the most extensively applied homogeneous catalytic processes in industry. The trigonal bipyramidal hydrido-rhodium complex is the catalytic species and usually contains two phosphorus centres. It was suggested that there was a relationship between the selectivity of the catalytic species and the bite angle of the diphosphine and as a result Casey *et al.* studied this relationship for different diphosphine ligands.[4] They found a very good correlation between the bite angle size and the regioselectivity, and it was suggested that the P-M-P bite angle in the diphosphines play an important role in determining the selectivity and rates in the catalytic reactions.

Another process that takes advantage of the wide angle and the selectivity that this leads to is, the nickel-catalysed hydrocyanation reaction.[5] This industrial process involves the addition of HCN

to alkenes, and is very useful in functionalizing organic substrates. The catalyst consists of a Ni(0) complex stabilised by *tris-o*-tolylphosphite in the presence of a Lewis acid.[6] It was chosen as it combined a large cone angle and good electronic properties. However, when incorporating diphosphines into the catalysts, no catalytic activity was exhibited. This is due to the mechanism involving a rate-determining reductive elimination of the alkyl cyanide. This results in the formation of a tetrahedral Ni(0) out of a square planar Ni(II) compound. The reaction is facilitated by electron-withdrawing ligands such as phosphites, whereas this reaction becomes more difficult when donating ligands such as phosphines are used. Therefore, the reaction proceeds faster when more electron-withdrawing phosphites or phosphinites are used. More recent research has also proved that bidentate diphosphines do generate very active catalysts, which are also quite resistant to deactivation, but basic phosphines still showed no activity in the hydrocyanation reaction.[1] It can therefore be seen that research in the area is needed to see whether diphosphines incorporated into catalysts can be manipulated into becoming better catalytic species.

Palladium catalysed copolymerisation of CO and alkenes is another catalytic process that uses wide angle diphosphines.[7] Indeed, research by Drent proved that catalysts of the form $[PdX_2(L\text{-}L)]$ where (L-L) was the bidentate diphosphine chelating in a *cis* fashion, and X was a weakly coordinating anion, exhibited excellent CO/ethene copolymerisation. Moreover, coordinating diphosphines that were ideal for this were $Ph_2P(CH_2)_2PPh_2$, $Ph_2P(CH_2)_4PPh_2$ and $Ph_2P(CH_2)_3PPh_2$.[8] It was also shown that the number of carbon atoms in the backbone had a dramatic influence on the activity and selectivity, as shown in Table 5.1.1.

Table 5.1.1: The effect of the variation of the chain length of bidentate diphosphines of the form $Ph_2P(CH_2)_mPPh_2$[8] on the rate of catalytic reaction.

m	Reaction rate /g (g Pd)$^{-1}$ h^{-1}
1	1
2	1000
3	6000
4	2300
5	1800
6	5

It can be seen that the P-M-P bite angle in these transition metal complex catalysts play an important role in the catalytic process, indeed in determining the selectivity and rates of the reactions.[1] Other studies involve the coordination of *o*-$C_6H_4(CH_2PPh_2)_2$ to platinum metal complexes, in the catalytic process of platinum-tin catalysed hydroformylation.[9] Platinum chloride – diphosphine – tin(II) halide systems have been explored, in the asymmetric induction in the hydroformylation of butenes, and it was revealed that by using $Ph_2P(CH_2)_4PPh_2$, a diphosphine with the number of carbons in the backbone being four, the activity is strikingly raised.

Fig 5.1.2: *o*-$C_6H_4(CH_2PPh_2)_2$.

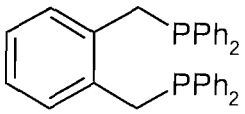

Even though it can be seen that the sterically demanding wide angles of diphosphine ligands are of great importance in industrial processes, it is surprising however, that the coordination chemistry of *o*-$C_6H_4(CH_2PPh_2)_2$ to transition metal ions has been largely neglected. Venanzi and coworkers have reported the preparation of some mononuclear metal complexes and halide bridged dimers involving *o*-$C_6H_4(CH_2PPh_2)_2$, including a dimeric complex of Ag(I) as the metal centre with one chelating *o*-$C_6H_4(CH_2PPh_2)_2$ ligand at each metal centre, and bridging halide ions, which was structurally characterised,[10] and is shown in Fig 5.1.3.

Fig 5.1.3: View of $[Ag_2Cl_2(o\text{-}C_6H_4(CH_2PPh_2)_2)_2]^{+}$.[10]

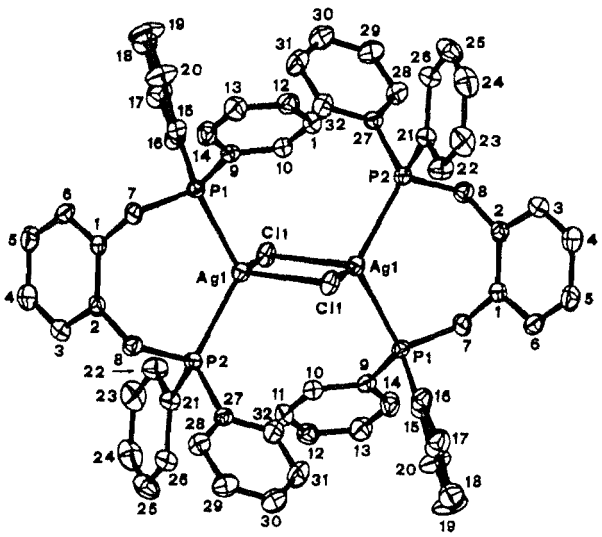

They also describe complexes with the empirical formula of $[MX(o\text{-}C_6H_4(CH_2PPh_2)_2)]$, by reacting silver nitrates and halides, with $o\text{-}C_6H_4(CH_2PPh_2)_2$. The $^{31}P\{^1H\}$ NMR for the complex above is a resonance at 0.8 ppm, with coupling constant of $^1J_{(107,109Ag-31P)} = 359$ Hz. Venanzi also describes the synthesis and limited characterisation of $[MX_2(o\text{-}C_6H_4(CH_2PPh_2)_2)]$ complexes where M = Ni, Pd, Pt and X = Cl, Br.[11] [12] These complexes are also synthesised and discussed in this work, but in some cases the geometries and coordination environments are found to have differed from what was believed in the earlier work (see results and discussion). Venanzi concluded that by adding differing R groups onto the pendant arms of the wide angle diphosphine $o\text{-}C_6H_4(CH_2PPh_2)_2$, the ligand could be used for a systematic study of organometallic reactions, for example alkene insertions, therefore it can be seen that this ligand has a lot of potential in industrial processes.

Werner and co-workers, have also reported other platinum complexes involving $o\text{-}C_6H_4(CH_2PPh_2)_2$. Indeed one such compound incorporates a platinum dimer, with a selenium atom bridging, and an $o\text{-}C_6H_4(CH_2PPh_2)_2$ chelate ring on one platinum metal centre, as shown in Fig 5.1.4.

Fig 5.1.4: Platinum dimer with selenium bridge and $o\text{-}C_6H_4(CH_2PPh_2)_2$ chelate.[13]

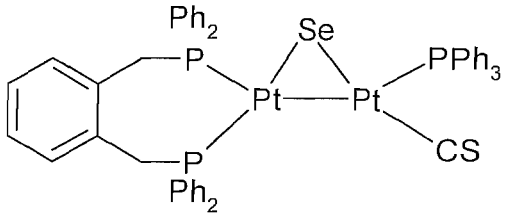

The above studies suggest that the ligand, $o\text{-}C_6H_4(CH_2PPh_2)_2$ is a versatile ligand, however its coordination to late transition metals has not been fully explored. This chapter details the study that was carried out on the $o\text{-}C_6H_4(CH_2PPh_2)_2$ ligand, including fully characterised metal complexes, in various geometries, such as square planar and tetrahedral geometries. All sections of the study were chosen to probe the ligating properties of the ligand, and six crystal structures were obtained, which show surprising variations in the phosphine bite angle, suggesting that the ligand is quite flexible in coordination.

5.2 Results and Discussion

5.2.1. Synthesis of *o*-$C_6H_4(CH_2PPh_2)_2$

The diphosphine *o*-$C_6H_4(CH_2PPh_2)_2$, was prepared as in the experimental section, by reaction of PPh_3 and lithium metal. The residual lithium was removed and then 0.8 molar equivalents of ^tBuCl, were added followed by addition of *o*-$C_6H_4(CH_2Cl)_2$. Upon heating the mixture, a white precipitate was formed, which was recrystallised from CH_2Cl_2/EtOH. Preliminary preparations of the ligand, resulted in small amounts of phosphine oxide present in the product, which from $^{31}P\{^1H\}$ NMR spectroscopy had a chemical shift of δ 30.8 ppm. This may be due to filtering and reducing the volume of the solvent in air. *o*-$C_6H_4(CH_2PPh_2)_2$ was more air sensitive than first thought; therefore during further preparations the resulting yield of 96% was achieved, as all procedures were undertaken in an inert atmosphere. $^{31}P\{^1H\}$ NMR spectra showed one peak at δ – 12.9 ppm, in accord with previous studies.[2] The ^1H NMR data suggested that the desired compound was formed, but due to the very small coupling constant between ^{31}P and ^1H, a slightly broad singlet was observed for the CH_2 signal in the spectrum, at δ 3.25 ppm. IR data on the ligand also provided evidence of pure product, with bands at 1600(w), 1484(m) and 1431(s) cm^{-1} indicating aromatic C=C stretches. Moreover, the absence of a strong P=O stretch between 1200 – 1100 cm^{-1} suggests no oxidation of the product.

5.2.2. Co, Rh and Ir Complexes

Three cobalt systems have been prepared and fully characterised, from $CoX_2.xH_2O$ (where X = Cl, Br, I) and one molar equivalent of *o*-$C_6H_4(CH_2PPh_2)_2$ in *iso*-propanol. [$CoCl_2$(L-L)], [$CoBr_2$(L-L)] and [CoI_2(L-L)] were isolated as brightly coloured blue, green and brown solids respectively, and were found to have distorted tetrahedral geometries.

Microanalytical results suggested that the desired products were formed. However associated CH_2Cl_2 was found to be present, which was supported by spectroscopic and crystallographic evidence. The magnetic moment measurements prove that the predicted high spin Co(II) species have been formed, consistent with others previously researched.[14] For example the magnetic moment for [$CoBr_2$(*o*-$C_6H_4(CH_2PPh_2)_2$)] was calculated as 4.41 μB, and Sacconi and Gelsomini obtained a magnetic moment for [$CoBr_2(Ph_2P(CH_2)_4PPh_2)$] as 4.50 μB.[14] Both the diffuse reflectance and solution UV/vis spectra for all three systems, suggest that the tetrahedral complexes are in the correct orientation, for example the diffuse reflectance absorptions for [$CoCl_2$(*o*-$C_6H_4(CH_2PPh_2)_2$)] at ν 30120, 25700, 22370, 16160, 15080, 13460, 10000 cm^{-1} are

consistent with other such compounds. For example, $[Co(Ph_2P(CH_2)_4PPh_2)Br_2]$ had a diffuse reflectance UV/vis spectrum of ν 20400, 18600, 16000, 15000, 10800, 8000, 6700 cm^{-1}.[14] Furthermore the far IR spectrum of $[CoCl_2(o\text{-}C_6H_4(CH_2PPh_2)_2)]$ shows a broad band at 318 cm^{-1}, which corresponds to the ν(Co-Cl). Group theory suggests that there should be two Co-Cl stretches (theory C_s: A' + A'') but as it is a broad band this suggests that there could be two overlapping bands. Crystals of $[CoCl_2(o\text{-}C_6H_4(CH_2PPh_2)_2)]$ were obtained and the data are shown in Fig 5.2.1 and Table 5.2.1, confirming the distorted tetrahedral coordination geometry in the solid state. The figure below is of the $[CoCl_2(o\text{-}C_6H_4(CH_2PPh_2)_2)]$ species. Selected bond angles and bond lengths are shown in Table 5.2.1.

Fig 5.2.1: View of the crystal structure of $[CoCl_2(o\text{-}C_6H_4(CH_2PPh_2)_2)]$, with the H atoms omitted for clarity. Ellipsoids are shown at the 50% probability level.

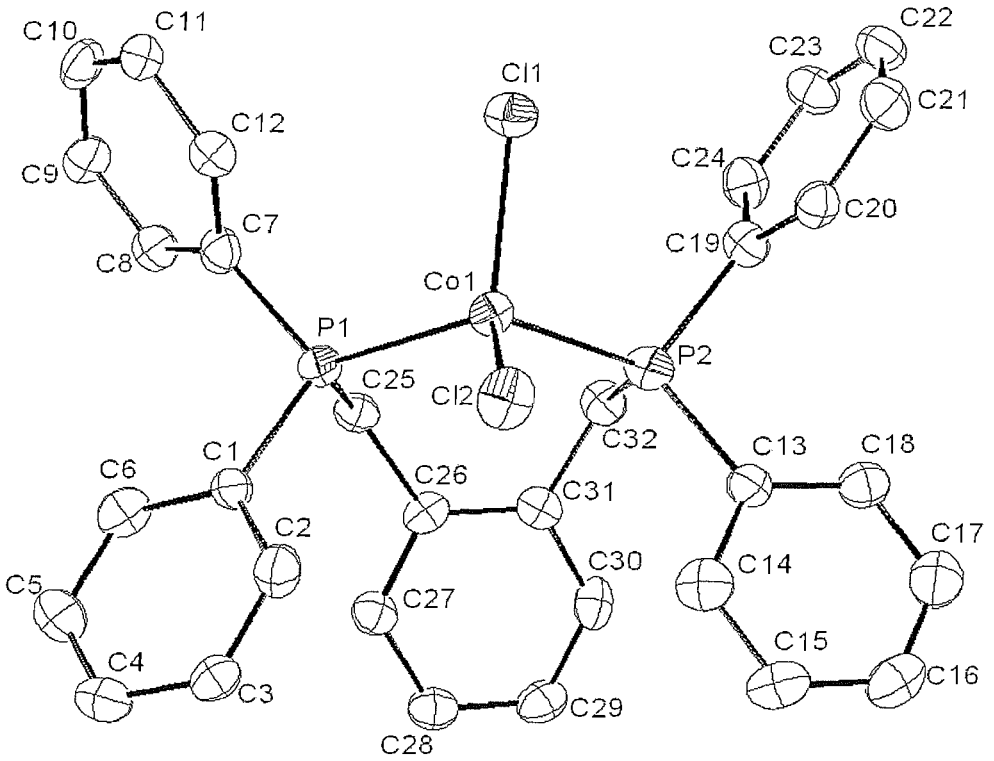

Table 5.2.1: Selected bond lengths (Å) and angles (°) for $[CoCl_2(o\text{-}C_6H_4(CH_2PPh_2)_2)]$.

Co1 – Cl1	2.2165(15)	P1 – Co1 – P2	106.18(5)
Co1 – Cl2	2.2045(15)	Cl1 – Co1 – Cl2	109.50(6)
Co1 – P1	2.4034(16)		
Co1 – P2	2.3795(16)		

Therefore it is apparent that larger chelate rings as in the $[CoX_2(o\text{-}C_6H_4(CH_2PPh_2)_2)]$ systems give tetrahedral metal centres[15] whereas more rigid diphosphines such as $o\text{-}C_6H_4(PPh_2)_2$ have been found to give square planar cations,[16] which could be due to the shortened pendant arms of the ligand and hence the smaller chelate ring, promoting the coordination around the metal centre.

In an attempt to further probe the versatility of the $o\text{-}C_6H_4(CH_2PPh_2)_2$ ligand, a reaction to investigate whether the ligand would promote higher coordination numbers and higher oxidation states of the metal centre was carried out. On reaction of $[CoCl_2(o\text{-}C_6H_4(CH_2PPh_2)_2)]$ in CH_2Cl_2 with NOCl (prepared *in situ* by heating $POCl_3$ and KNO_3) – used as it is a clean one electron oxidant at 273 K, an air sensitive dark blue – green solid was produced which was found to be a 5 coordinate Co(III) species of the form $[CoCl_3(o\text{-}C_6H_4(CH_2PPh_2)_2)]$. This is an interesting discovery as examples of high spin d^6 Co(III) complexes are rare.[17] The solution UV/vis spectrum is characteristic of the 5-coordinate geometry and the far infra red spectrum has three bands characteristic of the Co – Cl stretching modes (theory C_s: 2A' + A''), suggesting three chlorides coordinated around the metal centre. Examples of these rare compounds are of the form, $[Co\{Ph_2P(CH_2)_nPPh_2\}X_3]$ (X = Cl, Br; n = 4, 5). Indeed a specific example is $[Co\{Ph_2P(CH_2)_4PPh_2\}Cl_3]$ which is a deep blue colour with infra red Co-Cl bands of ν 355, 340, 300 cm^{-1}.[17] At room temperature $[CoCl_3(o\text{-}C_6H_4(CH_2PPh_2)_2)]$ decomposes in solution, but does survive as a solid in the freezer over a long period of time.

The rhodium(I) cation, $[Rh(o\text{-}C_6H_4(CH_2PPh_2)_2)_2]^+$, was prepared *via* two different routes. Method A was the reaction of $RhCl_3.3H_2O$ with two molar equivalents of $o\text{-}C_6H_4(CH_2PPh_2)_2$ in EtOH. A few drops of 40 % aqueous HBF_4 were added, and after stirring an orange precipitate was formed in good yield. The product expected from the preparation was a six coordinate rhodium(III) complex with two chelating $o\text{-}C_6H_4(CH_2PPh_2)_2$ ligands and two chlorides. However, the infrared spectrum of the product showed no Rh-Cl stretching modes, but there was evidence of coordinated $o\text{-}C_6H_4(CH_2PPh_2)_2$ ligand and a characteristic band for the BF_4^- anion. The positive ion electrospray MS spectrum (MeCN) showed peaks with the correct isotope distribution for [Rh(L-

$L)_2]^+$ and $[Rh(L\text{-}L)]^+$, but there was no evidence of any Cl containing species as the relevant isotope patterns and *m/z* peaks were absent.

By ^1H NMR spectroscopy the ligand resonances as mentioned above, had shifted to high frequency, indicating that the ligand was coordinated. Providing more evidence that the product formed was not the Rh(III) complex that was first thought and that it was indeed a planar Rh(I) complex, was the ^{31}P $\{^1H\}$ NMR spectrum. A resonance of a doublet at +11.6 ppm with a coupling constant of $^1J_{RhP}$ = 140 Hz, suggested one phosphorus environment, with a larger than expected coupling constant for a Rh(III) compound.[18] Together with the mass spectrometry data, these results are indeed indicative of the Rh(I) species.

In the solid state, X-ray crystallography provided unambiguous confirmation that the four coordinate, sterically crowded Rh(I) complex was the one formed, as Fig 5.2.2 (Table 5.2.2) shows. Orange single crystals were obtained by layering a $CHCl_3$ solution of the complex with hexane. The cationic species was found to be in a distorted square planar geometry, with one BF_4^- anion associated and two $CHCl_3$ solvent molecules associated, which was consistent with the NMR spectroscopic data. The Rh-P bond distances are in the range 2.31-2.34 Å and show similarities with other Rh(I) species,[19] for example $[RhCl(PPh_3)_3]$ $d(Rh\text{-}P_{transP})$ = 2.304-2.338 Å.[19, 20] The distortion in the square planar geometry is obvious from the sum of the P-Rh-P angles being 370°, which can be explained by the steric bulk of the *o*-$C_6H_4(CH_2PPh_2)_2$ ligand, the area around the metal centre that the bulky phenyl groups occupy. The P1···P2 and P3···P4 distances within the chelates are 3.28 and 3.37 Å, and the P1-Rh-P2 and P3-Rh-P4 angles within the chelate rings are 90.05(3) and 92.31(3) Å respectively.

Fig 5.2.2: Crystal structure of the cation in $[Rh(o\text{-}C_6H_4(CH_2PPh_2)_2)_2]BF_4.2CHCl_3$, with the H atoms and phenyl rings (except ipso carbons) omitted for clarity. Ellipsoids are shown at the 50% probability level.

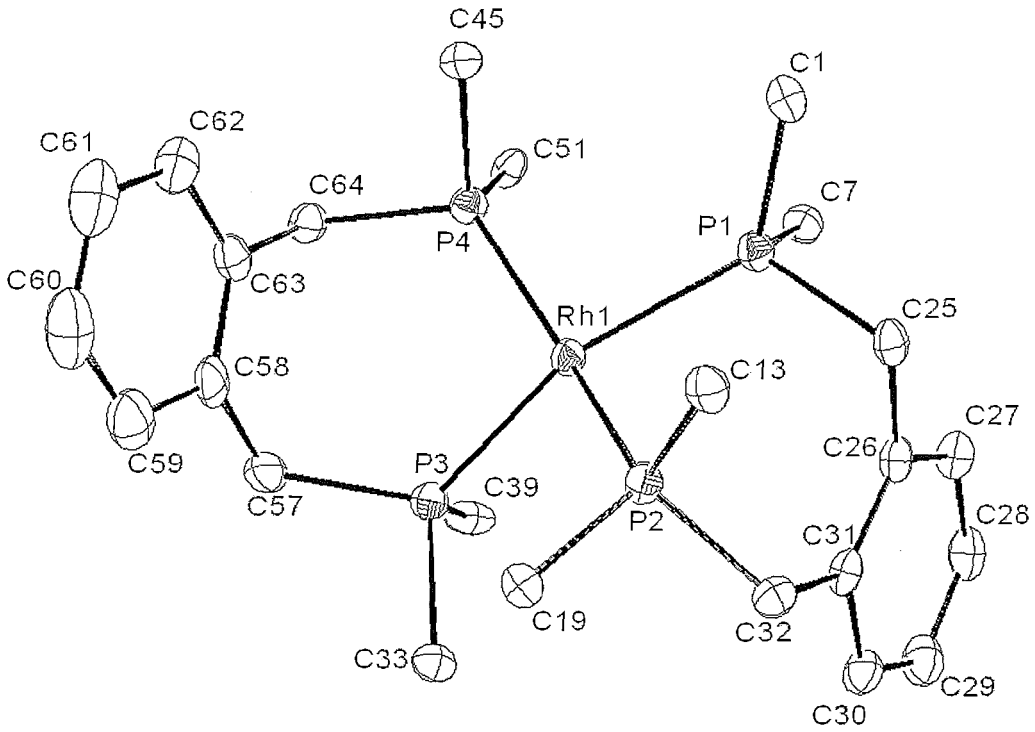

Table 5.2.2: Selected bond lengths (Å) and angles (°) for $[Rh(o\text{-}C_6H_4(CH_2PPh_2)_2)_2]BF_4.2CHCl_3$

Rh1-P1	2.3269(10)	P1-Rh1-P2	90.05(3)
Rh1-P2	2.3099(10)	P1-Rh1-P4	92.70(3)
Rh1-P3	2.3427(10)	P3-Rh1-P2	93.98(3)
Rh1-P4	2.3352(10)	P3-Rh1-P4	92.31(3)
P1-C1	1.833(4)		
P1-C7	1.818(4)		
P1-C25	1.855(4)		

The above result is of interest due the unexpected formation of the Rh(I) cationic species. In similar reactions with other phosphines, the Rh(III) cation is achieved. For example, using the same starting material and reacting it with $Ph_2P(CH_2)_2PPh_2$, the 6 coordinate $[RhCl_2(Ph_2P(CH_2)_2PPh_2)_2]^+$[21, 22] is produced. It can be argued therefore that the different reaction

pathway may be due to the steric bulk of o-$C_6H_4(CH_2PPh_2)_2$. The second method for the preparation of $[Rh(o\text{-}C_6H_4(CH_2PPh_2)_2)_2]^+$ (Method B), was the reaction of $[RhCl(cod)]_2$ and two molar equivalents of $AgBF_4$ refluxed in acetone. After cooling, the AgCl was filtered off and the yellow solution added to a solution of excess o-$C_6H_4(CH_2PPh_2)_2$ in toluene. After stirring for 24 h, the reaction was reduced to dryness and the residues were recrystallised from acetone/Et_2O. The orange solid was obtained in good yield. The $^{31}P\{^1H\}$ NMR spectroscopic data suggested that the product was indeed $[Rh(o\text{-}C_6H_4(CH_2PPh_2)_2)_2]BF_4$ with a doublet at 12.7 ppm (J = 138 Hz) which is in good accord to the data above.

In order to try to probe the versatility of the o-$C_6H_4(CH_2PPh_2)_2$ ligand, to see whether it would support higher coordination and oxidation states, a reaction of $[Rh(o\text{-}C_6H_4(CH_2PPh_2)_2)_2]BF_4$ and Cl_2 in CCl_4 was carried out. However the orange solid that resulted from the reaction was found to be the starting material. It can be concluded, therefore, that the steric bulk of two bidentate diphosphine o-$C_6H_4(CH_2PPh_2)_2$ ligands around a rhodium centre does not allow a six coordinate geometry.

Attempts were made to synthesise $[Rh(CO)\{o\text{-}C_6H_4(CH_2PPh_2)_2\}_2]^+$, *via* three different routes. The first route (Method A) was to react $[Rh\{o\text{-}C_6H_4(CH_2PPh_2)_2\}_2]BF_4$ with CO gas, in CH_2Cl_2. The reaction was monitored by IR spectroscopy and turned from orange to yellow in 5 minutes. Upon addition of Et_2O under an atmosphere of CO, yellow crystals formed, which were filtered and dried *in vacuo*. The yellow crystals were analysed by $^{31}P\{^1H\}$ NMR spectroscopy, which showed three broad resonances at 21.5, 15.9 and 8.5 ppm. This suggested that there was a mixture of products present. Due to the bulky Ph substituents present in the o-$C_6H_4(CH_2PPh_2)_2$ ligand, it was also predicted that there could be some dissociation of one or both of the ligands in solution. The ES^+ MS however, showed clusters of mass peaks at *ca. m/z* 1051and 1079 corresponding to $[Rh\{o\text{-}C_6H_4(CH_2PPh_2)_2\}_2]^+$ and $[Rh(CO)\{o\text{-}C_6H_4(CH_2PPh_2)_2\}_2]^+$ respectively. The IR spectra also suggested a mixture of products had been formed. For example, the solution IR spectrum showed CO bands at 2020 m and 1983 s cm^{-1} and the Nujol mull showed bands at 2033 w, 2015 w, 1974 s cm^{-1}. From these data it was clear that the desired complex had not been synthesised cleanly.

The second route (Method B) employed to prepare $[Rh(CO)\{o\text{-}C_6H_4(CH_2PPh_2)_2\}_2]^+$ was by reacting $[Rh_2Cl_2(CO)_4]$ and 4 molar equivalents of o-$C_6H_4(CH_2PPh_2)_2)_2$ in CH_2Cl_2 in the presence of NH_4PF_6 at 0°C. The reaction was carried out excluding light, and was stirred for 5 h. The mixture was allowed to warm to room temperature and stirred for a further 2.5 h, filtered and

reduced in volume. Hexane was added to precipitate a solid, which was obtained *via* filtration in moderate yield. The IR spectroscopic data suggested that the complex was pure with one carbonyl band at 2019 cm^{-1} in the solution IR spectrum. This was further confirmed in the Nujol mull IR spectrum with a band at 2010 cm^{-1}. The presence of the PF_6^- anion was also confirmed by bands at 840 and 557 cm^{-1}. The ES^+ MS also confirmed the presence of the desired species with a cluster of mass peaks at *ca. m/z* 1051 corresponding to $[Rh(o\text{-}C_6H_4(CH_2PPh_2)_2)_2]^+$. The $^{31}P\{^1H\}$ NMR spectrum however was complex. At -70°C three broad resonances were evident, suggesting that there was more than one species present.

The third attempt (Method C) at obtaining $[Rh(CO)(o\text{-}C_6H_4(CH_2PPh_2)_2)_2]^+$ was *via* a similar route to Method B. $[Rh_2Cl_2(CO)_4]$ and 4 molar equivalents of $o\text{-}C_6H_4(CH_2PPh_2)_2$ were reacted in CH_2Cl_2 with stirring, at room temperature. The $^{31}P\{^1H\}$ NMR spectrum at -80°C showed a doublet of triplets at 8.4 ($J_{Rh\text{-}P(eq)}$ = 90.6 Hz, $J_{P(ax)\text{-}P(eq)}$ = 37.4 Hz) ppm, a doublet of triplets at -9.16 ($J_{Rh\text{-}P(ax)}$ = 111.1, $J_{P(ax)\text{-}P(eq)}$ = 38.3 Hz) ppm and a singlet at -13.3 ppm. The two doublet of triplets suggests a trigonal bipyramidal geometry around the Rh(I), with the CO in the equatorial position, as shown in Fig 5.2.3. The singlet at -13.3 ppm suggests the presence of some free ligand or the uncoordinated end of a $\kappa^1\text{-}o\text{-}C_6H_4(CH_2PPh_2)_2$ ligand.

Fig 5.2.3: Proposed structure of $[Rh(CO)\{o\text{-}C_6H_4(CH_2PPh_2)_2\}_2]Cl$.

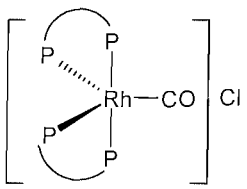

The IR spectra showed one carbonyl band at 1940 cm^{-1} (Nujol mull) and 1927 cm^{-1} (CH_2Cl_2), which was significantly different from the two attempts above (Method A and B), however the ES^+ MS showed the same cluster of mass peaks at *ca. m/z* 1051 corresponding to $[Rh(o\text{-}C_6H_4(CH_2PPh_2)_2)_2]^+$ (parent – CO). Yellow single crystals were obtained of the product and it was found that in the solid state the product was $[Rh(CO)Cl(o\text{-}C_6H_4(CH_2PPh_2)_2)(\kappa^1\text{-}o\text{-}C_6H_4(CH_2PPh_2)_2)].CH_2Cl_2$. There was some disorder in the CO group bound to the rhodium(I) centre which was found to be dioxygen (C65 and O1 occupy the same position in the difference map). This suggests that the product is very sensitive to oxygen, and can help to explain why there were mixtures of products formed in the different methods used. Fig 5.2.4 shows the

structure of [Rh(CO)Cl(*o*-$C_6H_4(CH_2PPh_2)_2$)(κ^1-*o*-$C_6H_4(CH_2PPh_2)_2$)] incorporating the disorder model. A second attempt to obtain crystallographic data on the compound was unsuccessful, as the data was weak and showed evidence of the free end of the κ^1-*o*-$C_6H_4(CH_2PPh_2)_2$ ligand being oxidised. These findings suggest that this system is much more sensitive to oxidation than first thought. The crystallographic evidence suggests that the bulky Ph substituents of the ligand make it impossible for both ligands to coordinate in a bidentate manner to the Rh(I) centre. However the $^{31}P\{^1H\}$ NMR spectroscopic data from Method C, suggested that the desired complex was formed. Unfortunately the chemistry appears to be quite complicated, with variable degrees of oxygenation occurring for each method used, and so the complex was not pursued in more detail.

Fig 5.2.4: View of the crystal structure of [Rh(CO)Cl(*o*-$C_6H_4(CH_2PPh_2)_2$)(κ^1-*o*-$C_6H_4(CH_2PPh_2)_2$)].CH_2Cl_2 incorporating the disorder model of the dioxygen with a numbering scheme adopted. H atoms and phenyl rings (with the exception of *ipso*-carbons) have been omitted for clarity. Ellipsoids are shown at the 50% probability level. †

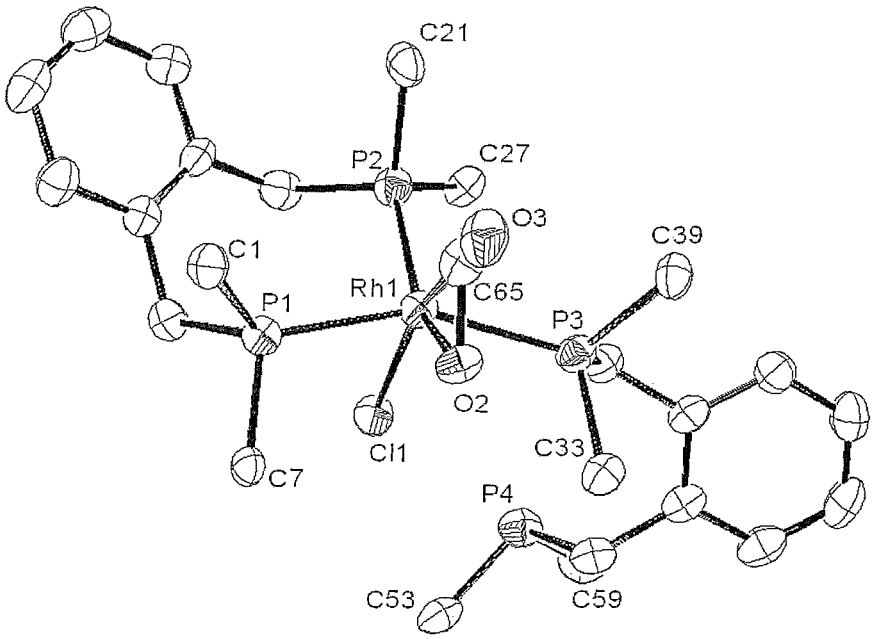

† Formula: $C_{65.49}H_{58}Cl_3O_{1.51}P_4Rh$, Formula weight: 1202.32, Crystal system: Monoclinic, Space Group: $P2_1/c$, a = 22.221(5), b = 14.940(4), c = 18.954(2) Å, $\alpha/°$ = 90, $\beta/°$ = 113.460(15), $\gamma/°$ = 90. Z = 4, Unique reflections: 13166, no. of parameters: 687, $R1$ [$I_o > 2\sigma(I_o)$] = 0.0615, $R1$ [all data] = 0.1426, wR_2 [$I_o > 2\sigma(I_o)$] = 0.1293, wR_2 [all data] = 0.1626.

Rhodium(I) and iridium(I) complexes of the type $[M'(o\text{-}C_6H_4(CH_2PPh_2)_2)(cod)]PF_6$ (where M' = Rh, Ir) were prepared from $[M'Cl(cod)]_2$ (where M' = Rh, Ir) and $o\text{-}C_6H_4(CH_2PPh_2)_2$, in good yield, in the presence of one molar equivalent of NH_4PF_6 in CH_2Cl_2. These complexes were prepared to obtain data on Rh(I) and Ir(I) complexes, that could be compared to that of $[Rh(o\text{-}C_6H_4(CH_2PPh_2)_2)_2]BF_4$ and therefore further the understanding of the coordination chemistry that occurs at these metal centres.

$[Rh(o\text{-}C_6H_4(CH_2PPh_2)_2)(cod)]PF_6$ was synthesised as an orange solid and analysed by phosphorus NMR spectroscopy, which suggested that the compound was pure. Two signals were recorded, suggesting two phosphorus environments. The first was a doublet at 10.3 ppm with coupling constant $^1J_{RhP}$ = 146 Hz, suggesting that the $o\text{-}C_6H_4(CH_2PPh_2)_2$ phosphorus atoms coordinated to the Rh(I) centre were in the same environment. The coupling constant was typical of a Rh(I) bidentate diphosphine complex, as researched previously.[19, 23] The second phosphorus signal was a septet at -143.8 ppm corresponding to the PF_6 anion associated with the complex. Microanalysis results also confirmed the purity of the compound. The ^1H NMR spectrum also proves beyond doubt that the desired product was formed with resonances at 7.70-7.50 (m), 6.85 (m), 6.40 (m) 4.40 (br m) 3.90 (br m) and 2.0-2.2 (m) which corresponded to phenyl protons, the xylyl unit, cod, ($o\text{-}C_6H_4(CH_2PPh_2)_2$, CH_2) and cod protons respectively.

$[Ir(o\text{-}C_6H_4(CH_2PPh_2)_2)(cod)]PF_6$ was isolated as a dark red solid and the results after spectroscopic analysis were very similar to that of the above rhodium analogue. Phosphorus NMR spectroscopy showed a singlet at -1.8 ppm corresponding to one phosphorus environment around the metal centre, and a septet at -143.8 ppm, confirming the presence of the PF_6^- anion. Again microanalysis confirmed the desired product, and positive ion electrospray MS showed the presence of the $[Ir(o\text{-}C_6H_4(CH_2PPh_2)_2)(cod)]^+$ at m/z = 775. ^1H NMR spectra data resulted in similar resonances to that of the analogous rhodium complex above. All the analytical data suggests that the compounds are the desired compounds and are similar to other Ir(I) complexes that have been researched previously.[23,24]

5.2.3. Ni, Pd and Pt Complexes

$[NiX_2(o\text{-}C_6H_4(CH_2PPh_2)_2)]$ where X = Cl, Br, was prepared using the appropriate hydrated nickel dihalide, dissolved in isopropanol, and with addition of one molar equivalent of $o\text{-}C_6H_4(CH_2PPh_2)_2$. $[NiBr_2(o\text{-}C_6H_4(CH_2PPh_2)_2)]$ was a brick red solid with a percentage yield of 87% and $[NiCl_2(o\text{-}C_6H_4(CH_2PPh_2)_2)]$ was a pink solid with a percentage yield of 76%. The diffuse reflectance and solution UV/vis data from $[NiBr_2(o\text{-}C_6H_4(CH_2PPh_2)_2)]$ and $[NiCl_2(o\text{-}C_6H_4(CH_2PPh_2)_2)]$ suggested that the complexes were square planar in geometry, which differs from work carried out by Venanzi and coworkers[12] who suggested they are tetrahedral in geometry, due to the absence of viable ^1H NMR spectra. However the ^1H NMR spectroscopic data from the isolated solids, suggested that both compounds had coordinated $o\text{-}C_6H_4(CH_2PPh_2)_2$ present with a doublet, at δ 3.65 and aromatics of around δ 7.50-7.20(m) and 6.90-6.70(m) ppm. The experimental magnetic moments of both compounds confirmed that they were diamagnetic. Another indication that the assignment is correct is the far infrared bands of both compounds, which for $[NiBr_2(o\text{-}C_6H_4(CH_2PPh_2)_2)]$ and $[NiCl_2(o\text{-}C_6H_4(CH_2PPh_2)_2)]$ give two Ni-X stretching vibrations indicative of a *cis*-NiX_2 unit[14] (theory taking into consideration the xylyl backbone: C_s: A' + A'').

The unexpected result above is interesting due to other related compounds adopting tetrahedral geometries. For example, the Ni(II) complex $[NiX_2(Ph_2P(CH_2)_4PPh_2)]$, with the $Ph_2P(CH_2)_4PPh_2$ forming a seven membered chelate ring similar to that of $o\text{-}C_6H_4(CH_2PPh_2)_2$, adopts a tetrahedral geometry.[14] However $Ph_2P(CH_2)_4PPh_2$ is a much more flexible ligand, suggesting that the rigidity of $o\text{-}C_6H_4(CH_2PPh_2)_2$ promotes the square planar geometry. Providing further evidence for this, the *o*-phenylene diphosphine, $o\text{-}C_6H_4(PPh_2)_2$ forms a square planar complex with Ni(II),[25] as it has the same rigid back-bone present in $o\text{-}C_6H_4(CH_2PPh_2)_2$. The basic xylene backbone is the same, but $o\text{-}C_6H_4(CH_2PPh_2)_2$ has a further carbon in the pendant arms of the ligand, which when coordinated forms seven-membered chelates, instead of five-membered chelates as in the $o\text{-}C_6H_4(PPh_2)_2$ case. This can also be explained by the strong ligand field exerted by the $o\text{-}C_6H_4(PPh_2)_2$ and $o\text{-}C_6H_4(CH_2PPh_2)_2$.

As with the further reaction of $[CoCl_2(o\text{-}C_6H_4(CH_2PPh_2)_2)]$ with NOCl at 273 K, to form the 5 coordinate $[CoCl_3(o\text{-}C_6H_4(CH_2PPh_2)_2)]$ species, reaction of $[NiCl_2(o\text{-}C_6H_4(CH_2PPh_2)_2)]$ with NOCl in CH_2Cl_2 resulted in an orange-brown, unstable solid, which upon analysis by solution UV/vis spectroscopy was found to be $[NiCl_3(o\text{-}C_6H_4(CH_2PPh_2)_2)]$ as the results compared well to the result for $[CoCl_3(o\text{-}C_6H_4(CH_2PPh_2)_2)]$. Examples of Ni(III)[26] species are not as rare as the high

spin d^6 Co(III) species, but are of great interest as it is another indication that *o*-$C_6H_4(CH_2PPh_2)_2$ can promote higher oxidation states than first predicted. An example of this type of complex is $[Ni\{o\text{-}C_6H_4(PPh_2)_2\}Cl_3]$, a dark green compound, with three infra red bands at 346, 311, 297 cm^{-1} similar to $[NiCl_3(o\text{-}C_6H_4(CH_2PPh_2)_2)]$ (theory C_s: 2A' + A''). As well as the infrared spectrum, the electronic spectrum was also recorded and bands indicating a distorted square pyramid structure was observed, which was similar to that of previously reported Ni(III) species.[26]

Three systems of palladium complexes incorporating *o*-$C_6H_4(CH_2PPh_2)_2$ were prepared as in the experimental section. A neutral palladium species $[PdCl_2(o\text{-}C_6H_4(CH_2PPh_2)_2)]$, in a square planar geometry, was prepared by reacting one equivalent of *o*-$C_6H_4(CH_2PPh_2)_2$ with Na_2PdCl_4 which was dissolved in EtOH. The reaction afforded a pale solid in a yield of 58% and was found to be pure by microanalysis. Fig 5.2.5 shows the structure of $[PdCl_2(o\text{-}C_6H_4(CH_2PPh_2)_2)]$ which contains bond lengths and angles similar to other palladium complexes.[12] The molecule has crystallographic *m* symmetry, with a Pd-P bond length of 2.2572(11) and a Pd-Cl distance of 2.3536 Å. The P1-Pd-P1' angle in the chelate of 100.04(6)° is much more obtuse than those seen in the Rh(I) species described above, which can be explained by the fact that there is a lot less steric bulk around the metal centre when only one *o*-$C_6H_4(CH_2PPh_2)_2$ ligand needs to be accommodated. This is also reflected in the P1···P1' distance of 3.46 Å which is much larger than of the above $[Rh(o\text{-}C_6H_4(CH_2PPh_2)_2)_2]^+$ cation.

Fig 5.2.5: Crystal Structure of $[PdCl_2(o\text{-}C_6H_4(CH_2PPh_2)_2)]$ with the H atoms omitted for clarity. Ellipsoids are shown at the 50% probability level.

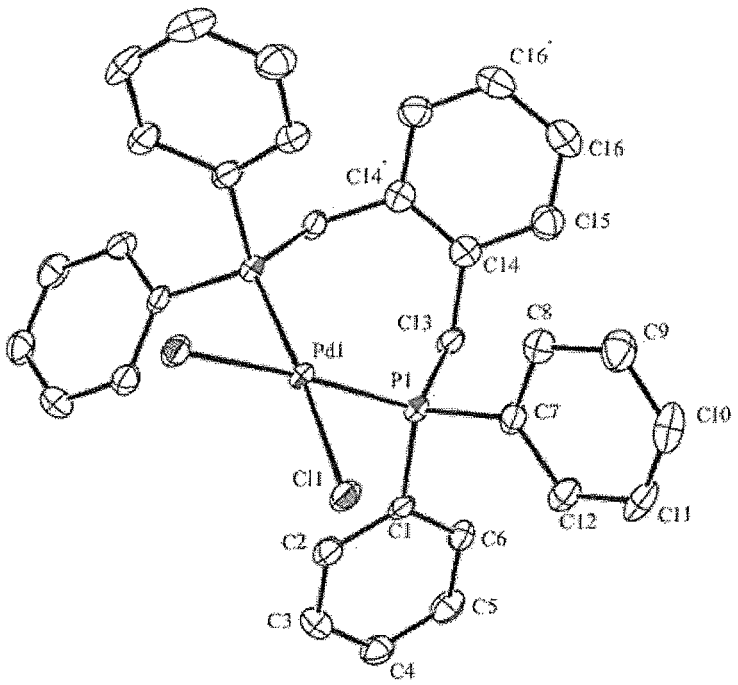

Table 5.2.3: Selected bond lengths (Å) and angles (°) for $[PdCl_2(o\text{-}C_6H_4(CH_2PPh_2)_2)]$.

Pd1-P1	2.2572(11)	P1 Pd1P1'	100.04(6)
Pd1-Cl1	2.3536(11)	P1Pd1Cl1'	174.91(4)
P1-C1	1.813(4)	P1Pd1Cl1	84.95(4)
P1-C7	1.818(4)	Cl1Pd1Cl1'	90.04(5)
P1-C13	1.835(4)		

All bond angles quoted, for bonds containing atoms marked with ('), for example P1', have a symmetry operation of x - y+1/2 z.

Other analytical techniques also proved that the compound is pure. The ^1H NMR spectrum suggests the aromatics of $o\text{-}C_6H_4(CH_2PPh_2)_2$ are complexed, with resonances of δ 7.9(m) and 7.5(m) [24H] ppm, and a doublet at δ 3.6 [4H] indicated the CH_2. $^{31}P\{^1H\}$ NMR spectroscopy

indicated one phosphorus environment with a resonance at δ 16.35 ppm. IR data suggests the presence of the Pd-Cl bond with bands at υ 316(m) and 304(m) cm^{-1}, which is in accordance with the data obtained by Venanzi and coworkers.[12] Again the data for the Pd-Cl bond agrees with the theory of two infra red active bands (theory C_s: A' + A'').

Another system prepared with a palladium metal centre, was $[Pd_2Cl_2(o\text{-}C_6H_4(CH_2PPh_2)_2)_2](PF_6)_2$. This was prepared by dissolving $PdCl_2$ in MeCN. One molar equivalent of $o\text{-}C_6H_4(CH_2PPh_2)_2$ was added followed by one molar equivalent of $TlPF_6$ to remove the excess chloride in the system. The resulting compound, was recovered as a yellow solid, with a percentage yield of 44%. Microanalytical data suggested that the complex was analytically pure. The $^{31}P\{^1H\}$ NMR spectrum showed one phosphorus environment in the dimer with a resonance at δ 27.27(s), and a septet at δ 143.65 ppm, indicating the presence of the PF_6^- counter ions. IR data also confirmed the presence of the PF_6^- with bands at υ 843(s) cm^{-1} and 561(s) cm^{-1} indicating P-F stretching modes and bending modes respectively. The presence of the Pd-Cl bond was also indicated by a band at 315(m) cm^{-1}. Electrospray mass spectrometry shows peaks at *m/z* 617 and 658 which indicated the following species respectively - $[PdCl(o\text{-}C_6H_4(CH_2PPh_2)_2)]^+$, and $([PdCl(o\text{-}C_6H_4(CH_2PPh_2)_2)(MeCN)]^+$, which were both formed *via* cleavage of the chloro bridges. It is assumed that $o\text{-}C_6H_4(CH_2PPh_2)_2$ is promoting the chosen pathway rather than cleaving both Pd – Cl bonds due to its steric bulk, preferring only one ligand around each metal centre.

Crystallographic studies on the structure of $[Pd_2Cl_2(o\text{-}C_6H_4(CH_2PPh_2)_2)_2](PF_6)_2.2CH_2Cl_2$ confirms a dinuclear $\mu^2\text{-}Cl_2$ palladium dication with a chelating $o\text{-}C_6H_4(CH_2PPh_2)_2$ bound to each Pd centre to give a distorted square planar geometry. There is a centre of inversion at the centre of the $Pd_2\text{-}\mu^2\text{-}Cl_2$ core. The Pd-P bond distances are 2.2481(10) and 2.2657(10) Å, very similar to Pd-P in the mononuclear complex above. The P1-Pd-P2 angle in this species is 98.00(4)° and d(P1···P2) is 3.41 Å.

Fig 5.2.6: Crystal structure of $[Pd_2Cl_2(o\text{-}C_6H_4(CH_2PPh_2)_2)_2]^{2+}$ from $[Pd_2Cl_2(o\text{-}C_6H_4(CH_2PPh_2)_2)_2](PF_6)_2.2CH_2Cl_2$, with the H atoms and phenyl rings (except ipso carbons) omitted for clarity. Ellipsoids are shown at the 50% probability level.

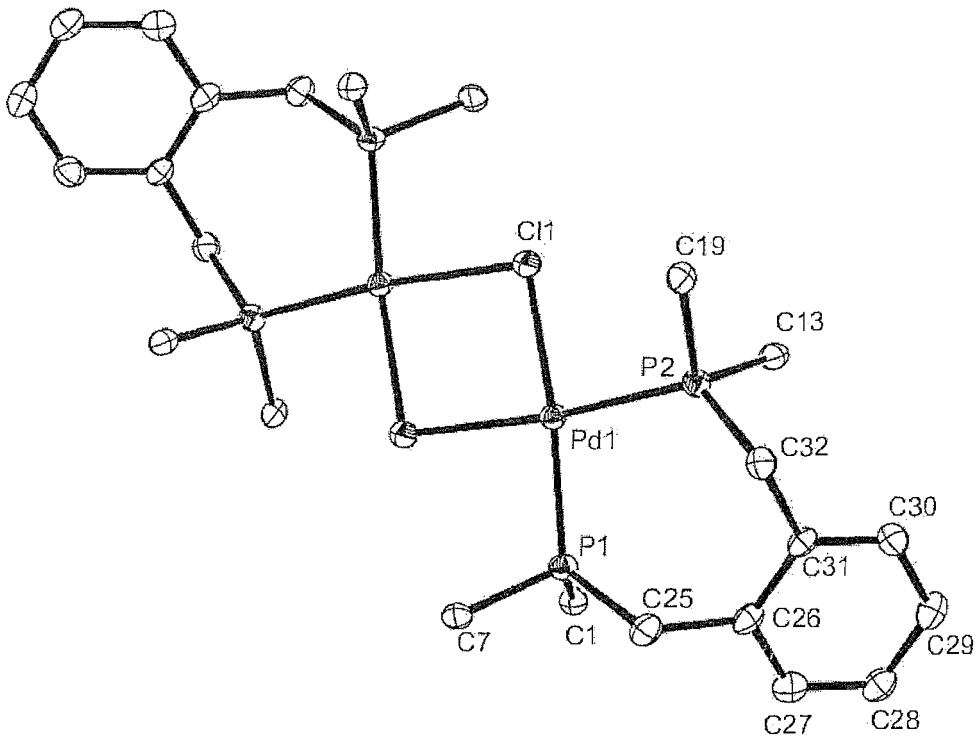

Table 5.2.4: Selected bond lengths (Å) and angles (°) for $[Pd_2Cl_2(o\text{-}C_6H_4(CH_2PPh_2)_2)_2](PF_6)_2.2CH_2Cl_2$

Pd1-P1	2.2481(10)	P1 Pd1 P2	98.00(4)
Pd1-P2	2.2657(10)	P2 Pd1 Cl1	90.93(4)
Pd1-Cl1	2.3917(10)	P1 Pd1 Cl1'	88.11(4)
P1-C1	1.818(4)		
P1-C7	1.821(4)		
P1-C25	1.821(4)		

All bond angles quoted, for bonds containing atoms marked with ('), for example Cl1', have a symmetry operation of 2-x, 2-y, 1-z.

The last palladium system explored was the homoleptic *bis*-ligand ion with square planar geometry and the molecular formula of $[Pd\{o\text{-}C_6H_4(CH_2PPh_2)_2\}_2](BF_4)_2$. This was prepared by dissolving $Pd(NO_3)_2$ in deionised water then adding two equivalents of $o\text{-}C_6H_4(CH_2PPh_2)_2$, dissolved in EtOH and CH_2Cl_2. An excess of HBF_4 was added and the reaction was stirred. A yellow precipitate was recovered with a yield of 69%. Similar studies have been investigated by Fox *et al.* in 1993.[27] The ^1H NMR spectrum shows a resonance at δ 8.0 – 7.20(m) [56H] ppm indicating that the aromatic rings of $o\text{-}C_6H_4(CH_2PPh_2)_2$ were present. The coordination of the CH_2 in the ligand was also indicated by a resonance at δ 3.65(d) ppm [8H]. $^{31}P\{^1H\}$ NMR spectroscopy also indicated purity of the compound by one resonance at δ 7.12 ppm suggesting one phosphorus environment. IR data also enforced the fact that the compound was pure by the presence of BF_4^- indicated by bands at υ 1095(w), 1067(s) cm^{-1} (B-F stretch), and 505(s), 491(s) cm^{-1} (δB-F). However, there was no evidence of any remaining nitrate or H_2O/OH^- in the product. These data, together with microanalyses, are consistent with the formulation of $[Pd\{o\text{-}C_6H_4(CH_2PPh_2)_2\}_2](BF_4)_2$. The Pd(II) centre is likely to be rather crowded, however this formulation is not unreasonable given the structural evidence for the distorted planar $[Rh(o\text{-}C_6H_4(CH_2PPh_2)_2)_2]^+$ cation described above.

An analogous complex to the $[PdCl_2(o\text{-}C_6H_4(CH_2PPh_2)_2)]$, was prepared from $K_2[PtCl_4]$. A solution of $K_2[PtCl_4]$ in CH_2Cl_2/EtOH, was prepared, and one molar equivalent of $o\text{-}C_6H_4(CH_2PPh_2)_2$ was added. Acetone was then added to give a homogeneous solution which was stirred for 72 h. before filtering and concentrating the filtrate *in vacuo* to give a white solid. Analysis of this species suggests that similar chemistry to that of $[PdCl_2(o\text{-}C_6H_4(CH_2PPh_2)_2)]$ has occurred and the neutral compound is indeed $[PtCl_2(o\text{-}C_6H_4(CH_2PPh_2)_2)]$, with a 98% yield. The ^1H NMR spectrum indicated the phenyl rings of $o\text{-}C_6H_4(CH_2PPh_2)_2$ were present by resonances at δ 8.00-7.80 (m) and 7.65-7.35(m) [28H] ppm and with a doublet at δ 3.85 [4H] ppm, which indicated both CH_2's in the coordinated $o\text{-}C_6H_4(CH_2PPh_2)_2$. The $^{31}P\{^1H\}$ NMR spectrum shows a singlet at –1.8 ppm with ^{195}Pt satellites ($^2J_{PtP}$ = 3584 Hz), consistent with the literature data.[28] This can be seen in Fig 5.2.7.

As there was some confusion as to whether the product was indeed the neutral species or the dinuclear $[Pt_2Cl_2(o\text{-}C_6H_4(CH_2PPh_2)_2)_2]Cl_2$, as with the palladium case above, a conductivity experiment was carried out in $MeNO_2$ solution. The complex was seen to be a non-electrolyte, which suggests the neutral species. The ^{195}Pt NMR spectrum shows a triplet at –4503 ppm, in accord with a P_2Cl_2 donor set at Pt(II).[12,28] An example from the literature researched by Hope

and co-workers is [Pt(Ph_2PCH=$CHPPh_2$)Cl_2] for which the ^{195}Pt NMR spectrum is a triplet at -4467 ppm.[28]

Fig 5.2.7: $^{31}P\{^1H\}$ NMR spectrum of [$PtCl_2$(*o*-C_6H_4(CH_2PPh_2)$_2$)] in CH_2Cl_2/$CDCl_3$.

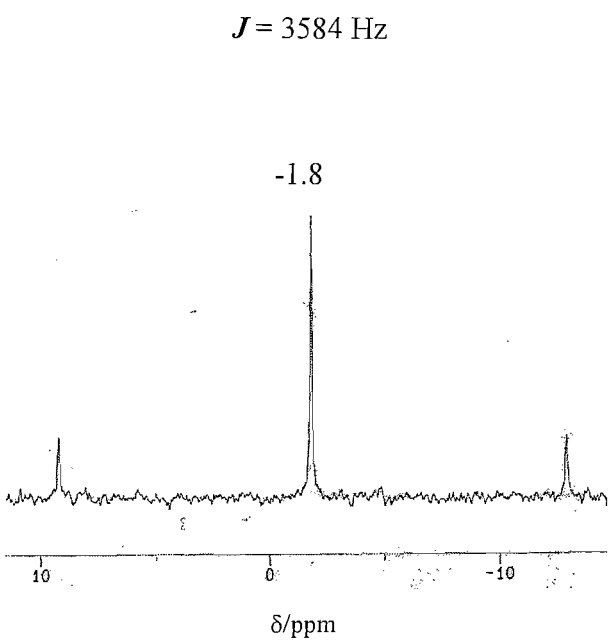

When [$PtCl_2$(*o*-C_6H_4(CH_2PPh_2)$_2$)] was dissolved in CH_2Cl_2 and treated with Cl_2/CCl_4 a yellow precipitate formed. In a Cl_2 saturated solution, $^{31}P\{^1H\}$ NMR spectroscopy suggested that this compound was [$PtCl_4$(*o*-C_6H_4(CH_2PPh_2)$_2$)], as the resonance produced was a singlet at -4.76 with platinum satellites $J_{Pt\text{-}P}$= 2160 Hz, which is approximately half the coupling constant for the starting material, and indicative of a Pt(IV)[28,29] complex. In the absence of Cl_2 the complex reverted back to the Pt(II) starting material, however, and this was also seen in the phosphorus NMR spectrum. In the IR spectrum, the desired product was confirmed by bands at 344 (w), 299 (w), 288 (w) indicating Pt-Cl stretches. Group theory, (theory C_s: 2A' + A'') indicates there should be four IR active bands, and the absence of the fourth could be explained by the weak spectrum. An example of similar compounds from the literature is [Pt($Ph_2P(CH_2)_2PPh_2$)Cl_4] which has IR ν(Pt-Cl) bands at 347 (m), 290 (s), 274 (s).[29] Similar treatment of [$PdCl_2$(*o*-C_6H_4(CH_2PPh_2)$_2$)] did not result in a colour change, and the $^{31}P\{^1H\}$ NMR spectrum was unchanged.

5.2.4. Cu, Ag and Au Complexes

The distorted tetrahedral complexes $[Cu(o\text{-}C_6H_4(CH_2PPh_2)_2)_2]BF_4$ and $[Ag(o\text{-}C_6H_4(CH_2PPh_2)_2)_2]BF_4$ were prepared from $[Cu(NCMe)_4]BF_4$ or $AgBF_4$ respectively and two equivalents of $o\text{-}C_6H_4(CH_2PPh_2)_2$ in CH_2Cl_2 excluding light. The colourless solutions afforded the *bis*-diphosphine complexes as above in high yield. The stoichiometry was confirmed by microanalysis. From analysis such as ^1H NMR spectroscopy, the data for both suggested that the complexes included two $o\text{-}C_6H_4(CH_2PPh_2)_2$ ligands by the chemical shifts at δ 7.80-6.60(m) [54H] (aromatic-H) and 3.65(m) [8H] (CH_2). $^{31}P\{^1H\}$ NMR spectroscopy indicated that there was indeed one phosphorus environment with a single broad singlet resonance at δ –8.74 (bs) ppm in the case of the Cu(I) complex, similar to literature examples[30] and two overlapping doublets indicating the silver to phosphorus coupling for both silver isotopes in the Ag(I) complex. (δ – 1.52 ppm with coupling constants of $^2J_{^{107}Ag-^{31}P} = 226$ Hz and $^2J_{^{109}Ag-^{31}P} = 257$ Hz).[31] In the case of the Ag(I) species the coupling constants are consistent with tetrahedral P_4-coordination in solution (compare for example the tetrahedral $[Ag(Ph_2P(CH_2)_2PPh_2)_2]^+$ $J(^{107}Ag\text{-}^{31}P) = 231$ and $J(^{109}Ag\text{-}^{31}P) = 266$ Hz[30]). The dihalo-bridged complexes $[Ag_2Cl_2(o\text{-}C_6H_4(CH_2PPh_2)_2)_2]$ (distorted tetrahedral P_2Cl_2 coordination) give $J(^{107}Ag\text{-}^{31}P) = 359$ and $J(^{109}Ag\text{-}^{31}P) = 413$ Hz, small reductions in the J values occur as the Cl is replaced by Br or I.[30] A *pseudo*-tetrahedral *bis*- $o\text{-}C_6H_4(CH_2PPh_2)_2$ coordination environment at Cu(I) is confirmed by the observation of a broad ^{63}Cu NMR resonance at +193 ppm which does not change significantly upon cooling. Phosphorus-copper coupling is not observed in either the $^{31}P\{^1H\}$ or ^{63}Cu NMR spectra. Electrospray mass spectroscopy for both species also suggested the right compound with peaks corresponding to the respective parent ions $(M^+ + H)^+$.

Fig 5.2.8: Isotope simulation for $[Ag(o\text{-}C_6H_4(CH_2PPh_2)_2)_2]BF_4$ compared to the actual mass spectrum.

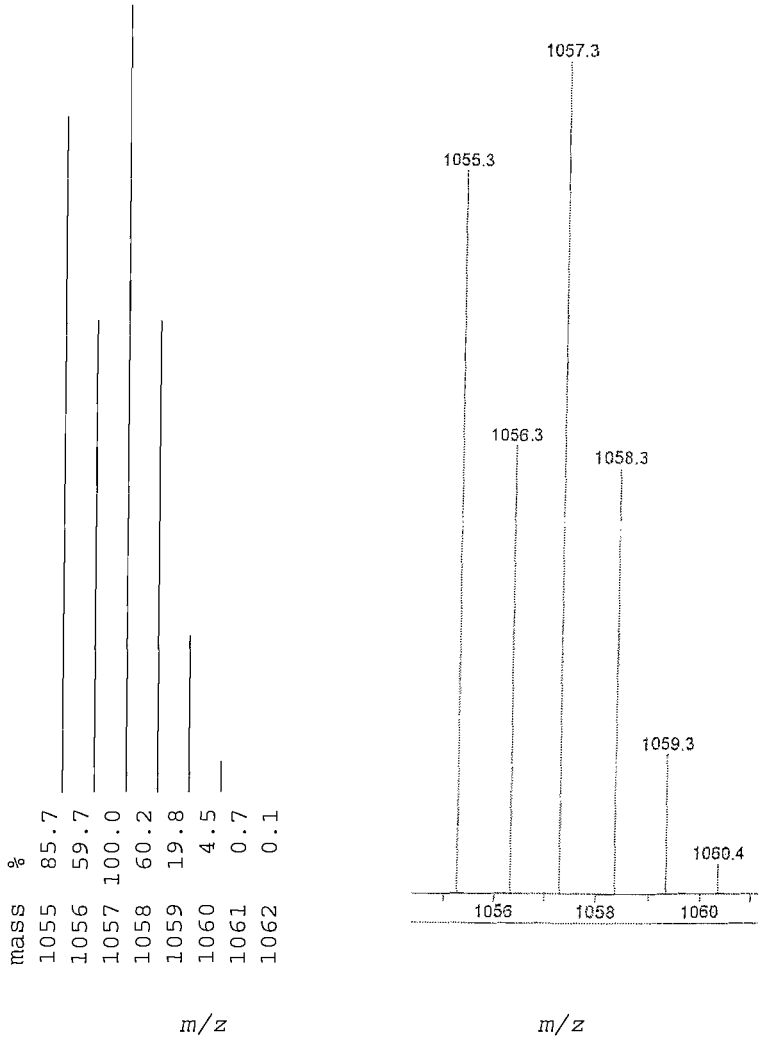

The IR data also suggests pure complexes with the presence of the BF_4^- anion with bands at 1097(w) cm^{-1} (B-F stretch), 504(w) cm^{-1} (B-F bend).

The coordination environment of the Ag(I) complex was confirmed by X-ray crystallographic studies. It was found to be the desired compound, with two solvated CH_2Cl_2 molecules associated. The structure of the cation shown (Fig 5.2.9), confirms two chelating $o\text{-}C_6H_4(CH_2PPh_2)_2$ ligands bonding in a bidentate manner to the silver metal centre. The geometry at the Ag(I) is distorted tetrahedral, which is consistent with the other analytical data. A summary of the main bond lengths and angles is displayed in Table 5.2.5. One point to note is that the P---P distances across

the chelate are 0.5 Å larger than in $[Rh(o\text{-}C_6H_4(CH_2PPh_2)_2)_2]^+$, reflecting the structural flexibility of the 7-membered chelate ring incorporating the somewhat rigid *o*-xylyl unit. The P–Ag-P angles are also over 10-12° larger than in the *bis*-*o*-$C_6H_4(CH_2PPh_2)_2$ complex $[Rh(o\text{-}C_6H_4(CH_2PPh_2)_2)_2]BF_4$. This is yet another indication of the flexibility of the ligand.

Fig 5.2.9: Crystal structure of $[Ag(o\text{-}C_6H_4(CH_2PPh_2)_2)_2]^+$ in $[Ag(o\text{-}C_6H_4(CH_2PPh_2)_2)_2]BF_4.2CH_2Cl_2$, with the H atoms and phenyl rings (except ipso carbons) omitted for clarity. Ellipsoids are shown at 50% probability level.

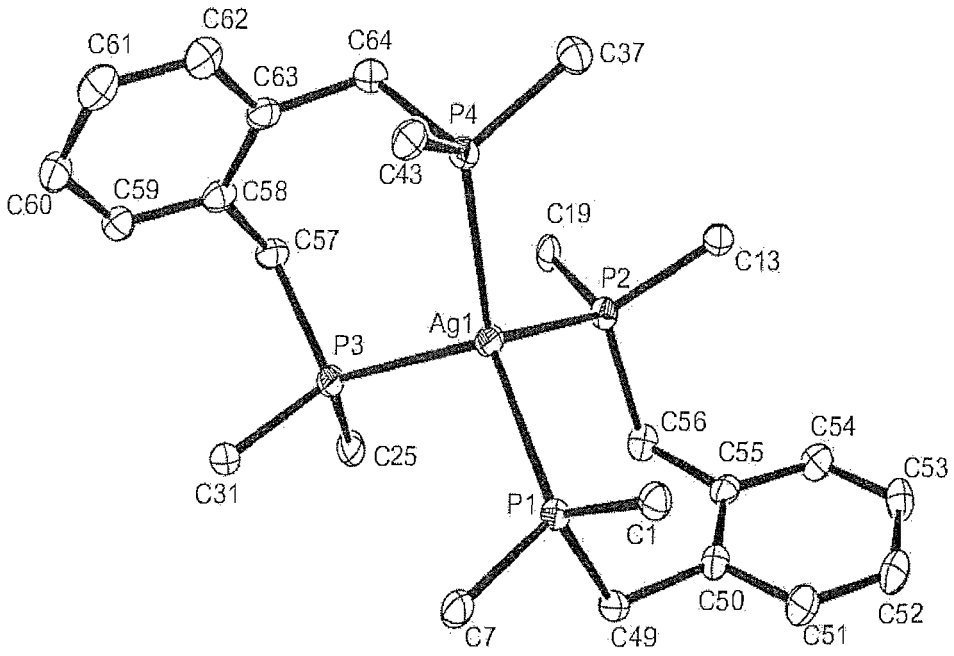

Table 5.2.5: Selected bond lengths (Å) and bond angles (°) for $[Ag(o\text{-}C_6H_4(CH_2PPh_2)_2)_2]BF_4.2CH_2Cl_2$

Ag1-P1	2.4691(9)	P1-Ag1-P2	102.88(3)
Ag1-P2	2.5222(9)	P1-Ag1-P3	110.69(3)
Ag1-P3	2.5385(9)	P2-Ag1-P4	108.32(3)
Ag1-P4	2.4787(9)	P3-Ag1-P4	104.21(3)
P1-C1	1.821(4)		
P1-C7	1.827(4)		
P1-C49	1.856(4)		

Other studies in the area have discussed the coordination of Ag(I) and *o*-$C_6H_4(CH_2PPh_2)_2$ but in a 1:1 ratio, whereby one ligand is coordinated to one metal centre, in a dimer, with halide bridges. The structures have the general form of $[Ag_2X_2(o\text{-}C_6H_4(CH_2PPh_2)_2)_2]$ (X = Cl or I) and exhibit distorted tetrahedral geometries around each metal centre.[10] However the P-Ag-P angles within the chelate rings are closer to the ideal tetrahedral value in the halo-bridged complexes than in the $[Ag(o\text{-}C_6H_4(CH_2PPh_2)_2)_2]^+$ cation, even though the Ag-P bonds are similar in length. The increase in distance between the chelating phosphorus centres can be seen to be due to the steric bulk of the *o*-$C_6H_4(CH_2PPh_2)_2$ ligand, as in the Ag(I) dimer complexes only one *o*-$C_6H_4(CH_2PPh_2)_2$ ligand is chelating, and so is not as distorted.

Two gold species were attempted using [AuCl(tht)],[32] with all reactions carried in the absence of light. $[Au_2Cl_2(o\text{-}C_6H_4(CH_2PPh_2)_2)]$ was prepared using a 2:1 ratio of [AuCl(tht)] and *o*-$C_6H_4(CH_2PPh_2)_2$ in CH_2Cl_2 and stirred. The resulting white solid (yield 23%) was treated as light sensitive and analysed by ^1H NMR spectroscopy, ^{31}P $\{^1H\}$ NMR spectroscopy and infrared. ^1H NMR spectroscopy suggested that the complex contained coordinated ligand with resonances at δ 3.90 (d) [4H] (CH_2), 7.60 – 7.10 (m) [24H] (Aromatics) ppm, which showed a slight shift upfield from the free ligand values. The $^{31}P\{^1H\}$ NMR spectrum showed a resonance at δ 30.5 (s) ppm, suggesting one phosphorus environment. The $^{31}P\{^1H\}$ NMR spectrum of the related $[Au_2Cl_2(Ph_2P(CH_2)_2PPh_2)]$ displays a similar coordination shift, giving $\delta(^{31}P)$ = +31.5 ppm.[33] These data together with ^1H NMR spectroscopic data confirm the formulation as $[(AuCl)_2(o\text{-}C_6H_4(CH_2PPh_2)_2)]$, probably involving linear Au-Cl coordination at each P atom of a bridging diphosphine. Infrared analysis also suggests that the compound is as stated by observing the presence of the Au – Cl bond with a band at υ 319cm^{-1}.

The second gold species to be prepared was the analogous compound to that of the Ag(I) above, $[Au(o\text{-}C_6H_4(CH_2PPh_2)_2)_2]PF_6$, using a 1:2:1 ratio of [AuCl(tht)], *o*-$C_6H_4(CH_2PPh_2)_2$ and $TlPF_6$. The reaction was carried out again excluding light in CH_2Cl_2 and yielded a white solid (66%). By ^{31}P $\{^1H\}$ NMR the compound was confirmed to have one coordinated *o*-$C_6H_4(CH_2PPh_2)_2$ phosphorus environment with a resonance at δ 0.76(s) ppm. The presence of the PF_6^- anion was also shown by a septet at -143.8 ppm. ^1H NMR spectroscopy showed coordination of two equivalents of *o*-$C_6H_4(CH_2PPh_2)_2$ with resonances at δ 3.75 (bs) [8H], (CH_2), 7.50 – 7.10 (m) [48H] (Aromatics) ppm, with appropriate integral patterns. Electrospray mass spectrometry confirmed the $[Au(o\text{-}C_6H_4(CH_2PPh_2)_2)_2]^+$ cation as being the dominant species with a cluster of mass peaks at *m/z* of 1145, corresponding to the correct isotope pattern, with a lower intensity

cluster corresponding to a fragment ion derived from loss of one o-$C_6H_4(CH_2PPh_2)_2$. To help complete the story, IR data prove that the compound contains the PF_6^- anion with peaks at υ 850 (s) (υPF_6^-), 560 (s) (δPF_6^-) cm^{-1}. As well as the strong evidence from the spectroscopic data described that the compound was the bis- o-$C_6H_4(CH_2PPh_2)_2$ product, crystals were successfully grown and the X-ray crystal structure was obtained.

Fig 5.2.10: Crystal structure of $[Au(o\text{-}C_6H_4(CH_2PPh_2)_2)_2]^+$ in $[Au(o\text{-}C_6H_4(CH_2PPh_2)_2)_2]PF_6.2CDCl_3$, with the H atoms and phenyl rings (except ipso carbons) omitted for clarity. Ellipsoids are shown at the 50% probability level.

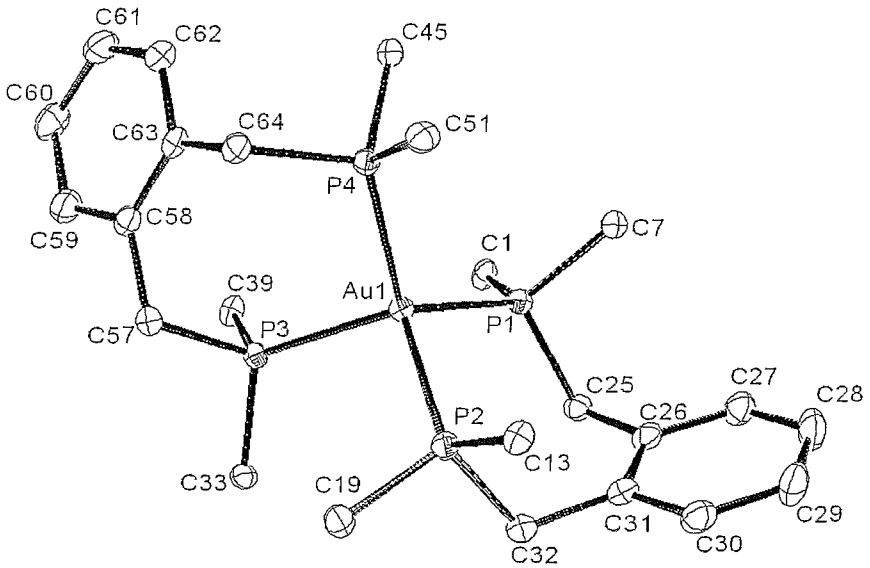

Table 5.2.6: Selected bond lengths (Å) and bond angles (°) for $[Au(o\text{-}C_6H_4(CH_2PPh_2)_2)_2]PF_6.2CDCl_3$

Au1-P1	2.4086(7)	P1-Au1-P2	103.62(2)
Au1-P2	2.4255(7)	P1-Au1-P4	116.16(2)
Au1-P3	2.4301(7)	P3-Au1-P2	102.94(2)
Au1-P4	2.4006(7)	P3-Au1-P4	103.65(2)
P1-C1	1.822(3)		
P1-C7	1.824(3)		
P1-C25	1.853(3)		

Comparison of the structure above with the Ag(I) analogue reveals a small but significant shortening of the metal-phosphorus bond distances in the 5d Au(I) complex.

5.3 Conclusion

The sterically demanding wide-angle diphosphine *o*-$C_6H_4(CH_2PPh_2)_2$, is preorganised for *cis*-chelation. Complexes have been synthesised incorporating transition metals from Group 9-11, and six crystal structures have been obtained. From these a significant advantage to this ligand can be recognised. The P---P distance, and hence the bite angle, varies more than half an angstrom between complexes, therefore it is a very flexible ligand, even with the relatively rigid back bone. The ligand favours low coordination numbers, as work on [Rh(*o*-$C_6H_4(CH_2PPh_2)_2)_2$]BF_4 and [Pd_2Cl_2(*o*-$C_6H_4(CH_2PPh_2)_2)_2$]$(PF_6)_2$ has shown. The reason for this can be predicted as due to the very bulky phenyl rings on the phosphorus centres. Many complexes showed evidence of dichloromethane or chloroform in the ^{1}H NMR spectra. Four out of the six crystal structures showed evidence of solvation of one or more solvent molecules for each metal centre. This suggests that the bulky ligand, when coordinated to metal centres creates large cavities in the structures that are stabilised by solvation.

Chemical oxidation reactions were carried out and [$PtCl_4$(*o*-$C_6H_4(CH_2PPh_2)_2$)], [$NiCl_3$(*o*-$C_6H_4(CH_2PPh_2)_2$)] and [$CoCl_3$(*o*-$C_6H_4(CH_2PPh_2)_2$)] were prepared and characterised by phosphorus NMR spectroscopy, Infrared spectroscopy and solution UV/vis spectroscopy. It can therefore be seen that the ligand, when exposed to extreme conditions can support higher oxidation states and coordination numbers. Indeed the d^6 Co(III) complex above is a rare discovery as not many are known,[17] so it can be deduced that *o*-$C_6H_4(CH_2PPh_2)_2$ is a very versatile ligand.

5.4 Experimental

Solvents were dried using known literature methods[34] prior to use and all preparations were undertaken using standard Schlenk techniques under a N_2 atmosphere.

***o*-$C_6H_4(CH_2PPh_2)_2$:** Solid PPh_3 (15.0 g, 57.2 mmol) and excess (4 equivalents) lithium (1.59 g, 228.8 mmol) were added to thf (100 cm^3). The solution turned blood red and was stirred overnight. The residual lithium was removed and then 0.8 equivalents of ^tBuCl (5 cm^3, 46 mmol) added drop wise to the reaction mixture. The solution turned violet and was stirred for 15 minutes. A solution of 0.4 equivalents of *o*-$C_6H_4(CH_2Cl_2)_2$ (4.0 g, 23 mmol) in thf (15 mL) was added to the reaction mixture drop wise and refluxed for 1 h. The mixture turned a yellow-brown and a white precipitate was formed. The reaction mixture was hydrolysed by a degassed, aqueous, saturated solution of NH_4Cl, the organic layer was separated and dried over degassed $MgSO_4$. Excess solvent was removed to produce a cream solid, which was recrystallised in minimum CH_2Cl_2. A white precipitate was produced with addition of ethanol (10 cm^3), which was filtered, and dried *in vacuo* (yield 11.82 g, 96%). ^1H NMR ($CDCl_3$): δ 7.25 (m) [20H] (Ph), 6.70 (m) [2H] (o-$C_6\underline{H}_4$), 6.60 (m) [2H] (o-$C_6\underline{H}_4$), 3.25(br,s) [4H] ($C\underline{H}_2$) ppm. $^{31}P\{^1H\}$ NMR (MeCN/$CDCl_3$): δ –12.94(s) ppm. IR (CsI disk): υ 3071w, 3052 w, 3018 w, 2985 w cm^{-1} (C-H stretches), 1600 w, 1484 m cm^{-1}, 1431 s cm^{-1} (Aromatics C=C). $^{13}C\{^1H\}$ NMR ($CDCl_3$): δ 133, 130, 129, 126 (aromatics), 33.5(d) ($\underline{C}H_2$) J = 16.8 Hz. All spectroscopic data are in accord with the literature.[12]

[$CoCl_2$(*o*-$C_6H_4(CH_2PPh_2)_2$)]: $CoCl_2.6H_2O$ (0.075 g, 0.316 mmol) was dissolved in isopropanol (20 cm^3). One molar equivalent of *o*-$C_6H_4(CH_2PPh_2)_2$ (0.150 g, 0.316 mmol) dissolved in CH_2Cl_2 (10 cm^3) was added and the reaction mixture was stirred for *ca.* 30 mins. to give a turquoise solid. The solvent was concentrated to *ca* 5 cm^3 *in vacuo* and the solid was collected by filtration, washed with *iso*-propanol and dried *in vacuo* (yield 67%). Required for $[C_{32}H_{28}Cl_2CoP_2].¼CH_2Cl_2$: C, 61.9; H, 4.6%. Found: C, 62.4; H, 4.3%. UV/vis (diffuse reflectance): v 6120, 7750, 13460, 15080, 16155, 25700 sh cm^{-1}; (CH_2Cl_2 solution): v 13590 (ε_{mol} 1000 $cm^{-1}mol^{-1}dm^3$), 15625 (900), 16920 (1060) cm^{-1}. IR (Nujol mull): υ 318 br m cm^{-1}. Magnetic moment = 4.68 μ_B.

[$CoCl_3$(*o*-$C_6H_4(CH_2PPh_2)_2$)]: Treatment of a CH_2Cl_2 solution of [$CoCl_2$(*o*-$C_6H_4(CH_2PPh_2)_2$)] with a stream of NOCl at *ca* –15°C leads to immediate formation of a deep green-blue solution which, upon pumping to dryness *in vacuo* affords a green-blue solid. IR (Nujol mull): υ 349, 321, 311 cm^{-1}. UV/vis (CH_2Cl_2 solution): v 6580, 16130, 16530 sh, 28570 cm^{-1}. †

[$CoBr_2$(*o*-$C_6H_4(CH_2PPh_2)_2$)]: Method as above, but using $CoBr_2.6H_2O$. Green solid (yield 62%). Required for [$C_{32}H_{28}Br_2CoP_2$]: C, 55.4; H, 4.1%. Found: C, 55.4; H, 3.7%. UV/vis (diffuse reflectance): ν 6540, 7605, 13265, 15130, 15875, 31850 cm^{-1}; (CH_2Cl_2 solution): 13280 (ε_{mol} 1580 $cm^{-1}mol^{-1}dm^3$), 15040 (1560), 16050 (1460) cm^{-1}. IR (Nujol mull): υ 243 br w cm^{-1}. Magnetic moment = 4.41 μ_B.

[CoI_2(*o*-$C_6H_4(CH_2PPh_2)_2$)]: Method as above, but using CoI_2. Brown-green solid (yield 55%). Required for [$C_{32}H_{28}CoI_2P_2$]1½CH_2Cl_2: C, 44.0; H, 3.4%. Found: C, 43.7; H, 3.1%. UV/vis (diffuse reflectance): ν 6610, 7350, 12770, 14045, 14730, 20830 sh, 2500 sh cm^{-1}; (CH_2Cl_2 solution): 12805 (ε_{mol} 920 $cm^{-1}mol^{-1}dm^3$), 13965 (885), 14840 (770) cm^{-1}. Magnetic moment = 4.84 μ_B.

[Rh(*o*-$C_6H_4(CH_2PPh_2)_2)_2$]BF_4

Method A: $RhCl_3.3H_2O$ (0.042 g, 0.16 mmol) was dissolved in EtOH (20 cm^3). Two molar equivalents of *o*-$C_6H_4(CH_2PPh_2)_2$ (0.15 g, 0.316 mmol) dissolved in CH_2Cl_2 (10 cm^3) was then added, together with 40% aqueous HBF_4 (1 cm^3). The resulting mixture was stirred at room temperature for 30 mins. Concentrating the mixture *in vacuo* gave an orange precipitate, which was filtered, washed with diethyl ether and dried *in vacuo* (Yield 52%). Required for [$C_{64}H_{56}BF_4P_4Rh$].2$CHCl_3$: C, 57.5; H, 4.2%. Found: C, 58.3; H, 4.6%. ^1H NMR ($CDCl_3$): 7.00 – 7.40 (m) [40H] (Ph), 6.90 (m) [4H] (*o*-$C_6\underline{H}_4$), 6.35 (m) [4H] (*o*-$C_6\underline{H}_4$), 3.65 (br s) [8H] ($C\underline{H}_2$). $^{31}P\{^1H\}$ NMR (CH_2Cl_2/$CDCl_3$): δ 11.6 ppm (d, $^1J_{RhP}$ = 140 Hz). IR spectrum (Nujol mull): ν 1060 s, 506 s cm^{-1}. Electrospray MS (MeCN): *m/z* 1051 [Rh(*o*-$C_6H_4(CH_2PPh_2)_2)_2]^+$, 557 [Rh(*o*-$C_6H_4(CH_2PPh_2)_2)]^+$, 475 [*o*-$C_6H_4(CH_2PPh_2)_2$+H]$^+$.

Method B: [RhCl(cod)]$_2$ (0.20 g, 0.40 mmol) and $AgBF_4$ (0.162 g, 0.84 mmol) were heated to reflux in acetone (10 cm^3) for 30 minutes, during which time a white precipitate was formed. The reaction was cooled to room temperature, and then filtered. The resultant yellow solution was added drop wise to a solution of excess *o*-$C_6H_4(CH_2PPh_2)_2$ (0.96 g, 0.2 mmol) in toluene (20 cm^3). The orange solution was then stirred at room temperature for 24 h. The reaction was then reduced to dryness, and then dissolved in minimum acetone. Et_2O (10 cm^3) was added to precipitate a solid. The orange solid was filtered, washed with hexane (10 cm^3) then dried *in vacuo*. (Yield: 0.66 g, 73%). $^{31}P\{^1H\}$ NMR (CH_2Cl_2/$CDCl_3$): δ 12.7 ppm (d, $^1J_{RhP}$ = 138 Hz). All other analytical data are as above.

Attempted preparation of $[Rh(CO)\{o\text{-}C_6H_4(CH_2PPh_2)_2\}_2]^+$

Method A: $[Rh(o\text{-}C_6H_4(CH_2PPh_2)_2)_2]BF_4$ (0.20 g, 0.18 mmol) was dissolved in dry CH_2Cl_2 (20 cm^3) under N_2. CO gas was bubbled through the solution for 30 minutes, whereby the solution changed from orange to yellow. The reaction was monitored by IR spectroscopy. Et_2O (20 cm^3) was added to crystallise yellow crystals, that were filtered and dried *in vacuo*. (Yield: 0.2 g, 93%). $^{31}P\{^1H\}$ NMR ($CH_2Cl_2/CDCl_3$): δ 21.5 (br s) 15.9 (br s), 8.5 (br s) ppm. ES^+ MS (MeCN): *m/z* 1051 $[Rh(o\text{-}C_6H_4(CH_2PPh_2)_2)_2]^+$, 1079 $[Rh(CO)(o\text{-}C_6H_4(CH_2PPh_2)_2)_2]^+$. IR ($CH_2Cl_2$): υ 2020 m, 1983 s (CO) cm^{-1}. IR (Nujol mull): υ 2033 w, 2015 w, 1974 s (CO) cm^{-1}. ‡

Method B: $[Rh_2Cl_2(CO)_4]$ (0.060 g, 0.15 mmol), $o\text{-}C_6H_4(CH_2PPh_2)_2)_2$ (0.29 g, 0.62 mmol) and NH_4PF_6 (0.055 g, 0.34 mmol) were dissolved in dry CH_2Cl_2 (15 cm^3) at 0°C, excluding light and was stirred for 5 h. The reaction was allowed to warm to room temperature and stirred for a further 2.5 h. The reaction mixture was then filtered and the resulting yellow solution was reduced in volume to *ca.* 2 cm^3 and hexane (10 cm^3) was added to precipitate a solid. The yellow solid was filtered and dried *in vacuo*. (Yield: 0.15 g, 40%). IR (Nujol mull): υ 2010 m (CO), 840 s, 557 s (PF_6^-) cm^{-1}. IR (CH_2Cl_2): υ 2019 s (CO) cm^{-1}. ES^+ MS (MeCN): *m/z* 1051 $[Rh(o\text{-}C_6H_4(CH_2PPh_2)_2)_2]^+$. $^{31}P\{^1H\}$ NMR (- 70°C, $CH_2Cl_2/CDCl_3$): δ 25.0 – 20.0 (br m) 17.0 – 12.0 (br m), 11.0 – 6.0 (br m) ppm. ‡

Method C: $Rh_2Cl_2(CO)_4]$ (0.050 g, 0.13 mmol) and $o\text{-}C_6H_4(CH_2PPh_2)_2)_2$ (0.26 g, 0.54 mmol) were dissolved in dry CH_2Cl_2 (15 cm^3) and the reaction was stirred for 1.5 h. The reaction mixture was then reduced in volume to *ca.* 2 cm^3 and hexane (10 cm^3) was added to precipitate a solid. The orange solid was isolated by filtration and dried *in vacuo*. (Yield: 55%). $^{31}P\{^1H\}$ NMR (-70°C; $CH_2Cl_2/CDCl_3$): δ 8.4 (dt) (J = 90.6, 37.4 Hz), -9.16 (dt) (J = 111, 38 Hz), -13.3 (s) ppm. IR (Nujol mull): υ 1940 s (CO) cm^{-1}. IR (CH_2Cl_2): υ 1927 s (CO) cm^{-1}. ES^+ MS (MeCN): *m/z* 1051 $[Rh(o\text{-}C_6H_4(CH_2PPh_2)_2)_2]^+$. ‡

$[Rh(cod)(o\text{-}C_6H_4(CH_2PPh_2)_2)]PF_6$: $[RhCl(cod)]_2$[35] (0.078 g, 0.16 mmol) was dissolved in a degassed solution of CH_2Cl_2 (20 cm^3). NH_4PF_6 (0.057 g, 0.35 mmol) and $o\text{-}C_6H_4(CH_2PPh_2)_2$ (0.15 g, 0.32 mmol) were added to the mixture and the reaction was stirred under nitrogen for 30 minutes. The reaction mixture changed from yellow to red and the white precipitate (NH_4Cl) was filtered off. The solution was reduced in volume to ~ 5 cm^3 *in vacuo*. Upon addition of diethyl ether (10 cm^3) an orange precipitate formed which was filtered and washed with diethyl ether (2 x 10 cm^3). The orange solid was dried *in vacuo* (yield 0.145 g, 55.4%). Required for

$[C_{40}H_{40}F_6P_3Rh].½CH_2Cl_2$: C, 55.7; H, 4.7%. Found: C, 56.1; H, 3.9%. ^1H NMR ($CDCl_3$): δ 7.70-7.50 (m) [20H] (Ph), 6.85 (m) [2H] (*o*-$C_6\underline{H}_4$), 6.40 (m) [2H] (*o*-$C_6\underline{H}_4$), 4.40 (br m) [4H] (cod C$\underline{H}$), 3.90 (br m) [4H] (*o*-$C_6H_4(CH_2PPh_2)_2$, C$\underline{H}_2$), 2.0-2.2 (m) [8H] (cod C$\underline{H}_2$). $^{31}P\{^1H\}$ NMR ($CH_2Cl_2/CDCl_3$): δ 10.3 ppm (d, $^1J_{RhP}$ = 146 Hz) [2P], -143.8 (septet, PF_6^-) [1P]. IR (Nujol mull): υ 840 s, 557 s cm^{-1}.

[Ir(cod)(*o*-$C_6H_4(CH_2PPh_2)_2$)]PF_6: Method as above, using $[Ir_2Cl_2(cod)_2]$,[36] giving an orange–red solid (yield 0.164 g, 56%). Required for $[C_{40}H_{40}F_6IrP_3].CH_2Cl_2$: C, 49.0; H, 4.2%. Found: C, 48.3; H, 3.7%. ^1H NMR ($CDCl_3$): δ 7.70-7.30 (m) [20H] (Ph), 6.85 (m) [2H] (*o*-$C_6\underline{H}_4$), 6.40 (m) [2H] (*o*-$C_6\underline{H}_4$), 4.18 (br m) [4H] (cod C$\underline{H}$), 3.92 (br m) [4H] (*o*-$C_6H_4(CH_2PPh_2)_2$, C$\underline{H}_2$), 1.7-2.0 (m) [8H] (cod C$\underline{H}_2$). $^{31}P\{^1H\}$ NMR ($CH_2Cl_2/CDCl_3$): δ -1.8 ppm (s) [2P], -143.8 (septet, PF_6^-) [1P]. IR (Nujol mull): υ 841 s, 557 s cm^{-1}. Electrospray MS (MeCN): m/z 775 [Ir(cod)(*o*-$C_6H_4(CH_2PPh_2)_2$)]$^+$.

[$NiCl_2$(*o*-$C_6H_4(CH_2PPh_2)_2$)]: $NiCl_2.6H_2O$ (0.075 g, 0.316 mmol) was dissolved in *iso*-propanol (20 cm^3) and one mol. equiv. of *o*-$C_6H_4(CH_2PPh_2)_2$ (0.15 g, 0.316 mmol) was added. Stirring the reaction mixture for 1 h. afforded a deep pink solid which was filtered and dried *in vacuo*. Recrystallisation from CH_2Cl_2 gave a deep pink solid (yield 76%). Required for $[C_{32}H_{28}Cl_2NiP_2].1½CH_2Cl_2$: C, 55.0; H, 4.3%. Found: C, 55.5; H, 5.0%. ^1H NMR ($CDCl_3$): δ 6.90-7.40 (br m) [20H] (Ph), 6.70 (br m) [2H] (*o*-$C_6\underline{H}_4$), 6.30 (br m) [2H] (*o*-$C_6\underline{H}_4$), 3.40 (br m) [4H] (C$\underline{H}_2$) ppm. UV/vis (diffuse reflectance): 20325, 29415, 37310 cm^{-1}; (CH_2Cl_2 solution): 20410 (ε_{mol} 510 $cm^{-1}mol^{-1}dm^3$). IR (Nujol mull): υ 337 m, 322 m cm^{-1}.

[$NiCl_3$(*o*-$C_6H_4(CH_2PPh_2)_2$)]: Treatment of a CH_2Cl_2 solution of [$NiCl_2$(*o*-$C_6H_4(CH_2PPh_2)_2$)] with a stream of NOCl at *ca.* –50°C gave a deep orange-brown solution, from which an orange brown solid was obtained upon pumping to dryness *in vacuo*. IR (Nujol mull): ν 340, 312, 300 sh cm^{-1}. UV/vis (CH_2Cl_2 solution): 12900 v br, 21050, 28570 cm^{-1}. †

[$NiBr_2$(*o*-$C_6H_4(CH_2PPh_2)_2$)]: Prepared as above with $NiBr_2.3H_2O$ (0.086 g, 0.316 mmol) and *o*-$C_6H_4(CH_2PPh_2)_2$ (0.15 g, 0.316 mmol) to afford a brick red solid (yield 87%). Required for $[C_{32}H_{28}Br_2NiP_2].1½CH_2Cl_2$: C, 49.0; H, 3.8%. Found: C, 48.3; H, 4.9%. ^1H NMR ($CDCl_3$): δ 6.70-7.50 (br m) [24H] (Ar-C$\underline{H}$), 3.80 (br m) [4H] (C$\underline{H}_2$) ppm. UV/vis (diffuse reflectance): 19600, 24040, 29240 cm^{-1}; (CH_2Cl_2 solution): 19920 (ε_{mol} 450 $cm^{-1}mol^{-1}dm^3$), 25000 (1485), 30675 (3140) cm^{-1}. IR (Nujol mull): υ 282 w, 262 w cm^{-1}.

[$PdCl_2$(*o*-$C_6H_4(CH_2PPh_2)_2$)]: Na_2PdCl_4 (0.093 g, 0.316 mmol) was dissolved in EtOH (20 cm^3). One molar equivalent of *o*-$C_6H_4(CH_2PPh_2)_2$ (0.15 g, 0.316 mmol) was added in EtOH (~5 cm^3). The reaction mixture was stirred overnight, and a pale cream precipitate formed. After filtering and drying *in vacuo* a cream solid was recovered (yield 58%). Required for $[C_{32}H_{28}Cl_2P_2Pd].CH_2Cl_2$: C, 53.8; H, 4.1%. Found: C, 54.2; H, 4.2%. ^{1}H NMR ($CDCl_3$): δ 7.85-7.98 (m), 7.44-7.60 (m) [20H] (Ph), 6.88 (m) [2H] (*o*-$C_6\underline{H}_4$), 6.15 (m) [2H] (*o*-$C_6\underline{H}_4$), 3.75 (br d, *J* = 10 Hz) [4H] ($C\underline{H}_2$). $^{31}P\{^1H\}$ NMR (CH_2Cl_2/$CDCl_3$): δ 16.4 ppm. IR (CsI disk): υ 3064 w, 2971 w, 2933 w, 1586 w, 1481 m, 1433 s, 1360 m, 1188 w, 1103 s, 1073 w, 1027 w, 1000 m, 867 w, 837 m, 746 s, 700 s, 504 s, 452 w, 316 m, 304 m cm^{-1}.

[Pd_2Cl_2(*o*-$C_6H_4(CH_2PPh_2)_2)_2$]$(PF_6)_2$: $PdCl_2$ (0.056 g, 0.316 mmol) was dissolved in MeCN (20 cm^3), by refluxing for 1h. One molar equivalent of *o*-$C_6H_4(CH_2PPh_2)_2$ (0.15 g, 0.316 mmol) was added to the reaction mixture, followed by one equivalent of $TlPF_6$ (0.11 g, 0.316 mmol). The resulting reaction mixture was stirred overnight and then filtered. The yellow filtrate was reduced to ~5 cm^3. Cold diethyl ether (~10 cm^3) was added dropwise to precipitate a yellow solid, which was filtered and dried *in vacuo* (yield 44%). Required for $[C_{64}H_{56}Cl_2F_{12}P_6Pd_2]$: C, 50.5; H, 3.7%. Found: C, 50.9; H, 3.8%. ^{1}H NMR ($CDCl_3$): δ 7.40-7.90 (m) [40H], (Ph), 6.80 (m) [4H] (*o*-$C_6\underline{H}_4$), 6.20 (m) [4H] (*o*-$C_6\underline{H}_4$), 3.90 (br d, *J* = 12 Hz) [8H], ($C\underline{H}_2$). $^{31}P\{^1H\}$ NMR (CH_2Cl_2/$CDCl_3$): δ 27.3 (s) [4P] (-P-Ph), -143.7 (septet) [2P] (PF_6^-) ppm. IR (CsI disk): υ 3082 w, 3067 w, 3031 w, 2932 w, 1587 w, 1485 w, 1437 s, 1356 m, 1185 w, 1167 w, 1106 m, 1068 w, 1002 m, 843 br s, 777 m, 746 m, 696 m, 561 s, 501 m, 457 m, 374 w, 315 m cm^{-1}. Electrospray MS (MeCN): *m/z* 617 [PdCl(*o*-$C_6H_4(CH_2PPh_2)_2$)]$^+$, 658 [PdCl(*o*-$C_6H_4(CH_2PPh_2)_2$)(MeCN)]$^+$.

[Pd(*o*-$C_6H_4(CH_2PPh_2)_2)_2$]$(BF_4)_2$: *o*-$C_6H_4(CH_2PPh_2)_2$ (0.15 g, 0.316 mmol) was dissolved in a mixture of EtOH (20 cm^3) and CH_2Cl_2 (10 cm^3). $Pd(NO_3)_2$ (0.036 g, 0.158 mmol) was dissolved in deionised H_2O (~10 cm^3) and added forming an orange solution. An excess of 40 % aqueous HBF_4 (2 cm^3) was then added, and the reaction was stirred for 1h. The solution was reduced in volume until a yellow precipitate formed which was filtered and dried *in vacuo* (yield 69%). Required for $[C_{64}H_{56}B_2F_8P_4Pd]$: C, 62.5; H, 4.6%. Found: C, 63.0; H, 4.9%. ^{1}H NMR ($CDCl_3$): δ 7.30 – 7.80 (m) [40H] (Ph), 6.20-6.80 (m) [8H] (*o*-$C_6\underline{H}_4$), 3.70 (br m) ppm [8H] ($C\underline{H}_2$). $^{31}P\{^1H\}$ NMR (CH_2Cl_2/$CDCl_3$): δ 7.1 ppm. IR (Nujol mull): υ 1067s, 505s cm^{-1}.

[$PtCl_2$(*o*-$C_6H_4(CH_2PPh_2)_2$)]: K_2PtCl_4 (0.13 g, 0.316 mmol) was dissolved in deionised H_2O (10 cm^3) and added to EtOH (20 cm^3) whilst stirring. One equivalent of *o*-$C_6H_4(CH_2PPh_2)_2$ (0.15 g, 0.316 mmol) dissolved in CH_2Cl_2 (10 cm^3) was added. The reaction mixture was stirred for 3h, and the subsequent two layers were combined with the addition of acetone (10 cm^3). After stirring for 72 hrs, the mixture was filtered and then reduced in volume until a cream precipitate formed which was filtered and dried *in vacuo* (yield 98%). Required for [$C_{32}H_{28}Cl_2P_2Pt$]: C, 51.9; H, 3.8%. Found: C, 51.1; H, 3.9%. ^{1}H NMR ($CDCl_3$): δ 7.90-8.00 (m), 7.45-7.60 (m) [20H] (Ph), 6.90 (m) [2H] (*o*-$C_6\underline{H}_4$), 6.20 (m) [2H] (*o*-$C_6\underline{H}_4$), 3.95 (br d, J = 11 Hz) [4H] ($C\underline{H}_2$) ppm. $^{31}P\{^1H\}$ NMR (CH_2Cl_2/$CDCl_3$): δ –1.8 ppm, $^1J_{Pt\text{-}P}$ = 3584 Hz. ^{195}Pt NMR: -4503 (t, $^1J_{PtP}$ = 3584 Hz). IR (Nujol Mull): υ 326 w, 304 w cm^{-1}. Conductivity $\Lambda_M/\Omega^{-1}.cm^2.mol^{-1}$ (10^{-3} $mol.dm^{-3}$ $MeNO_2$): 11.0. Electrospray MS (MeCN): *m/z* 745 [PtCl(*o*-$C_6H_4(CH_2PPh_2)_2$)(MeCN)]$^+$.

[$PtCl_4$(*o*-$C_6H_4(CH_2PPh_2)_2$)]: Treatment of a CH_2Cl_2 solution of [$PtCl_2$(*o*-$C_6H_4(CH_2PPh_2)_2$)] with Cl_2 in CCl_4 gave a bright yellow solution, which upon concentrating *in vacuo* produced a bright yellow solid. Required for [$C_{32}H_{28}Cl_4P_2Pt$].CH_2Cl_2: C, 44.2; H, 3.4%. Found: C, 44.8; H, 3.4 %. $^{31}P\{^1H\}$ NMR (CH_2Cl_2/$CDCl_3$): δ –4.8 ppm, $^1J_{Pt\text{-}P}$ = 2160 Hz. IR (Nujol Mull): υ 344, 299, 288 cm^{-1}.

[Cu(*o*-$C_6H_4(CH_2PPh_2)_2)_2$](BF_4): [Cu($NCMe)_4$](BF_4) (0.044 g, 0.158 mmol) was dissolved in CH_2Cl_2 (20 cm^3) and stirred. Two molar equivalents of *o*-$C_6H_4(CH_2PPh_2)_2$ (0.15 g, 0.136 mmol) were added, and the reaction was stirred for 2 h. The solution was reduced in volume to ~5 cm^3 and hexane (15 cm^3) was added to precipitate a solid. This was filtered and the white solid was dried *in vacuo* (yield 92%). Required for [$C_{64}H_{56}BCuF_4P_4$].$2CH_2Cl_2$: C, 62.5; H, 4.8%. Found: C, 62.5; H, 4.9%. ^{1}H NMR ($CDCl_3$): δ 7.70-6.80 (br m) [44H] (Ar-C$\underline{H}$), 6.30 (br m) [4H] (*o*-$C_6\underline{H}_4$) 3.65 (br m) [8H] ($C\underline{H}_2$). $^{31}P\{^1H\}$ NMR: δ –8.7 (s) ppm. ^{63}Cu NMR: δ +193 ppm. Electrospray MS (MeCN): *m/z* 1011 [Cu(*o*-$C_6H_4(CH_2PPh_2)_2)_2$]$^+$, 578 [Cu(*o*-$C_6H_4(CH_2PPh_2)_2$)](MeCN)]$^+$, 537 [Cu(*o*-$C_6H_4(CH_2PPh_2)_2$)]$^+$. IR (CsI disk): υ 3059 w, 2964 w, 2927 w, 1590 w, 1482 m, 1437 s, 1359 w, 1272 w, 1186 m, 1159 w, 1096 s, 1062 br s, 1003 w, 865 m, 842 m, 766 m, 735 s, 700 s, 504 s, 486 s, 445 w, 342 w cm^{-1}.

[Ag(*o*-$C_6H_4(CH_2PPh_2)_2)_2$](BF_4): $AgBF_4$ (0.031 g, 0.158 mmol) was dissolved in CH_2Cl_2 (20 cm^3) in a foil wrapped reaction vessel to exclude light, at 0°C. Two equivalents of *o*-$C_6H_4(CH_2PPh_2)_2$ (0.15 g, 0.316 mmol) were dissolved in CH_2Cl_2 (10 cm^3) and added dropwise whilst stirring to the reaction mixture, keeping the temperature at 0°C. After stirring for 2 h, the white precipitate was

recovered by filtration, and dried *in vacuo* to afford a white solid (yield 82%). The solid was stored in a foil wrapped container to exclude light. Required for $[C_{64}H_{56}AgBF_4P_4].1½CH_2Cl_2$: C, 61.9; H, 4.7%. Found: C, 62.4; H, 5.1%. ^{1}H NMR ($CDCl_3$): δ 6.95-7.30 (m) [40H] (Ph), 6.65 (br m) [4H] (*o*-$C_6\underline{H}_4$), 6.20 (br m) [4H] (*o*-$C_6\underline{H}_4$), 3.65 (br s) [8H] ($C\underline{H}_2$) ppm. ^{31}P{^{1}H} NMR ($CH_2Cl_2/CDCl_3$): δ −1.5 (2 x d, $^1J_{107Ag-31P}$ = 226 Hz, $^1J_{109Ag-31P}$ = 257 Hz). Electrospray MS (MeCN): *m/z* 1055 [^{107}Ag(*o*-$C_6H_4(CH_2PPh_2)_2)_2$]$^+$, 1057 [^{109}Ag(*o*-$C_6H_4(CH_2PPh_2)_2)_2$]$^+$. IR (Nujol Mull): υ 1059 m, 504 m cm^{-1}.

[Au(*o*-$C_6H_4(CH_2PPh_2)_2)_2$]PF_6: *o*-$C_6H_4(CH_2PPh_2)_2$ (0.15 g, 0.316 mmol) was dissolved in CH_2Cl_2 (20 cm^3). AuCl(tht) (50.7 mg, 0.158 mmol) was added to the reaction vessel, followed by $TlPF_6$ (55.2 mg, 0.158 mmol). The vessel was wrapped in foil to exclude light. This was stirred for 1h, and filtered to remove TlCl. The volume was reduced to ~5 cm^3 and a white precipitate formed, which was filtered and dried *in vacuo* (yield 66%). The resulting fine white powder was stored in a sample bottle excluding light. Required for $[C_{64}H_{56}AuF_6P_5].CH_2Cl_2$: C, 56.7; H, 4.2%. Found: C, 57.3; H, 3.9%. ^{1}H NMR ($CDCl_3$): δ 7.10-7.35 (m) [40H] (Ph), 6.40 (m) [4H] (*o*-$C_6\underline{H}_4$), 5.83 (m) [4H] (*o*-$C_6\underline{H}_4$), 3.75 (br s) [8H], ($C\underline{H}_2$) ppm. ^{31}P{^{1}H} NMR ($CH_2Cl_2/CDCl_3$): δ 0.8 (s) [4P] (P-Ph), -143.9 (sep) [1P] (PF_6) ppm. Electrospray MS (MeCN): *m/z* 1145 [Au(*o*-$C_6H_4(CH_2PPh_2)_2)_2$]$^+$, 671 [Au(*o*-$C_6H_4(CH_2PPh_2)_2$)]$^+$. IR (Nujol Mull): υ 850 br s, 560 s cm^{-1}.

[$(AuCl)_2$(*o*-$C_6H_4(CH_2PPh_2)_2$)]: *o*-$C_6H_4(CH_2PPh_2)_2$ (0.072 g, 0.152 mmol) was dissolved in CH_2Cl_2 (20 cm^3). [AuCl(tht)] (0.098 g, 0.304 mmol) was added and the vessel was wrapped in foil to exclude light. The reaction mixture was stirred for 30 minutes at room temperature, and then reduced in volume to ~5 cm^3. The resulting white precipitate was filtered and dried *in vacuo* to afford a fine white powder (yield 23%), which was placed in a foil wrapped container. ^{1}H NMR ($CDCl_3$): δ 7.30 – 7.60 (m) [20H] (Ph), 6.86 (m) [2H] (*o*-$C_6\underline{H}_4$), 6.35 (m) [2H] (*o*-$C_6\underline{H}_4$), 3.92 (br) [4H] ($C\underline{H}_2$) ppm. ^{31}P {^{1}H} NMR ($CH_2Cl_2/CDCl_3$): δ 30.5 (s) ppm. IR (Nujol Mull): υ 319 m cm^{-1}. †

5.5 X-Ray Crystallography

Details of the crystallographic data collection and refinement parameters are given in Table 5.5.1. Small blue crystals of [$CoCl_2$(*o*-$C_6H_4(CH_2PPh_2)_2$)] were obtained by vapour diffusion of diethyl ether into a CH_2Cl_2 solution of the complex. Orange crystals of [Rh(*o*-$C_6H_4(CH_2PPh_2)_2)_2$]BF_4.2$CHCl_3$ were obtained by liquid diffusion of hexane into a solution of the complex in $CHCl_3$, while yellow crystals of [$PdCl_2$(*o*-$C_6H_4(CH_2PPh_2)_2$)].2CH_2Cl_2 and [Pd_2Cl_2(*o*-

$C_6H_4(CH_2PPh_2)_2)_2](PF_6)_2$ and colourless crystals of $[Ag(o\text{-}C_6H_4(CH_2PPh_2)_2)_2]BF_4.2CH_2Cl_2$ and $[Au(o\text{-}C_6H_4(CH_2PPh_2)_2)_2]PF_6.2CH_2Cl_2$ were grown by liquid diffusion of hexane into a CH_2Cl_2 solution of the appropriate complex. Data collection used a Nonius Kappa CCD diffractometer (T = 120 K) and with graphite-monochromated Mo-K_α X-radiation (λ = 0.71073 Å). Structure solution and refinement were routine.[37, 38] Selected bond lengths and angles are given in Tables 5.2.1 – 5.2.6.

† Microanalysis was not obtained due to decomposition of the complex over time in air. (decomposition occurred in transit to Strathclyde)

‡ Microanalysis was not obtained due to mixtures of products formed.

Table 5.5.1: Crystallographic Parameters (L = *o*-$C_6H_4(CH_2PPh_2)_2$)

Complex	**$[CoCl_2(L)]$**	**$[Rh(L)_2]BF_4.2CHCl_3$**	**$[PdCl_2(L)].2CH_2Cl_2$**	**$[Pd_2Cl_2(L)_2](PF_6)_2$**	**$[Ag(L)_2]BF_4.2CH_2Cl_2$**	**$[Au(L)_2]PF_6.2CH_2Cl_2$**
Formula	$C_{32}H_{28}Cl_2CoP_2$	$C_{66}H_{58}BCl_6F_4P_4Rh$	$C_{34}H_{32}Cl_6P_2Pd$	$8C_{64}H_{56}Cl_2F_{12}P_6Pd_2$	$C_{66}H_{60}AgBCl_4F_4P_4$	$C_{66}H_{60}AuCl_4F_6P_5$
M	604.31	1377.42	821.72	1522.61	1313.50	1460.76
Crystal System	monoclinic	monoclinic	Monoclinic	triclinic	triclinic	monoclinic
Space Group	$P2_1/c$	$P2_1/c$	$P2_1/m$	P-*1*	P-*1*	$P2_1/n$
a/Å	8.431(3)	12.5675(2)	10.0854(7)	9.6898(4)	11.8886(3)	11.32970(10)
b/Å	18.217(3)	24.5759(7)	17.7620(15)	13.1151(7)	14.8588(3)	24.0180(3)
c/Å	18.075(5)	20.1428(6)	10.5702(7)	13.8233(7)	14.8588(3)	22.8978(2)
α/°	90	90	90	66.043(2)	85.0570(10)	90
β/°	93.54(2)	100.595(2)	115.727(4)	86.115(3)	89.6220(10)	93.7570(10)
γ/°	90	90	90	75.645(3)	86.0290(10)	90
U/Å^3	2770.8(13)	6115.2(3)	1705.8(2)	1554.17(13)	3074.28(12)	6217.48(11)
Z	4	4	2	1	2	4
μ(Mo-Kα)/cm^{-1}	9.49	7.00	11.32	8.96	6.58	2.726
Unique Reflns	6330	13925	3756	7038	14004	14231
No. of params.	334	739	202	388	721	739
$R1$ [$I_o > 2\sigma(I_o)$]	0.0692	0.0570	0.0539	0.0512	0.0571	0.0301
$R1$ [all data]	0.1668	0.1041	0.0746	0.0751	0.0775	0.0425
wR_2 [$I_o > 2\sigma(I_o)$]	0.1174	0.1082	0.1116	0.1041	0.1393	0.0642
wR_2 [all data]	0.1464	0.1236	0.1202	0.1142	0.1527	0.0694

5.6 References

[1] See Z. Freixa, P. W. N. M. van Leeuwen, *Dalton Trans.*, 2003, 1890.

[2] R. F. Heck, D. S. Breslow, *J. Am. Chem. Soc.*, 1961, **83**, 4023.

[3] R. F. Heck, D. S. Breslow, *J. Am. Chem. Soc.*, 1962, **84**, 2499.

[4] C. P. Casey, G. T. Whiteker, M. G. Melville, L. M. Petrovich, J. A. Gavney Jr., D. R. Powell, *J. Am. Chem. Soc.*, 1992, **114**, 5535.

[5] P. W. N. M. van Leeuwen, P. C. J. Kamer, J. N. H. Reek, P. Dierkes, *Chem. Rev.*, 2000, **100**, 2741.

[6] (a) W. C. Seidel, C. A. Tolman, U.S. Pat. 3,850,973, 1973 (to Du Pont); *Chem. Abstr.* 1975, **82**, 97704.

(b) C. M. King, W. C. Seidel, C. A. Tolman, U.S. Pat. 3,925,445, 1975 (to Du Pont); *Chem. Abstr.* 1976, **84**, 88921.

(c) M. Rapport, U.S. Pat. 4,371,- 474, 1983 (to Du Pont); *Chem. Abstr.* 1983, **98**, 125452.

[7] K. Angermund, W. Bauman, E. Dinjus, R. Fornika, H. Gorls, M. Kessler, C. Kruger, W. Leitner, F. Lutz, *Chem. Eur. J.*, 1997, **3**, 755.

[8] E. Drent, J. A. M. Broekhoven, M. J. Doyle, *J. Organomet. Chem.*, 1991, **417**, 235.

[9] T. Hayashi, Y. Kawabata, T. Isoyama, I. Ogata, *Bull. Chem. Soc. Jpn.*, 1981, **54**, 673.

[10] F. Caruso, M. Camalli, H. Rimml, L. M. Venanzi, *Inorg. Chem.*, 1995, **34**, 673.

[11] H. Rimml, L. M. Venanzi, *Phosphorus Sulfur*, 1987, **30**, 297.

[12] M. Camalli, F. Caruso, S. Chaloupka, E. M. Leber, H. Rimml, L. M. Venanzi, *Helv. Chim. Acta*, 1990, **73**, 2263.

[13] M. Ebner, H. Otto, H. Werner, *Angew. Chem., Int. Ed. Engl.*, 1985, **24**, 518.

[14] L. Sacconi, J. Gelsomini, *Inorg. Chem.*, 1968, 7(2), 291.

[15] W. DeW. Horrocks Jr., G. R. van Hecke, D. DeW. Hall, *Inorg. Chem.*, 1967, **4**, 694.

[16] W. Levason, C. A. McAuliffe, *Inorg. Chim. Acta.*, 1975, **14**, 127.

[17] W. Levason, M. D. Spicer, *J. Chem. Soc., Dalton Trans.*, 1990, 719.

[18] G. Canepa, C. D. Brandt, H. Werner, *Organometallics*, **23**, 2004, 1140.

[19] M. J. Bennett, P. B. Donaldson, *Inorg. Chem.*, 1977, **16**, 655.

[20] J. A. Osborn, G. Wilkinson, *Inorg. Synth.*, 1967, **10**, 67.

[21] W. Levason, C. A. McAuliffe, *Inorg. Chim. Acta*, 1976, **16**, 167.

[22] W. Levason, C. A. McAuliffe, *J. Chem. Soc., Dalton Trans.*, 1974, 2238.

[23] W. Levason, S. D. Orchard, G.Reid, J. M. Street, *J. Chem. Soc., Dalton Trans.*, 2000, 2537.

[24] G. L. Geoffrey, M. S. Wrighton, G. S. Hammond, H. B. Gray, *J. Am. Chem. Soc.*, 1974, **96**, 3105.

[25] W. Levason, C. A. McAuliffe, *Inorg. Chim. Acta,* 1974, **11**, 33.

[26] L. R. Gray, S. J. Higgins, W. Levason, M. Webster, *J. Chem. Soc., Dalton Trans.*, 1984, 459.

[27] M. A. Fox, Pei-Wei Wang, *Inorg. Chem.*, 33, 1994, 2938.

[28] E. G. Hope, W. Levason, N. A. Powell, *Inorg. Chim. Acta,* 1986, **115**, 187.

[29] D. J. Gulliver, W. Levason, K. G. Smith, *J. Chem. Soc. Dalton Trans.*, 1981, 2153.

[30] J. R. Black, W. Levason, M. D. Spicer, M. Webster, *J. Chem. Soc., Dalton Trans.*, 1993, 3129.

[31] S. J. Berners Price, C. Brevard, A. Pagelot, P. J. Sadler, *Inorg. Chem.*, 1985, **24**, 4278.

[32] R. Uson, A. Laguna, M. Laguna, *Inorg. Synth.*, **26**, 1989, 85.

[33] S. J. Berners-Price, M. A. Mazid, P. J. Sadler, *J. Chem. Soc., Dalton Trans.*, 1984, 969.

[34] R. J. Errington, "Advanced Practical Inorganic and Metal Organic Chemistry", Blackie Academic and Professional London, 1997.

[35] G. Giordano, R. H. Crabtree, *Inorg. Synth.*, 1979, **19**, 218.

[36] J. L. Herde, J. C. Lambert, C. V. Senoff, *Inorg. Synth.*, 1974, **15**, 18.

[37] SHELXS-97, program for crystal structure solution, G. M. Sheldrick, University of Göttingen, Germany 1997.

[38] SHELXL-97, program for crystal structure refinement, G. M. Sheldrick, University of Göttingen, Germany 1997.

Chapter 6

Synthesis and Spectroscopic studies of Transition metal carbonyl complexes of $Ph_2Sb(CH_2)_3SbPh_2$ and $Me_2Sb(CH_2)_3SbMe_2$.

6.1 Introduction

The coordination chemistry of distibine ligands has received limited exploration compared to the many hundreds of papers dealing with bi- and polydentate phosphorus and arsenic ligands, and has generally been confined to soft metals in low oxidation states, for example low valent metal carbonyls (other relevant distibine studies are recorded in chapters 2, 3 and 4 of this publication).

There are two types of distibine ligands that are of interest, which are as follows; distibinoalkanes of the form $R_2Sb(CH_2)_mSbR_2$ (m = 1 or 3), and distibinobenzenes of the form o-$C_6H_4(SbR_2)_2$ (R = Me or Ph). Distibinomethanes have been found to act as mondentates or bridging ligands, but do not seem to act as chelating ligands with metal carbonyls.[1] This can be explained by the extensive ring strain in the resulting four-membered chelate ring. In contrast the distibinobenzenes tend to act as bidentate chelating ligands in direct parallel to o-$C_6H_4(CH_2PPh_2)_2$ in chapter 5.

$Me_2Sb(CH_2)_3SbMe_2$ and o-$C_6H_4(SbMe_2)_2$ react with $M(CO)_6$ (M = Cr, Mo, W) to form complexes of the form $[M(CO)_4(L\text{-}L)]$ with the appropriate bidentate distibine forming a chelating ring.[2-4] However the behaviour of ligands such as $Ph_2SbCH_2SbPh_2$ or $Me_2SbCH_2SbMe_2$ is not as straight-forward. They react with Group 6 metal carbonyls complexes, resulting in a variety of different products which are dependent on the conditions of the reaction. For example complexes of the type $[M(CO)_5\{\eta^1\text{-}Ph_2SbCH_2SbPh_2\}]$ (M = W, Mo) can be prepared by reacting $[Et_4N][M(CO)_5Br]$ with the ligand in a 1:1 ratio, or by a photolysis route.[5] However, when $[Et_4N][Cr(CO)_5Br]$ is reacted with $Ph_2SbCH_2SbPh_2$, a mixture of $[Cr(CO)_5\{\eta^1\text{-}Ph_2SbCH_2SbPh_2\}]$ and $[Cr_2(CO)_{10}\{\mu\text{-}Ph_2SbCH_2SbPh_2\}]$ is formed. This suggests that the coordination of one stibine group acts to reduce the reactivity of the second, but it can also be argued that steric effects may play an important role.

A detailed study of Group 6 carbonyls with $Ph_2SbCH_2SbPh_2$ has been reported which investigated four types of complex; $[M(CO)_5(\eta^1\text{-}L\text{-}L)]$, $[(CO)_5M(\mu\text{-}L\text{-}L)M(CO)_5]$, *cis*-$[(CO)_4M(\mu\text{-}L\text{-}L)_2M(CO)_4]$ and *fac*-$[M(CO)_3(\eta^1\text{-}L\text{-}L)_3]$ (where M = W, Mo, Cr and L-L = $Ph_2SbCH_2SbPh_2$).[5] Fig 6.1.1 shows the reaction schemes summarising the synthesis of these complexes and Fig 6.1.2 shows a representative crystal structure of *cis*-$[(CO)_4M(\mu\text{-}L\text{-}L)_2M(CO)_4]$.[5]

Fig 6.1.1: Reaction schemes involving $Ph_2SbCH_2SbPh_2$ and Group 6 carbonyls.[5]

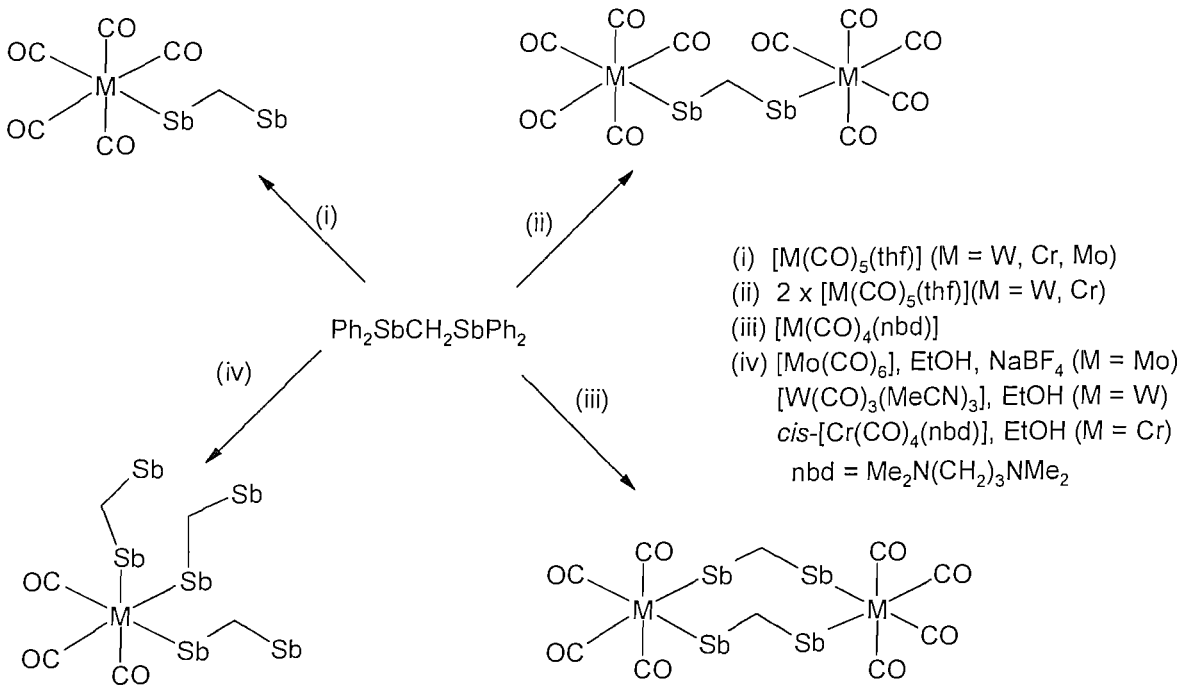

Fig 6.1.2: Crystal structure of *cis*-$[(CO)_4W(Ph_2SbCH_2SbPh_2)W(CO)_4]$.[5]

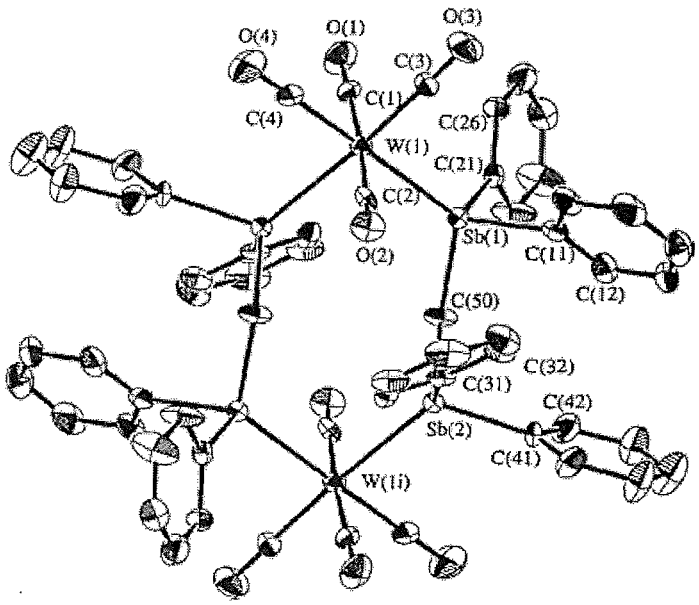

Similar reactions with $Me_2SbCH_2SbMe_2$ have been carried out, [5] however the pyrophoric nature of the ligand made it difficult to isolate pure samples of the complexes that involved η^1-$Me_2SbCH_2SbMe_2$, as they were very unstable. This was due to the strong donor properties and the air sensitivity of the free $SbMe_2$ fragment.[5]

Other research that has been carried out involving metal carbonyls and ligands such as $Ph_2SbCH_2SbPh_2$ and $Me_2SbCH_2SbMe_2$, involves reacting $[Mn_2(CO)_{10}]$ in the presence of $[\{(Cp)Fe(CO)_2\}_2]$ to form complexes of the type $[Mn_2(CO)_8(L\text{-}L)]$ (L-L = $Ph_2SbCH_2SbPh_2$, $Me_2SbCH_2SbMe_2$).[6] A photolysis method was also successful in producing $[Mn_2(CO)_6(Ph_2SbCH_2SbPh_2)_2]$.[7] $[Fe(CO)_4\{\eta^1\text{-}Ph_2SbCH_2SbPh_2\}]$ is prepared in good yield from $[Fe_2(CO)_9]$ in thf, and the X-ray structure of the complex shows that the iron metal centre is in a trigonal bipyramidal geometry, with the antimony atom occupying an axial site.

Reaction of metal carbonyls and *o*-$C_6H_4(CH_2SbMe_2)_2$ and related compounds have been researched recently by Levason *et al.*[8] For example, the ligands *o*-$C_6H_4(CH_2SbMe_2)_2$, 1,3-$C_6H_4(CH_2SbMe_2)_2$ and 1,4-$C_6H_4(CH_2SbMe_2)_2$ have been fully characterised and complexed with tungsten, iron and nickel metal centres. The generic synthesis for these ligands is shown in Chapter 2 of this Thesis. Levason and co-workers have isolated compounds including $[Ni(CO)_2(o\text{-}C_6H_4(CH_2SbMe_2)_2)]$, $[W(CO)_4(o\text{-}C_6H_4(CH_2SbMe_2)_2)]$ and $[\{Fe(CO)_4\}_2(o\text{-}C_6H_4(CH_2SbMe_2)_2)]$[8]. They developed high yielding, clean, convenient, syntheses for new distibine ligands with xylyl and phenylene backbones. The reactions used to establish the Me-Sb-C linkage, are of great interest and significance in stibine chemistry as they advance the understanding of the systems.[8] The metal carbonyl complexes that the above research obtained showed that the 1,3-$C_6H_4(CH_2SbMe_2)_2$ and 1,4-$C_6H_4(CH_2SbMe_2)_2$ ligands exhibit monodentate and bridging, bidentate coordination modes, while *o*-$C_6H_4(CH_2SbMe_2)_2$ has produced both bridging, bidentate and 7-membered chelate ring complexes. Research in Chapter 2 also shows that the wide angle distibine $\{CH_2(o\text{-}C_6H_4CH_2SbMe_2)\}_2$ binds to selected transition metals in an unprecedented 11-membered *cis*-chelate.

In this Chapter the coordination chemistry of $Ph_2Sb(CH_2)_3SbPh_2$ and $Me_2Sb(CH_2)_3SbMe_2$ will be investigated with transition metal carbonyl complexes, including $[Cr(CO)_6]$, $[Cr(CO)_4(C_7H_8)]$, $[Mo(CO)_4(C_7H_8)]$, $[W(CO)_4(piperidine)_2]$, $[Fe_2(CO)_9]$, $[Co_2(CO)_8]$, $[Mn_2(CO)_{10}]$ and $[Ni(CO)_4]$ in order to probe the electronic properties of the ligands with a view to comparing the bonding properties of these ligands against other literature examples and other analogous phosphines.

6.2 Results and Discussion

6.2.1. Ligand Synthesis

$Ph_2Sb(CH_2)_3SbPh_2$ was prepared as an air stable white solid in moderate yield (44%), from the reaction of $SbPh_3$, 2 molar equivalents of Na, and $Br(CH_2)_3Br$ in liquid ammonia. $Ph_2Sb(CH_2)_3SbPh_2$ is a versatile ligand, as it can be handled in air, and therefore is an ideal ligand to study first. The analogous ligand $Me_2Sb(CH_2)_3SbMe_2$ was successfully synthesised by preparing Me_3SbBr_2 from $SbCl_3$ and three equivalents of MeMgI, then brominating the resulting Me_3Sb. The Me_3SbBr_2, an air stable white solid was then reacted with 4 molar equivalents of Na in liquid ammonia, and the resulting Me_2Sb^- Na^+ was reacted with 1,3-dibromopropane to afford the air sensitive yellow oil (yield 50 %) with no need to distill. The ligand was found to have a density of 1.90 g cm^{-1} and by ^1H NMR spectroscopy the oil was pure with resonances at 1.70 (q) [2H] (CH_2), 1.40 (t) [4H] (CH_2), 0.65 (s) [12H] (CH_3) ppm. The $^{13}C\{^1H\}$ NMR spectrum also gave resonances at 24.45 (s) (central CH_2), 19.60 (s) (CH_2Sb), -5.00 (s) (CH_3) ppm. Both ligands were prepared in order to probe their coordination and ligating properties with the purpose of further understanding the underlying chemistry. They are direct analogues, differing only in the R groups attached to the antimony.

6.2.2. Complexes of W, Mo and Cr

$[W(CO)_4(Ph_2Sb(CH_2)_3SbPh_2)]$ was prepared in poor yield from $[W(CO)_4(piperidine)_2]$ and one molar equivalent of $Ph_2Sb(CH_2)_3SbPh_2$, in ethanol. The microanalytical data suggests that the desired product was formed with a molecule of CH_2Cl_2 associated. This assumption was further supported by the observation of dichloromethane in the ^1H NMR at 5.3 ppm. APCI+ mass spectrometry suggested that the desired product was formed, due to the highest mass isotope pattern corresponding to the parent ion, while the infra red spectrum showed four clear carbonyl bands at υ 2015(s), 1916(sh), 1902(vs), 1882(sh) cm^{-1}. This corresponds to symmetry rules, (Theory C_s: 3A' + A''), indicative of a *cis*-chelating ligand and a distorted octahedral complex, as shown in Figure 6.2.1.

Fig 6.2.1: $[M(CO)_4(Ph_2Sb(CH_2)_3SbPh_2)]$ proposed structure with C_s symmetry.

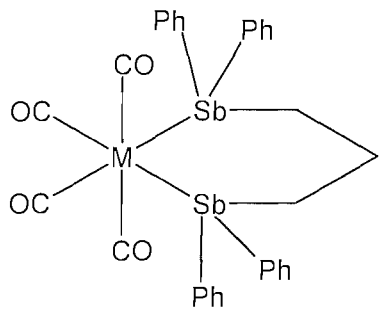

Where M = W, Cr, Mo

The analogous tungsten complex incorporating $Me_2Sb(CH_2)_3SbMe_2$ was prepared in a similar way to the above, in ethanol, with one molar equivalent of $[W(CO)_4(piperidine)_2]$ and $Me_2Sb(CH_2)_3SbMe_2$. The resultant pale yellow solid was isolated in moderate yield (37 %). From the analytical data it can be seen that the desired product was synthesised. For example the ^1H NMR, carried out in CD_2Cl_2 due to its poor solubility in $CDCl_3$, suggested that the ligand was coordinated to the metal centre by resonances indicative of $Me_2Sb(CH_2)_3SbMe_2$, shifted to higher frequency due to coordination. The $^{13}C\{^1H\}$ NMR was carried out in dmso/d^6-dmso also due to the low solubility of the complex, and showed resonances at -1.9 ($\underline{C}H_3$), 16.6 ($\underline{C}H_2Sb$), 24.4 ($CH_2\underline{C}H_2$), 203.5 CO ($^1J_{WC}$ = 120Hz), 208.2 CO ($^1J_{WC}$ = 165Hz). APCI+ mass spectrometry, showed mass peaks at *m/z* 569, 557, 543 and 528 which correspond to $[W(CO)_2(MeSb(CH_2)_3SbMe_2)]^+$, $[W(CO)(Me_2Sb(CH_2)_3SbMe_2)]^+$, $[W(CO)(MeSb(CH_2)_3SbMe_2)]^+$, and $[W(Me_2Sb(CH_2)_3SbMe_2)]^+$ respectively. Although in this instance there is no higher mass peaks corresponding to the parent ion, the result indicates that the complex is easily fragmented with dissociation of CO. The last analytical technique employed was infra-red spectroscopy. A solution infra-red spectrum in CH_2Cl_2 and a nujol mull of the product were carried out and three bands in the carbonyl region of the spectrum were recorded, in both cases. However, one of the three bands was very broad, and so it could be suggested that the fourth band is hidden under the broad bands, and thus would correspond to the theoretical values, the C_s point group, and infra red active symmetry operations, (C_s: 3A' + A''). $[W(CO)_4(Ph_2Sb(CH_2)_3SbPh_2)]$ and

$[W(CO_4)(Me_2Sb(CH_2)_3SbMe_2)]$ agree with previously reported tungsten complexes such as $[W(CO)_4(SbPh_3)_2]$.[9,10]

The preparation of $[Cr(CO)_4(Ph_2Sb(CH_2)_3SbPh_2)]$ proved to be solvent dependent, as initial attempts using $[Cr(CO)_4(C_7H_8)]$ in ethanol or methylcyclohexane, and $[Cr(CO)_6]$ in ethanol produced pale yellow solids in very small quantities and on analysis by infra-red spectroscopy no carbonyl bands were observed. It can be suggested that the methods resulted in air sensitive complexes, which decomposed during recrystallisation. After further attempts two methods were executed in moderate yield. $[Cr(CO)_6]$ and $Ph_2Sb(CH_2)_3SbPh_2$ in ethanol with $NaBH_4$ as a catalyst gave a yellow/green waxy solid. The second method was a variation of the failed attempt above using equal molar equivalents of $[Cr(CO)_4(C_7H_8)]$[11] and $Ph_2Sb(CH_2)_3SbPh_2$ in methylcyclohexane. The high yielding pale green solid that resulted from the reaction after stirring under nitrogen and heating, was identified by microanalysis. The $^{13}C\{^1H\}$ NMR spectrum showed the presence of carbonyl resonances with signals at 228.9 and 222.9 ppm, which was further supported by solution infra-red bands at 2004 s, 1911 s, 1895 s (CO stretches) cm^{-1}. (Theory: C_s as above). The infra-red nujol mull showed similar bands, suggesting that the compound was the same geometry in the solution and solid state. The presence of coordinated ligand was proved by the ^1H NMR spectrum, and APCI mass spectrometry and showed the presence of chromium and coordinated ligand at *m/z* 646.4 ($[Cr(Ph_2Sb(CH_2)_3SbPh_2)]^+$). The analogous complex $[Cr(CO)_4(Me_2Sb(CH_2)_3SbMe_2)]$ was prepared in ethanol, with equal molar equivalents of $[Cr(CO)_4(C_7H_8)]$ and $Me_2Sb(CH_2)_3SbMe_2$. After stirring overnight, and refluxing, recrystallisation from CH_2Cl_2 and hexane afforded the pale green solid. Analytical data are consistent with the solid being the desired product. The nujol mull infra-red spectrum is consistent with C_s symmetry, with four IR active bands. The solution infra-red spectrum also had four bands in the carbonyl region. The APCI+ mass spectrometry follows the trend of the tungsten compounds above, whereby the CO's dissociate in the column, however a parent ion peak is observed at *m/z* 509 $[Cr(CO)_4(Me_2Sb(CH_2)_3SbMe_2)]^+$. There is also a mass peak at *m/z* 481 corresponding to $(P\text{-}CO)^+$. The ^1H NMR and $^{13}C\{^1H\}$ NMR spectra also suggest coordinated ligand as described for the chromium complex above.

$[Mo(CO)_4(Ph_2Sb(CH_2)_3SbPh_2)]$ was prepared from $[Mo(CO)_4(C_7H_8)]$ and one molar equivalent of $Ph_2Sb(CH_2)_3SbPh_2$, in methylcyclohexane. The work up procedure was as with the analogous chromium complex. The resulting pale yellow solid was isolated in good yield (81 %) and the microanalytical results confirmed the purity. The ^1H NMR spectrum showed resonances

indicative of coordinated ligand, and the $^{13}C\{^{1}H\}$ NMR spectrum showed two carbonyl environments indicative of such complexes at 211.0 and 215.6 ppm.[5] The ^{95}Mo NMR spectrum suggested that there was one molybdenum containing species with one peak at -1849 ppm, as seen with other such compounds.[5] It was confirmed that the product was not $[Mo(CO)_6]$ as the ^{95}Mo NMR resonance for this is -2325 ppm.[5] The other analytical techniques used were APCI+ mass spectroscopy, whereby clusters of mass peaks were present for the complex, following dissociation of COs, as was seen in above complexes. There was however no parent ion, but peaks at *m/z* 746, 718 and 690 corresponding to $[Mo(CO)_2(Ph_2Sb(CH_2)_3SbPh_2)]^+$, $[Mo(CO)(Ph_2Sb(CH_2)_3SbPh_2)]^+$ and $[Mo(Ph_2Sb(CH_2)_3SbPh_2)]^+$ respectively, were seen. The infra-red spectrum of the complex also supported the other characterisation techniques as both solution and solid infra-reds spectra confirmed the C_s point group with four bands in the carbonyl region. The analogous molybdenum complex to the one above, $[Mo(CO)_4(Me_2Sb(CH_2)_3SbMe_2)]$ was prepared in ethanol, with one molar equivalent of $Me_2Sb(CH_2)_3SbMe_2$, after stirring overnight and then refluxing, the yellow solution was reduced to dryness. The pale brown solid was recrystallised from CH_2Cl_2 and hexane, in very low yield. Analytical techniques such as $^{13}C\{^{1}H\}$ NMR spectrum showed coordinated ligand was present along with the correct number of carbonyl environments. ^{95}Mo NMR spectroscopy also proved that there was one molybdenum environment with a resonance at -1843 ppm, which is similar to the analogous $Ph_2Sb(CH_2)_3SbPh_2$ complex. The solution infra-red spectrum showed three bands in the carbonyl region of the spectrum, but one of these was very broad, thus a fourth band could have been overlapped. Indeed the solid infra-red spectrum showed four bands in the carbonyl region of the spectrum, indicative of the correct C_s symmetry. Table 6.2.1 shows the IR and $^{13}C\{^{1}H\}$ NMR data for the above 6 complexes compared with literature examples.

Table 6.2.1: IR and ^{13}C $\{^1H\}$ NMR spectroscopic data for complexes with W, Mo and Cr metal centres.

Complex	CO chemical shift ppm	υ (CO) /cm^{-1}	Ref
$[W(CO)_4(Ph_2Sb(CH_2)_3SbPh_2)]$	201.5 (116)[a], 205.1 (165)[a]	2012(s), 1920(sh), 1900(vs), 1869(s).	
$[W(CO)_4(Me_2Sb(CH_2)_3SbMe_2)]$	203.5 (120)[a], 208.2 (165)[a]	2009(s), 1886(vs, br),1869(sh).	
$[W(CO)_4(Ph_2P(CH_2)_3PPh_2)]$	203.2, 206.0	2016, 1923, 1901, 1888 (Toluene)	12
$[W(CO)_5(Ph_2SbCH_2SbPh_2)]$	196.7 (126)[a], 199.0 (162)[a]	2066(m), 1983(m), 1918(s)	5
$[W(CO)_4(o\text{-}C_6H_4(CH_2SbMe_2)_2)]$	201.7, (126)[a], 206.1 (160)[a]	2012(vs), 1935(sh), 1901(vs), 1873(sh)	8
$[Cr(CO)_4(Ph_2Sb(CH_2)_3SbPh_2)]$	222.8, 228.9	2000(s), 1916(m), 1897(s), 1865(s).	
$[Cr(CO)_4(Me_2Sb(CH_2)_3SbMe_2)]$	223.7, 229.	1993(s), 1903(sh), 1888(vs,br), 1862(sh).	
$[Cr(CO)_4(Ph_2P(CH_2)_3PPh_2)]$	222.0, 226.9	2015, 1935, 1907, 1890 (Toluene)	12
$[Cr(CO)_5(Ph_2SbCH_2SbPh_2)]$	217.6, 223.0	2056(m), 1982(m), 1922(s)	5
$[Mo(CO)_4(Ph_2Sb(CH_2)_3SbPh_2)]$	211.0, 215.6	2015(s), 1928(m), 1906(vs), 1872(s).	
$[Mo(CO)_4(Me_2Sb(CH_2)_3SbMe_2)]$	213.0, 218.4	2013(m), 1946(sh), 1894(vs,br) 1866(sh).	
$[Mo(CO)_4(Ph_2P(CH_2)_3PPh_2)]$	208.6, 213.2	2015, 1930, 1883 (Toluene)	12
$[Mo(CO)_5(Ph_2SbCH_2SbPh_2)]$	206.5, 210.5	2068(m), 1991(m), 1935(s)	5

a = $^1J_{WC}$ Hz ($^{183}W - ^{13}C$), all above IR data is from Nujol mulls unless stated.

6.2.3. Complexes of Co, and Mn

The substitution chemistry of $[Co_2(CO)_8]$ with bidentate Group 15 ligands is complicated, with a variety of stoichiometries observed depending on the ligand being used, leading to several isomers being identified.[1,13] For many of these Group 15 ligands, the ionic $[Co(CO)_3(L\text{-}L)][Co(CO)_4]_2$ complexes form first and then transform to neutral dimers of the form $[Co_2(CO)_6(L\text{-}L)]$ on warming in solution. In other cases this further transformation does not take place and the $[Co(CO)_3(L\text{-}L)][Co(CO)_4]_2$ species is obtained.[13]

The reaction of $[Co_2(CO)_8]$ and $Ph_2Sb(CH_2)_3SbPh_2$ in toluene, afforded a rather unstable red-brown solid in good yield, which decomposed in solution after a few hours, and in the solid state decomposed more slowly (1-2 days). Microanalysis suggested that the solid had a composition corresponding to $[Co_2(CO)_6(Ph_2Sb(CH_2)_3SbPh_2)]$, however it was very poorly soluble in chlorocarbon or hydrocarbon solvents which hindered the spectroscopic studies. Indeed, due to this fact we were prevented from obtaining $^{13}C\{^1H\}$ or ^{59}Co NMR spectroscopic data. However, the solution infra-red spectrum suggested the desired product, with carbonyl bands at 2055 s, 1970 s cm^{-1}. A nujol mull infra-red spectrum of the product also reinforced this by similar bands at 2033 m, 1976 s cm^{-1}. There was a significant absence of bridging carbonyl bands in both media,

which have been observed in previous work on complexes of the form $[Co_2(CO)_6(R_2SbCH_2SbR_2)]$.[1] Comparison of the pattern in the carbonyl region of the IR spectrum with extensive work carried out by Thornhill and Manning,[13] for cobalt carbonyl diphosphine and diarsine complexes has led to a tentative structural formulation as an oligo- or poly-meric $[\{Co(CO)_3(Ph_2Sb(CH_2)_3SbPh_2)Co(CO)_3\}_n]$ with unbridged $Co_2(CO)_6$ units linked by bridging distibine into oligomers. Further stirring or heating of this compound with more $Ph_2Sb(CH_2)_3SbPh_2$ resulted in substantial decomposition, indeed complete loss of CO bands in the IR spectrum.

The reaction of $Me_2Sb(CH_2)_3SbMe_2$ with $[Co_2(CO)_8]$, was not as straight forward as first expected. It was assumed that due to the reactivity of the $Me_2Sb(CH_2)_3SbMe_2$ ligand, the reaction would proceed faster, but after reacting one molar equivalent of $[Co_2(CO)_8]$ with $Me_2Sb(CH_2)_3SbMe_2$ in toluene, the red brown solid was obtained and found to be subtly different. Again the solid was poorly soluble in most organic solvents. The analytical techniques, did not suggest that the analogous compound to $[\{Co(CO)_3(Ph_2Sb(CH_2)_3SbPh_2)Co(CO)_3\}_n]$ had been obtained. The infra-red spectrum did show two bands in the CO region of the spectrum, however the ^{59}Co NMR spectrum indicated the presence of the $[Co(CO)_4]^-$ anion with a resonance at -2999 ppm.[14] A resonance for a cobalt environment in a cationic species was not obtained possibly due to the peak being too broad to see. The $^{13}C\{^1H\}$ NMR spectrum also supported the evidence of the $[Co(CO)_4]^-$ anion being present with a CO peak at 195.8 ppm. The other peak at 194.4 was due to the carbonyls of the cationic species. There is only one CO peak for each due to the fluxionality of the COs in cobalt complexes of this type.[13] More evidence to suggest that the product is an ionic species is the mass spectrometry of the solid. The positive ion electrospray mass spectrometry spectrum showed peaks at 751, 777 and 803 corresponding to $[Co(Me_2Sb(CH_2)_3SbMe_2)_2]^+$, $[Co(CO)(Me_2Sb(CH_2)_3SbMe_2)_2]^+$, $[Co(CO)_2(Me_2Sb(CH_2)_3SbMe_2)_2]^+$ respectively, and the negative ion electrospray MS spectrum showed one mass peak at *m/z* 171 corresponding to the $[Co(CO)_4]^-$ anion. The ^1H NMR spectrum showed the presence of coordinated ligand, which indicates that the ligand is present in the cationic species, however all the analysis above is not sufficient to propose a certain structure for the product.

$[Mn_2(CO)_8(Ph_2Sb(CH_2)_3SbPh_2)]$ was prepared using two different approaches, a chemical procedure and photolysis. In the chemical synthesis, $[Mn_2(CO)_{10}]$ was dissolved in toluene with one equivalent of $Ph_2Sb(CH_2)_3SbPh_2$ and 0.2 equivalents of $[\{(Cp)Fe(CO)_2\}_2]$. After refluxing for 24 hours and work up the brown solid was recovered in high yield. The photolysis of $[Mn_2(CO)_{10}]$

and $Ph_2Sb(CH_2)_3SbPh_2$ in toluene over 12 hours, afforded the same compound, as proved by all analytical techniques, but there was significant decomposition *via* this route. Other such manganese carbonyl complexes have been researched previously and provide comparative geometries and structures.[7,15,16] Microanalysis proved the purity and the infra-red spectroscopy data suggests carbonyl bands at 2055 s, 2034 w, 1977 vbr s, 1966 sh, 1953 s sh, 1914 sh cm^{-1} in both mull and solution infra red. These CO bands rule out the diaxial formulation (1 strong CO band) of the structure, but are similar to the equatorial, equatorial pattern reported for $[Mn_2(CO)_8$(distibinomethane)], although the longer backbone of $Ph_2Sb(CH_2)_3SbPh_2$ could result in further significant twisting of the Mn units away from the eclipsed geometry, and this is shown in Fig. 6.2.2. The ^1H NMR spectrum, although having broad peaks shows coordination of the ligand and the $^{13}C\{^1H\}$ NMR spectrum indicates the desired product by resonances at around 217.9 (s, CO), 217.2 (s, CO), 214.5 (s, CO) ppm for both techniques, although these partially overlap and are broadened by the ^{55}Mn quadrupole which makes the number of resonances uncertain. The $^{13}C\{^1H\}$ NMR spectrum also showed two methylene environments in the propane backbone, shifted from free ligand, indicating that both Sb atoms were coordinated to a manganese metal centre.

Fig 6.2.2: Possible structure of $[Mn_2(CO)_8(Ph_2Sb(CH_2)_3SbPh_2)]$

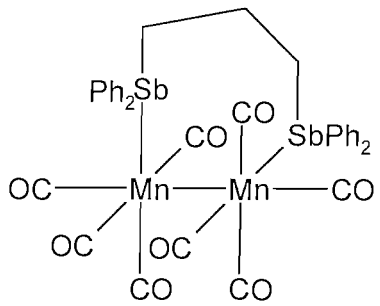

6.2.4. Complexes of Fe

$[Fe(CO_4)(Ph_2Sb(CH_2)_3SbPh_2)]$, a red brown oil, was prepared from a 1:1 ratio of $[Fe(CO)_9]$ and $Ph_2Sb(CH_2)_3SbPh_2$ in thf. The ^1H NMR spectrum shows the presence of coordinated ligand with resonances at 1.8-2.0 (m), 7.1-7.6 (m) ppm, and the $^{13}C\{^1H\}$ NMR spectrum provides further evidence for this along with a carbonyl resonance at 213.3 ppm, however two were expected. This

can be explained by fluxionality of the carbonyls at the metal centre. The three carbonyl bands in the solution IR spectrum are consistent with an axially substituted trigonal bypyramid local geometry (theory C_{3v}: $2A_1 + E$), but the solid IR spectrum is not consistent. There is however, a very broad band in the carbonyl region of the solid IR spectrum (1913 vbr) which could suggest that two of the stretching modes have overlapped. The data acquired can be compared to similar iron complexes from literature. (see Table 6.2.2). Further evidence that the desired product has been achieved is shown in the APCI+ mass spectroscopy. A mass peak at *m/z* 763 corresponds to the parent ion. The second complex synthesised from $Ph_2Sb(CH_2)_3SbPh_2$ and iron as the metal centre, was $[\{Fe(CO)_4\}_2(Ph_2Sb(CH_2)_3SbPh_2)]$. The proposed structure for this complex is shown in Fig 6.2.3. The red brown oil, was prepared from a 1:2 ratio of $Ph_2Sb(CH_2)_3SbPh_2$ to $[Fe(CO)_9]$ in thf. The IR data collected on the oil, shows very good correlation with literature data on similar iron complexes (see Table 6.2.2). The carbonyl resonances in the $^{13}C\{^1H\}$ NMR spectra compare well with the above iron complex and show one resonance, due to the fluxionality described above and can be seen in the literature and Table 6.2.2 below. The APCI+ mass spectrometry showed the major mass peak at *m/z* 762, corresponding to $[Fe(CO)_4(Ph_2Sb(CH_2)_3SbPh_2)]^+$. This was not unexpected however, due to the weakness of the C–Sb bonds, and fragmentation could have occurred in the mass spectrometer.

The third iron complex to be synthesised using $[Fe_2(CO)_9]$ was $[\{Fe(CO)_4\}_2(Me_2Sb(CH_2)_3SbMe_2)]$, prepared from a 2:1 ratio of $[Fe_2(CO)_9]$ and $Me_2Sb(CH_2)_3SbMe_2$ in thf, in a 50 % yield. The resulting dark red oil, was examined by $^{13}C\{^1H\}$ NMR spectroscopy. Resonances were seen that corresponded to the coordinated ligand, and one carbonyl resonance. The infra-red spectra (solution in CH_2Cl_2, and solid as a nujol mull) showed four IR bands in the carbonyl region, which do not corresponds with the theory, (C_3v: $2A_1 + E$) for local symmetry. However this can be explained by the fact that there are minor impurities in the product as indicated by the ^1H NMR data as complex multiplets. Comparisons of the compounds made and literature examples can be seen in Table 6.2.2. As the complex was an oil, microanalysis was not carried out, but from the data it can be suggested that the complex's structure incorporates the $Me_2Sb(CH_2)_3SbMe_2$ ligand bridging the two iron metal centres. The proposed structure is shown in Fig. 6.2.3.

Fig. 6.2.3: Proposed structure of $[\{Fe(CO)_4\}_2(Ph_2Sb(CH_2)_3SbPh_2)]$ and $[\{Fe(CO)_4\}_2(Me_2Sb(CH_2)_3SbMe_2)]$.

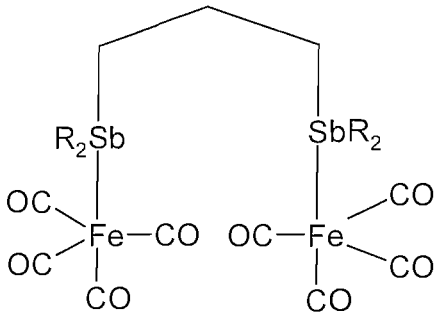

The above structure is proposed as the data collected for these complexes correlates closely with the literature data, which have similar structures. Such compounds are shown in Table 6.2.2 below.

Table 6.2.2: Selected IR and ^{13}C $\{^1H\}$ NMR data of complexes with Fe metal centres.

Complex	CO δ /ppm	υ (CO) /cm^{-1}	Ref
$[Fe(CO)_4(Ph_2Sb(CH_2)_3SbPh_2)]$	213.3	2041 s, 1913 vbr	
$[\{Fe(CO)_4\}_2(Ph_2Sb(CH_2)_3SbPh_2)]$	213.2	2041 s, 2060 sh, 1913 vbr	
$[\{Fe(CO)_4\}_2(Me_2Sb(CH_2)_3SbMe_2)]$	213.6	2042 m, 1965 m, 1932 s,br, 1914 sh	
$[Fe(CO)_4(Ph_2SbCH_2SbPh_2)]$		2043 m, 1970 w, 1940 s, 1933 m	15
$[Fe(CO)_4(1,4\text{-}C_6H_4(SbMe_2)_2)]$		2043 s, 1966 m, 1933 s (CH_2Cl_2)	8
$[\{Fe(CO)_4\}_2(Me_2SbCH_2SbMe_2)]$	213.6	2038 s, 1961 s, 1928 s	15
$[\{Fe(CO)_4\}_2(1,2\text{-}C_6H_4(CH_2SbMe_2)_2)]$	213.3	2033, 1964, 1935	8
$[\{Fe(CO)_4\}_2(1,3\text{-}C_6H_4(CH_2SbMe_2)_2)]$	213.3	2043, 1959, 1938	8
$[\{Fe(CO)_4\}_2(1,4\text{-}C_6H_4(CH_2SbMe_2)_2)]$	213.4	2041, 1965, 1932	8

6.2.5. Complexes of Ni

As with other nickel carbonyl complexes that incorporate distibine ligands,[6,8] the products from the reaction of $[Ni(CO)_4]$ and $Ph_2Sb(CH_2)_3SbPh_2$, and $[Ni(CO)_4]$ and $Me_2Sb(CH_2)_3SbMe_2$ were unstable and decomposed significantly in a few hours at room temperature with the deposition of black solids. Despite this however, spectroscopic data were obtained so that correlation of the electronic properties of these complexes and literature examples could be achieved. The reaction of $[Ni(CO)_4]$ and $Me_2Sb(CH_2)_3SbMe_2$ in CH_2Cl_2 proceeded with the visible evolution of carbon monoxide, and the colourless waxy solid that resulted after removing the CH_2Cl_2, was found to contain one species. The waxy solid was proved to be $[(CO)_3Ni\{\mu\text{-}Me_2Sb(CH_2)_3SbMe_2\}Ni(CO)_3]$ by the characteristic CO resonance at 197.1 ppm in the $^{13}C\{^1H\}$ NMR spectrum and the two IR active carbonyl stretches at 2067 s and 1991 vs in the IR spectrum (Local symmetry:C_{3v} : $A_1 + E$). The presence of one Me resonance and two methylene resonances in the ^1H and $^{13}C\{^1H\}$ NMR spectra confirm that the complex incorporates bidentate coordination of the distibine ligand. The reaction was repeated with a deficit of $[Ni(CO)_4]$, and the product was found to be a mixture of the tricarbonyl and a dicarbonyl nickel species. However, none of the frequencies of the three Me and five methylene resonances in the ^1H or $^{13}C\{^1H\}$ NMR spectra corresponded to $[(CO)_3Ni\{\mu\text{-}Me_2Sb(CH_2)_3SbMe_2\}Ni(CO)_3]$ or free ligand. From this and other literature data which can be seen in Table 6.2.3, we tentatively formulate the tricarbonyl as $[(CO)_3Ni\{\eta^1\text{-}Me_2Sb(CH_2)_3SbMe_2\}]$ and the dicarbonyl as $[Ni(CO)_2\{Me_2Sb(CH_2)_3SbMe_2\}]$, with the latter containing a chelating distibine ligand. Attempts were made to convert the mixture to the dicarbonyl species, with heating or prolonged stirring, but unfortunately these failed with substantial decomposition of the products being the only outcome.

From an excess of $[Ni(CO)_4]$ and $Ph_2Sb(CH_2)_3SbPh_2$ in a CH_2Cl_2 solution an inseparable mixture was obtained. The reaction was a lot slower than that of the $Me_2Sb(CH_2)_3SbMe_2$ ligand with $[Ni(CO)_4]$, and after a few hours stirring at room temperature, *in situ* infra-red spectroscopy studies showed a mixture of tricarbonyl and dicarbonyl complexes, with unchanged $[Ni(CO)_4]$ also present. The solution darkened over time, indicating the instability of the complexes, but some spectroscopic data was obtained. The yellow oil was analysed via ^1H NMR spectroscopy, $^{13}C\{^1H\}$ NMR spectroscopy and infra-red spectroscopy. The $^{13}C\{^1H\}$ NMR spectrum showed the presence of four major CH_2 resonances, suggesting two different ligand environments around the metal centre. Therefore, the tentative formulations for the major products are $[\{Ni(CO)_3\}_2\{\mu\text{-}Ph_2Sb(CH_2)_3SbPh_2\}]$ and $[Ni(CO)_2(Ph_2Sb(CH_2)_3SbPh_2)]$. Comparisons between these complexes reported here and other literature compounds can be seen in Table 6.2.3.

Table 6.2.3: Spectroscopic data for $[Ni(CO)_3(L)]$ or $[(CO)_3Ni(L)Ni(CO)_3]$

Ligand	ν (CO) (cm^{-1})[a]	^{13}C (δ CO)(ppm)[a]	Ref
[Ni(CO)$_3$(L)]			
$Ph_2Sb(CH_2)_3SbPh_2$	2071, 1996	196.8	b
$Me_2Sb(CH_2)_3SbMe_2$	2067, 1989	197.1	b
m-$C_6H_4(CH_2SbMe_2)_2$	2068, 1993	197.0	8
p- $C_6H_4(CH_2SbMe_2)_2$	2068, 1993	197.1	8
m- $C_6H_4(SbMe_2)_2$	2070, 1995	196.9	8
$Me_2SbCH_2SbMe_2$	2067, 1994	197.1	6
$Ph_2SbCH_2SbPh_2$	2072, 2004	196.3	6
$SbEt_3$	2067, 1996	197.9	21, 22
$SbPh_3$	2074, 2004	196.5	21
[Ni(CO)$_2$(L)]			
$Ph_2Sb(CH_2)_3SbPh_2$	2005, 1947	201.8	b
$Me_2Sb(CH_2)_3SbMe_2$	1992, 1933	201.5	b
o-$C_6H_4(CH_2SbMe_2)_2$	2002, 1939	201.0	8
m- $C_6H_4(SbMe_2)_2$	2000, 1941	201.0	8

a = chlorocarbon solvents (CH_2Cl_2 and $CDCl_3$)

b = This work

Literature examples such as work carried out by Levason and coworkers recently,[6,8] suggest that such complexes form readily. This is due to the nickel carbonyl being easily substituted due to less electron density being placed into the π^* CO molecular orbital, than phosphine or arsine analogues, resulting in weaker bonds. Comparison with Tolmans extensive study [17] of the $\nu_1(A_1)$ modes in $[Ni(CO)_3L]$ (L = phosphine ligand) complexes shows the electronic properties of these two ligands are similar to trialkylphosphines.

Fig. 6.2.4 shows a summary of the reaction schemes of all the complexes synthesised in this work.

Fig 6.2.4: Syntheses of the metal carbonyl distibinopropane complexes

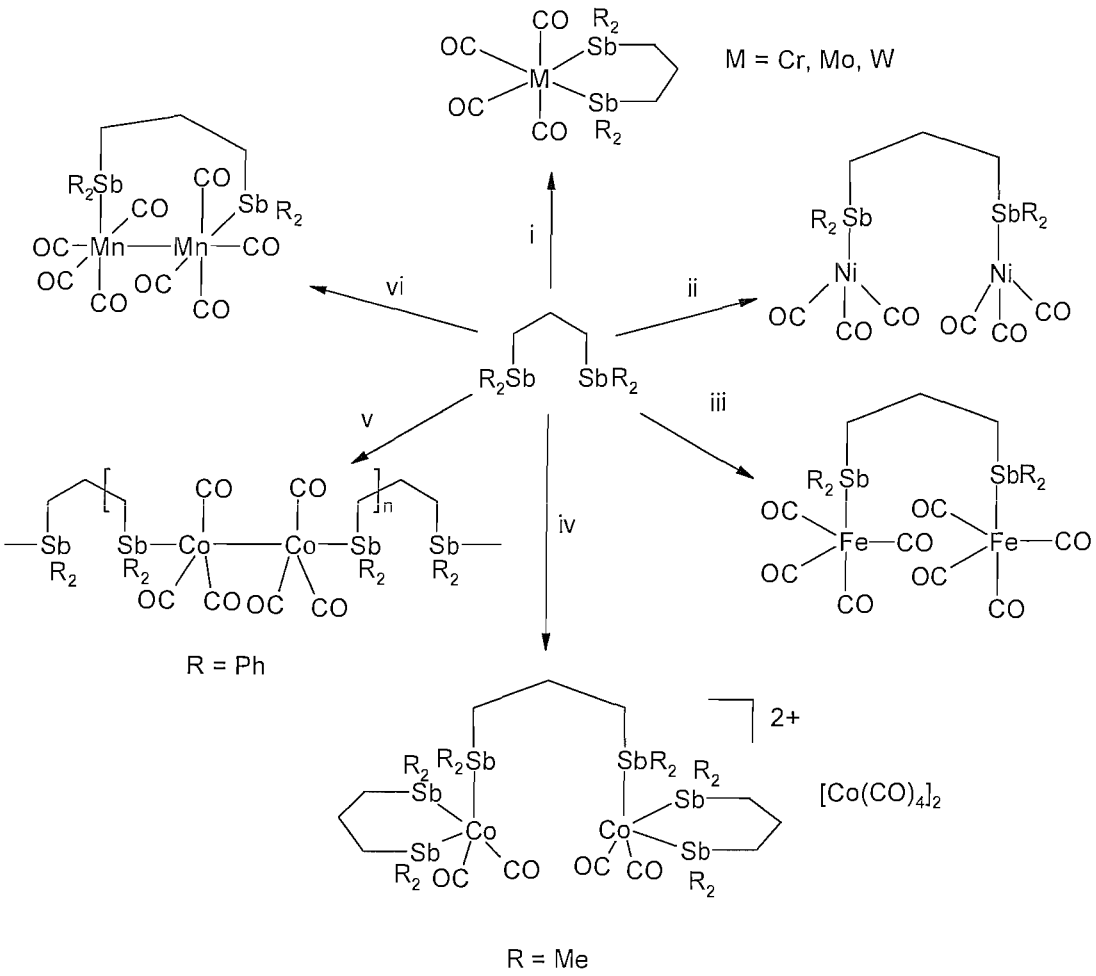

Reagents: i. $[M(CO)_4(nbd)]$ in EtOH, M = Cr, Mo or $[W(CO)_4(pip)_2]$ in EtOH; ii. $[Ni(CO)_4]$ in CH_2Cl_2; iii. $[Fe_2(CO)_9]$ in thf; iv and v. $[Co_2(CO)_8]$ in toluene; vi. $[Mn_2(CO)_{10}]$ in toluene with $[CpFe(CO)_2]_2$.

6.3 Conclusion

The coordination chemistry of the flexibile C_3 linked distibine ligands $Ph_2Sb(CH_2)_3SbPh_2$ and $Me_2Sb(CH_2)_3SbMe_2$, has been investigated with transition metal carbonyl species from Group 6, Mn, Fe, Co and Ni. The ligands were prepared by sodium/liquid ammonia synthesis, in good yield. $Ph_2Sb(CH_2)_3SbPh_2$ is an air stable white solid, and $Me_2Sb(CH_2)_3SbMe_2$ as a yellow air sensitive oil. Reactions with both ligands afforded the following products. Displacement of an olefin or amine from $[M(CO)_4(C_7H_8)]$ or $[W(CO)_4(piperidine)_2]$ resulted in complexes of the form $[M(CO)_4(L\text{-}L)]$ (M = Cr, Mo, W) (L-L = $Ph_2Sb(CH_2)_3SbPh_2$, $Me_2Sb(CH_2)_3SbMe_2$). Reactions with $[Co_2(CO)_8]$ and the appropriate ligand afforded $[Co_2(CO)_6(Ph_2Sb(CH_2)_3SbPh_2)]$ and $[Co_2(CO)_4(Me_2Sb(CH_2)_3SbMe_2)][Co(CO)_4]_2$. $[Mn_2(CO)_8(Ph_2Sb(CH_2)_3SbPh_2)]$ was prepared from $[Mn_2(CO)_{10}]$ and $Ph_2Sb(CH_2)_3SbPh_2$. A mixture of $[\{Ni(CO)_3\}_2(Ph_2Sb(CH_2)_3SbPh_2)]$ and $[Ni(CO)_2(Ph_2Sb(CH_2)_3SbPh_2)]$ was prepared by reaction of $[Ni(CO)_4]$ and $Ph_2Sb(CH_2)_3SbPh_2$, whereas $[\{Ni(CO)_3\}_2(Me_2Sb(CH_2)_3SbMe_2)]$ was the product formed by reacting $Me_2Sb(CH_2)_3SbMe_2$ with nickel tetracarbonyl. By reacting $[Fe_2(CO)_9]$ with the appropriate ligand in a 2:1 ratio (Fe:L), $[\{Fe(CO)_4\}_2(L\text{-}L)]$ (L-L = $Ph_2Sb(CH_2)_3SbPh_2$, $Me_2Sb(CH_2)_3SbMe_2$) was formed, and using a 1:1 ratio (Fe:$Ph_2Sb(CH_2)_3SbPh_2$) $[Fe(CO)_4(Ph_2Sb(CH_2)_3SbPh_2)]$ was obtained. Where possible the products were characterisied by IR, NMR (^1H, $^{13}C\{^1H\}$, ^{55}Mn and ^{59}Co as appropriate) spectroscopy, mass spectrometry and microanalysis. $Ph_2Sb(CH_2)_3SbPh_2$ and $Me_2Sb(CH_2)_3SbMe_2$ are versatile ligands, which due to their flexible propane back bone can act as chelating ligands and also as a bridging ligand, between two metal centres.

6.4 Experimental

General experimental techniques and instrumentation are described in the appendix. $[Cr(CO)_4(C_7H_8)]$[11], $[Mo(CO)_4(C_7H_8)]$[11], and $[W(CO)_4(piperidine)_2]$[19], were prepared following known literature procedures. Other metal carbonyls were obtained commercially (Aldrich or Strem) and used as received.

$Ph_2Sb(CH_2)_3SbPh_2$: Liquid ammonia (500 cm^3) was condensed using acetone/CO_2 slush, and then sodium (4.0 g, 160 mmol) was added slowly to allow it to dissolve. The deep blue solution was left to stir for 30 minutes. Ph_3Sb (28.0 g, 80 mmol) was added slowly, and then reaction was left to stir for 90 minutes. NH_4Cl (4.27 g, 80 mol) was added to destroy the MeNa biproduct, and then the reaction was stirred for 30 minutes 1,3-dibromopropane (8.08 g, 40 mmol) was added dropwise, and the reaction was stirred overnight at room temperature to evaporate the liquid ammonia. The reaction was hydrolysed with deionised degassed H_2O (100 cm^3) and the organics were extracted with diethyl ether (100 cm^3). The aqueous layer was separated and washed with diethyl ether (2 x 100 cm^3), and then the combined organics were dried over anhydrous $MgSO_4$ for 3 hrs. The combined organics were reduced to dryness, the white solid was recrystallised from ethanol. (Yield 10.34 g, 40%). ^1H NMR ($CDCl_3$): δ 1.8-2.0 (m) [6H] ($C\underline{H}_2Sb$, $C\underline{H}_2$), 7.-7.5 (m) [20H] (SbPh) ppm. $^{13}C\{^1H\}$ NMR ($CDCl_3$) 25.1 ($\underline{C}H_2Sb$), 26.5 ($\underline{C}H_2CH_2$), 128.7, 128.9, 136.0, 137.9 (aryl $\underline{C}$) ppm. All spectroscopic data are in accord with the literature.[4]

$Me_2Sb(CH_2)_3SbMe_2$: Liquid ammonia (500 cm^3) was condensed using acetone/CO_2 slush, and then sodium (5.63 g, 0.24 mol) was added slowly to allow it to dissolve. The inky black solution was left to stir for 30 minutes. Me_3SbBr_2 [20] (20 g, 0.06 mol) was added slowly, and then reaction was left to stir for 90 minutes. NH_4Cl (3.2 g, 0.06 mol) was added to destroy the MeNa biproduct, and then the reaction was stirred for 30 minutes. 1,3-dibromopropane (6.06 g, 0.03 mol) was added dropwise, and the reaction was stirred overnight at RT to evaporate the liquid ammonia. The reaction was hydrolysed with deionised degassed H_2O (100 cm^3) and the organics were extracted with diethyl ether (100 cm^3). The aqueous layer was separated and washed with diethyl ether (2 x 100 cm^3), and then the combined organics were dried over $MgSO_4$ for 3 hrs. The combined organics were reduced to dryness and the resulting yellow oil (Yield 5.2 g, 50%), dried *in vacuo*. The density of the oil was found to be 1.90 g cm^{-1}. ^1H NMR ($CDCl_3$): δ 0.65 (s) [12H] ($C\underline{H}_3$), 1.40 (t) [4H] ($C\underline{H}_2$), 1.70 (q) [2H] ($C\underline{H}_2Sb$) ppm. $^{13}C\{^1H\}$ NMR ($CDCl_3$): δ -5.0 ($\underline{C}H_3$), 19.6 ($\underline{C}H_2Sb$), 24.7 ($\underline{C}H_2CH_2$) ppm. All spectroscopic data are in accord with the literature.[4]

[$Cr(CO)_4(Ph_2Sb(CH_2)_3SbPh_2)$]

Method 1: $[Cr(CO)_6]$ (0.48g, 0.22 mmol) and $Ph_2Sb(CH_2)_3SbPh_2$ (0.125g, 0.22 mmol) were dissolved in ethanol (50 cm^3), $NaBH_4$ (0.1g) was added and the mixture was refluxed for 2hrs during which the solution turned yellow. The solvent was removed *in vacuo*, and the residue shaken up with water (20 cm^3) and CH_2Cl_2 (20 cm^3). The organic layer was separated, dried ($MgSO_4$), and evaporated to small volume to produce a yellow powder, which was filtered and dried *in vacuo*.

Method 2: $[Cr(CO)_4(C_7H_8)]$ (0.13 g, 0.5 mmol) and $Ph_2Sb(CH_2)_3SbPh_2$ (0.297 g, 0.5 mmol) were dissolved in methylcyclohexane (50 cm^3) and stirred under N_2 overnight. The solution was warmed to 50°C for 2hrs, and left to stir for 48 hrs at room temperature. The reaction was warmed to reflux for 2 hrs, cooled and reduced in volume by 50 %. A pale green precipitate was formed, which was put in the freezer overnight to crystallise. The resulting pale green solid was filtered and dried *in vacuo*. (Yield: 0.094 mg, 84%). Anal. Found: C, 48.7; H, 3.4. Calc. for $C_{31}H_{26}CrO_4Sb_2$: C, 49.1; H, 3.5%. ^1H NMR ($CDCl_3$): δ 2.0-2.2 (m) [6H] ($C\underline{H}_2Sb$, $C\underline{H}_2$), 7.1-7.6 (m) [20H] (SbPh) ppm. $^{13}C\{^1H\}$ NMR ($CH_2Cl_2/CDCl_3$): δ 20.8 ($\underline{C}H_2Sb$), 23.5 ($\underline{C}H_2CH_2$), 129.5, 130.2, 133.1, 134.8 (aryl-$\underline{C}$), 222.8, 228.9 ($\underline{C}O$) ppm. MS (APCI): *m/z* 645 $[Cr(Ph_2Sb(CH_2)_3SbPh_2)]^+$. IR ($CH_2Cl_2$) ν 2004 s, 1911 sh, 1895 vs,br cm^{-1}; IR (Nujol mull) ν 2000 s, 1916 m, 1897 s, 1865 s cm^{-1}.

[$Mo(CO)_4(Ph_2Sb(CH_2)_3SbPh_2)$]: $[Mo(CO)_4(C_7H_8)]$ (0.15g, 0.5 mmol) and $Ph_2Sb(CH_2)_3SbPh_2$ (0.3g, 0.5 mmol) were dissolved in methylcyclohexane (50 cm^3) and the mixture stirred overnight. The solution was filtered, and the filtrate evaporated under reduced pressure to produce a pale yellow solid which was dried *in vacuo*. (Yield 0.33g, 81%). Anal. Found: C, 47.0; H, 3.1. Calc. for $C_{31}H_{26}MoO_4Sb_2$: C, 46.4; H, 3.3%. ^1H NMR ($CDCl_3$): δ 2.0-2.2 (m) [6H] ($C\underline{H}_2Sb$, $C\underline{H}_2$), 7.1-7.7(m) [20H], (SbPh) ppm. $^{13}C\{^1H\}$ NMR ($CH_2Cl_2/CDCl_3$): δ 20.9 ($\underline{C}H_2Sb$), 23.6 ($\underline{C}H_2CH_2$), 129.4, 130.1, 133.1,134.8 (aryl-$\underline{C}$), 211.0, 215.6 ($\underline{C}O$) ppm. ^{95}Mo NMR ($CH_2Cl_2/CDCl_3$): δ -1849 ppm. MS (APCI): *m/z* 746 $[Mo(CO)_2(Ph_2Sb(CH_2)_3SbPh_2)]^+$, 718 $[Mo(CO)(Ph_2Sb(CH_2)_3SbPh_2)]^+$, 690 $[Mo(Ph_2Sb(CH_2)_3SbPh_2)]^+$. IR ($CH_2Cl_2$): ν 2021 s, 1927 sh, 1912 vs, 1892 s cm^{-1}; IR (Nujol mull): ν 2015 s, 1928 m, 1906 vs, 1872 s cm^{-1}.

[$W(CO)_4(Ph_2Sb(CH_2)_3SbPh_2)$]: $[W(CO)_4(piperidine)_2]$ (0.23g, 0.5 mmol) and $Ph_2Sb(CH_2)_3SbPh_2$ (0.3g, 0.5 mmol) were refluxed gently in ethanol (30 cm^3), then the mixture was cooled and filtered. The solvent was removed *in vacuo*, the residue extracted with CH_2Cl_2, the solution

filtered, and the filtrate concentrated to *ca.* 10 cm^3. Addition of diethyl ether (10 cm^3) produced a yellow solid, which was separated and dried *in vacuo*. (Yield 0.11g, 24%). Anal. Found: C, 39.1; H, 3.0. Calc. for $C_{31}H_{26}O_4Sb_2W.CH_2Cl_2$: C, 39.4; H, 3.5%. ^1H NMR ($CDCl_3$): δ 2.2 (m) [6H] ($C\underline{H}_2Sb$, $C\underline{H}_2$) 5.4 (s) ($C\underline{H}_2Cl_2$), 7.3-7.6 (m) [20H], (SbPh) ppm. $^{13}C\{^1H\}$ NMR ($CH_2Cl_2/CDCl_3$): δ 20.0 ($\underline{C}H_2Sb$), 23.8 ($\underline{C}H_2CH_2$), 129.4, 130.3, 132.1, 134.7 (aryl-$\underline{C}$), 201.4 ($^1J_{WC}$ = 116Hz) 205.1($^1J_{WC}$ = 165Hz) ($\underline{C}O$) ppm. MS (APCI): *m/z* 891 $[W(Ph_2Sb(CH_2)_3SbPh_2)(CO)_4]^+$. IR ($CH_2Cl_2$): ν 2015 s, 1916 sh, 1902 vs, 1882 sh cm^{-1}; IR (Nujol mull): ν 2012 s, 1920 sh, 1900 vs, 1869 s cm^{-1}.

$[\{Fe(CO)_4\}_2(Ph_2Sb(CH_2)_3SbPh_2)]$: $[Fe_2(CO)_9]$ (0.92g, 2.6 mmol) and $Ph_2Sb(CH_2)_3SbPh_2$ (0.75g, 1.26 mmol) were dissolved in anhydrous thf (50 cm^3) and the solution was stirred at room temperature for 2 hrs. Filtration and removal of the volatiles under reduced pressure, afforded a viscous dark red-brown oil. (Yield: 1.14g, 97%). ^1H NMR ($CDCl_3$): δ 2.0(m) [4H] ($C\underline{H}_2Sb$), 2.3 (m) [2H] ($C\underline{H}_2$), 7.3-7.6 (m) [20H] (SbPh) ppm. $^{13}C\{^1H\}$ NMR ($CH_2Cl_2/CDCl_3$): δ 22.9 ($\underline{C}H_2Sb$), 25.9 ($\underline{C}H_2CH_2$), 129.4, 129.9, 131.2, 134.7 (aryl-$\underline{C}$), 213.2 ($\underline{C}O$) ppm. MS (APCI): *m/z* 762 $[Fe(CO)_4(Ph_2Sb(CH_2)_3SbPh_2)]^+$, 732 $[Fe(CO)_3(Ph_2Sb(CH_2)_3SbPh_2)]^+$, 678 $[Fe(CO)(Ph_2Sb(CH_2)_3SbPh_2)]^+$, 650 $[Fe(Ph_2Sb(CH_2)_3SbPh_2)]^+$. IR ($CH_2Cl_2$): ν 2044 s, 1967 m, 1934 s,br cm^{-1}. IR (Nujol mull): ν 2041 s, 2060 sh, 1913 vbr cm^{-1}.†

$[Fe(CO)_4(Ph_2Sb(CH_2)_3SbPh_2)]$: This was obtained also as a red-brown oil using a 1:1 $[Fe_2(CO)_9]$: $Ph_2Sb(CH_2)_3SbPh_2$ ratio. The NMR spectra show some contamination with $[\{Fe(CO)_4\}_2(Ph_2Sb(CH_2)_3SbPh_2)]$ and $Ph_2Sb(CH_2)_3SbPh_2$. ^1H NMR ($CDCl_3$): δ 1.8-2.0 (m) [6H], ($C\underline{H}_2Sb$, $C\underline{H}_2$), 7.1-7.6 (m) [20H] (SbPh) ppm. $^{13}C\{^1H\}$ NMR ($CH_2Cl_2/CDCl_3$): δ 23.4, 24.2 ($\underline{C}H_2Sb$), 25.6 ($\underline{C}H_2CH_2$), 128.9, 129.8, 131.0, 134.7, 136.0, 137.5 (aryl-$\underline{C}$), 213.3 ($\underline{C}O$) ppm. MS (APCI): *m/z* 763 $[Fe(CO)_4(Ph_2Sb(CH_2)_3SbPh_2)]^+$. IR ($CH_2Cl_2$): ν 2044 s, 1967 m, 1934 s,br cm^{-1}. IR (Nujol mull): ν 2041s, 1913 vbr cm^{-1}. †

$[Co_2(CO)_6(Ph_2Sb(CH_2)_3SbPh_2)]$: $[Co_2(CO)_8]$ (0.17 g, 0.5 mmol) was dissolved in dry toluene (50 cm^3) and filtered. $Ph_2Sb(CH_2)_3SbPh_2$ (0.297 g, 0.5 mmol) was dissolved in dry toluene (50 cm^3), and added to the toluene solution of $[Co_2(CO)_8]$. The reaction mixture was stirred for 1 hr and then filtered. The dark brown solution was put in the freezer overnight, and the red-brown solid was filtered and dried *in vacuo*. (Yield: 0.13 g, 42%).

The unstable red-brown solid was very poorly soluble in non-polar solvents. Anal. Found: C, 43.6; H, 3.4. Calc. for $C_{33}H_{26}Co_2O_6Sb_2$: C, 45.0; H, 3.0%. ^1H NMR ($CDCl_3$): δ 1.5-2.0 (m) [6H],

($C\underline{H}_2Sb$, $C\underline{H}_2$), 7.1-7.6 (m) [20H] (SbPh) ppm. IR (CH_2Cl_2): ν 1995 m, 1969 s,br, 1934 s,br cm^{-1}. IR (Nujol mull): ν 2004 sh, 1980 s,br, 1953 sh cm^{-1}.

$[Mn_2(CO)_8(Ph_2Sb(CH_2)_3SbPh_2)]$: $[Mn_2(CO)_{10}]$ (0.45 g, 1.15 mmol), $Ph_2Sb(CH_2)_3SbPh_2$ (0.683 g, 1.15 mmol) and $[\{(Cp)Fe(CO)_2\}_2]$ (0.08 g, 0.23 mmol) were dissolved in toluene (50 cm^3) and refluxed for 24 hrs. The dark brown solution was then cooled, reduced in volume to 50 % and then hexane (10 cm^3) was added to precipitate a solid. A waxy brown solid was collected by filtration, dissolved in minimum CH_2Cl_2, filtered through cotton wool, and reduced to dryness to afford a brown solid, which was dried *in vacuo*. (Yield: 0.32 g, 41%). Anal. Found: C, 44.6; H, 2.9 %. Calc. for $C_{35}H_{26}Mn_2O_8Sb_2$: C, 45.3; H, 2.8%. ^1H NMR ($CDCl_3$): δ 2.0-2.2 (br, s) [6H] ($C\underline{H}_2Sb$, $C\underline{H}_2$), 7.0-7.6 (br, m) [20H] (SbPh) ppm. $^{13}C\{^1H\}$ NMR ($CH_2Cl_2/CDCl_3$): δ 20.6 ($\underline{C}H_2Sb$), 21.6 ($\underline{C}H_2CH_2$), 129.3, 130.0, 134.6, 136.4 (aryl-$\underline{C}$), 214.5, 217.2, 217.9 ($\underline{C}O$) ppm. IR (CH_2Cl_2): ν 2034 w, 1977 vbr,s, 1966 sh, 1953 s,sh, 1914 sh cm^{-1}. IR (Nujol mull): ν 2023 w, 1966 s,br, 1947 sh, 1919 sh cm^{-1}.

$[\{Ni(CO)_3\}_2(Ph_2Sb(CH_2)_3SbPh_2)]$ and $[Ni(CO)_2(Ph_2Sb(CH_2)_3SbPh_2)]$

CARE: $[Ni(CO)_4]$ is volatile and extremely toxic: All reactions were conducted in a good fume cupboard and in sealed equipment fitted with bromine water scrubbers. Spectroscopic samples were also handled in the fume cupboard. Residues were destroyed with bromine-water.

A large excess of $Ni(CO)_4$ (*ca.* 1 cm^3) was added to a stirred solution of $Ph_2Sb(CH_2)_3SbPh_2$ (0.297 g, 0.55 mmol) in CH_2Cl_2 (20 cm^3). Carbon monoxide was rapidly evolved, and progress of the reaction was monitored by IR spectroscopy of aliquots of the solution at regular intervals. When reaction had ceased, the excess tetracarbonylnickel and the solvent were removed *in vacuo* to leave a yellow oil, which darkened overnight. Spectroscopic studies showed an inseparable mixture of the two complexes. ^1H NMR ($CDCl_3$): δ 2.0, 2.2 (m), 7.3-7.7(m) [20H] (SbPh) ppm. $^{13}C\{1H\}$ NMR ($CH_2Cl_2/CDCl_3$):δ 20.8, 22.8, 23.5, 24.0 ($\underline{C}H_3$, $\underline{C}H_2Sb$, $\underline{C}H_2$) 129.3, 129.8, 133.0, 134.9 (aryl-$\underline{C}$), 196.8 ($Ni(\underline{C}O)_3$), 201.8 ($Ni(\underline{C}O)_2$) ppm. IR (CH_2Cl_2): ν 2071 s, 1996 vs, 1947 m. IR (thin film): ν 2072 s, 2005 s, 1997 s, 1957 m cm^{-1}. †

$[W(CO)_4(Me_2Sb(CH_2)_3SbMe_2)]$: $[W(CO)_4(piperidine)_2]$ (0.26 g, 0.55 mmol) and $Me_2Sb(CH_2)_3SbMe_2$ (0.2 cm^3, 0.55 mmol) were refluxed gently in ethanol (30 cm^3), then the mixture was cooled and filtered. The solvent was removed *in vacuo*, the residue extracted with CH_2Cl_2, the solution filtered, and the filtrate concentrated to 10 cm^3. Addition of diethyl ether (10 cm^3) produced a yellow solid, which was separated and dried in vacuo. (Yield 0.13 g, 37%). ^1H

NMR (CD_2Cl_2): δ 1.3 (s) [12H] ($C\underline{H}_3$), 1.7 (m) [4H] ($C\underline{H}_2Sb$), 2.1 (m) [2H] ($C\underline{H}_2$) ppm. $^{13}C\{^1H\}$ NMR (dmso/d6-dmso): δ -1.9 ($\underline{C}H_3$), 16.6 ($\underline{C}H_2Sb$), 24.4 ($CH_2\underline{C}H_2$), 203.5 (^1J = 120Hz), 208.2 (^1J = 165Hz) ($\underline{C}O$) ppm. MS (APCI): *m/z* 569 $[W(CO)_2(MeSb(CH_2)_3SbMe_2)]^+$, 557 $[W(CO)(Me_2Sb(CH_2)_3SbMe_2)]^+$, 543 $[W(CO)(MeSb(CH_2)_3SbMe_2)]^+$, 528 $[W(Me_2Sb(CH_2)_3SbMe_2)]^+$. IR ($CH_2Cl_2$): ν 2011 m, 1896 vs,br, 1870 sh cm^{-1}. IR (Nujol mull): ν 2009 s, 1886 vs, br, 1869 sh cm^{-1}. †

$[Mo(CO)_4(Me_2Sb(CH_2)_3SbMe_2)]$: $[Mo(CO)_4(C_7H_8)]$ (0.17 g, 0.55 mmol) and $Me_2Sb(CH_2)_3SbMe_2$ (0.5 cm^3, 0.95 g, 0.55 mmol) were dissolved in degassed EtOH (25 cm^3) and the yellow solution was stirred overnight. The reaction was refluxed for 2 hrs, reduced to dryness and the residues dissolved in minimum CH_2Cl_2. Hexane (10 cm^3) was added to precipitate the pale brown solid which was filtered and dried *in vacuo*. (Yield: 0.031 g, 11%). Anal. Found: C, 23.8; H, 3.1 %. Calc. for $C_{11}H_{18}O_4Mo_1Sb_2$: C, 23.8; H, 3.3%. ^1H NMR ($CDCl_3$): δ 1.05 (s) [12H] ($C\underline{H}_3$), 1.55 [4H] ($C\underline{H}_2Sb$), 1.90 [2H] ($C\underline{H}_2$) ppm. $^{13}C\{^1H\}$ NMR (dmso/d^6 dmso): δ -1.6 ($\underline{C}H_3$), 17.8 ($\underline{C}H_2Sb$), 24.5 ($\underline{C}H_2CH_2$), 213.0, 218.4 ($\underline{C}O$) ppm. ^{95}Mo NMR (dmso/d^6-dmso): δ -1843 ppm. IR (CH_2Cl_2): ν 2014 m, 1903 vs,br, 1880 sh cm^{-1}. IR (Nujol mull): ν 2013 m, 1946 sh, 1894 vs,br, 1866 sh cm^{-1}.

$[Cr(CO)_4(Me_2Sb(CH_2)_3SbMe_2)]$: As above using $[Cr(CO)_4(C_7H_8)]$ (0.14 g, 0.55 mmol). The pale green solid was recrystallised from CH_2Cl_2 and Et_2O, and dried *in vacuo*. (Yield: 0.15 g, 54%). ^1H NMR ($CDCl_3$): δ 1.1 (s) [6H] ($C\underline{H}_3$), 1.6 (t) [4H] ($C\underline{H}_2Sb$), 1.9 (m) [2H] ($C\underline{H}_2$) ppm. $^{13}C\{^1H\}$ NMR ($CH_2Cl_2/CDCl_3$): δ -2.1 ($\underline{C}H_3$), 17.9 ($\underline{C}H_2Sb$), 24.0 ($\underline{C}H_2CH_2$), 223.7, 229.9 ($\underline{C}O$) ppm. MS (APCI): *m/z* 509 $[Cr(CO)_4(Me_2Sb(CH_2)_3SbMe_2)]^+$, 481 $[Cr(CO)_3(Me_2Sb(CH_2)_3SbMe_2)]^+$. IR ($CH_2Cl_2$): ν 1995 s, 1900 sh, 1885 s,vbr, 1875 sh cm^{-1}. IR (Nujol mull): ν 1993 s, 1903 sh, 1888 vs,br, 1862 sh cm^{-1}. †

$[\{Fe(CO)_4\}_2(Me_2Sb(CH_2)_3SbMe_2)]$: $[Fe_2(CO)_9]$ (0.8 g, 2.2 mmol) was dissolved in dry degassed thf (50 cm^3) and filtered. $Me_2Sb(CH_2)_3SbMe_2$ (0.38 g, 1.1 mmol) in a stock solution of CH_2Cl_2, was added and stirred for 30 minutes. The reaction was reduced to dryness and the dark red oil was dried *in vacuo*. (Yield: 0.74 g, 50%). ^1H NMR ($CDCl_3$): δ 0.8 – 2.3 (m) [18H]. $^{13}C\{^1H\}$ NMR ($CH_2Cl_2/CDCl_3$): δ -5.1 ($\underline{C}H_3$), 20.8 ($\underline{C}H_2Sb$), 25.6 ($\underline{C}H_2CH_2$), 213.6 ($\underline{C}O$) ppm. IR (CH_2Cl_2): ν 2055 s, 1968 m, 1927 vbr,s cm^{-1}. IR (Nujol mull): ν 2042 m, 1965 m, 1932 s,br, 1914 sh cm^{-1}. †

$[Co_2(CO)_4(Me_2Sb(CH_2)_3SbMe_2)][Co(CO)_4]_2$: $[Co_2(CO)_8]$ (0.38 g, 1.1 mmol) was dissolved in dry degassed toluene (50 cm^3) and filtered. $Me_2Sb(CH_2)_3SbMe_2$ (0.39 g, 1.1 mmol) was added to the reaction and then stirred for 1 hr. The brown precipitate produced was filtered and dried *in vacuo*. (Yield: 0.15g, 20%). ^1H NMR ($CH_2Cl_2/CDCl_3$): δ 0.6 (s) [4H], 0.8 (s) [8H], 1.2-1.7 (m) [6H] ($C\underline{H}_2Sb$, $C\underline{H}_2$) ppm. $^{13}C\{^1H\}$ NMR ($CH_2Cl_2/CDCl_3$): δ -2.6 ($\underline{C}H_3$), 18.8 ($\underline{C}H_2Sb$), 21.4 ($\underline{C}H_2CH_2$), 194.4, 195.8 ($\underline{C}O$) ppm. ^{59}Co NMR ($CH_2Cl_2/CDCl_3$): δ -2999.3 ppm ($w_{1/2}$ = 40 Hz). MS (ES+): *m/z* 751 $[Co(Me_2Sb(CH_2)_3SbMe_2)_2]^+$, 777 $[Co(CO)(Me_2Sb(CH_2)_3SbMe_2)_2]^+$, 803 $[Co(CO)_2(Me_2Sb(CH_2)_3SbMe_2)_2]^+$. MS (ES-): *m/z* 171 $[Co(CO)_4]^-$. IR (CH_2Cl_2): ν 1990 sh, 1972 s,br, 1885 s, br cm^{-1}. IR (Nujol mull): ν 1968 s,br, 1878 s,br cm^{-1}. †

$[\{Ni(CO)_3\}_2(Me_2Sb(CH_2)_3SbMe_2)]$: A large excess of $Ni(CO)_4$ (*ca.* 1 cm^3) was added to a stirred solution of $Me_2Sb(CH_2)_3SbMe_2$ (0.2 cm^3, 0.55 mmol) in CH_2Cl_2 (20 cm^3). Carbon monoxide was rapidly evolved, and progress of the reaction was monitored by IR spectroscopy of aliquots of the solution at regular intervals. When the reaction had ceased, the excess tetracarbonylnickel and the solvent was removed *in vacuo* to leave a yellow oil. ^1H NMR ($CDCl_3$): δ 1.0 (s) [12H] ($C\underline{H}_3$), 1.6 (m) [4H] ($C\underline{H}_2Sb$), 1.8 (m) [2H] ($C\underline{H}_2$) ppm. $^{13}C\{^1H\}$ NMR ($CH_2Cl_2/CDCl_3$): δ -3.4 ($\underline{C}H_3$), 19.1 ($\underline{C}H_2Sb$), 24.1 ($CH_2\underline{C}H_2$), 197.1 ($\underline{C}O$) ppm. IR (CH_2Cl_2): ν 2067 s, 1991 vs cm^{-1}. IR (thin film): ν 2069 s, 1996 br,s cm^{-1}.

Reaction using a deficit of $[Ni(CO)_4]$: ^1H NMR ($CDCl_3$): δ 0.68 (s), 0.96 (s), 0.98 (s), 1.4 – 1.85 (m) [6H] ($C\underline{H}_2Sb$, $C\underline{H}_2$) ppm. $^{13}C\{^1H\}$ NMR ($CH_2Cl_2/CDCl_3$): δ -4.9, -3.2, -1.4 ($\underline{C}H_3$), 18.3, 19.6, 20.9, 24.1, 24.9 ($\underline{C}H_2Sb$, $\underline{C}H_2$), 197.1, 201.5 ($\underline{C}O$) ppm. IR (CH_2Cl_2): ν 2066 s, 1991 vs, 1933 m cm^{-1}. IR (thin film): ν 2069 s, 2006 sh, 1996 br,s, 1950 m cm^{-1}. †

† Microanalysis was not obtained due to the very unstable nature of the complex.

6.5 References

[1] N. R. Champness, W. Levason, *Coord. Chem. Rev.*,1994, **133**,115; W. Levason, G. Reid, *Coord. Chem. Rev.*, 2006, **250**, 2565.

[2] E. Shewchuk, S. B Wild, *J. Organomet. Chem.*,1974, **71**, C1.

[3] E. Shewchuk, S. B Wild, *J. Organomet. Chem.*,1977, **128**, 115.

[4] T. Fukumoto, Y. Matsumura, R. Okawara, *Inorg. Nucl. Chem. Let.*, 1973, **9**, 711.

[5] A. M. Hill, N. J. Holmes, A. R. J. Genge, W. Levason, M. Webster, S. Rutschow, *J. Chem. Soc., Dalton Trans.*,1998, 825.

[6] A. M. Hill, W. Levason, M. Webster, I. Albers, *Organometallics,* 1997, **16**, 5641.

[7] A. R. J. Genge, N. J. Holmes, W. Levason, M. Webster, *Polyhedron,*1999, **18**, 2673.

[8] W. Levason, M. L. Matthews, G. Reid, M. Webster, *Dalton. Trans.*, 2004, 51.

[9] T. Fukumoto, Y. Matsuruma, R. Okawara, *Inorg. Nucl. Chem. Letters,* 1973, **9**, 711.

[10] J. Chatt, G. J. Leigh, N. J. Thankarajan, *J. Organomet. Chem.*,1971, **29**, 105.

[11] M. A. Bennett, L. Pratt, G. Wilkinson, *J. Chem. Soc.*, 1961, 2037.

[12] A. Tekkaya, S. J. Ozkar, *J. Organomet. Chem.*, 1999, **590**, 208.

[13] D. J. Thornhill, A. R. Manning, *J. Chem. Soc., Dalton. Trans.*, 1973, 2086.

[14] E. A. C. Lucken, K. Noack, D. F. Williams, *J. Chem. Soc. (A),*1967, 148.

[15] N. J. Holmes, W. Levason, M. Webster, *J. Organomet. Chem.*, 1998, **568,** 213.

[16] R. H. Reimann, E. Singleton, *J. Chem. Soc., Dalton Trans.*, 1976, 2109.

[17] C. A. Tolman, *Chem. Rev.*, 1977, **77**, 313.

[18] M. V. Barybin, M. K. Pomije, J. E. Ellis, *Inorg. Chim. Acta,* 1998, **269**, 58.

[19] D. J. Darensbourg, R. L. Kump, *Inorg. Chem.*, 1978, **17**, 2680.

[20] W. Levason, K. G. Smith, C. A. McAuliffe, F. P. McCullough, R. D. Sedgwick, S. G. Murray, *J. Chem. Soc., Dalton Trans.*, 1979, 1718.

[21] G. M. Bodner, M. P. May, L. E. McKinney, *Inorg. Chem.*, 1980, **19**, 1951.

[22] D. Benlian, M. Bigorgne, *Bull. Chem. Soc. Fr.*, 1963, 1583.

Appendix

Experimental Techniques and Instrumentation

Experimental Techniques

Unless otherwise stated, experiments were performed under dry N_2 or Ar atmospheres using standard Schlenk line techniques. The air sensitive distibine ligands were stored and handled in an inert dry box, with an N_2 atmosphere. Glassware was pre-dried prior to use. Unless otherwise stated, commercial reagents and solvents were used as received from Acros, Aldrich, Avocado and Fisher. Commerically available metal carbonyls were used as received from Aldrich and Strem, and precious metal salts were supplied by Johnson Matthey. Deuterated solvents were used as received from Aldrich and Apollo Scientific. Where stated solvents were dried and distilled from sodium/benzophenone (thf, Et_2O, toluene, hexane), calcium hydride (CH_2Cl_2, $CHCl_3$, acetonitrile) or magnesium/I_2 (EtOH).[1]

Instrumentation

Infrared spectra were recorded as either Nujol mulls between CsI plates or as CsI disks over the range 4000-200 cm^{-1}, while solution infrared spectra were recorded in CH_2Cl_2 solution over the range 2300–1700 cm^{-1}, using a Perkin-Elmer 983G spectrometer.

UV/vis spectra were recorded either as solids by diffuse reflectance or in CH_2Cl_2 solution using 1 cm path length quartz cells using a Perkin Elmer Lambda19 spectrometer.

Mass spectra were run by electron impact on a VG-70-SE Normal geometry double focusing spectrometer, by positive ion electrospray or by negative ion electrospray (MeCN solution) using a VG Biotech platform.

^1H NMR spectra were recorded in $CDCl_3$ (unless otherwise stated) using a Bruker AV300 and were referenced to Me_4Si ($\delta = 0$). $^{13}C\{^1H\}$, $^{31}P\{^1H\}$, ^{63}Cu and $^{195}Pt\{^1H\}$ NMR spectra were recorded in $CH_2Cl_2/CDCl_3$ or $(CH_3)_2CO/(CD_3)_2CO$ (unless otherwise stated), in 10 mm diameter tubes using a Bruker DPX400 spectrometer operating at 100.6, 162.0, 106.11 or 85.62 MHz respectively and were referenced to Me_4Si, external 85% H_3PO_4, $[Cu(NCMe)_4]BF_4$ and 1 mol. dm^{-3} $Na_2[PtCl_6]$ respectively ($\delta = 0$). For carbonyl compounds $[Cr(acac)_3]$ was added to the NMR spectroscopy samples prior to recording $^{13}C\{^1H\}$ NMR spectra.

Microanalyses were undertaken by the University of Strathclyde microanalytical service. Due to the unstable nature of some compounds, this was not possible, as the samples were in transit and decomposed. Novel ligands, where possible were analysed as air stable Sb(V) species.

Electrical conductivity measurements were recorded in 10^{-3} mol dm^{-3} $MeNO_2$ or CH_2Cl_2 solution using a Pye Conductivity Bridge and platinised platinum electrodes, calibrated with standard KCl solutions.

X-ray crystallography

Data collections for the structures reported in chapters 2, 3, 4 and 5, were carried out using an Enraf-Nonius Kappa CCD diffractometer with graphite monochromated Mo-Kα radiation (λ = 0.71073 Å) with the crystals held at 120 K in a nitrogen stream. Structure solution and refinement were routine with H-atoms normally introduced in calculated positions.[2-4] With the exception of $[Rh(CO)Cl(o\text{-}C_6H_4(CH_2PPh_2)_2)(\kappa^1\text{-}o\text{-}C_6H_4(CH_2PPh_2)_2)].CH_2Cl_2$ and $[RhCl_2(SbPh_3)_3(Ph)]$ which have weak data or have been reported previously, all *.cif files for the the crystal structures reported in this Thesis have been published. Table A1 below shows the structures reported along with the CCDC reference number.

Table A1: Crystal structures reported in this Thesis.

Complex	CCDC Number
$[CoCl_2(o\text{-}C_6H_4(CH_2PPh_2)_2)]$	204478
$[Rh\{o\text{-}C_6H_4(CH_2PPh_2)_2\}_2]BF_4.2CHCl_3$	240479
$[PdCl_2(o\text{-}C_6H_4(CH_2PPh_2)_2)]$	240480
$[Pd_2Cl_2\{o\text{-}C_6H_4(CH_2PPh_2)_2\}_2](PF_6)_2.2CH_2Cl_2$	240481
$[Ag\{o\text{-}C_6H_4(CH_2PPh_2)_2\}_2]BF_4.2CH_2Cl_2$	240482
$[Au\{o\text{-}C_6H_4(CH_2PPh_2)_2\}_2]PF_6.2CDCl_3$	240483
$[Me_3Pt(\mathbf{VI})I]$	285687
$[Me_3Pt\{Ph_2Sb(CH_2)_3SbPh_2\}I]$	285688
$[Me_3Pt\{Me_2Sb(CH_2)_3SbMe_2\}I]$	285689
$[Me_3Pt\{o\text{-}C_6H_4(CH_2SbMe_2)_2\}I]$	285690
$[Me_3Pt(SbPh_3)_2I]$	285691
$[(Me_3Pt)_2\{\mu\text{-}Ph_2SbCH_2SbPh_2\}(\mu\text{-}I)_2]$	285692
$[Rh(CO)\{Ph_2Sb(CH_2)_3SbPh_2\}_2]PF_6.¾CH_2Cl_2$	604224
$[RhCl_2\{Ph_2Sb(CH_2)_3SbPh_2\}\{PhClSb(CH_2)_3SbClPh\}]Cl.CHCl_3$	604225
$[PtCl_2(\mathbf{VI})]$	616260
$[W(CO)_4(\mathbf{VI})]$ ($P2_1/n$)	616261
$[W(CO)_4(\mathbf{VI})]$ (Cc)	616262

References

[1] R. J. Errington, "Advanced Practical Inorganic and Metal Organic Chemistry", Blackie Academic and Professional London, 1997.

[2] G. M. Sheldrick, SHELX-97, Program for Crystal Structure Refinement, University of Gottingen, Germany, (1997).

[3] G. M. Sheldrick, SHELX-97, Program for Crystal Structure Solution, University of Gottingen, Germany, (1997).

[4] L. J. Farrugia, WinGX-Version 1.64.05, An Integrated System of Windows Programs for the Solution, Refinement and Analysis of Single Crystal *X*-ray Diffraction Data, Department of Chemistry, University of Glasgow, UK, (2003).